

Classification of Flavonoid Metabolomes via Data Mining and Quantification of Hydroxyl NMR Signals

Yang Yu,[†] Guido F. Pauli,^{†,‡} Ling-Yi Huang,[†] Li-She Gan,[§] Richard B. van Breemen,[†] Dianpeng Li,[¶] James B. McAlpine,[‡] David C. Lankin,[†] and Shao-Nong Chen^{†,‡,*}

[†]UIC/NIH Center for Botanical Dietary Supplements Research, PCRPS and Department of Pharmaceutical Sciences, and
[‡]Institute for Tuberculosis Research, College of Pharmacy, University of Illinois at Chicago, Chicago, IL 60612, United States

[§]College of Pharmaceutical Sciences, Zhejiang University, Hangzhou, 310058, China

[¶]Guangxi Key Laboratory of Functional Phytochemicals Research and Utilization, Guangxi Institute of Botany, Chinese Academy of Sciences, Guilin 541006, China

■ SUPPORTING INFORMATION

■ TABLE OF CONTENTS

SUPPORTING INFORMATION PART & DESCRIPTION	PAGE
Section S1. Details of Experimental Procedures & Structure Elucidation	6
Section S1A. General Experimental Procedures	6
Section S1B. Building NMR Metabolomic Tools	6
Section S1C. Samples and Sample Preparation	6
Section S1D. Fractionation by HPLC	7
Section S1E. LC-MS conditions	7
Section S2. Structure Elucidation and Verification of 5-OH Flavonoids	9
Section S3. Structure Verification Of 5-OH Flavonoids	15
Figure S1. Original structure of licoisoflavanone B reported in the literature (A) vs. its revised structure determined as relicoisoflavanone B (B)	15
Figure S2. Original structure of licoisoflavanone C reported in the literature (A) vs. its revised structure determined as relicoisoflavanone C (B)	15
Figure S3. ^1H - ^1H COSY (—) and selected HMBC ($\text{H}\rightarrow\text{C}$) correlations of the original structure of licoisoflavanone B reported in the literature (A) vs. its revised structure determined as relicoisoflavanone B (B)	16
Figure S4. ^1H - ^1H COSY (—) and selected HMBC ($\text{H}\rightarrow\text{C}$) correlations of the original structure of licoisoflavanone C reported in the literature (A) vs. its revised structure determined as relicoisoflavanone C (B)	16
Section S4. Structure Elucidation and Verification Related Tables	17
Table S1. Comparison of the ^1H and ^{13}C NMR spectroscopic data of licoisoflavanone B vs. relicoisoflavanone B, compound 1, and licoisoflavanone C vs. relicoisoflavanone C	17
Table S2. The HMBC patterns of licoisoflavanone B vs. relicoisoflavanone B, compound 1, and licoisoflavanone C vs. relicoisoflavanone C	18
Table S3. The HMBC patterns mined from literature data of compounds isolated from licorice species (GU, GG, and GI)	19
Table S4. The metabolomic HMBC patterns from experimental data of GU/GG/GI MeOH fractions	22
Table S5. The HMBC patterns of 15 compounds identified in GU-MF-11, GU-MF-12, and GU-MF-14–20	23
Section S5. References Related to Structure Elucidation and Verification	24
Section S6. Further Supporting Figures & Tables	28
Figure S5. Comparison of the ^1H NMR spectra of WF, 50% MF, MF, and AF for GU	28
Figure S6. Comparison of the ^1H NMR spectra of GU-MF, GG-MF, and GI-MF	29
Figure S7. The chemical shifts of the 5-/2'-OH hydrogens and the three HMBC correlated carbons of the following flavonoid skeletons: flavonone, isoflavonone, flavononol, flavone, isoflavone, flavonol, its 3-O-methyl derivative, its 3-O-glycoside, dihydrochalcone, chalcone, and α -hydroxyl dihydrochalcone	30

Figure S8. The preparative HPLC profile of GU-MF at 254 nm, divided into 20 subfractions, GU-MF-1 to GU-MF-20	31
Figure S9. The 5-/2'-OH hydrogen chemical shifts and structures of the three model compounds, Y1, Y2, and Y3	32
Table S6. Bond lengths, second-order stabilization energies $\Delta E^{(2)}$, and natural charges of the hydrogen atoms of the C(4/1)=O...H-O-C(5/2') hydrogen bonds in the model compounds Y1, Y2, and Y3	33
Figure S10. B3LYP/6-31+G(d,p) optimized lowest energy 3D conformers of the model compounds, Y1, Y2, and Y3	34
Table S7. Energy analysis of the conformers of the model compounds, Y1, Y2, and Y3	35
Table S8. NBO analysis data for conformers of the model compounds, Y1, Y2, and Y3	35
Table S9. Second-order stabilization energies $\Delta E^{(2)}$ (kcal/mol) of the hydrogen bonds of the conformers of the model compounds, Y1, Y2, and Y3	36
Table S10. The relative percentage of the eight subtypes in GU, GG, and GI, respectively	36
Figure S11. The ^1H NMR spectrum of GU-MF	37
Figure S12. The HMBC spectrum of GU-MF	38
Figure S13. The ^1H NMR spectrum of GG-MF	39
Figure S14. The HMBC spectrum of GG-MF	40
Figure S15. The ^1H NMR spectrum of GI-MF	41
Figure S16. The HMBC spectrum of GI-MF	42
Figure S17. The ^1H NMR spectrum of GU-MF-11	43
Figure S18. The ^1H NMR spectrum of compound 13 in GU-MF-11	44
Figure S19. The ^1H NMR spectrum of compound 14 in GU-MF-11	45
Figure S20. The ^1H NMR spectrum of compound 11 in GU-MF-11	46
Figure S21. The ^1H NMR spectrum of compound 3 in GU-MF-11	47
Figure S22. The ^1H - ^1H COSY spectrum of GU-MF-11	48
Figure S23. The HSQC spectrum of GU-MF-11	49
Figure S24. The HMBC spectrum of GU-MF-11	50
Figure S25. The IT-TOF TIC spectrum of GU-MF-11	51
Figure S26. The (+)-HRESIMS and (-)-HRESIMS spectra of one of compounds 3, 11, and 13 in GU-MF-11	52
Figure S27. The (+)-HRESIMS and (-)-HRESIMS spectra of one of compounds 3, 11, and 13 in GU-MF-11	53
Figure S28. The (+)-HRESIMS and (-)-HRESIMS spectra of one of compounds 3, 11, and 13 in GU-MF-11	54
Figure S29. The (+)-HRESIMS and (-)-HRESIMS spectra of compound 14 in GU-MF-11	55
Figure S30. The ^1H NMR spectrum of GU-MF-12	56
Figure S31. The ^1H NMR spectrum of compound 8 in GU-MF-12	57
Figure S32. The ^1H NMR spectrum of compound 10 in GU-MF-12	58
Figure S33. The ^1H - ^1H COSY spectrum of GU-MF-12	59
Figure S34. The HSQC spectrum of GU-MF-12	60

Figure S35. The HMBC spectrum of GU-MF-12	61
Figure S36. The IT-TOF TIC spectrum of GU-MF-12	62
Figure S37. The (+)-HRESIMS and (-)-HRESIMS spectra of one of compounds 8 and 10 in GU-MF-12	63
Figure S38. The (+)-HRESIMS and (-)-HRESIMS spectra of one of the compounds 8 and 10 in GU-MF-12	64
Figure S39. The ^1H NMR spectrum of GU-MF-14	65
Figure S40. The ^1H NMR spectrum of compound 12 in GU-MF-14	66
Figure S41. The ^1H - ^1H COSY spectrum of GU-MF-14	67
Figure S42. The HSQC spectrum of GU-MF-14	68
Figure S43. The HMBC spectrum of GU-MF-14	69
Figure S44. The IT-TOF TIC spectrum of GU-MF-14	70
Figure S45. The (+)-HRESIMS and (-)-HRESIMS spectra of compound 12 in GU-MF-14	71
Figure S46. The ^1H NMR spectrum of GU-MF-15	72
Figure S47. The ^1H NMR spectrum of compound 15 in GU-MF-15	73
Figure S48. The ^1H NMR spectrum of compound 2 in GU-MF-15	74
Figure S49. The ^1H - ^1H COSY spectrum of GU-MF-15	75
Figure S50. The HSQC spectrum of GU-MF-15	76
Figure S51. The HMBC spectrum of GU-MF-15	77
Figure S52. The IT-TOF TIC spectrum of GU-MF-15	78
Figure S53. The (+)-HRESIMS and (-)-HRESIMS spectra of compound 15 in GU-MF-15	79
Figure S54. The (+)-HRESIMS and (-)-HRESIMS spectra of compound 2 in GU-MF-15	80
Figure S55. The ^1H NMR spectrum of GU-MF-16	81
Figure S56. The ^1H NMR spectrum of compound 5 in GU-MF-16	82
Figure S57. The ^1H - ^1H COSY spectrum of GU-MF-16	83
Figure S58. The HSQC spectrum of GU-MF-16	84
Figure S59. The HMBC spectrum of GU-MF-16	85
Figure S60. The IT-TOF TIC spectrum of GU-MF-16	86
Figure S61. The (+)-HRESIMS and (-)-HRESIMS spectra of compound 5 in GU-MF-16	87
Figure S62. The ^1H NMR spectrum of GU-MF-17	88
Figure S63. The ^1H NMR spectrum of compound 6 in GU-MF-17	89
Figure S64. The ^1H - ^1H COSY spectrum of GU-MF-17	90
Figure S65. The HSQC spectrum of GU-MF-17	91
Figure S66. The HMBC spectrum of GU-MF-17	92
Figure S67. The IT-TOF TIC spectrum of GU-MF-17	93
Figure S68. The (+)-HRESIMS and (-)-HRESIMS spectra of compound 6 in GU-MF-17	94
Figure S69. The ^1H NMR spectrum of GU-MF-18	95
Figure S70. The ^1H NMR spectrum of compound 1 in GU-MF-18	96
Figure S71. The ^1H - ^1H COSY spectrum of GU-MF-18	97
Figure S72. The HSQC spectrum of GU-MF-18	98
Figure S73. The HMBC spectrum of GU-MF-18	99

Figure S74. The IT-TOF TIC spectrum of GU-MF-18	100
Figure S75. The (+)-HRESIMS and (-)-HRESIMS spectra of compound 1 in GU-MF-18 with extracted ions (positive and negative) for m/z 423 and 421, respectively	101
Figure S76. The ^1H NMR spectrum of GU-MF-18-1	102
Figure S77. The ^1H NMR spectrum of compound 1 in GU-MF-18-1	103
Figure S78. The ^1H - ^1H COSY spectrum of GU-MF-18-1	104
Figure S79. The HSQC spectrum of GU-MF-18-1	105
Figure S80. The HMBC spectrum of GU-MF-18-1	106
Figure S81. Expansion of the HMBC spectrum of GU-MF-18-1	107
Figure S82. The IT-TOF TIC spectrum of GU-MF-18-1	108
Figure S83. The (+)-HRESIMS and (-)-HRESIMS spectra of compound 1 in GU-MF-18-1	109
Figure S84. The ^1H NMR spectrum of GU-MF-19	110
Figure S85. The ^1H NMR spectrum of compound 9 in GU-MF-19	111
Figure S86. The ^1H - ^1H COSY spectrum of GU-MF-19	112
Figure S87. The HSQC spectrum of GU-MF-19	113
Figure S88. The HMBC spectrum of GU-MF-19	114
Figure S89. The IT-TOF TIC spectrum of GU-MF-19	115
Figure S90. The (+)-HRESIMS and (-)-HRESIMS spectra of compound 9 in GU-MF-19	116
Figure S91. The ^1H NMR spectrum of GU-MF-20	117
Figure S92. The ^1H NMR spectrum of compound 7 in GU-MF-20	118
Figure S93. The ^1H NMR spectrum of compound 4 in GU-MF-20	119
Figure S94. The ^1H - ^1H COSY spectrum of GU-MF-20	120
Figure S95. The HSQC spectrum of GU-MF-20	121
Figure S96. The HMBC spectrum of GU-MF-20	122
Figure S97. The IT-TOF TIC spectrum of GU-MF-20	123
Figure S98. The (+)-HRESIMS and (-)-HRESIMS spectra of compound 7 in GU-MF-20	124
Figure S99. The (+)-HRESIMS and (-)-HRESIMS spectra of compound 4 in GU-MF-20	125
Section S7. Flowchart of Literature Mining	126
Section S8. SciFinder Literature Mining Results	127

SECTION S1. DETAILS OF EXPERIMENTAL PROCEDURES & STRUCTURE ELUCIDATION.

SECTION S1A. GENERAL EXPERIMENTAL PROCEDURES.

The HPLC purification was using a Shimadzu Prominence HPLC system with LC-20AB pump and SPD-20A UV/VIS detector (Kyoto, Japan) on GROM-SIL 120 ODS-4 HE column (300×20 mm, $5 \mu\text{m}$) from Watrex International (San Francisco, CA, USA). HRESIMS data were obtained on a Shimadzu LC-IT-TOF mass spectrometer. All the three species of licorice were extracted with an Accelerated Solvent Extraction (ASE 350) from Dionex Corporation (Sunnyvale, CA, USA). All collected HPLC fractions were dried using a Genevac miVac centrifugal vacuum concentrator (Ipswich, England). Freeze-drying was performed on a Labconco Freezone 4.5 (Kansas City, MO, USA). ^1H NMR and HMBC spectra of GU-MF, GG-MF, and GI-MF, as well as ^1H NMR, ^1H - ^1H COSY, HSQC, and HMBC (hmbcetgpd) spectra of GU-MF-18-1 were performed on a Bruker (Rheinstetten, Germany) Avance 600 MHz NMR spectrometer equipped with a 5 mm TXI cryoprobe, whereas ^1H NMR, ^1H - ^1H COSY, HSQC, and HMBC (hmbcgplndqf) spectra of GU-MF-1~GU-MF-20 were acquired on a Bruker Avance III DRX-500 spectrometer equipped with a 1.7 mm room temperature microprobe. ^1H / ^{13}C NMR chemical shifts were referenced to the residual dimethyl sulfoxide- d_5 (DMSO- d_6) solvent signals δ 2.500/39.510 in the corresponding ^1H / ^{13}C NMR spectra, respectively. All the ^{13}C NMR data were retrieved from either HSQC or HMBC spectra. Offline 1D and 2D NMR data processing was performed with Mnova NMR software package (v.6.0.2, MestReLab Research S.L., A Coruña, Spain) using default parameters, or with NUTS Pro (v. 201004, Acorn NMR Inc., Livermore, CA, USA) using a Lorentz-Gaussian window function (line broadening = -0.3 Hz, Gaussian factor = 0.05). Three times zero fillings were applied prior to Fourier transformation, and the resulting NMR spectra were subjected to manual phase adjustment and automatic baseline correction using polynomial functions.

SECTION S1B. BUILDING NMR METABOLOMIC TOOLS.

The NMR metabolomic tools were built on the basis of our previous studies and developed methodologies, as described in references ¹⁻⁹.

SECTION S1C. SAMPLES AND SAMPLE PREPARATION.

10 gram of each DNA verified licorice raw material was extracted with EtOH:*i*-PrOH:H₂O (90:5:5), using the ASE 350 setup at 80 °C, for 30 min of static time at 1500 psi, for a total of 45 min of extraction.

The extractions were performed for three times to yield three licorice extract (GU, GG, and GI). Each extract was fractionated on XAD-2 (Sigma-Aldrich, St Louis, MO, USA) column with H₂O (WF), 50% MeOH (50% MF), MeOH (MF), and Acetone (AF), respectively. The 5-OH flavonoids/flavanoids/2'-OH chalcones were enriched into methanol fractions, GU-MF, GG-MF, and GI-MF. To validate the method, GU-MF was further fractionated with HPLC on ODS semi-prep column to yield twenty subfractions, GU-MF-1~GU-MF-20. To make the NMR spectra of GU-MF-18 less complicated for elucidation and validation of structure **1**, GU-MF-18 was further separated over a Sephadex LH-20 column to get two fractions, and compound **1** was concentrated in GU-MF-18-1.

NMR samples of GU-MF, GG-MF, and GI-MF were prepared at the following weights: GU-MF, 25.1 mg; GG-MF, 25.1 mg; GI-MF, 25.1 mg, followed by the addition of 600 μL of 99.9% DMSO-*d*₆ (Cambridge Isotope Laboratory (CIL), Inc., Andover, MA, USA). Next, the solutions were transferred to 5 mm NMR tubes. NMR sample of GU-MF-18-1 was prepared at the following weight: 1.82 mg, followed by the addition of 175 μL of 99.9% DMSO-*d*₆. Meanwhile, GU-MF-1~GU-MF-20 were prepared at the following weights: GU-MF-1, 1.27 mg; GU-MF-2, 1.13 mg; GU-MF-3, 3.20 mg; GU-MF-4, 0.46 mg; GU-MF-5, 1.31 mg; GU-MF-6, 0.66 mg; GU-MF-7, 1.37 mg; GU-MF-8, 0.85 mg; GU-MF-9, 1.42 mg; GU-MF-10, 2.34 mg; GU-MF-11, 2.35 mg; GU-MF-12, 1.71 mg; -13, 1.07 mg; -14, 2.36 mg; -15, 3.32 mg; -16, 2.48 mg; -17, 1.05 mg; -18, 2.43 mg; -19, 1.70 mg; -20, 1.53 mg, followed by the addition of 45 μL of "100%" DMSO-*d*₆ (CIL). Next, the 35 μL solutions were transferred to 1.7 mm NMR tubes.

SECTION S1D. FRACTIONATION BY HPLC.

The elution of GU-MF in HPLC was achieved with a gradient of acetonitrile (A) and aqueous 0.1% acetic acid (B) starting with 35% A from 0 to 2.5 min, reaching 35-70% A over 2.5-35 min, keeping 70-76% A over 35-75 min, getting 76-80% A over 75-90 min, achieving 80-90% A over 90-100 min, reaching 90-100% A over 100-105 min, and keeping 100% A over 105-115 min, with a flow rate of 0.8 mL/min. 20 subfractions were acquired from above HPLC fractionation (Figure S8, Supporting information).

SECTION S1E. LC-MS CONDITIONS.

Each sample of GU-MF-1~20 was analyzed using high resolution accurate mass measurement with data-dependent product ion MS/MS on a Shimadzu LCMS-ITTOF hybrid mass spectrometer equipped with a Shimadzu Prominence UFLC-XR HPLC system. Separations were obtained using a Waters (Milford, MA,

USA) XTerra C18, 1.0 × 150 mm, 3.5 μm HPLC column. The mobile phase consisted of a 18 min gradient from water containing 0.1% formic acid to acetonitrile. The flow rate was 0.2 mL/min, and the column temperature was 35 °C.

In the electrospray source, the nitrogen nebulizing gas flow was 1.5 L/min, the heating gas flow was 10 L/min, the interface temperature 200 °C, the CDL temperature 200 °C, and the heat block 200 °C. Positive and negative ion electrospray mass spectra were recorded from *m/z* 100 to 1000. For positive and negative scan, product ion mass spectra were recorded in 0.375 s using unit resolution selection in the ion trap and a resolving power about 10,000 in the time-of-flight (TOF) sector. The detector voltage was 1.65 kV.

The predicted formulas were calculated based on the Software in Shimadzu IT-TOF instrument: Accurate Mass Calculator. The ppm values for each constituent was included.

The elution of GU-MF-11 in HPLC was achieved with a gradient of acetonitrile (A) and aqueous 0.1% formic acid (B) starting with 35% A from 0 to 3.0 min, reaching 35-55% A over 3.0-14.0 min, getting 55-100% A over 14.0-15.5 min, keeping 100% A over 15.5-18.0 min, with a flow rate of 0.2 mL/min.

The elution of GU-MF-12 in HPLC was achieved with a gradient of acetonitrile (A) and aqueous 0.1% formic acid (B) starting with 20% A from 0 to 0.5 min, reaching 20-30% A over 0.5-3.0 min, getting 30-50% A over 3.0-10.0 min, achieving 50-100% A over 10.0-15.5 min, keeping 100% A over 15.5-18.0 min, with a flow rate of 0.2 mL/min.

The elution of GU-MF-14~GU-MF-16 in HPLC were achieved with a gradient of acetonitrile (A) and aqueous 0.1% formic acid (B) starting with 25% A from 0 to 0.5 min, reaching 25-35% A over 0.5-3.0 min, getting 35-55% A over 3.0-10.0 min, achieving 55-100% A over 10.0-15.5 min, keeping 100% A over 15.5-18.0 min, with a flow rate of 0.2 mL/min.

The elution of GU-MF-17~GU-MF-20 in HPLC were achieved with a gradient of acetonitrile (A) and aqueous 0.1% formic acid (B) starting with 30% A from 0 to 0.5 min, reaching 30-40% A over 0.5-3.0 min, getting 40-60% A over 3.0-10.0 min, achieving 60-100% A over 10.0-15.5 min, keeping 100% A over 15.5-18.0 min, with a flow rate of 0.2 mL/min.

SECTION S2. STRUCTURE ELUCIDATION AND VERIFICATION OF 5-OH FLAVONOIDs.

According to the developed methodology, two compounds (**10** and **8**) were identified in GU-MF-12, which belonged to different subtype structures, type II-1 and II-3. In the ^1H NMR and HMBC spectra of GU-MF-12 (Figures S30–32, S35, Supporting Information), the NMR data (δ_{H} 12.90, 1H, s, 5-OH; δ_{C} 159.6, C-5; 98.5, C-6; 104.5, C-10; 13.22, 1H, s, 5-OH; δ_{C} 158.8, C-5; 111.1, C-6; 104.5, C-10) established two major 5-OH flavonoids, respectively, including one (structural type II-1) 5,7-dihydroxyl-8-prenyl flavones/isoflavones for **10**, and one (structural type II-3) 5,7-dihydroxyl-6-prenyl flavones/isoflavones for **8**. The structures of the two compounds were deduced together. The HSQC spectrum (Figure S34, Supporting Information) of GU-MF-12 revealed two isoflavone characteristic crossed-peaks of H-2/C-2 signals at δ_{H} 8.38/ δ_{C} 153.9 and δ_{H} 8.28/ δ_{C} 153.9 for **10** and **8**, respectively. The integral value of H-2 in **8** and **10** indicated the quantity of two compounds are almost equal. The NMR data ($\delta_{\text{H/C}}$ 7.38/130.2, 2H, d, J = 8.2 Hz, CH-2', 6'; 6.81/115.1, 2H, d, J = 8.2 Hz, CH-3', 5'; and $\delta_{\text{H/C}}$ 7.36/130.2, 2H, d, J = 8.2 Hz, CH-2', 6'; 6.82/115.1, 2H, d, J = 8.2 Hz, CH-3', 5') showed that both of compounds **10** and **8** had 4'-hydroxyl substituted B rings, which were proved by the COSY correlations (Figure S33, Supporting Information) of H-2'/H-3' and H-5'/H-6' as well as the HMBC correlations (Figure S35, Supporting Information) from H-2', H-3', H-5', and H-6' to C-4' (δ_{C} 157.4) for both of **10** and **8**. Considering the (−)-HRESIMS (Figures S37 and S38, Supporting Information) at m/z 337.1035 [M − H][−] (calcd for $\text{C}_{20}\text{H}_{17}\text{O}_5^-$, 337.1081) and m/z 337.1044 [M − H][−] (calcd for $\text{C}_{20}\text{H}_{17}\text{O}_5^-$, 337.1081) for **10** and **8**, or vise versa, their structures were determined as lupiwighteone¹⁰ and wighteone,¹⁰ respectively.

Compound **12** in GU-MF-14, a major 5-OH flavonoid, was identified as type II-2, 5,7-dihydroxyl flavonones/isoflavanones (δ_{H} 12.85, 1H, s, 5-OH; δ_{C} 161.8, C-5; 98.9, C-6; 104.6, C-10) on the basis of its ^1H NMR data and HMBC spectra (Figures S39, S40, and S43, Supporting Information). Its ^1H NMR data and HSQC spectrum (Figures S39, S40, and S42, Supporting Information) of GU-MF-14 revealed the presence of one singlet proton signal (δ_{H} 8.17, 1H, s, H-2; δ_{C} 155.5, C-2) having the same peak area as proton resonance 12.85 ppm in **12**, indicating **12** was an isoflavone. Combined with its ^1H - ^1H COSY spectrum (Figure S41, Supporting Information), two AB coupling system aromatic protons (δ_{H} 6.33, 1H, d, J = 8.2 Hz, H-5'; 6.88, 1H, d, J = 8.2 Hz, H-6'; δ_{C} 107.3, C-5'; 131.2, C-6') and a 1',2',3',4'-tetrasubstituted B ring were determined in **12**, which was proved by the HMBC correlations (Figure S43, Supporting Information) from H-5' to C-1' (δ_{C} 111.2), C-3' (δ_{C} 109.8), and C-4' (δ_{C} 153.7); from H-6' to C-3 (δ_{C} 120.6),

C-2' (δ_{C} 151.0), and C-4'. The NMR data (δ_{H} 6.67, 1H, d, J = 10.0 Hz, H-1''; 5.68, 1H, d, J = 10.0 Hz, H-2''; δ_{C} 116.8, C-1''; 128.7, C-2'') revealed that **12** possessed a 2,2-dimethylpyran ring with the same pattern as that of licoisoflavone B,¹⁰ which was proved by the HMBC correlations (Figure S43, Supporting Information) from H-1'' to C-2', C-3', C-4', and C-3'' (δ_{C} 75.5); from H-2'' to C-3', C-3'', C-4'' (δ_{C} 27.3), and C-5'' (δ_{C} 27.3); from H-4'' (δ_{H} 1.37, 3H, s) to C-3'' and C-5''; from H-5'' (δ_{H} 1.37, 3H, s) to C-3''. Taking into account the (−)-HRESIMS (Figure S45, Supporting Information) at m/z 351.0878 [M − H][−] (calcd for $\text{C}_{20}\text{H}_{15}\text{O}_6^-$, 351.0874), **12** was elucidated as licoisoflavone B.¹⁰

Compounds **2** and **15** in GU-MF-15 were identified. Analysis of ¹H NMR data and HMBC spectra (Figures S46–48, S51, Supporting Information) of GU-MF-15 revealed the presence of two major 5-OH flavonoids, including one (structural type I-1) 5,7-dihydroxyl-8-prenyl flavonone/isoflavanone (δ_{H} 12.27, 1H, s, 5-OH; δ_{C} 161.4, C-5; 95.4, C-6; 102.0, C-10), and one (structural type II-2) 5,7-dihydroxyl flavone/isoflavone (δ_{H} 12.91, 1H, s, 5-OH; δ_{C} 161.9, C-5; 99.1, C-6; 104.3, C-10).

Analysis of the ¹H NMR and HSQC spectrum (Figures S46–48, and S50, Supporting Information) of GU-MF-15 revealed the presence of one methylene (δ_{H} 4.48, 1H, t, J = 11.0 Hz, H-2a; 4.44, 1H, dd, J = 11.0, 5.5 Hz, H-2b; δ_{C} 70.0, C-2) and one methine (δ_{H} 4.26, 1H, dd, J = 11.0, 5.5 Hz, H-3; δ_{C} 45.6, C-3), with the same peak area as proton resonance 12.27 ppm in **2**, indicating compound **2** was an isoflavanone. The NMR data (δ_{H} 6.31, 1H, d, J = 8.3 Hz, H-5'; 6.67, 1H, d, J = 8.3 Hz, H-6'; δ_{C} 106.8, C-5'; 126.7, C-6') showed that there was a 1',2',3',4'-tetrasubstituted B ring in **2**, which was supported by HMBC correlations (Figure S51, Supporting Information) from H-5' to C-1' (δ_{C} 113.9), C-3' (δ_{C} 116.1), and C-4' (δ_{C} 154.9); from H-6' to C-3 (δ_{C} 45.6), C-2' (δ_{C} 153.8), and C-4'. Considering the (−)-HRESIMS (Figure S54, Supporting Information) at m/z 423.1779 [M − H][−] (calcd for $\text{C}_{25}\text{H}_{27}\text{O}_6^-$, 423.1813), **2** was determined as 3'-(γ,γ -dimethylallyl)-kievitone.¹¹

Analysis of the ¹H NMR and HSQC spectrum (Figures S46–48, S50, Supporting Information) of GU-MF-15 revealed the presence of one singlet proton signal (δ_{H} 8.35, 1H, s, H-2; δ_{C} 154.1, C-2) with the same peak area as proton resonance 12.91 ppm in **15**, indicating that compound **15** was an isoflavone. The NMR data (δ_{H} 7.27, 1H, d, J = 2.0 Hz, H-2'; 6.80, 1H, d, J = 8.2 Hz, H-5'; 7.29, 1H, dd, J = 8.2, 2.0 Hz, H-6'; δ_{C} 126.7, C-2'; 115.5, C-5'; 129.5, C-6') showed that there was a 1',3',4'-trisubstituted B ring in **15**, which was proved by the HMBC correlations (Figure S51, Supporting Information) from H-2' to C-3 (δ_{C} 121.8), C-4'

(δ_c 152.3), C-6' (δ_c 129.5), and C-1'' (δ_c 121.4); from H-5' to C-1' (δ_c 123.2), C-3' (δ_c 120.5), and C-4'; from H-6' to C-3, C-2' and C-4'. The NMR data (δ_H 6.43, 1H, d, J = 9.8 Hz, H-1''; 5.77, 1H, d, J = 9.8 Hz, H-2''; δ_c 121.4, C-1''; 131.2, C-2'') revealed the presence of a 2,2-dimethylpyran ring in **15** with the same pattern as that of isoderrone, which was proved by the HMBC correlations (Figure S51, Supporting Information) from H-1'' to C-4' and C-3'' (δ_c 76.3); from H-2'' to C-3' and C-3''; from H-4'' (δ_H 1.39, 3H, s) to C-2'' (δ_c 131.2), C-3'', and C-5'' (δ_c 27.5); from H-5'' (δ_H 1.39, 3H, s) to C-2'', C-3'', and C-4'' (δ_c 27.5). Considering the (−)-HRESIMS (Figure S53, Supporting Information) at m/z 335.0893 [M − H][−] (calcd for C₂₀H₁₅O₅[−], 335.0925), **15** was determined as isoderrone.¹⁰

Compound **5** was identified in GU-MF-16. The ¹H NMR data and HMBC spectra (Figures S55–56, S59, Supporting Information) revealed the presence of one major 5-OH flavonoid, one (structural type II-3) 5,7-dihydroxyl-6-prenyl flavones/isoflavones (δ_H 13.26, 1H, s, 5-OH; δ_c 158.8, C-5; 111.1, C-6; 104.1, C-10). The NMR data (δ_H 8.20, 1H, s, H-2; δ_c 153.4, C-2) with the same peak area as proton resonance 13.26 ppm in **5** revealed that compound **5** was an isoflavone. The NMR data (δ_H 6.88, 1H, brs, H-2'; 6.67, 1H, brs, H-6'; δ_c 113.9, C-2'; 120.3, C-6') revealed that there was a 1',3',4',5'-tetrasubstituted B ring in **5**, which was proved by the HMBC correlations (Figure S59, Supporting Information) from H-2' to C-3' (δ_c 144.2), C-4' (δ_c 143.1), and C-6' (δ_c 120.3), and from H-6' to C-2' (δ_c 113.9), C-4', and C-1''' (δ_c 28.2). Taking into account the (−)-HRESIMS (Figure S61, Supporting Information) at m/z 421.1639 [M − H][−] (calcd for C₂₅H₂₅O₆[−], 421.1657), **5** was determined as isoangustone A.¹⁰

Compound **6** was identified in GU-MF-17. The ¹H NMR data and HMBC spectrum (Figures S62–63, S66, Supporting Information) revealed the presence of one major 5-OH flavonoid, one (structural type II-3) 5,7-dihydroxyl-6-prenyl flavones/isoflavones (δ_H 13.21, 1H, s, 5-OH; δ_c 158.9, C-5; 111.2, C-6; 104.2, C-10). The NMR data (δ_H 8.30, 1H, s, H-2; δ_c 153.7, C-2) with the same peak area as proton resonance 13.21 ppm in **6** revealed that compound **6** was an isoflavone. ¹H NMR data (δ_H 6.91 and 6.72, each 1H, brs, H-2' and H-6'; δ_c 116.8 and 117.3, C-2' and C-6') revealed that there was a 1',3',4',5'-tetrasubstituted B ring in **6**, which was proved by the HMBC correlations (Figure S66, Supporting Information) from H-2' to C-3' (δ_c 145.2), C-4' (δ_c 140.0), and C-6' (δ_c 117.3); from H-6' to C-2' (δ_c 116.8), C-4', and C-1''' (δ_c 121.9). The NMR data (δ_H 6.38, 1H, d, J = 10.0 Hz, H-1''; 5.75, 1H, d, J = 10.0 Hz, H-2''; δ_c 121.9 and 131.1) revealed that **6** possessed a 2,2-dimethylpyran ring with the same pattern as that of **14**. Considering the (−)

HRESIMS (Figure S68, Supporting Information) at m/z 419.1490 [$M - H$]⁻ (calcd for C₂₅H₂₃O₆⁻, 419.1500), compound **6** was determined as gancaonin H.¹²

A major component of GU-MF-18 was identified as **1** (δ_H 12.56, 1H, s, 5-OH; δ_C 161.0, C-5; 107.6, C-6; 101.7, C-10), a new 5,7-dihydroxyl-6-prenyl flavonone/isoflavonone (subtype I-3), based on its 1D ¹H NMR and HMBC data (Figures S69–70, S73, Supporting Information). The HSQC spectrum (Figure S72, Supporting Information) revealed the presence of one methylene (δ_H 4.47, 1H, t, J = 11.0 Hz, H-2a; 4.38, 1H, dd, J = 11.0, 5.5 Hz, H-2b; δ_C 69.7, C-2), one methine (δ_H 4.26, 1H, dd, J = 11.0, 5.5 Hz, H-3; δ_C 46.2, C-3), one singlet (δ_H 5.98, 1H, s, H-8; δ_C 94.2, C-8), two AB-coupled aromatic hydrogens (δ_H 6.27, 1H, d, J = 8.2 Hz, H-5'; 6.82, 1H, d, J = 8.2 Hz, H-6'; δ_C 107.7, C-5'; 130.1, C-6'), and two olefinic hydrogens (δ_H 6.68, 1H, d, J = 10.0 Hz, H-1'''; 5.67, 1H, d, J = 10.0 Hz, H-2'''; δ_C 116.9, C-1'''; 129.0, C-2'''), all with the same resonance area as the δ_H 12.56 LFR singlet in **1**. The COSY spectrum confirmed the presence of four spin systems (bold bonds in Figure S71, Supporting Information). The HMBC correlations (Figure S73, Supporting Information) from H-5' to C-1' (δ_C 115.6) and C-3' (δ_C 110.1), from H-6' to C-3 (δ_C 46.2), C-2' (δ_C 150.6) and C-4' (δ_C 152.5), from H-1''' to C-4' and C-3''' (δ_C 75.1), from H-2''' to C-3' and C-3''', from H-4''' to C-2''' (δ_C 129.0), C-3''', and C-5''' (δ_C 27.4), and from H-5''' to C-2''' and C-3''' revealed that **1** was closely related to **3**, having the same B-ring and an isoflavonone C-ring. Their difference was the presence vs. lack of a C-6 prenyl substituent in **1** vs. **3**. Elucidation of **1** as the new 6-prenyl-licoisoflavanone was ultimately supported by the molecular formula (C₂₅H₂₆O₆) of **1** assigned via (−)-HRESIMS (Figure S75, Supporting Information) at m/z 421.1654 [$M - H$]⁻ (calcd for C₂₅H₂₅O₆⁻, 421.1657), reflecting an increase of one prenyl group. This was corroborated by concentrating **1** from GU-MF-18 via Sephadex LH-20 gel chromatography and subsequent NMR and MS data analysis of GU-MF-18-1 (Figures S76–83, Supporting Information).

Compound **9** was identified in GU-MF-19. The ¹H NMR data and HMBC spectrum (Figures S84–85, S88, Supporting Information) revealed the presence of one major 5-OH flavonoid (δ_H 13.21, 1H, s, 5-OH; δ_C C-5 156.7; C-6, 111.7; C-10, 104.6), which showed high similarity to those of structural type II-3 (5,7-dihydroxyl-6-prenyl flavones/isoflavones). Comparison of their NMR data indicated that the C-5 was shielded by $\Delta\delta_C$ −2.1 in **9**, suggesting that there is likely an additional 8-prenyl group in **9**. The ¹H NMR data (δ_H 8.38, 1H, s, H-2) with the same peak area as proton resonance 13.21 ppm in **9** revealed that

compound **9** was an isoflavone. Analysis of ^1H NMR data and HSQC spectrum (δ_{H} 7.38, 2H, d, J = 8.2 Hz, H-2',6'; 6.82, 2H, brd, J = 8.2 Hz, H-3',5'; δ_{C} 130.2 and 115.1, C-2',6' and C-3',5') revealed that compound **9** had a 4'-hydroxyl substituted B ring (Figures S84–S85, S87, Supporting Information), which was proved by the COSY correlations (Figure S86, Supporting Information) of H-2'/H-3' and H-5'/H-6' and HMBC correlations (Figure S88, Supporting Information) from H-2' and H-6' to C-4' (δ_{C} 157.4). Considering the (−)-HRESIMS (Figure S90, Supporting Information) at m/z 405.1704 [M − H][−] (calcd for C₂₅H₂₅O₅[−], 405.1707), **9** was determined as 6,8-diprenylgenistein.¹³

Compounds **4** and **7** were identified in GU-MF-20. The ^1H NMR data and 2D HMBC spectrum (Figures S91–S93, S96, Supporting Information) revealed the presence of two major 5-OH flavonoids, two (structural type II-3) 5,7-dihydroxyl-6-prenyl flavones/isoflavones (δ_{H} 13.10, 1H, s, 5-OH; δ_{C} 158.6, C-5; 111.0, C-6; 104.2, C-10; δ_{H} 13.17, 1H, s, 5-OH; δ_{C} 159.0, C-5; 111.2, C-6; 104.1, C-10). Analysis of the ^1H NMR data and HSQC spectrum (Figures S91–S93, S95, Supporting Information) of GU-MF-20 revealed the presence of two singlet proton signals (δ_{H} 8.16, 8.33, each 1H, s, H-2) possessing the same peak area as proton resonances 13.10 in **4** and 13.17 in **7**, respectively, indicating that both of **4** and **7** are isoflavones.

Combined with its ^1H - ^1H COSY spectrum (Figure S94, Supporting Information), two AB coupling system aromatic protons (δ_{H} 6.32, 1H, d, J = 8.3 Hz, H-5' and 6.88, 1H, brd, J = 8.3 Hz, H-6'; δ_{C} 107.4 and 131.2, C-5' and C-6') in B-ring for **4**, and three ABX coupling system aromatic protons (δ_{H} 7.26, 1H, d, J = 2.3 Hz, H-2'; 6.79, 1H, d, J = 8.3 Hz, H-5'; 7.29, 1H, dd, J = 8.3, 2.3 Hz, H-6'; δ_{C} 126.8, C-2'; 115.5, C-5'; 129.6, C-6') in B-ring for **7** were determined. Thus, the 1',2',3',4'-tetrasubstituted B ring in **4** and 1',3',4'-trisubstituted B ring in **7** were determined, which was proved by the HMBC correlations (Figure S96, Supporting Information) from H-5' to C-1' (δ_{C} 111.3) and C-3' (δ_{C} 110.0), and from H-6' to C-2' (δ_{C} 151.1) in **4**; from H-2' to C-6' (δ_{C} 129.6), and from H-6' to C-2' (δ_{C} 126.8) in **7**. There were also double bonds in **4** (δ_{H} 6.67, 1H, d, J = 9.8 Hz, H-1'''; 5.68, 1H, d, J = 9.8 Hz, H-2'''; δ_{C} 116.9 and 128.8, C-1''' and C-2''') and **7** (δ_{H} 6.43, 1H, d, J = 9.8 Hz, H-1'''; 5.78, 1H, d, J = 9.8 Hz, H-2'''; δ_{C} 121.5 and 131.2, C-1''' and C-2'''), respectively, indicating both of **4** and **7** possessed 2,2-dimethylpyran rings with the same pattern as those of **12** and **15**, respectively, which were proved by the HMBC correlations (Figure S96, Supporting Information) from H-1''' to C-3''' (δ_{C} 75.3), from H-2''' to C-3' (δ_{C} 110.0) and C-3'', from H-4''' to C-2''' (δ_{C} 128.8), C-3'', and C-5''' (δ_{C} 27.5), and from H-5''' to C-2'' and C-3'' in **4**; from H-1''' to C-3''' (δ_{C}

76.4), from H-2''' to C-3' (δ_{C} 120.5) and C-3''', from H-4''' to C-2''' (δ_{C} 131.2), C-3''', and C-5''' (δ_{C} 27.6), and from H-5''' to C-2''' and C-3''' in **7**. Considering the (−)-HRESIMS (Figures S98 and S99, Supporting Information) at m/z 419.1476 [M − H][−] (calcd for C₂₅H₂₃O₆[−], 419.1500) and m/z 403.1537 [M − H][−] (calcd for C₂₅H₂₃O₅[−], 403.1551) for **4** and **7**, respectively, their structures were determined as angustone B¹⁴ for **4** and isochandalone¹⁵ for **7**.

SECTION S3. STRUCTURE VERIFICATION OF 5-OH FLAVONOIDs.

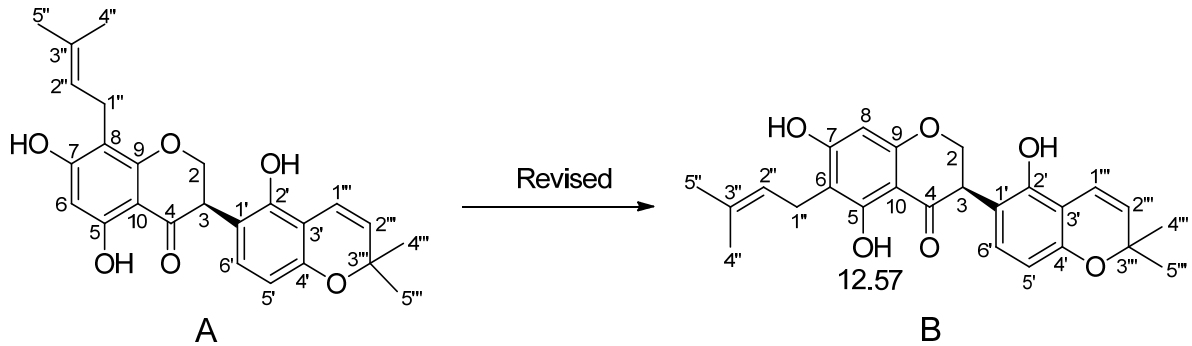


Figure S1. Original structure of licoisoflavanone B reported in the literature (A) vs. its revised structure determined as relicoisoflavanone B (B).

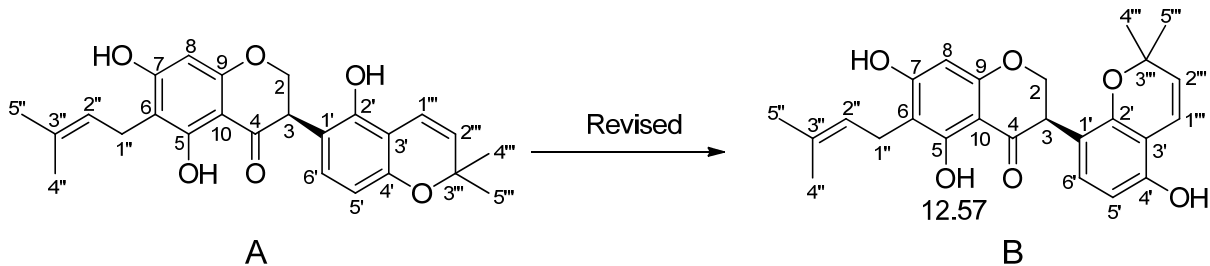


Figure S2. Original structure of licoisoflavanone C reported in the literature (A) vs. its revised structure determined as relicoisoflavanone C (B).

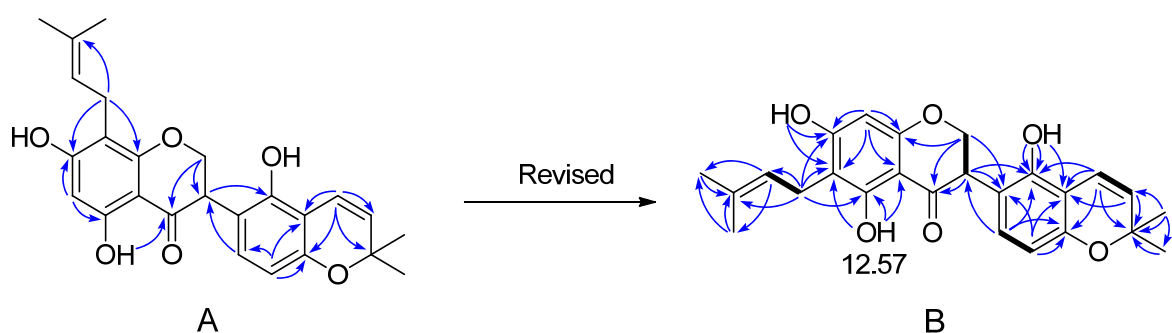


Figure S3. ^1H - ^1H COSY (—) and selected HMBC ($\text{H} \rightarrow \text{C}$) correlations of the original structure of licoisoflavanone B reported in the literature (A) vs. its revised structure determined as relicoisoflavanone B (B).

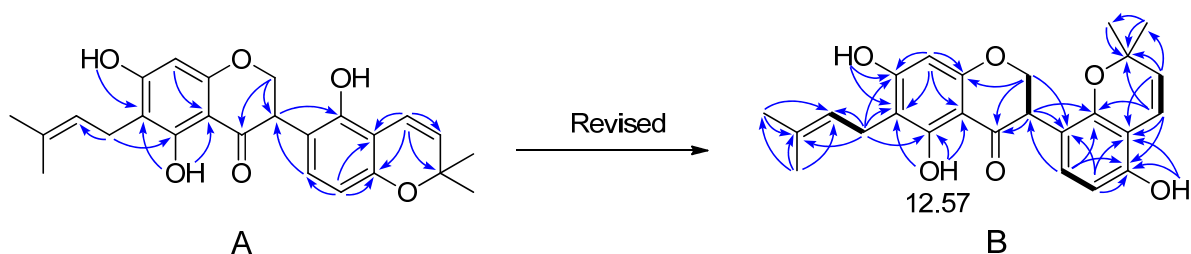


Figure S4. ^1H - ^1H COSY (—) and selected HMBC ($\text{H} \rightarrow \text{C}$) correlations of the original structure of licoisoflavanone C reported in the literature (A) vs. its revised structure determined as relicoisoflavanone C (B).

SECTION S4. STRUCTURE ELUCIDATION AND VERIFICATION RELATED TABLES.

Table S1. Comparison of the ^1H and ^{13}C NMR spectroscopic data of licoisoflavanone B vs. relicoisoflavanone B, compound 1, and licoisoflavanone C vs. relicoisoflavanone C (all in $\text{DMSO}-d_6$).

	licoisoflavanone B ^a		relicoisoflavanone B ^b		1		licoisoflavanone C ^a		relicoisoflavanone C ^b	
	δ_{H}	δ_{C}	δ_{H}	δ_{C}	$\delta_{\text{H}}^{\text{c}}$	$\delta_{\text{C}}^{\text{d}}$	δ_{H}	δ_{C}	δ_{H}	δ_{C}
2	4.36 m 4.46 m	70.2	4.36 m 4.46 m	70.2	4.38 dd (11.0, 5.5) 4.47 t (11.0)	69.7	4.33 m	70.2	4.33 m	70.3
3	4.25 q	46.8	4.25 q	46.8	4.26 dd (11.0, 5.5)	46.2	4.13 q	46.5	4.13 q	46.5
4		197.9		197.9		197.3		197.8		197.8
5		164.4		161.4		161.0		164.2		161.3
6	5.98 s	94.6		108.1		107.6		108.0		108.0
7		161.4		164.4		163.9		161.3		164.2
8		108.1	5.98 s	94.6	5.96 s	94.2	5.97 s	94.4	5.97 s	94.6
9		161.1		161.1		160.5		161.0		161.0
10		102.1		102.1		101.7		102.5		102.5
1'		116.1		116.1		115.6		109.4		113.8
2'		151.2		151.2		150.6		151.1		151.3
3'		110.6		110.6		110.1		113.8		109.4
4'		153.1		153.1		152.5		153.1		153.1
5'	6.26 d (8.4)	108.3	6.26 d (8.4)	108.3	6.27 d (8.4)	107.7	6.32 d (8.0)	108.0	6.32 d (8.0)	108.0
6'	6.81 d (8.4)	130.5	6.81 d (8.4)	130.5	6.82 d (8.4)	130.1	6.78 d (8.0)	130.6	6.78 d (8.0)	130.6
1''	3.12 d (6.8)	21.1	3.12 d (6.8)	21.1	3.11 d (7.0)	20.7	3.11 d (6.8)	21.1	3.11 d (6.8)	21.1
2''	5.13 t (6.4)	123.1	5.13 t (6.4)	123.1	5.13 tt (7.0, 1.2)	122.6	5.12 t (6.4)	123.1	5.12 t (6.4)	123.1
3''		130.7		130.7		130.1		125.8		130.6
4''	1.69 s	18.1	1.69 s	18.1	1.69 s	17.6	1.69 s	25.9	1.61 s	25.9
5''	1.62 s	25.9	1.62 s	25.9	1.61 s	25.4	1.61 s	18.1	1.69 s	18.1
1'''	6.67 d (10.0)	117.4	6.67 d (10.0)	117.4	6.67 d (10.0)	116.9	6.54 d (10.0)	117.2	6.54 d (10.0)	117.2
2'''	5.66 d (10.0)	129.5	5.66 d (10.0)	129.5	5.68 d (10.0)	129.0	5.59 d (10.0)	128.8	5.59 d (10.0)	128.8
3'''		75.5		75.5		75.1		76.3		76.3
4'''	1.34 s	27.8	1.34 s	27.8	1.34 s	27.4	1.23 s	27.5	1.23 s	27.5
5'''	1.34 s	27.8	1.34 s	27.8	1.34 s	27.4	1.23 s	27.9	1.23 s	27.9
OH	12.57 s		12.57 s		12.56 s		12.57 s		12.57 s	
OH	10.74 s		10.74 s				10.73 s		10.73 s	
OH	9.17 s		9.17 s				9.64 s		9.64 s	

^a Data were measured in 400 MHz for ^1H and 100 MHz for ^{13}C .

^b Relicoisoflavanone B is the revised structure of licoisoflavanone B; relicoisoflavanone C is the revised structure of licoisoflavanone C.

^c The resonance data were obtained from the ^1H NMR spectrum of GU-MF-18-1 using the residual solvent signals ($\delta_{\text{H}} 2.50$) as a reference.

^d The resonance data were extracted from the HSQC and HMBC spectra of GU-MF-18-1, and chemical shifts were referenced to the solvent peaks ($\delta_{\text{C}} 39.51$).

Table S2. The HMBC patterns of licoisoflavanone B vs. relicoisoflavanone B, compound 1, and licoisoflavanone C vs. relicoisoflavanone C (all in DMSO-*d*₆).

Compound Name	Structural Type	MHz (¹ H)	Chemical shift (ppm)			
			5-OH	C-5	C-6	C-10
licoisoflavanone B*	Type I-1	400	12.57	164.4	94.6	102.1
relicoisoflavanone B*	Type I-3	400	12.57	161.4	108.1	102.1
1	Type I-3	600	12.56	161.0	107.6	101.7
licoisoflavanone C*	Type I-3	400	12.57	164.2	108.0	102.5
relicoisoflavanone C*	Type I-3	400	12.57	161.3	108.0	102.5

*Chemical shifts were referenced to 40.00 ppm of DMSO-*d*₆ as reported in reference 26.

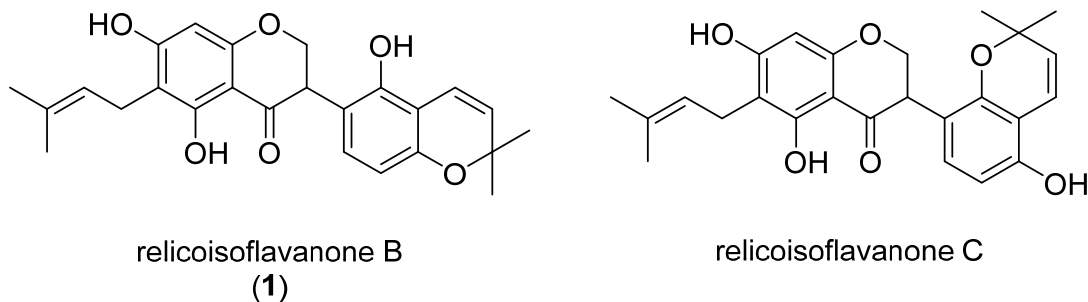


Table S3. The HMBC patterns mined from literature data of compounds isolated from licorice species (GU, GG, and GI).

No.	Name Given in the Literature	Structural Type	Solvent	MHz (¹ H)	5-OH/ 2'-OH	C-5/ C-2'	C-6/ C-3'	C-10/ C-1'	Plant source(s)	References Isolation	NMR data
1	sophoraflavanone B	Type I-1	DMSO-d ₆	400, 600	12.08	161.1	95.2	101.7	GU,GI	16,17	18
2	pinocembrin	Type I-2	DMSO-d ₆	500	12.10	163.5	95.9	101.8	GU,GG	19,20	21
3	sigmoidin B	Type I-2	DMSO-d ₆	300	12.12	163.5	95.7	101.8	GU	22	23
4	naringenin	Type I-2	DMSO-d ₆	200	12.20	163.8	95.3	101.7	GU,GG,GI	24, 25, 26	27
5	licoflavanone	Type I-2	DMSO-d ₆	300	12.21	163.5	95.9	101.7	GU,GG	28, 29	30
6	licoisoflavanone	Type I-2	DMSO-d ₆	400	12.29	163.9	96.0	102.0	GU,GG	31, 32	10
7	6-prenylnaringenin	Type I-3	DMSO-d ₆	400, 600	12.41	160.5	107.5	101.6	GU,GG,GI	28, 33, 17	18
8	2'-hydroxyisolupalbigenin	Type II-1	DMSO-d ₆	400	12.79	159.3	98.4	104.6	GU,GI	10, 26	10
9	licoflavone C	Type II-1	DMSO-d ₆	400	12.90	159.5	98.8	104.2	GU,GG,GI	34, 35, 36	26
9	licoflavone C	Type II-1	Acetone-d ₆	400	13.00	161.0	99.3	107.4	GU,GG,GI	34, 35, 36	36
10	lupiwighteone	Type II-1	DMSO-d ₆	400	12.90	159.6	98.8	104.0	GU,GG,GI	22, 25, 37	10
11	isolupalbigenin	Type II-1	DMSO-d ₆	400	12.90	159.6	98.8	104.0	GU	10	10
12	2,3-dehydrokievitone	Type II-1	DMSO-d ₆	400	12.92	159.9	98.8	104.9	GG,GI	38, 26	26
13	licoisoflavone C	Type II-1	DMSO-d ₆	400	12.93	159.9	98.8	104.8	GI	26	26
14	gancaonin L	Type II-1	DMSO-d ₆	400	12.94	159.6	98.4	104.4	GU,GG	39, 40	10
15	licoisoflavone B	Type II-2	DMSO-d ₆	400	12.85	161.8	98.9	104.6	GU,GG,GI	41, 42, 26	10
16	licoisoflavone A	Type II-2	DMSO-d ₆	400	12.86	161.8	98.9	104.6	GU,GG,GI	41, 35, 26	10
17	abiochanin A	Type II-2	DMSO-d ₆	400	12.91	161.9	99.3	104.0	GU	10	10
18	isoderrone	Type II-2	DMSO-d ₆	400	12.91	162.0	99.0	104.4	GU,GI	10, 43	10
19	semilicoisoflavone B	Type II-2	DMSO-d ₆	400	12.94	162.4	99.4	104.8	GU,GG,GI	44, 35, 26	26
20	apigenin	Type II-2	DMSO-d ₆	400	12.95	161.6	99.2	103.5	GU	45	46
21	genistein	Type II-2	DMSO-d ₆	400	12.95	162.0	99.0	104.5	GU,GG,GI	10, 33, 26	10
22	3'-isoprenylgenistein	Type II-2	DMSO-d ₆	400	12.95	162.4	99.3	104.9	GU	24	24
23	chrysoeriol	Type II-2	DMSO-d ₆	400	12.96	161.5	98.9	103.7	GU	47	48
24	pratensein	Type II-2	DMSO-d ₆	400	12.96	162.0	99.0	104.5	GU	10	10
25	luteolin	Type II-2	DMSO-d ₆	400	12.97	161.5	98.9	103.8	GG	49	50
26	epimedokoreanin D	Type II-2	DMSO-d ₆	400	12.98	161.5	98.8	103.7	GU	51	52
27	allolicoisoflavone B	Type II-2	DMSO-d ₆	400	12.98	161.9	99.2	103.9	GU,GI	53, 26	10
28	glycyrrhisoflavone	Type II-2	DMSO-d ₆	400	13.00	162.5	99.4	104.9	GU,GI	45, 26	26
28	glycyrrhisoflavone	Type II-2	Acetone-d ₆	90, 300, 500	13.06	163.9	99.8	106.2	GU,GI	45, 26	74
29	angustone B	Type II-3	DMSO-d ₆	80	13.07	158.8	111.3	104.6	GG,GI	42, 41	14
30	angustone A	Type II-3	DMSO-d ₆	400	13.11	158.6	111.0	104.4	GU,GI	10, 26	10

31	gancaonin A	Type II-3	DMSO- <i>d</i> ₆	400	13.15	159.0	111.3	104.5	GU	22	22
32	gancaonin B	Type II-3	DMSO- <i>d</i> ₆	400	13.17	158.9	111.3	104.4	GU	22	22
33	gancaonin O	Type II-3	DMSO- <i>d</i> ₆	300	13.20	158.3	110.8	103.5	GU	39	54
34	gancaonin H	Type II-3	DMSO- <i>d</i> ₆	400	13.22	158.9	111.2	104.3	GU,GI	24, 41	12
35	wighteone	Type II-3	DMSO- <i>d</i> ₆	400	13.23	158.8	111.0	104.2	GU,GG,GI	55, 33, 26	10
36	6-C-prenylorobol	Type II-3	DMSO- <i>d</i> ₆	400	13.26	158.8	111.0	104.2	GU	10	10
37	2',4'-dihydroxy-chalcone	Type III-1	DMSO- <i>d</i> ₆	500	13.40	165.8	102.6	113.0	None	None	56
37	2',4'-dihydroxy-chalcone	Type III-1	CDCl ₃	400/500/	13.33	166.9	103.9	114.8	None	None	
				600							75
38	isoliquiritigenin	Type III-1	DMSO- <i>d</i> ₆	400	13.58	165.8	102.6	113.0	GU,GG,GI	10, 57, 58	10
39	licoagrochalcone A	Type III-1	DMSO- <i>d</i> ₆	400	13.60	166.2	103.1	113.5	GG,GI	59, 58	26
39	licoagrochalcone A	Type III-1	Acetone- <i>d</i> ₆	400	13.66	167.6	103.8	114.5	GG,GI	59, 58	61
40	homobutein	Type III-1	DMSO- <i>d</i> ₆	400	13.63	165.8	102.5	113.0	GU	10	10
41	isobavachalcone	Type III-2	DMSO- <i>d</i> ₆	400	14.02	164.0	114.9	113.2	GU,GG,GI	60, 61, 26	62
41	isobavachalcone	Type III-2	MeOH- <i>d</i> ₄	200		165.0	116.6	114.5	GU,GG,GI	60, 61, 26	76
42	glabranin	Type I-1	CDCl ₃	400	12.12	162.3	96.9	103.3	GU,GG,GI	63, 20, 17	77
43	8-prenyleriodictyol	Type I-1	Acetone- <i>d</i> ₆	400/500	12.14	163.0	96.3	103.3	GU,GI	64, 17	78
44	gancaonin E	Type I-1	Acetone- <i>d</i> ₆	400	12.14	163.0	96.4	103.4	GU	22	22
45	euchestraflavanone A	Type I-1	DMSO- <i>d</i> ₆	n/a	None	None	None	None	GI	26	None
46	3'-(γ,γ -dimethylallyl)-kievitone	Type I-1	DMSO- <i>d</i> ₆	None	None	None	None	None	GU	65	None
47	dihydrolicoisoflavone	Type I-2	Acetone- <i>d</i> ₆	300		165.4	96.6	102.8	GU	44	79
48	(2S)-3'-(2-hydroxy-3-methylbut-3-enyl)-4',5,7-trihydroxy-dihydroflavanone	Type I-2	DMSO- <i>d</i> ₆	None	None	None	None	None	GU	28	
49	glyasperin F	Type I-2	MeOH- <i>d</i> ₄	500		165.7	97.2	103.6	GU	44	80
50	isoglabranin	Type I-3	CDCl ₃	400	12.36	161.2	107.0	102.9	GG,GI	25, 17	81
51	6-prenyleriodictyol	Type I-3	DMSO- <i>d</i> ₆	None	None	None	None	None	GU,GI	66, 17	None
52	paratocarpin L	Type I-3	DMSO- <i>d</i> ₆	None	None	None	None	None	GI	41	None
53	glisoflavanone	Type I-3	Acetone- <i>d</i> ₆	500	12.31	162.7	109.2	102.6	GU,GI	53, 26	53
54	gancaonin M	Type II-1	Acetone- <i>d</i> ₆	400	12.95	161.5	99.5	106.3	GU	39	39
55	vogelin C	Type II-1	DMSO- <i>d</i> ₆	None	None	None	None	None	GU	55	None
56	glyurallin B	Type II-1	DMSO- <i>d</i> ₆	None	None	None	None	None	GU,GI	31, 41	None
57	orobol	Type II-2	DMSO- <i>d</i> ₆	None	None	None	None	None	GU	24	None
58	allolicoisoflavone A	Type II-2	DMSO- <i>d</i> ₆	None	None	None	None	None	GU	44	None
59	gancaonin Q	Type II-3	Acetone- <i>d</i> ₆	400	13.31	160.2	112.3	105.2	GU,GI	67, 26	67
60	6,5'-diprenylluteolin	Type II-3	Acetone- <i>d</i> ₆	500	13.31	160.2	112.3	105.3	GU	47	47
61	luteone	Type II-3	DMSO- <i>d</i> ₆	None	None	None	None	None	GU	10	None
62	gancaonin N	Type II-3	Acetone- <i>d</i> ₆	400	13.03	160.4	112.3	105.9	GU	39	39

63	isoangustone A	Type II-3	DMSO- <i>d</i> ₆	None	None	None	None	GU	65	None
64	isochandalone	Type II-3	DMSO- <i>d</i> ₆	None	None	None	None	GI	26	None
65	5-prenylbutein	Type III-1	Acetone- <i>d</i> ₆	500	13.68	167.4	103.6	GI	58	82
66	kanzonol B	Type III-1	DMSO- <i>d</i> ₆	None	None	None	None	GG,GI	59, 26	None
67	licochalcone G	Type III-1	DMSO- <i>d</i> ₆	None	None	None	None	GI	58	None
68	isoliquiritin	Type III-1	DMSO- <i>d</i> ₆	None	None	None	None	GU,GG	68, 69	None
69	isoliquiritin apioside	Type III-1	DMSO- <i>d</i> ₆	None	None	None	None	GU,GG,GI	68, 69, 70	None
70	6"- <i>O</i> -acetylisoliquiritin	Type III-1	DMSO- <i>d</i> ₆	None	None	None	None	GU	71	None
71	1-(2,4-dihydroxyphenyl)-3-[4-methoxy-3-(3-methylbut-2-enyl)-phenyl]prop-2-en-1-one	Type III-1	DMSO- <i>d</i> ₆	None	None	None	None	GU	60	None
72	morachalcone A	Type III-2	Acetone- <i>d</i> ₆	300		164.5	115.9	GG	40	83
73	corylifol B	Type III-2	DMSO- <i>d</i> ₆	None	None	None	None	GI	41	None
74	kanzonol C	Type III-2	Acetone- <i>d</i> ₆	400	14.02			GG,GI	72,	84,
			CDCl ₃	400	13.88				58	72
75	2,3',4,4'-tetrahydroxy-3,5'-diprenylchalcone	Type III-2	DMSO- <i>d</i> ₆	None	None	None	None	GG	40	None
76	6",6"-dimethylpyrano[2",3":4,5]-3'- γ,γ -dimethylallyl-2',3,4'-trihydroxychalcone	Type III-2	DMSO- <i>d</i> ₆	None	None	None	None	GG	38	None

Table S4. The metabolomic HMBC patterns from experimental data of GU/GG/GI MeOH fractions (all in DMSO-*d*6).^a

Structural Type	MHz (¹ H)	5-/2'-OH	C-5 ^b /C-2 ^b	C-6 ^b /C-3 ^b	C-10 ^b /C-1 ^b	Plant/Fraction Source
Type I-1	600	12.11	160.8	95.4	101.7	GI-MF
Type I-1	600	12.27	161.5	95.5	102.1	GU-MF
Type I-2	600	12.12	163.6	95.9	101.8	GI-MF
Type I-2	600	12.13	163.6	95.9	101.8	GI-MF
Type I-2	600	12.14	163.6	95.9	101.9	GU-MF
Type I-2	600	12.14	163.6	95.9	101.8	GI-MF
Type I-2	600	12.15	163.6	95.9	101.8	GI-MF
Type I-2	600	12.15	163.7	95.9	101.9	GG-MF
Type I-2	600	12.15	163.6	95.9	101.9	GU-MF
Type I-2	600	12.15	163.6	95.9	101.8	GI-MF
Type I-2	600	12.16	163.8	95.9	101.9	GG-MF
Type I-2	600	12.29	163.9	95.9	102.1	GU-MF
Type I-2	600	12.31	163.9	95.9	102.2	GU-MF
Type I-2	600	12.32	163.9	95.9	102.2	GU-MF
Type I-3	600	12.41	160.7	107.5	101.6	GU-MF
Type I-3	600	12.42	160.5	107.6	101.5	GU-MF
Type I-3	600	12.57	161.0	107.7	102.0	GU-MF
Type I-3	600	12.59	161.0	107.6	102.1	GU-MF
Type II-1	600	12.80	159.4	98.4	104.5	GU-MF
Type II-1	600	12.90	159.1	98.4	103.7	GI-MF
Type II-1	600	12.91	159.5	98.5	104.5	GU-MF
Type II-1	600	12.91	159.1	98.4	103.7	GI-MF
Type II-1	600	12.92	159.6	98.6	104.6	GU-MF
Type II-2	600	12.86	161.9	99.0	104.7	GU-MF
Type II-2	600	12.92	162.0	99.1	104.5	GU-MF
Type II-2	600	12.96	162.1	99.1	104.5	GU-MF
Type II-2	600	12.96	162.0	99.0	104.4	GU-MF
Type II-2	600	12.97	161.4	98.9	103.6	GI-MF
Type II-2	600	12.97	162.0	99.0	104.4	GU-MF
Type II-2	600	12.97	161.4	98.9	103.6	GI-MF
Type II-2	600	12.98	161.4	99.0	103.5	GI-MF
Type II-2	600	13.01	162.0	99.0	104.5	GU-MF
Type II-3	600	13.12	158.8	111.0	104.5	GU-MF
Type II-3	600	13.12	158.8	111.0	104.5	GU-MF
Type II-3	600	13.22	158.8	111.1	104.4	GU-MF
Type II-3	600	13.22	158.3	111.1	103.6	GI-MF
Type II-3	600	13.22	158.8	111.1	104.4	GU-MF
Type II-3	600	13.23	158.8	111.1	104.3	GU-MF
Type II-3	600	13.24	158.8	111.1	104.3	GU-MF
Type II-3	600	13.25	158.8	111.1	104.3	GU-MF
Type II-3	600	13.28	158.8	111.0	104.3	GU-MF
Type III-1	600	13.54	165.8	102.6	113.0	GU-MF
Type III-1	600	13.54	165.8	102.6	113.0	GI-MF
Type III-1	600	13.54	165.8	102.6	113.0	GG-MF
Type III-1	600	13.62	165.8	102.6	113.0	GU-MF
Type III-1	600	13.62	165.8	102.6	113.0	GG-MF
Type III-1	600	13.62	165.8	102.6	113.0	GI-MF
Type III-1	600	13.64	165.8	102.6	112.9	GI-MF
Type III-2	600	13.96	163.7	115.0	112.4	GG-MF
Type III-2	600	14.01	163.6	114.9	112.3	GG-MF
Type III-2	600	14.02	163.7	114.9	112.3	GG-MF
Type III-2	600	14.04	163.7	115.0	112.3	GG-MF

^a Chemical shifts (ppm) were referenced to the solvent peaks (δ_{H} 2.50 and δ_{C} 39.51).

^b The resonance data were extracted from the HMBC spectrum.

Table S5. The HMBC patterns of 15 compounds identified in GU-MF-11, GU-MF-12, and GU-MF-14–20 (all in DMSO-*d*₆).

No.	Name Given in the Literature	Structural Type	MHz (¹ H)	Chemical Shift ^a				Fraction Source
				5-OH	C-5 ^b	C-6 ^b	C-10 ^b	
2	3'-(γ , γ -dimethylallyl)-kievitone	Type I-1	500	12.27	161.4	95.4	102.0	GU-MF-15
3	licoisoflavanone	Type I-2	500	12.28	163.9	96.0	102.1	GU-MF-11
1	6-prenyl-licoisoflavanone	Type I-3	500	12.56	161.0	107.6	101.7	GU-MF-18
10	lupiwigteone	Type II-1	500	12.90	159.6	98.5	104.5	GU-MF-12
11	licoisoflavone A	Type II-2	500	12.84	162.0	98.9	104.7	GU-MF-11
12	licoisoflavone B	Type II-2	500	12.85	161.8	98.9	104.6	GU-MF-14
15	isoderrone	Type II-2	500	12.91	161.9	99.1	104.3	GU-MF-15
14	semilicoisoflavone B	Type II-2	500	12.94	162.0	99.1	104.5	GU-MF-11
13	glycyrrhisoflavone	Type II-2	500	12.99	162.0	99.0	104.6	GU-MF-11
4	angustone B	Type II-3	500	13.10	158.6	111.0	104.2	GU-MF-20
7	isochandalone	Type II-3	500	13.17	159.0	111.2	104.1	GU-MF-20
6	gancaonin H	Type II-3	500	13.21	158.9	111.2	104.2	GU-MF-17
8	wigteone	Type II-3	500	13.22	158.8	111.1	104.5	GU-MF-12
5	isoangustone A	Type II-3	500	13.26	158.8	111.1	104.1	GU-MF-16
9	6,8-diprenylgenistein	none	500	13.21	156.7	111.7	104.6	GU-MF-19

^a Chemical shifts (ppm) were referenced to the solvent peaks (δ _H 2.50 and δ _C 39.51).

^b The resonance data were extracted from the HMBC spectrum.

SECTION S5. REFERENCES RELATED TO STRUCTURE ELUCIDATION AND VERIFICATION

- (1) Nam, J. W.; Phansalkar, R. S.; Larkin, D. C.; Bisson, J.; McAlpine, J. B.; Leme, A. A.; Vidal, C. M. P.; Ramirez, B.; Niemitz, M.; Bedran-Russo, A.; Chen, S. N.; Pauli, G. F. *J. Org. Chem.* **2015**, *80*, 7495–7507.
- (2) Gao, W.; Napolitano, J. G.; Larkin, D. C.; Kim, J. Y.; Jin, Y. Y.; Lee, H.; Suh, J. W.; Chen, S. N.; Pauli, G. F. *Magn. Reson. Chem.* **2017**, *55*, 239–244.
- (3) Napolitano, J. G.; Simmler, C.; McAlpine, J. B.; Larkin, D. C.; Chen, S. N.; Pauli, G. F. *J. Nat. Prod.* **2015**, *78*, 658–665.
- (4) Napolitano, J. G.; Larkin, D. C.; McAlpine, J. B.; Niemitz, M.; Korhonen, S. P.; Chen, S.-N.; Pauli, G. F. *J. Org. Chem.* **2013**, *78*, 9963–9968.
- (5) Napolitano, J. G.; Larkin, D. C.; Graf, T. N.; Friesen, J. B.; Chen, S. N.; McAlpine, J. B.; Oberlies, N. H.; Pauli, G. F. *J. Org. Chem.* **2013**, *78*, 2827–2839.
- (6) Napolitano, J. G.; Larkin, D. C.; Chen, S. N.; Pauli, G. F. *Magn. Reson. Chem.* **2012**, *50*, 569–575.
- (7) Napolitano, J. G.; Gödecke, T.; Rodríguez-Brasco, M. F.; Jaki, B. U.; Chen, S. N.; Larkin, D. C.; Pauli, G. F. *J. Nat. Prod.* **2012**, *75*, 238–248.
- (8) Qiu, F.; Imai, A.; McAlpine, J. B.; Larkin, D. C.; Burton, I.; Karakach, T.; Farnsworth, N. R.; Chen, S. N.; Pauli, G. F. *J. Nat. Prod.* **2012**, *75*, 432–443.
- (9) Dong, S. H.; Nikolić, D.; Simmler, C.; Qiu, F.; van Breemen, R. B.; Soejarto, D. D.; Pauli, G. F.; Chen, S. N. *J. Nat. Prod.* **2012**, *75*, 2168–2177.
- (10) Ji, S.; Li, Z. W.; Song, W.; Wang, Y. R.; Liang, W. F.; Li, K.; Tang, S. N.; Wang, Q.; Qiao, X.; Zhou, D. M.; Yu, S. W.; Ye, M. *J. Nat. Prod.* **2016**, *79*, 281–292.
- (11) Bojase, G.; Wanjala, C. C. W.; Majinda, R. R. T. *Phytochemistry* **2001**, *56*, 837–841.
- (12) Fukai, T.; Wang, Q. H.; Kitagawa, T.; Kusano, K.; Nomura, T.; Litaka, Y. *Heterocycles* **1989**, *29*, 1761–1772.
- (13) Sekine, T.; Inagaki, M.; Ikegami, F.; Fujii, Y.; Ruangrungsi, N. *Phytochemistry* **1999**, *52*, 87–94.
- (14) Lane, G. A.; Newman, R. H. *Phytochemistry* **1987**, *26*, 295–300.
- (15) Tahara, S.; Orihara, S.; Ingham, J. L.; Mizutani, J. *Phytochemistry* **1989**, *28*, 901–911.
- (16) Hayashi, H.; Zhang, S. L.; Nakaizumi, T.; Shimura, K.; Yamaguchi, M.; Inoue, K.; Sarsenbaev, K.; Ito, M.; Honda, G. *Chem. Pharm. Bull.* **2003**, *51*, 1147–1152.
- (17) Zhou, B.; Wan, C. X. *J. Asian Nat. Prod. Res.* **2015**, *17*, 256–261.
- (18) Stevens, J. F.; Ivancic, M.; Hsu, V. L.; Deinzer, M. L. *Phytochemistry* **1997**, *44*, 1575–1585.
- (19) Zhu, X. M.; Di, Y. T.; Peng, S. L.; Wang, M. K.; Ding, L. S. *Chin. Tradit. Herb. Drugs* **2003**, *34*, 198–201.
- (20) Biondi, D. M.; Rocco, C.; Ruberto, G. *J. Nat. Prod.* **2003**, *66*, 477–480.
- (21) An, N.; Yang, S. L.; Zou, Z. M.; Xu, L. Z. *Chin. Tradit. Herb. Drugs* **2006**, *37*, 663–664.
- (22) Fukai, T.; Wang, Q. H.; Nomura, T. *Heterocycles* **1989**, *29*, 1369–1378.
- (23) Ndom, J. C.; Mbafor, J. T.; Fomum, Z. T.; Martin, M. T.; Bodo, B. *Magn. Reson. Chem.* **1993**, *31*, 210–211.
- (24) Wang, Q.; Miao, W. J.; Xiang, C.; Guo, D. A.; Ye, M. *Chin. Tradit. Herb. Drugs* **2014**, *45*, 31–36.
- (25) Biondi, D. M.; Rocco, C.; Ruberto, G. *J. Nat. Prod.* **2005**, *68*, 1099–1102.
- (26) Lin, Y.; Kuang, Y.; Li, K.; Wang, S.; Ji, S.; Chen, K.; Song, W.; Qiao, X.; Ye, M. *Bioorg. Med. Chem.* **2017**, *25*, 5522–5530.
- (27) Jeon, S. H.; Chun, W.; Choi, Y. J.; Kwon, Y. S. *Arch. Pharm. Res.* **2008**, *31*, 978–982.

- (28) Zhou, B.; Wan, C. X. *Chin. Tradit. Herb. Drugs* **2016**, *47*, 21–25.
- (29) Fukui, H.; Goto, K.; Tabata, M. *Chem. Pharm. Bull.* **1988**, *36*, 4174–4176.
- (30) Nkengfack, A. E.; Sanson, D. R.; Tempesta, M. S.; Fomum, Z. T. *J. Nat. Prod.* **1989**, *52*, 320–324.
- (31) Shibano, M.; Henmi, A.; Matsumoto, Y.; Kusano, G.; Miyase, T.; Hatakeyama, Y. *Heterocycles* **1997**, *45*, 2053–2060.
- (32) Montoro, P.; Maldini, M.; Russo, M.; Postorino, S.; Piacente, S.; Pizza, C. *J. Pharm. Biomed. Anal.* **2011**, *54*, 535–544.
- (33) Hayashi, H.; Yasuma, M.; Hiraoka, N.; Ikeshiro, Y.; Yamamoto, H.; Yesilada, E.; Sezik, E.; Honda, G.; Tabata, M. *Phytochemistry* **1996**, *42*, 701–704.
- (34) Guo, Z. H.; Niu, X. L.; Xiao, T.; Lu, J. J.; Li, W.; Zhao, Y. Q. *J. Funct. Foods* **2015**, *14*, 324–336.
- (35) Fang, S. Q.; Leng, K.; Duan, J. A.; Li, C. Y.; Wei, J. H.; Zheng, Y. F.; Peng, G. P. *Chin. Tradit. Pat. Med.* **2015**, *37*, 2443–2448.
- (36) Kajiyama, K.; Demizu, S.; Hiraga, Y.; Kinoshita, K.; Koyama, K.; Takahashi, K.; Tamura, Y.; Okada, K.; Kinoshita, T. *J. Nat. Prod.* **1992**, *55*, 1197–1203.
- (37) Lin, Y.; Kuang, Y.; Li, K.; Wang, S.; Song, W.; Qiao, X.; Sabir, G.; Ye, M. *Bioorg. Med. Chem.* **2017**, *25*, 3706–3713.
- (38) Li, K.; Ji, S.; Song, W.; Kuang, Y.; Lin, Y.; Tang, S. N.; Cui, Z. X.; Qiao, X.; Yu, S. W.; Ye, M. *J. Nat. Prod.* **2017**, *80*, 334–346.
- (39) Fukai, T.; Wang, Q. H.; Takayama, M.; Nomura, T. *Heterocycles* **1990**, *31*, 373–382.
- (40) Kuroda, M.; Mimaki, Y.; Honda, S.; Tanaka, H.; Yokota, S.; Mae, T. *Bioorg. Med. Chem.* **2010**, *18*, 962–970.
- (41) Song, W.; Qiao, X.; Chen, K.; Wang, Y.; Ji, S.; Feng, J.; Li, K.; Lin, Y.; Ye, M. *Anal. Chem.* **2017**, *89*, 3146–3153.
- (42) Li, Y. J.; Chen, J.; Li, Y.; Li, Q.; Zheng, Y. F.; Fu, Y.; Li, P. *J. Chromatogr. A* **2011**, *1218*, 8181–8191.
- (43) Fukai, T.; Nomura, T. *Phytochemistry* **1995**, *38*, 759–765.
- (44) Gafner, S.; Bergeron, C.; Villinski, J. R.; Godejohann, M.; Kessler, P.; Cardellina, J. H.; Ferreira, D.; Feghali, K.; Grenier, D. *J. Nat. Prod.* **2011**, *74*, 2514–2519.
- (45) Li, S. P.; Li, W.; Wang, Y. H.; Asada, Y.; Koike, K. *Bioorg. Med. Chem. Lett.* **2010**, *20*, 5398–5401.
- (46) Li, W.; Dai, R. J.; Yu, Y. H.; Li, L.; Wu, C. M.; Luan, W. W.; Meng, W. W.; Zhang, X. S.; Deng, Y. L. *Biol. Pharm. Bull.* **2007**, *30*, 1123–1129.
- (47) Bai, H.; Li, W.; Koike, K.; Pei, Y. P.; Dou, D. Q.; Chen, Y. J.; Wang, Y. H.; Nikaido, T. *Heterocycles* **2004**, *63*, 2091–2095.
- (48) Park, Y.; Moon, B. H.; Yang, H.; Lee, Y.; Lee, E.; Lim, Y. *Magn. Reson. Chem.* **2007**, *45*, 1072–1075.
- (49) Khalaf, I.; Vlase, L.; Lazar, D.; Corcova, A.; Ivanescu, B.; Lazar, M. I. *Farmacia* **2010**, *58*, 416–421.
- (50) Park, Y.; Moon, B. H.; Lee, E.; Lee, Y.; Yoon, Y.; Ahn, J. H.; Lim, Y. *Magn. Reson. Chem.* **2007**, *45*, 674–679.
- (51) Fang, S. Q.; Qu, Q. Y.; Zheng, Y. F.; Zhong, H. H.; Shan, C. X.; Wang, F.; Li, C. Y.; Peng, G. *P. J. Sep. Sci.* **2016**, *39*, 2068–2078.
- (52) Li, W. K.; Pan, J. Q.; Lü, M. J.; Zhang, R. Y.; Liao M. C.; Xiao, P. G. *Acta Pharmaceutica Sinica* **1996**, *31*, 29–32.

- (53) Hatano, T.; Aga, Y.; Shintani, Y.; Ito, H.; Okuda, T.; Yoshida, T. *Phytochemistry* **2000**, *55*, 959–963.
- (54) Dias, A. C. P.; Tomás-Barberán, F. A.; Fernandes-Ferreira, M.; Ferreres, F. *Phytochemistry* **1998**, *48*, 1165–1168.
- (55) Luo, L. P.; Shen, L. M.; Sun, F.; Ma, Z. J. *Food Chem.* **2013**, *138*, 315–320.
- (56) Zhang, Y. L.; Mei, R. Q.; Liu, X.; Liu, G. M.; Wu, B. *Chin. Tradit. Herb. Drugs* **2014**, *45*, 2293–2298.
- (57) Chin, Y. W.; Jung, H. A.; Liu, Y.; Su, B. N.; Castoro, J. A.; Keller, W. J.; Pereira, M. A.; Kinghorn, A. D. *J. Agric. Food Chem.* **2007**, *55*, 4691–4697.
- (58) Dao, T. T.; Nguyen, P. H.; Lee, H. S.; Kim, E.; Park, J.; Lim, S. I.; Oh, W. K. *Bioorg. Med. Chem. Lett.* **2011**, *21*, 294–298.
- (59) Asada, Y.; Li, W.; Yoshikawa, T. *Phytochemistry* **1998**, *47*, 389–392.
- (60) Feng, K. P.; Chen, R. D.; Li, J. H.; Tao, X. Y.; Liu, J. M.; Zhang, M.; Dai, J. G. *J. Asian Nat. Prod. Res.* **2016**, *18*, 253–259.
- (61) Asada, Y.; Li, W.; Yoshikawa, T. *Phytochemistry* **1998**, *47*, 389–392.
- (62) Wang, H. M.; Yan, Z. H.; Lei, Y. N.; Sheng, K.; Yao, Q. W.; Lu, K.; Yu, P. *Tetrahedron Lett.* **2014**, *55*, 897–899.
- (63) Yuldashev, M. P. *Chem. Nat. Compd.* **1998**, *34*, 508–509.
- (64) Jia, S. S.; Liu, D.; Wang, H. Q.; Suo, Z. X. *Acta Pharmaceutica Sinica* **1993**, *28*, 623–625.
- (65) Eerdunbayaer; Orabi, M. A. A.; Aoyama, H.; Kuroda, T.; Hatano, T. *Molecules* **2014**, *19*, 13027–13041.
- (66) Ye, R. G.; Fan, Y. H.; Ma, C. M. *J. Agric. Food Chem.* **2017**, *65*, 510–515.
- (67) Fukai, T.; Wang, Q. H.; Nomura, T. *Phytochemistry* **1991**, *30*, 1245–1250.
- (68) Kitagawa, I.; Hori, K.; Uchida, E.; Chen, W. Z.; Yoshikawa, M.; Ren, J. L. *Chem. Pharm. Bull.* **1993**, *41*, 1567–1572.
- (69) Kitagawa, I.; Chen, W. Z.; Hori, K.; Harada, E.; Yasuda, N.; Yoshikawa, M.; Ren, J. L. *Chem. Pharm. Bull.* **1994**, *42*, 1056–1062.
- (70) Li, G. N.; Simmler, C.; Chen, L. Y.; Nikolic, D.; Chen, S. N.; Pauli, G. F.; van Breemen, R. B. *Eur. J. Pharm. Sci.* **2017**, *109*, 182–190.
- (71) Lee, J. E.; Lee, J. Y.; Kim, J.; Lee, K.; Choi, S. U.; Ryu, S. Y. *Arch. Pharm. Res.* **2015**, *38*, 1299–1303.
- (72) Kinoshita, T.; Kajiyama, K.; Hiraga, Y.; Takahashi, K.; Tamura, Y.; Mizutani, K. *Chem. Pharm. Bull.* **1996**, *44*, 1218–1221.
- (73) Shirataki, Y.; Noguchi, M.; Yokoe, I.; Tomimori, T.; Komatsu, M. *Chem. Pharm. Bull.* **1991**, *39*, 1568–1572.
- (74) Hatano, T.; Kagawa, H.; Yasuhara, T.; Okuda, T. *Chem. Pharm. Bull.* **1988**, *36*, 2090–2097.
- (75) Zhang, X. J.; Li, L. Y.; Wang, S. S.; Que, S.; Yang, W. Z.; Zhang, F. Y.; Gong, N. B.; Cheng, W.; Liang, H.; Ye, M.; Jia, Y. X.; Zhang, Q. Y. *Tetrahedron* **2013**, *69*, 11074–11079.
- (76) Pistelli, L.; Spera, K.; Flamini, G.; Mele, S.; Morelli, I. *Phytochemistry* **1996**, *42*, 1455–1458.
- (77) Peralta, M. A.; Santi, M. D.; Agnese, A. M.; Cabrera, J. L.; Ortega, M. G. *Phytochemistry lett.* **2014**, *10*, 260–267.
- (78) Fukai, T.; Zeng, L.; Nomura, T.; Zhang, R. Y.; Lou, Z. C. *Nat. Medicines* **1996**, *50*, 247–251.
- (79) Dubois, J. L.; Sneden, A. T. *J. Nat. Prod.* **1995**, *58*, 629–632.
- (80) McKee, T. C.; Bokesch, H. R.; McCormick, J. L.; Rashid, M. A.; Spielvogel, D.; Gustafson, K. R.; Alavanja, M. M.; Cardellina, J. H.; Boyd, M. R. *J. Nat. Prod.* **1997**, *60*, 431–438.
- (81) Popoola, O. K.; Marnewick, J. L.; Rautenbach, F.; Ameer, F.; Iwuoha, E. I.; Hussein, A. A.

Molecules **2015**, *20*, 7143–7155.

- (82) Yenesew, A.; Induli, M.; Derese, S.; Midiwo, J. O.; Heydenreich, M.; Peter, M. G.; Akala, H.; Wangui, J.; Liyala, P.; Waters, N. C. *Phytochemistry* **2004**, *65*, 3029–3032.
- (83) Monache, G. D.; Rosa, M. C. D.; Scurria, R.; Vitali, A.; Cuteri, A.; Monacelli, B.; Pasqua, G.; Botta, B. *Phytochemistry* **1995**, *39*, 575–580.
- (84) Fukai, T.; Nishizawa, J.; Nomura, T. *Phytochemistry* **1994**, *35*, 515–519.

SECTION S6. FURTHER SUPPORTING FIGURES & TABLES

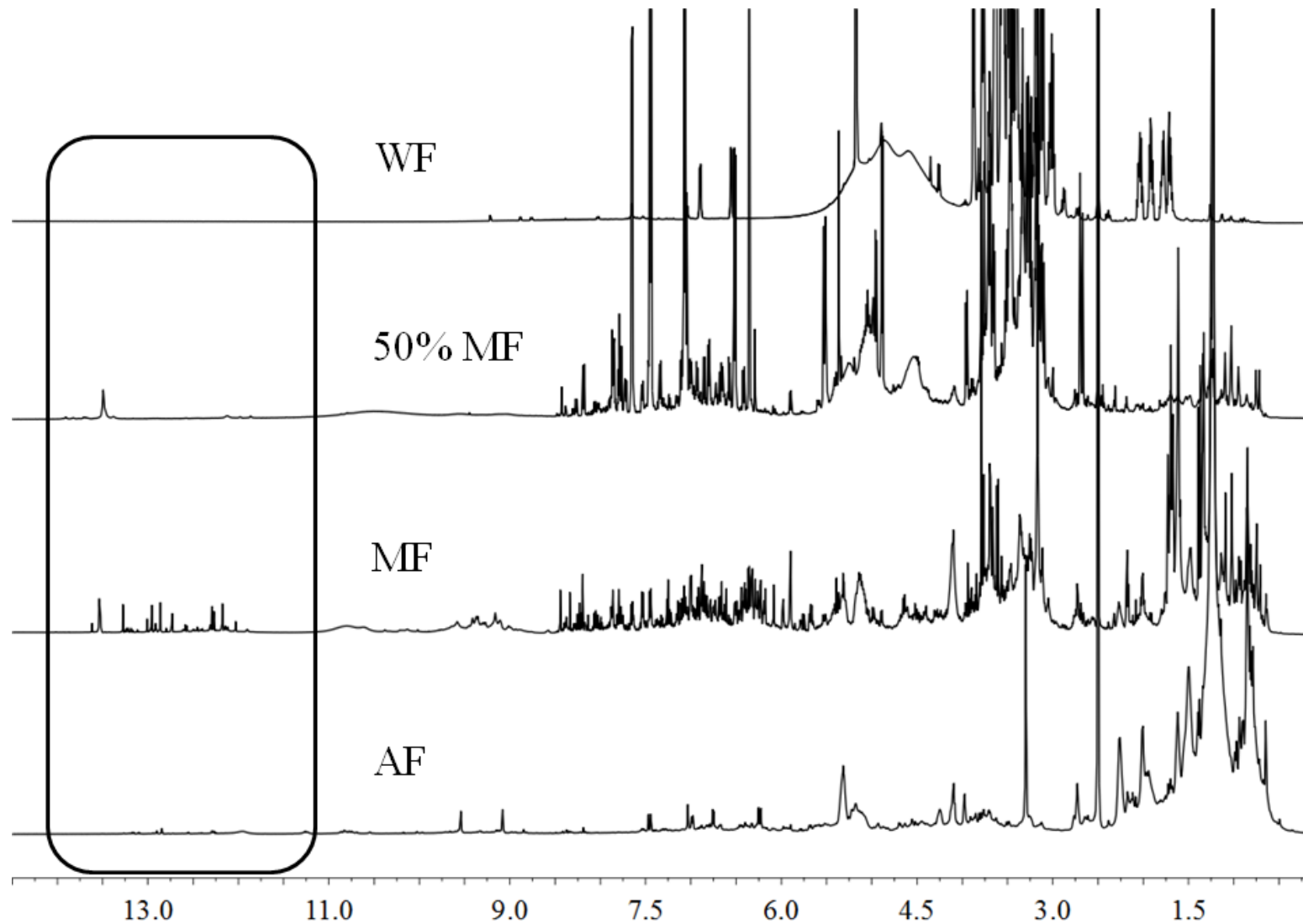


Figure S5. Comparison of the ^1H NMR spectra of WF, 50% MF, MF, and AF for GU in $\text{DMSO}-d_6$.

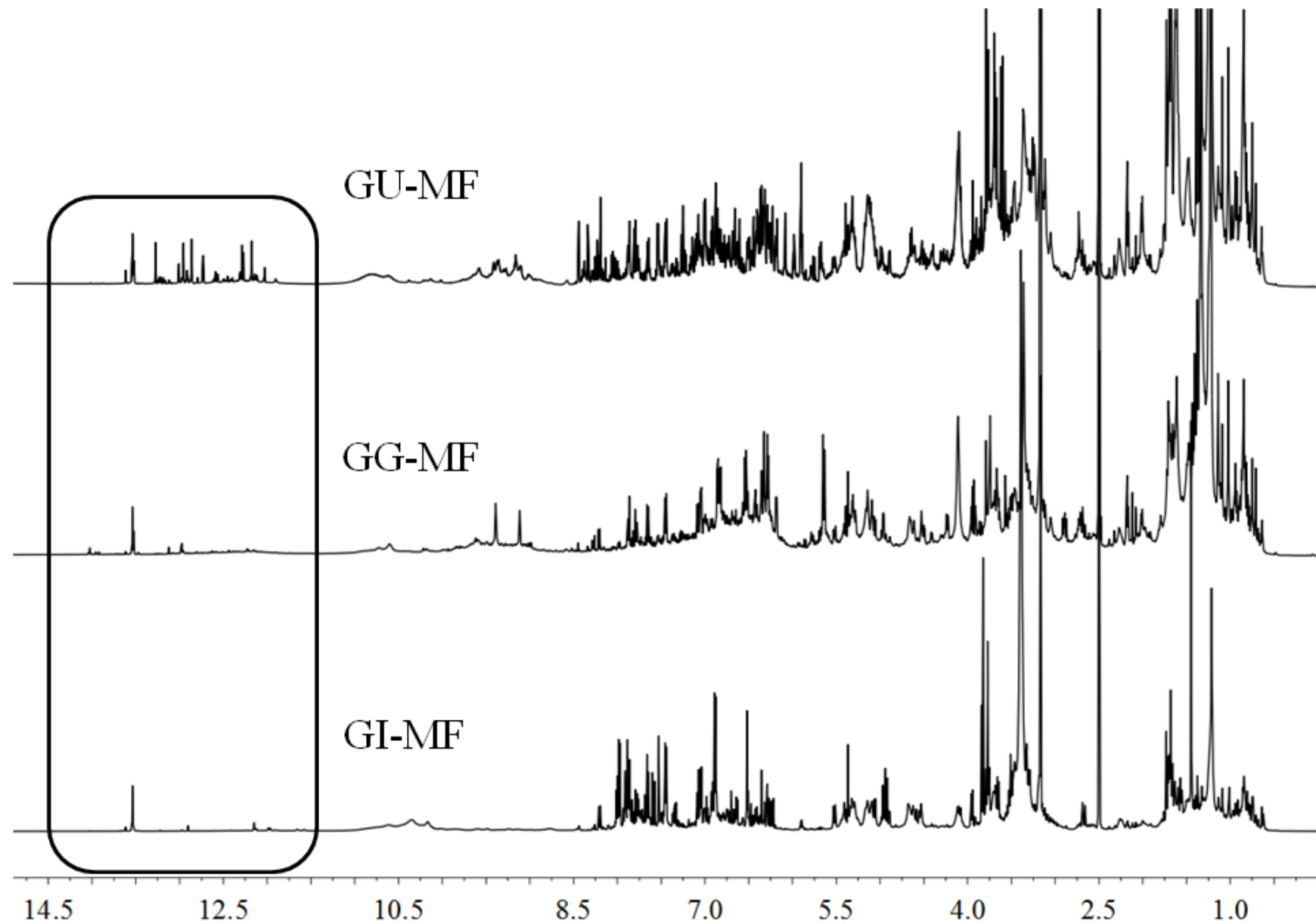


Figure S6. Comparison of the ^1H NMR spectra of GU-MF, GG-MF, and GI-MF in $\text{DMSO}-d_6$.

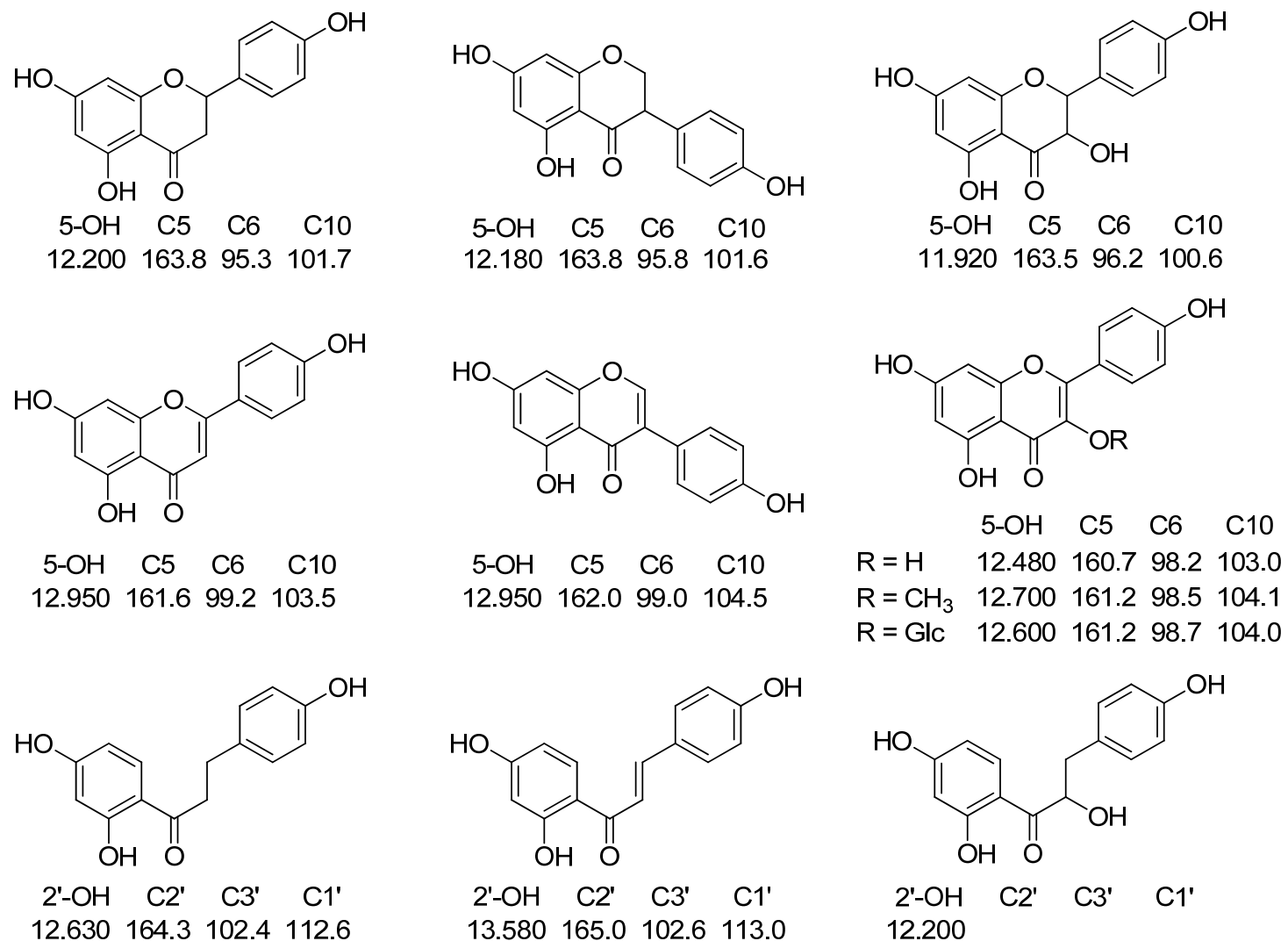


Figure S7. The chemical shifts of the 5-/2'-OH hydrogens and the three HMBC correlated carbons of the following flavonoid skeletons: flavonone, isoflavonone, flavononol, flavone, isoflavone, flavonol, its 3-O-methyl derivative, its 3-O-glycoside, dihydrochalcone, chalcone, and α -hydroxyl dihydrochalcone (all in DMSO-*d*₆).

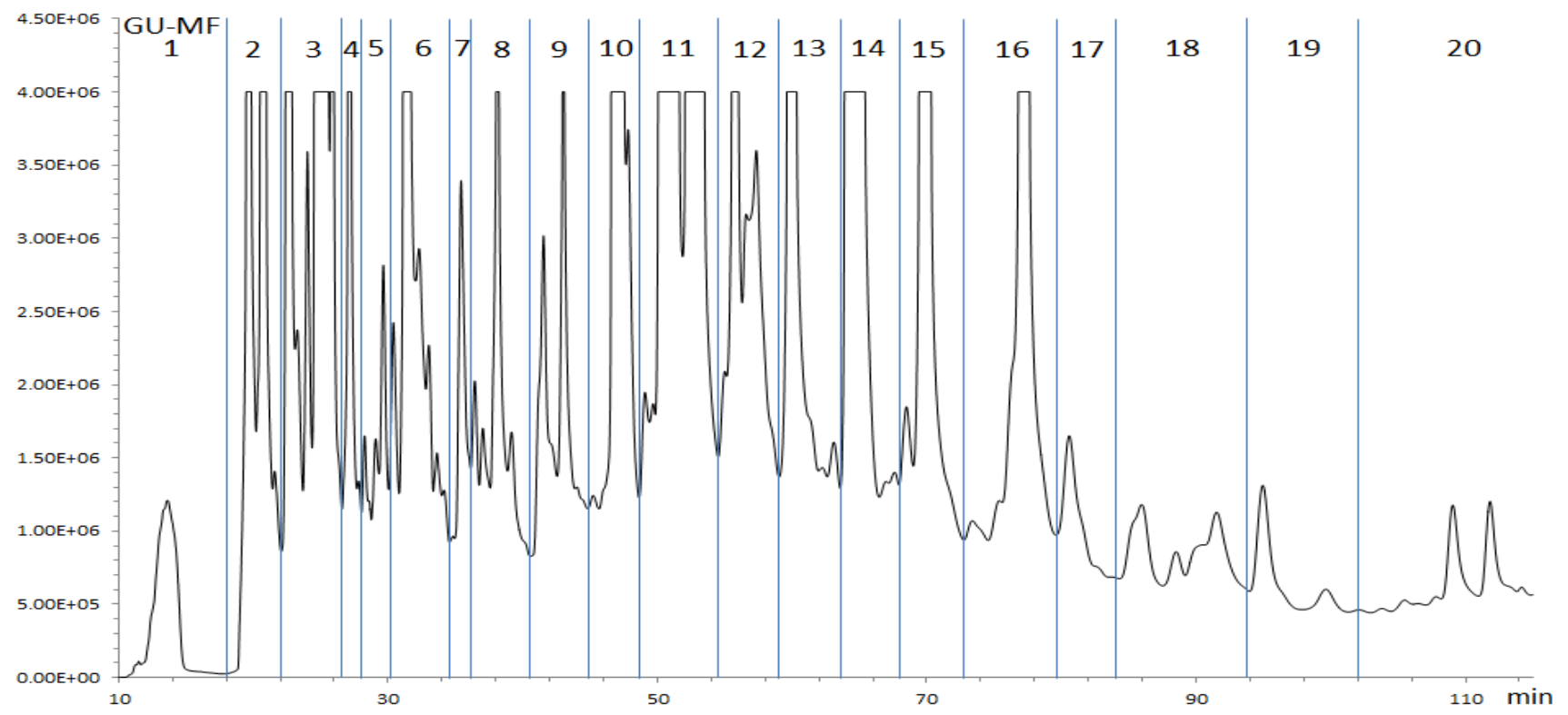


Figure S8. The preparative HPLC profile of GU-MF at 254 nm, divided into 20 subfractions, GU-MF-1 to GU-MF-20.

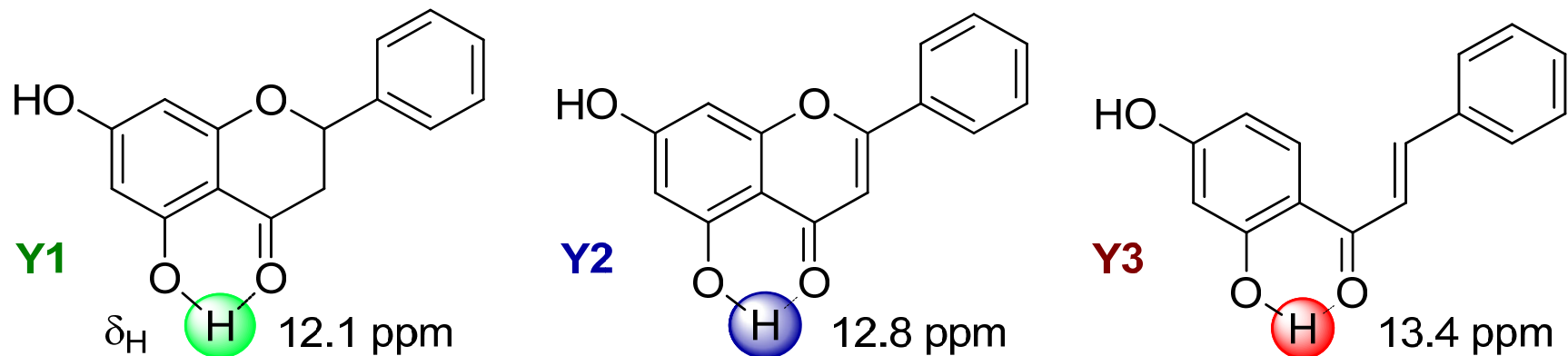


Figure S9. The 5-/2'-OH hydrogen chemical shifts and structures of the three model compounds, Y1, Y2, and Y3 in DMSO-*d*₆. In order to theoretically explain the above rules of 5-OH hydrogen chemical shifts for flavanones, flavonoids, and chalcones, three model compounds, Y1, Y2, and Y3, were chosen and further studied by using Natural Bond Orbital (NBO) analysis. Firstly, conformational searching were carried out via Monte Carlo searching using molecular mechanism with MMFF94 force field in the Spartan 08 program.¹ The results showed two lowest energy conformers for each compound (Fig. S10). Subsequently, the conformers were re-optimized using DFT at the B3LYP/6-31+G(d,p) level in vacuum with the Gaussian 09 program.² The B3LYP/6-31+G(d,p) harmonic vibrational frequencies were further calculated to confirm their stability. The second-order perturbation stabilization energies ΔE^2 (an indicator of intensity of the 4=O...H-O-5 or 1=O...H-O-2' hydrogen bond)³ and natural charges on the three related atoms were calculated on each conformer via Natural Bond Orbital (NBO) analysis at the WB97XD/6-311++G(2d,2p) level. The final data for the compounds were obtained by averaging those of the conformers according to their relative Gibbs free energy (ΔG) and Boltzmann distribution theory.

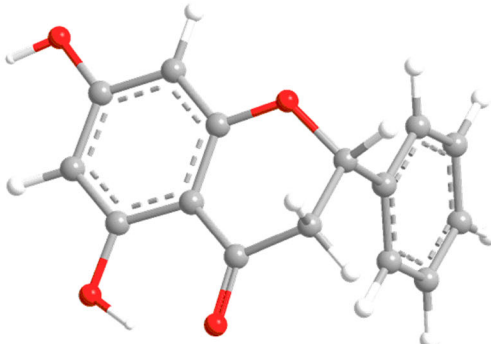
Table S6. Bond lengths, second-order stabilization energies $\Delta E^{(2)}$, and natural charges of the hydrogen atoms of the C(4/1)=O...H-O-C(5/2') hydrogen bonds in the model compounds Y1, Y2, and Y3.

Compound	Donor→Acceptor	R(O...H)(nm)	$\Delta E^{(2)}$ (Kcal/mol)	Natural Charge
Y1	E(LP(O=C(4))→RY*(H-O-C(5)))	0.170428	0.56	0.51274
Y2	E(LP(O=C(4))→RY*(H-O-C(5)))	0.168642	0.58	0.51489
Y3	E(LP(O=C(4/1))→RY*(H-O-C(5/2')))	0.159827	0.73	0.51162

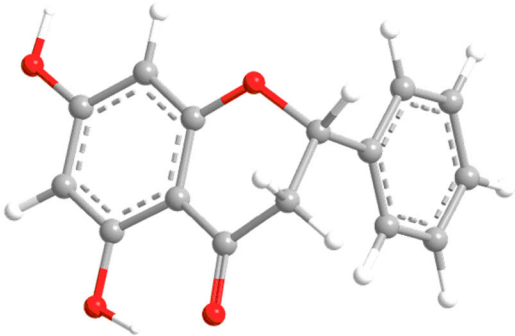
The results showed a decrease of hydrogen bond lengths and increase of second-order stabilization energies from Y1 to Y3, which is consistent with the increase of 5-/2'-OH proton chemical shifts of these compounds and indicating the hydrogen bonds play important roles in the NMR behavior of the 5-/2'-OH protons. However, the electron density on the hydrogen atom of the 5-/2'-OH plays less important role in the determination of the chemical shifts because the order of natural charges on these hydrogen atoms are inconsistent with the NMR observation.

Methods & References

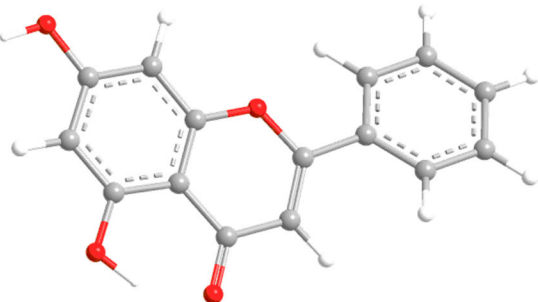
- 1) *Spartan 08*; Wavefunction Inc.:Irvine, CA.
- 2) *Gaussian 09*, Revision A.1, Frisch, M. J.; Trucks, G. W.; Schlegel, H. B.; Scuseria, G. E.; Robb, M. A.; Cheeseman, J. R.; Scalmani, G.; Barone, V.; Mennucci, B.; Petersson, G. A.; Nakatsuji, H.; Caricato, M.; Li, X.; Hratchian, H. P.; Izmaylov, A. F.; Bloino, J.; Zheng, G.; Sonnenberg, J. L.; Hada, M.; Ehara, M.; Toyota, K.; Fukuda, R.; Hasegawa, J.; Ishida, M.; Nakajima, T.; Honda, Y.; Kitao, O.; Nakai, H.; Vreven, T.; Montgomery, Jr., J. A.; Peralta, J. E.; Ogliaro, F.; Bearpark, M.; Heyd, J. J.; Brothers, E.; Kudin, K. N.; Staroverov, V. N.; Kobayashi, R.; Normand, J.; Raghavachari, K.; Rendell, A.; Burant, J. C.; Iyengar, S. S.; Tomasi, J.; Cossi, M.; Rega, N.; Millam, J. M.; Klene, M.; Knox, J. E.; Cross, J. B.; Bakken, V.; Adamo, C.; Jaramillo, J.; Gomperts, R.; Stratmann, R. E.; Yazyev, O.; Austin, A. J.; Cammi, R.; Pomelli, C.; Ochterski, J. W.; Martin, R. L.; Morokuma, K.; Zakrzewski, V. G.; Voth, G. A.; Salvador, P.; Dannenberg, J. J.; Dapprich, S.; Daniels, A. D.; Farkas, Ö.; Foresman, J. B.; Ortiz, J. V.; Cioslowski, J.; Fox, D. J. Gaussian, Inc., Wallingford CT, 2009.
- 3) J. Phys. Chem. B 2008, 112, 5088-5097.



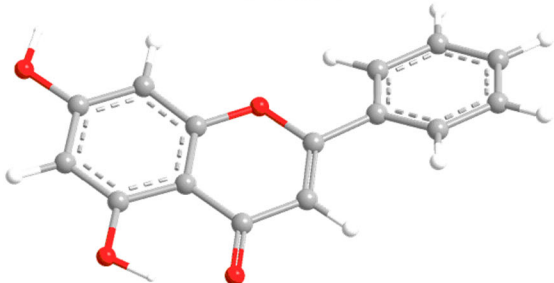
Y1C1



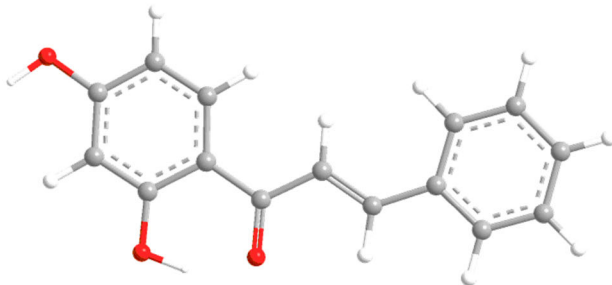
Y1C2



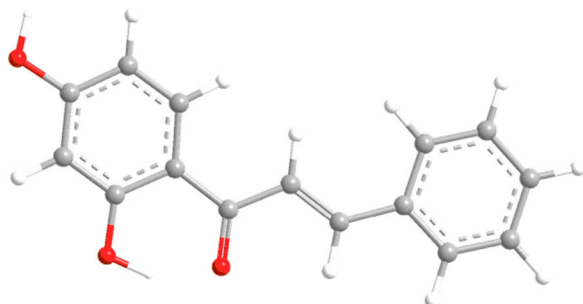
Y2C1



Y2C2



Y3C1



Y3C2

Figure S10. B3LYP/6-31+G(d,p) optimized lowest energy 3D conformers of the model compounds, Y1, Y2, and Y3. In order to obtain the final spectra, all simulated spectra of the conformers of each compound were averaged according to their energies and the Boltzmann distribution theory expressed as:

$$\frac{N_i^*}{N} = \frac{g_i e^{-\varepsilon_i / k_B T}}{\sum g_i e^{-\varepsilon_i / k_B T}}$$

Table S7. Energy analysis of the conformers of the model compounds, Y1, Y2, and Y3.

conf.	Gibbs free energy (298.15 K)		
	G (Hartree)	ΔG (Kcal/mol)	Boltzmann Distribution
Y1C1	-879.586629	0	0.618004
Y1C2	-879.586175	0.284890	0.381996
Y2C1	-878.406073	0	0.730286
Y2C2	-878.405133	0.589859	0.269714
Y3C1	-804.361161	0	0.677843
Y3C2	-804.360459	0.440512	0.322157

Table S8. NBO analysis data for conformers of the model compounds, Y1, Y2, and Y3: natural charges on hydrogen bond related atoms.

Y1C1	Natural Charge	Y1C2	Natural Charge
4=O	-0.6452	4=O	-0.64405
5-O	-0.68451	5-O	-0.68231
5-O-H	0.51312	5-O-H	0.51212

Y2C1	Natural Charge	Y2C2	Natural Charge
4=O	-0.66364	4=O	-0.66269
5-O	-0.68754	5-O	-0.68577
5-O-H	0.51521	5-O-H	0.51402

Y3C1	Natural Charge	Y3C2	Natural Charge
1=O	-0.65874	1=O	-0.65739
2'-O	-0.68947	2'-O	-0.68688
2'-O-H	0.51182	2'-O-H	0.51121

Table S9. Second-order stabilization energies $\Delta E^{(2)}$ (kcal/mol) of the hydrogen bonds of the conformers of the model compounds, Y1, Y2, and Y3.

	$\Delta E^{(2)}$ (kcal/mol)
Y1C1	0.56
Y1C2	0.55
Y2C1	0.58
Y2C2	0.57
Y3C1	0.75
Y3C2	0.68

Table S10. The relative percentage of the eight subtypes in GU, GG, and GI, respectively.

Structural Type		GU (%)	GG (%)	GI (%)
Type I-1	A	7.92	0	1.02
Type I-2	B	17.82	4.55	20.40
Type I-3	C	6.41	0	0
Type II-1	D	3.74	0	8.49
Type II-2	E	32.90	0	2.96
Type II-3	F	17.04	0	1.48
Type III-1	G	14.17	75.70	65.65
Type III-2	H	0	19.75	0

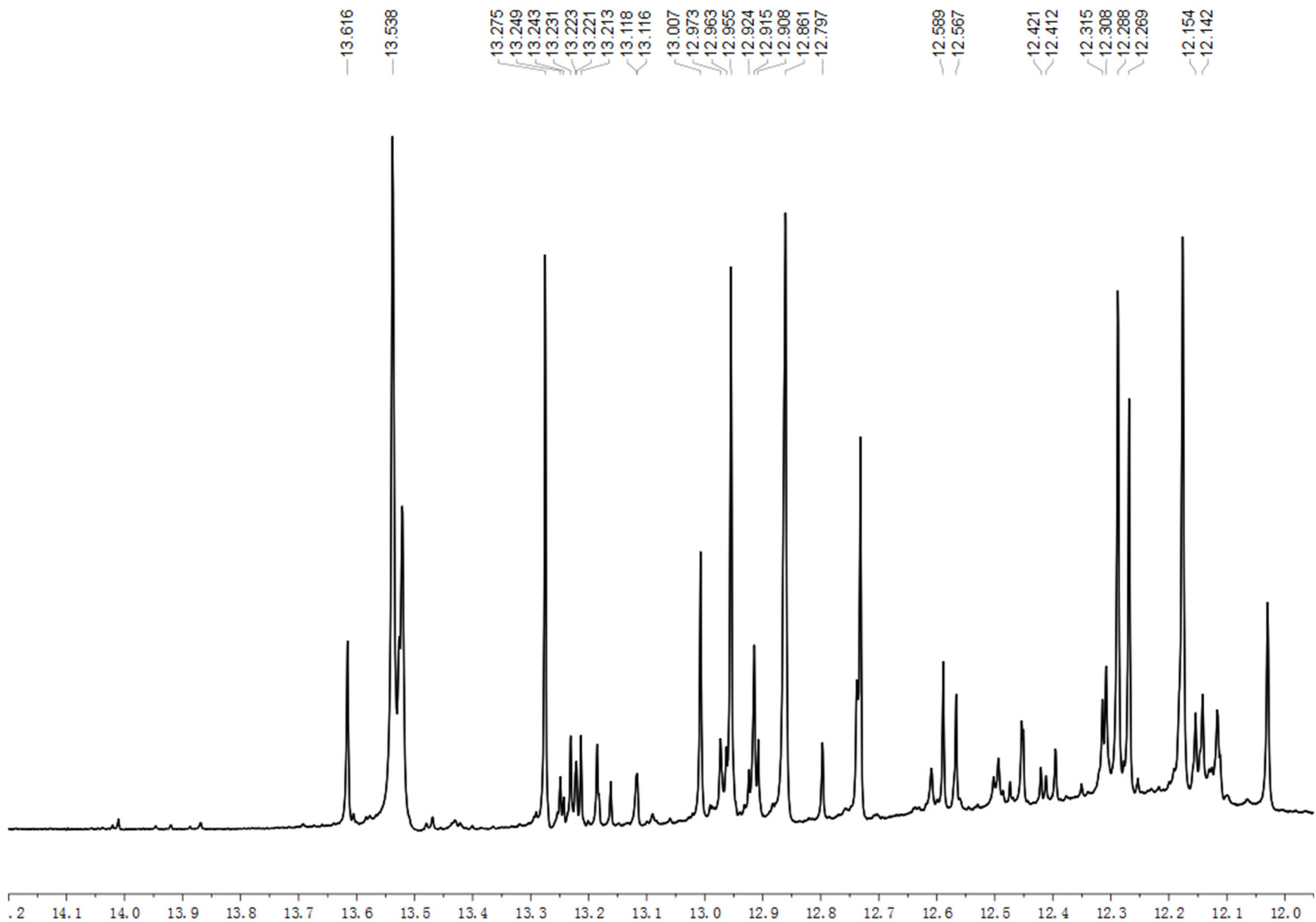


Figure S11. The ^1H NMR spectrum of GU-MF in $\text{DMSO}-d_6$.

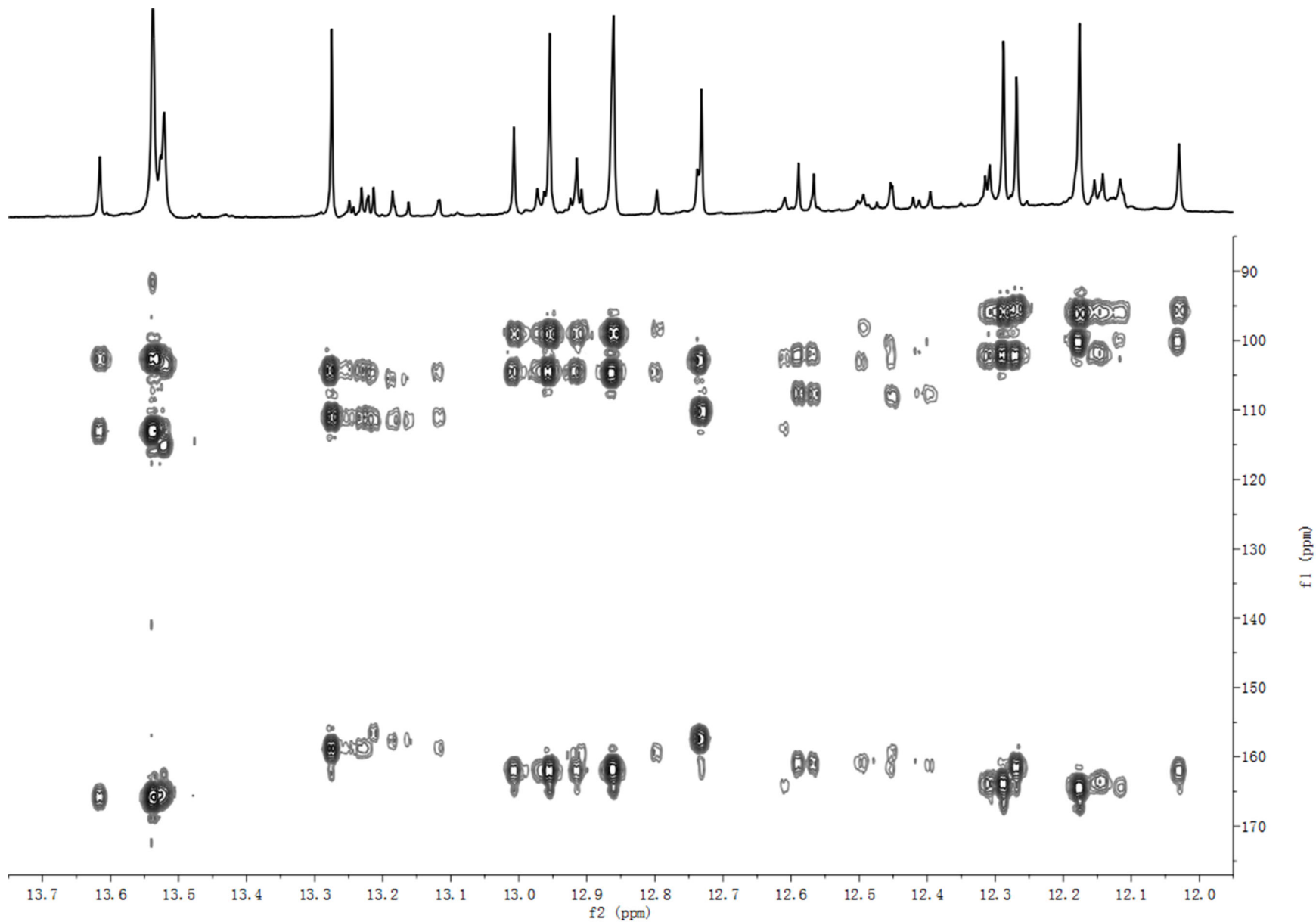


Figure S12. The HMBC spectrum of GU-MF in $\text{DMSO}-d_6$.

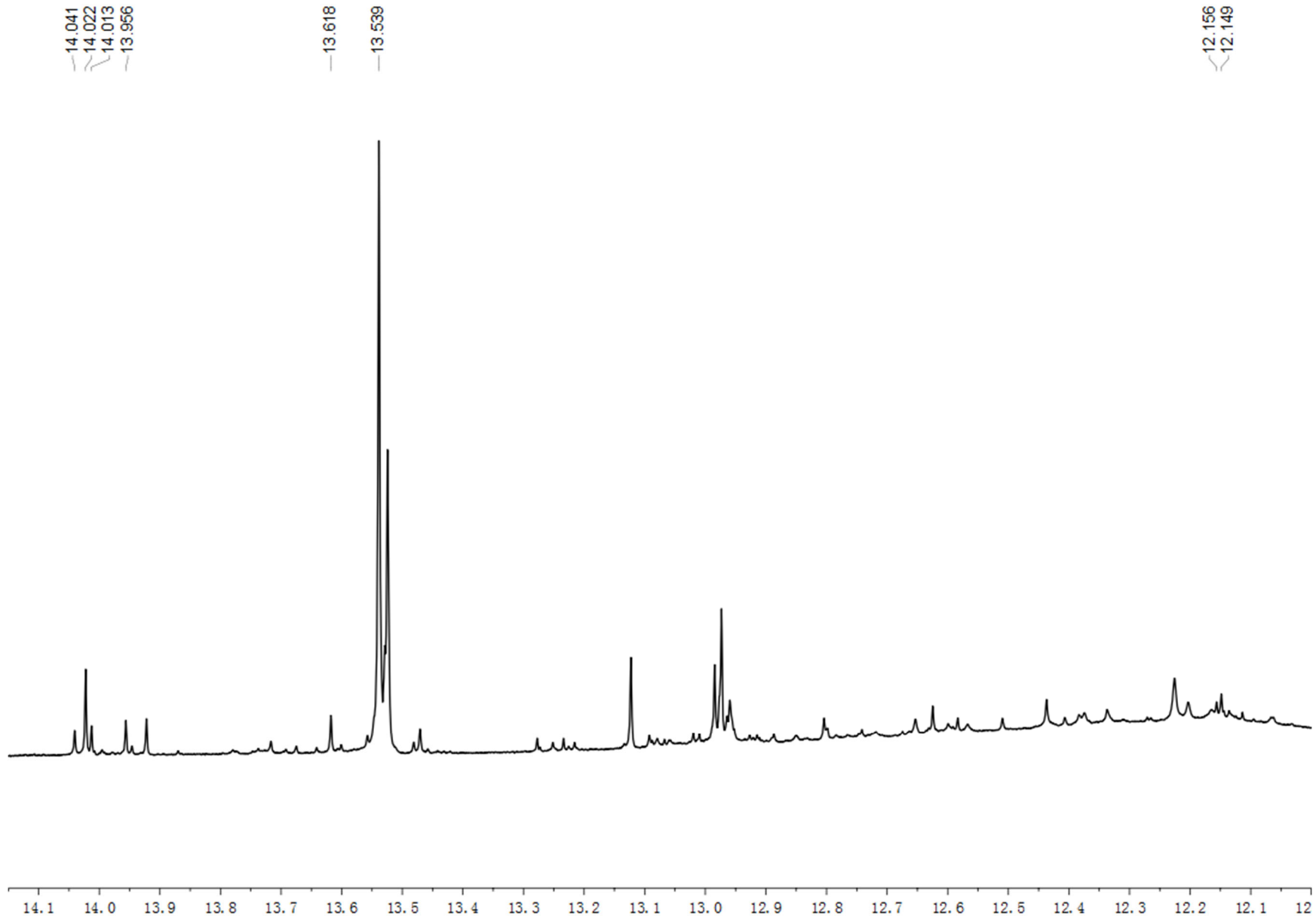


Figure S13. The ^1H NMR spectrum of GG-MF in $\text{DMSO}-d_6$.

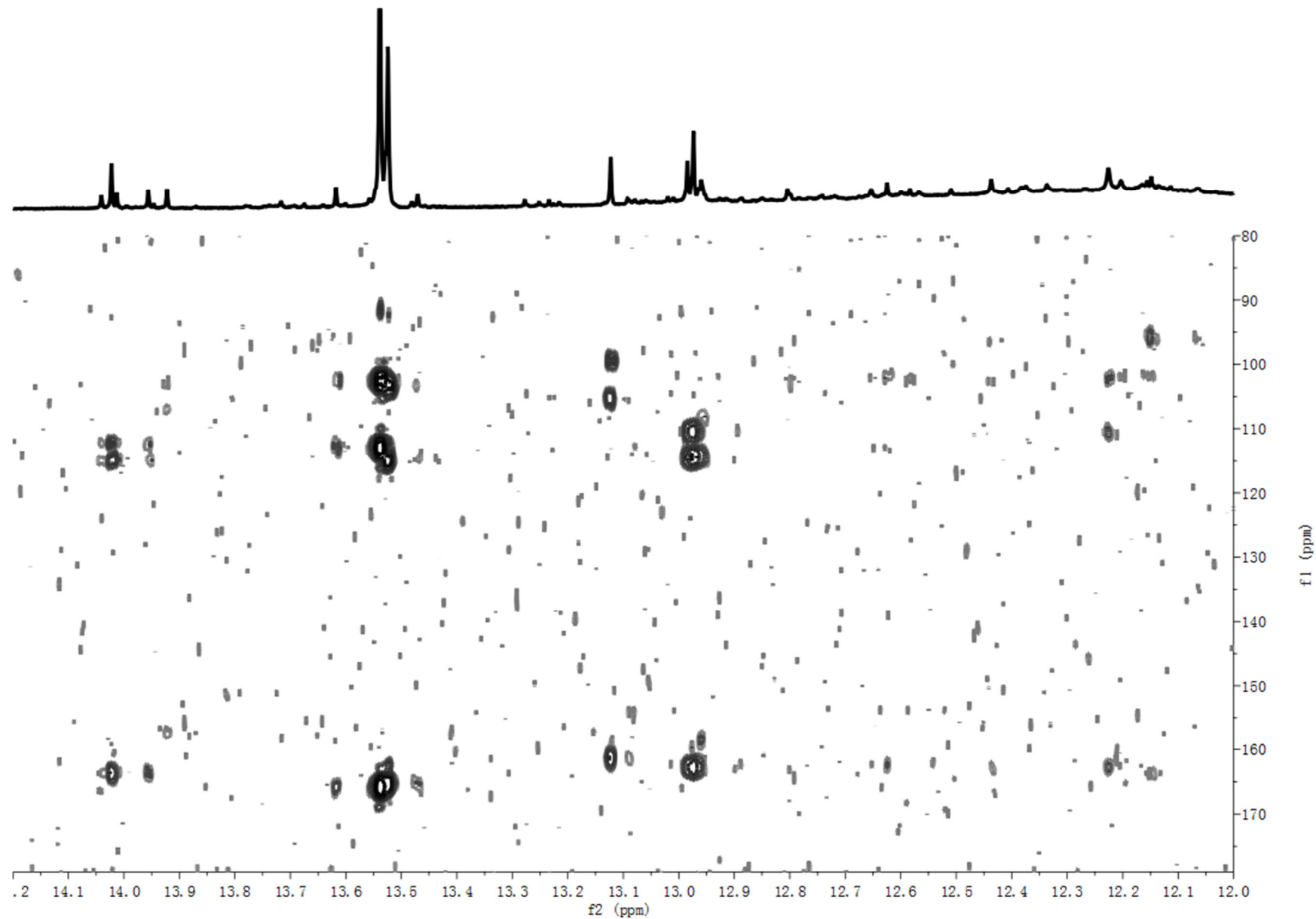


Figure S14. The HMBC spectrum of GG-MF in $\text{DMSO}-d_6$.

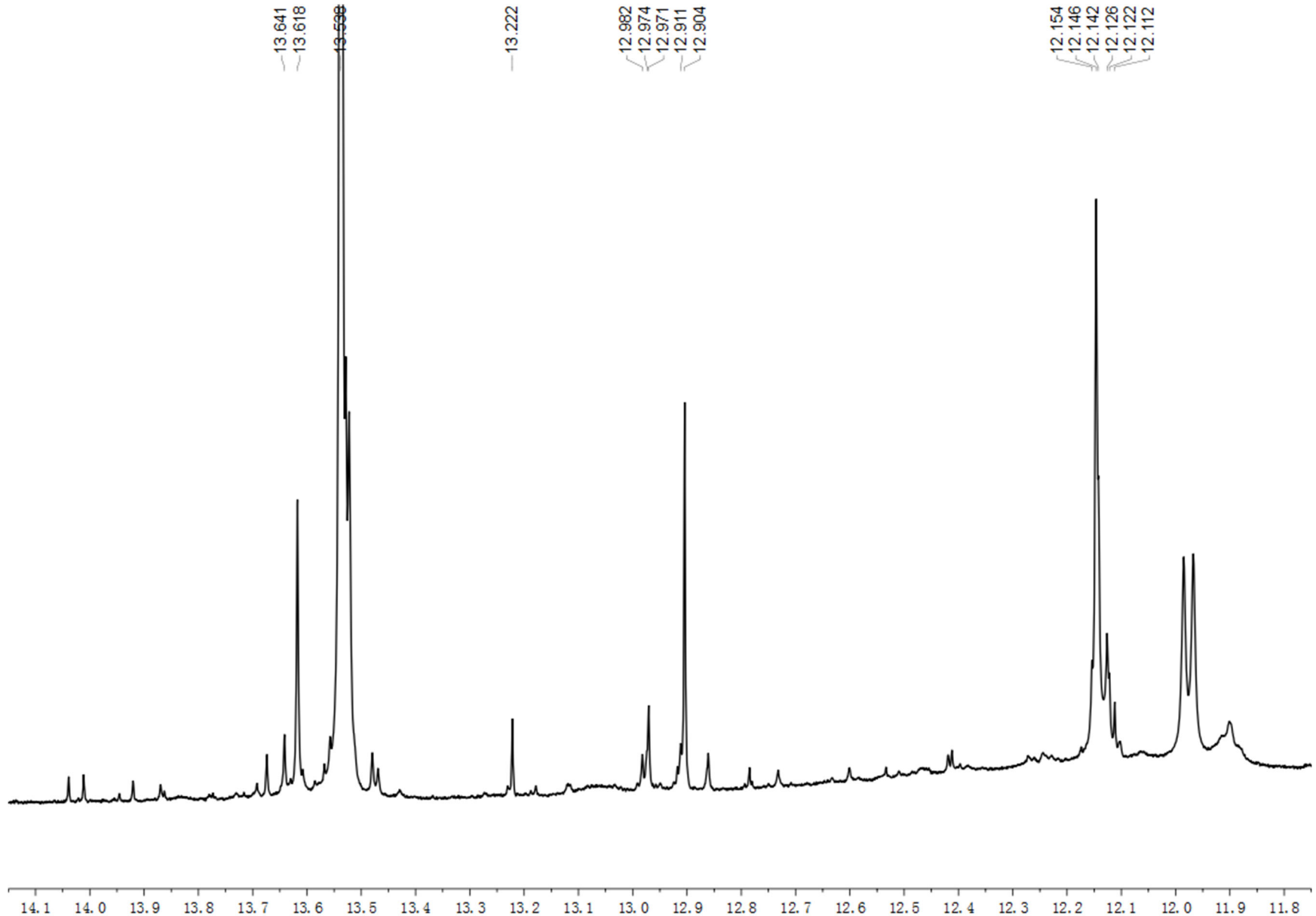


Figure S15. The ^1H NMR spectrum of GI-MF in $\text{DMSO}-d_6$.

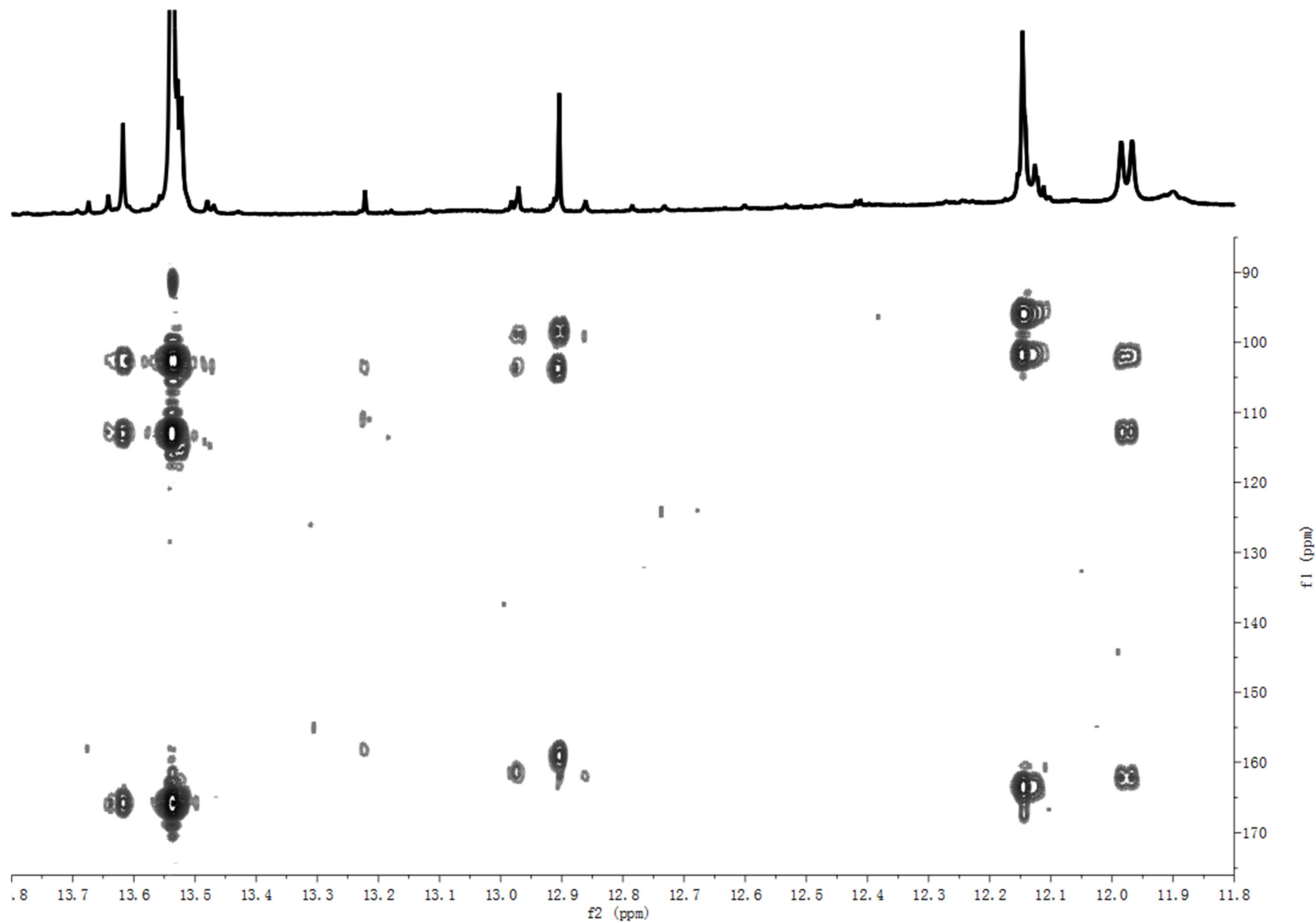


Figure S16. The HMBC spectrum of GI-MF in $\text{DMSO}-d_6$.

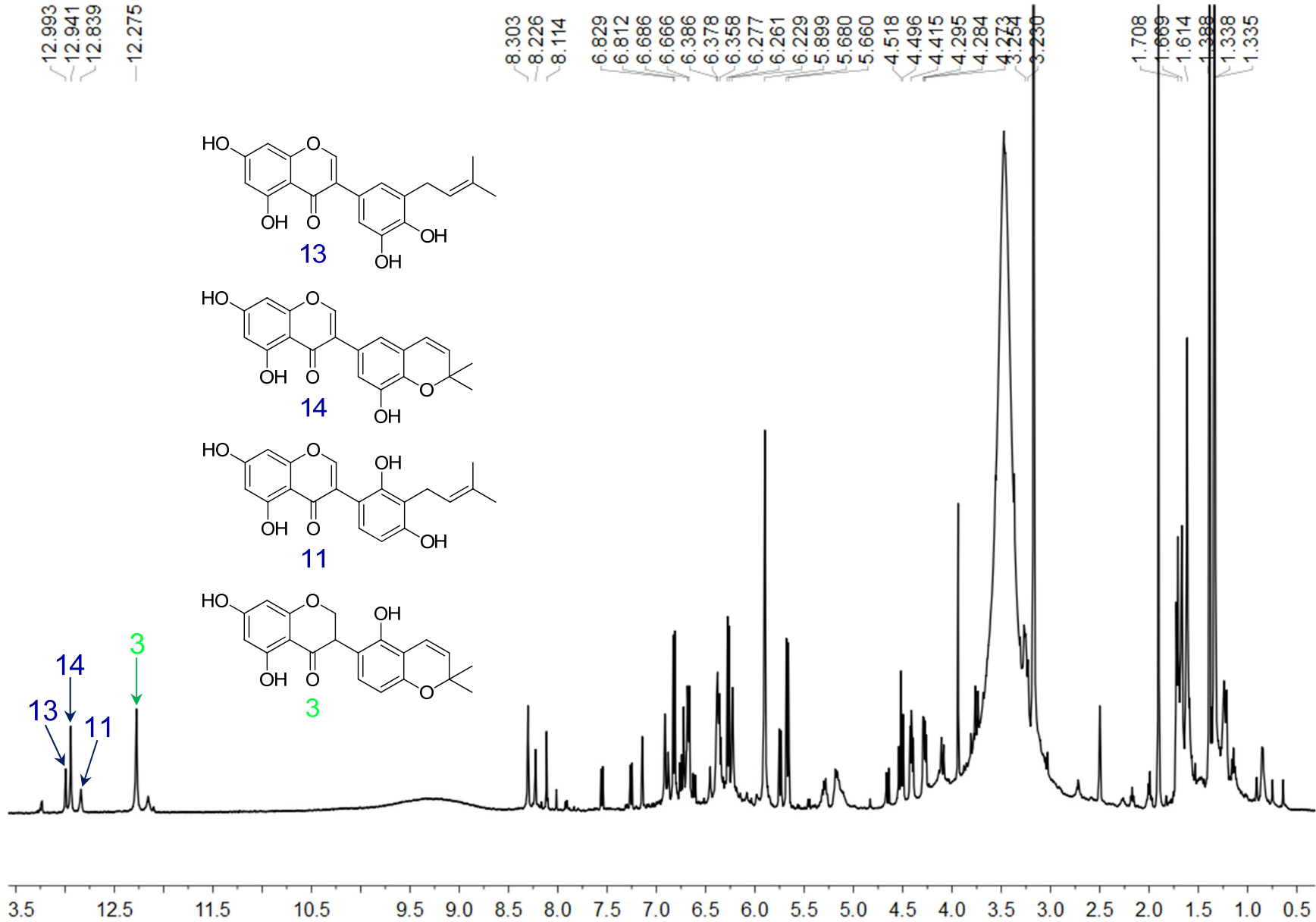


Figure S17. The ^1H NMR spectrum of GU-MF-11 in $\text{DMSO}-d_6$.

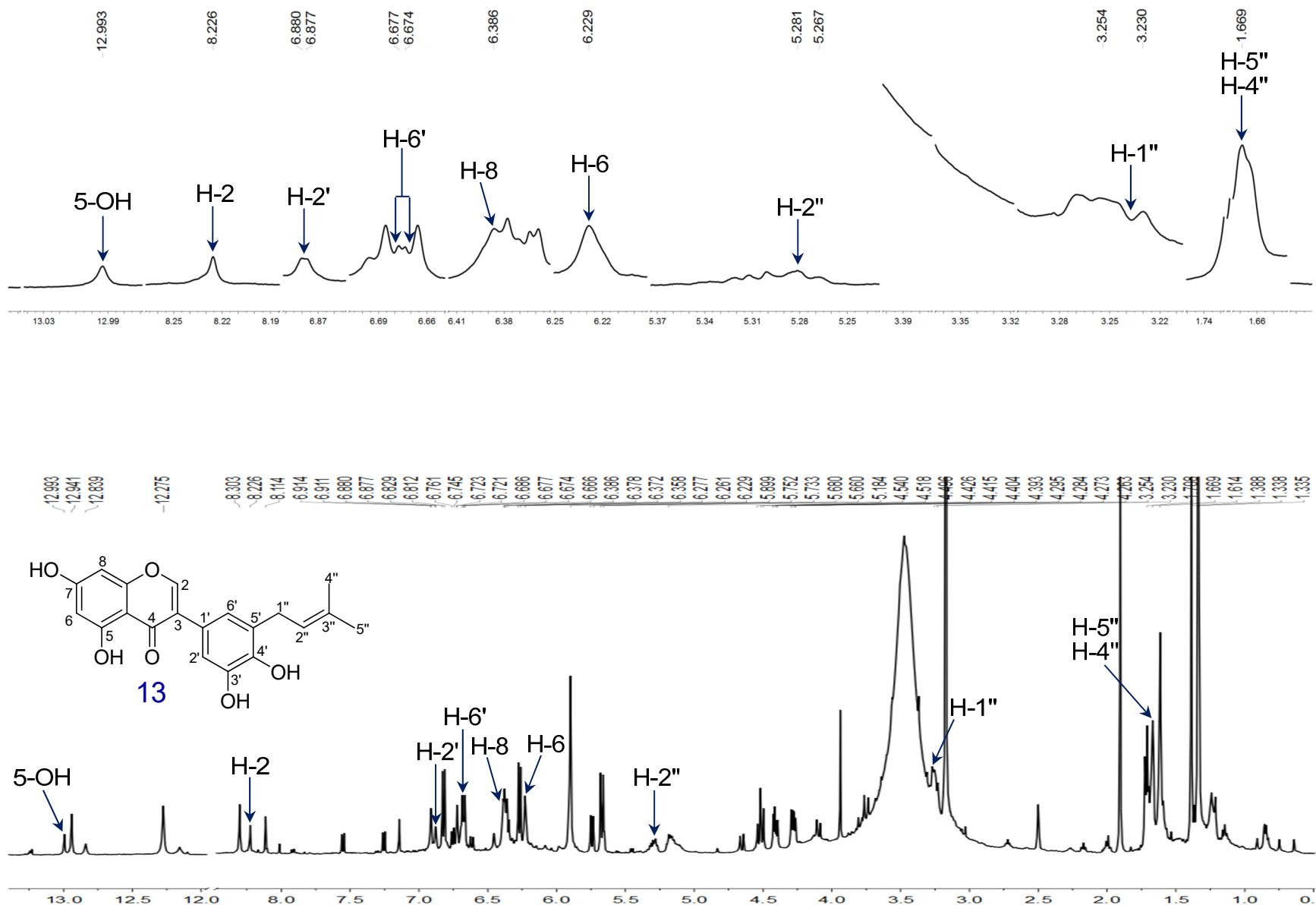


Figure S18. The ^1H NMR spectrum of compound **13** in GU-MF-11 in $\text{DMSO}-d_6$.

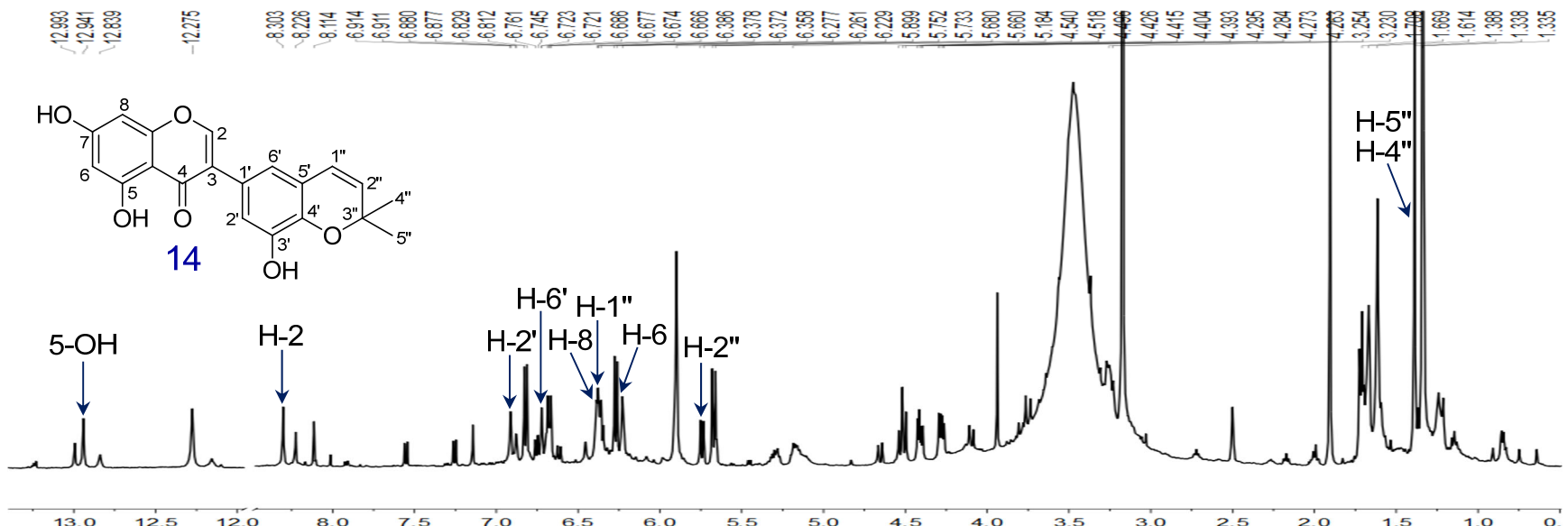
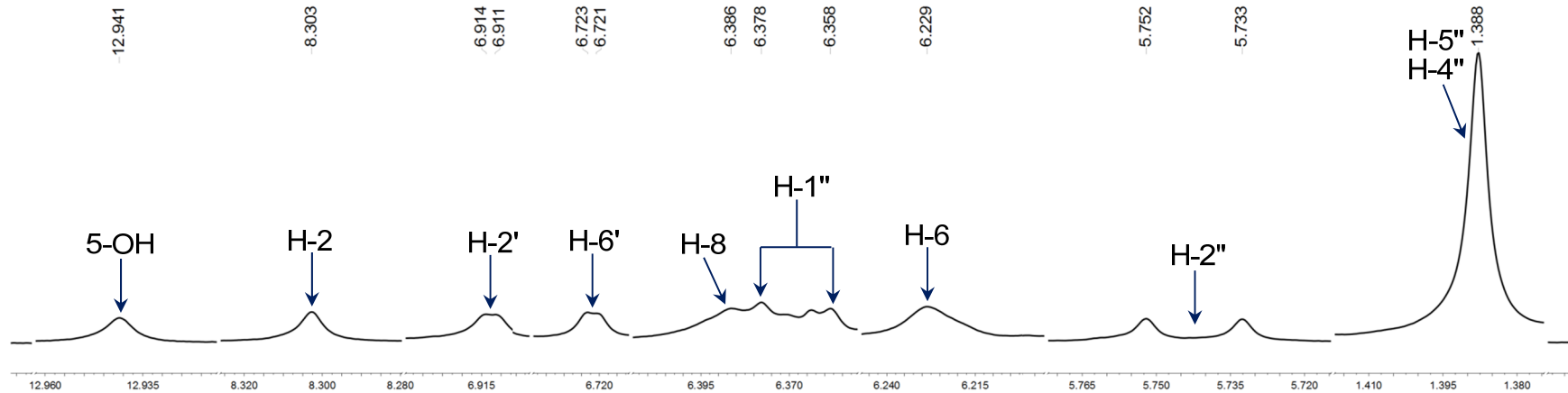


Figure S19. The ^1H NMR spectrum of compound **14** in GU-MF-11 in $\text{DMSO}-d_6$.

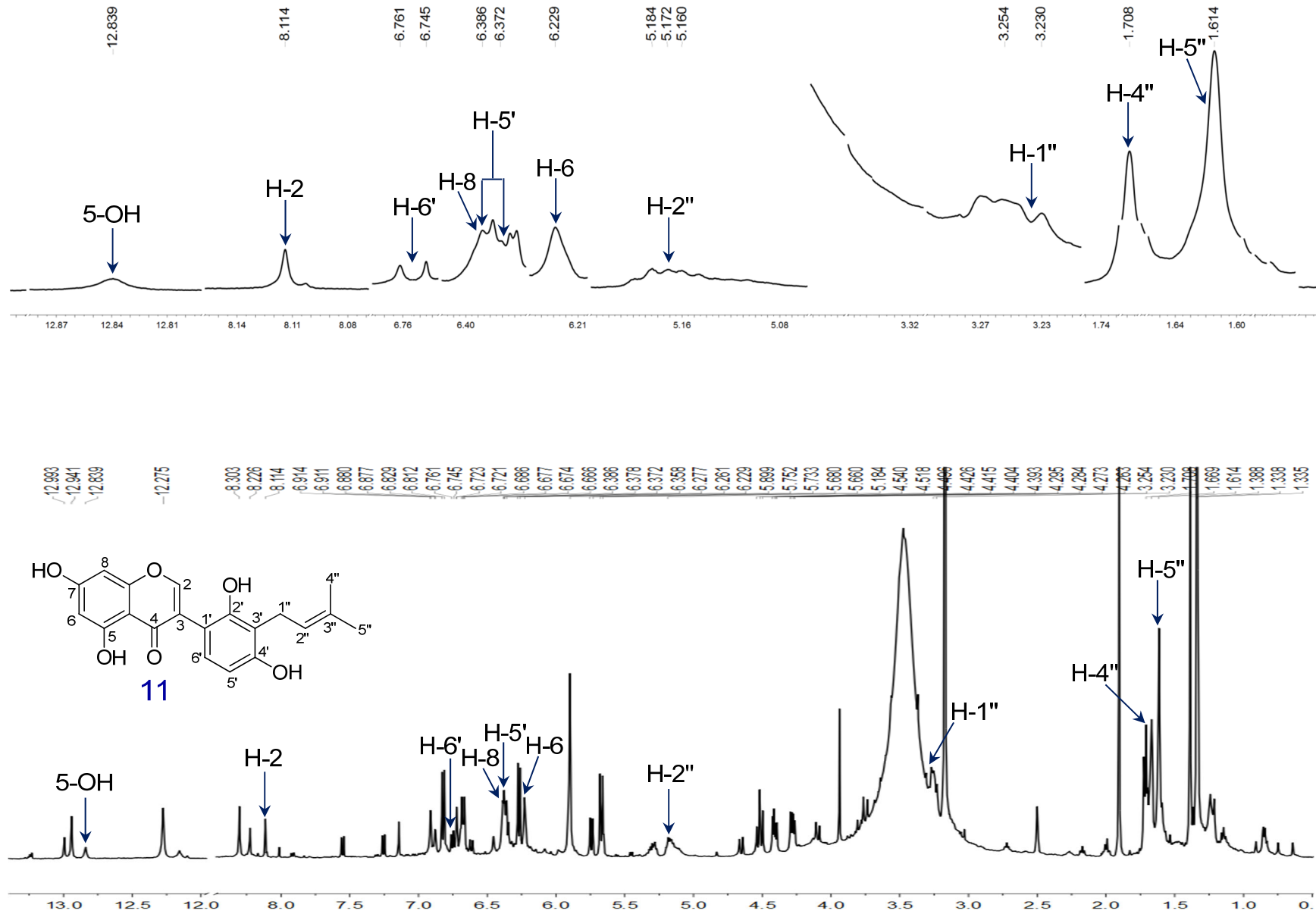


Figure S20. The ^1H NMR spectrum of compound **11** in GU-MF-11 in $\text{DMSO}-d_6$.

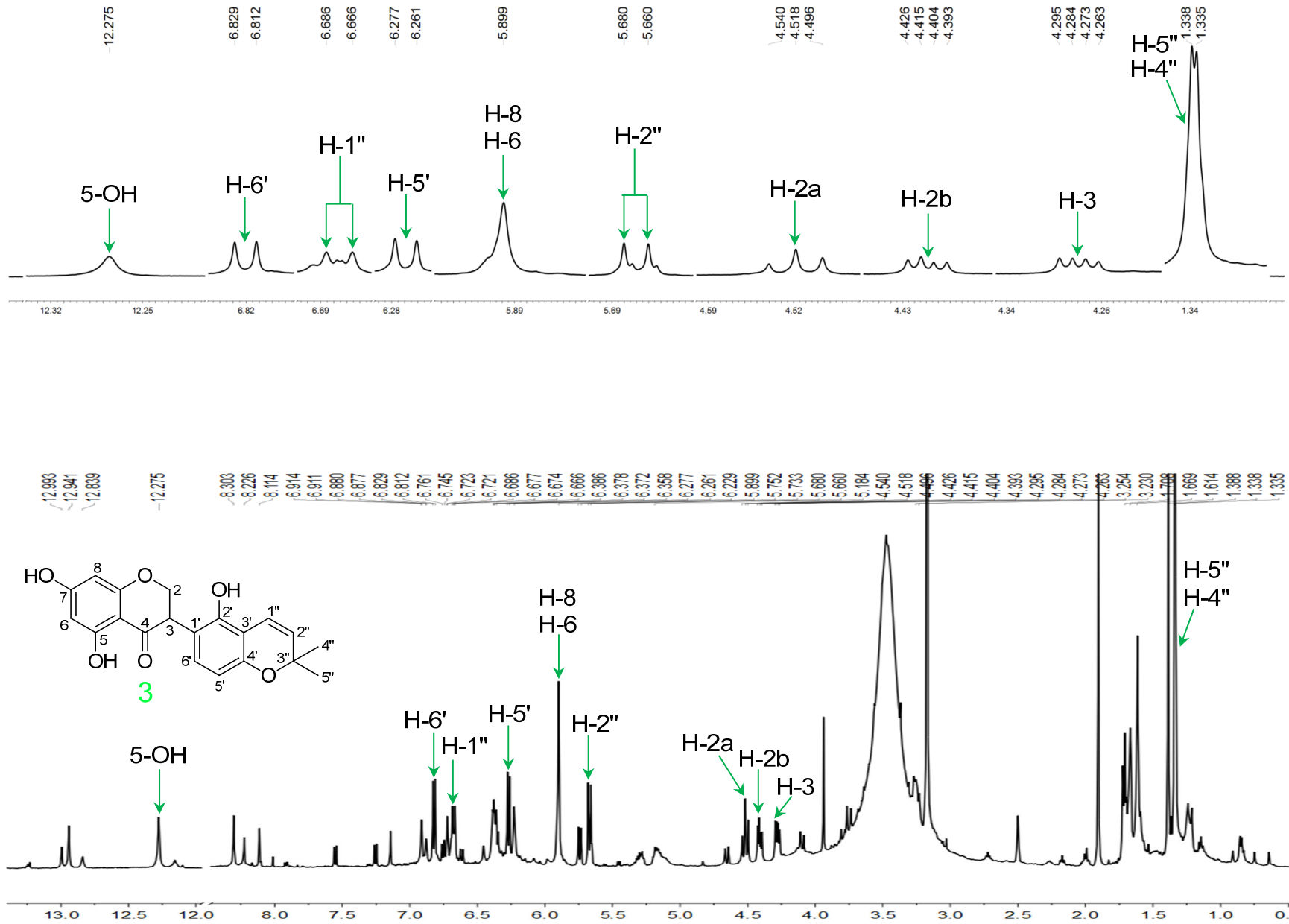


Figure S21. The ^1H NMR spectrum of compound 3 in GU-MF-11 in $\text{DMSO}-d_6$.

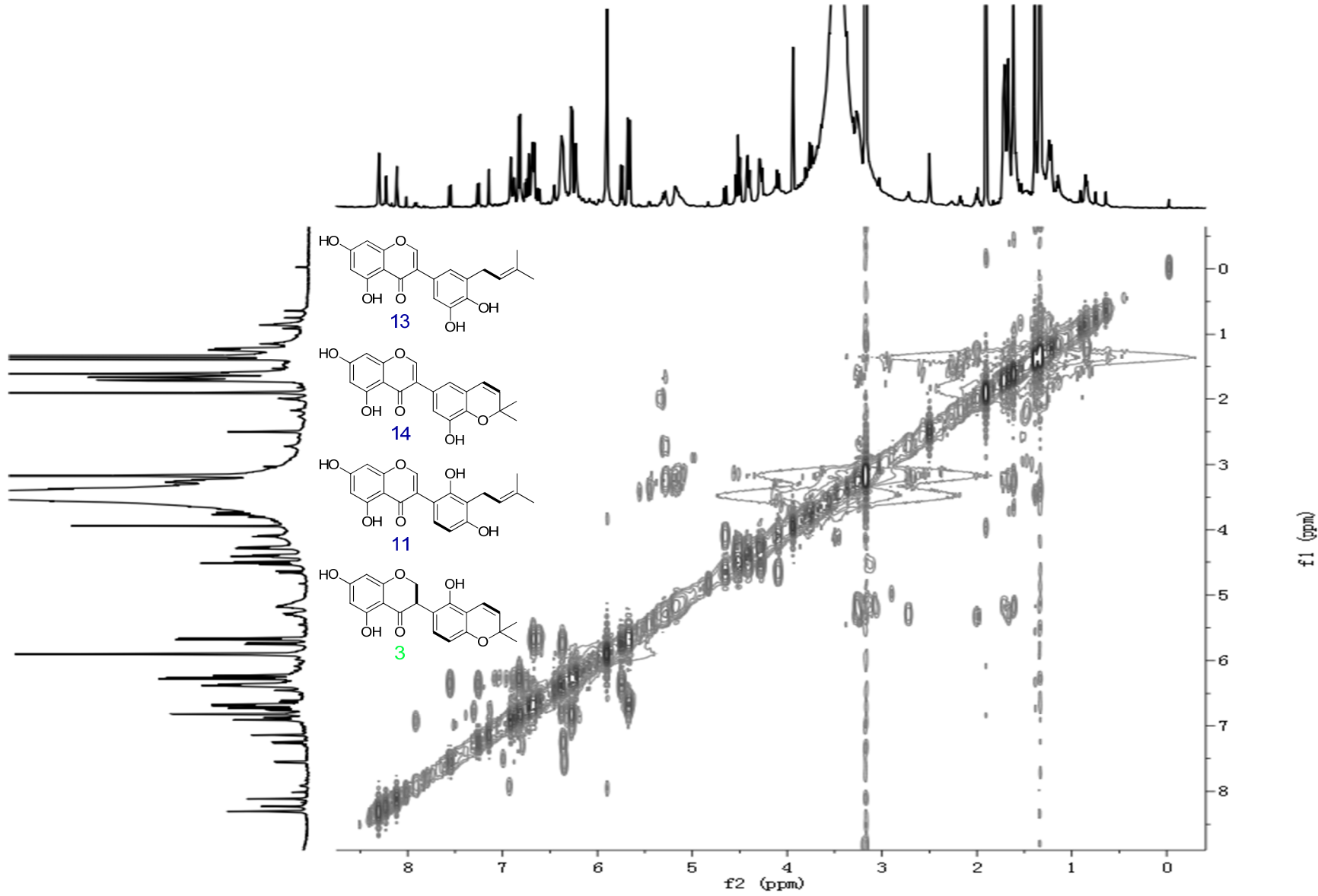


Figure S22. The ${}^1\text{H}$ - ${}^1\text{H}$ COSY spectrum of GU-MF-11 in $\text{DMSO}-d_6$.

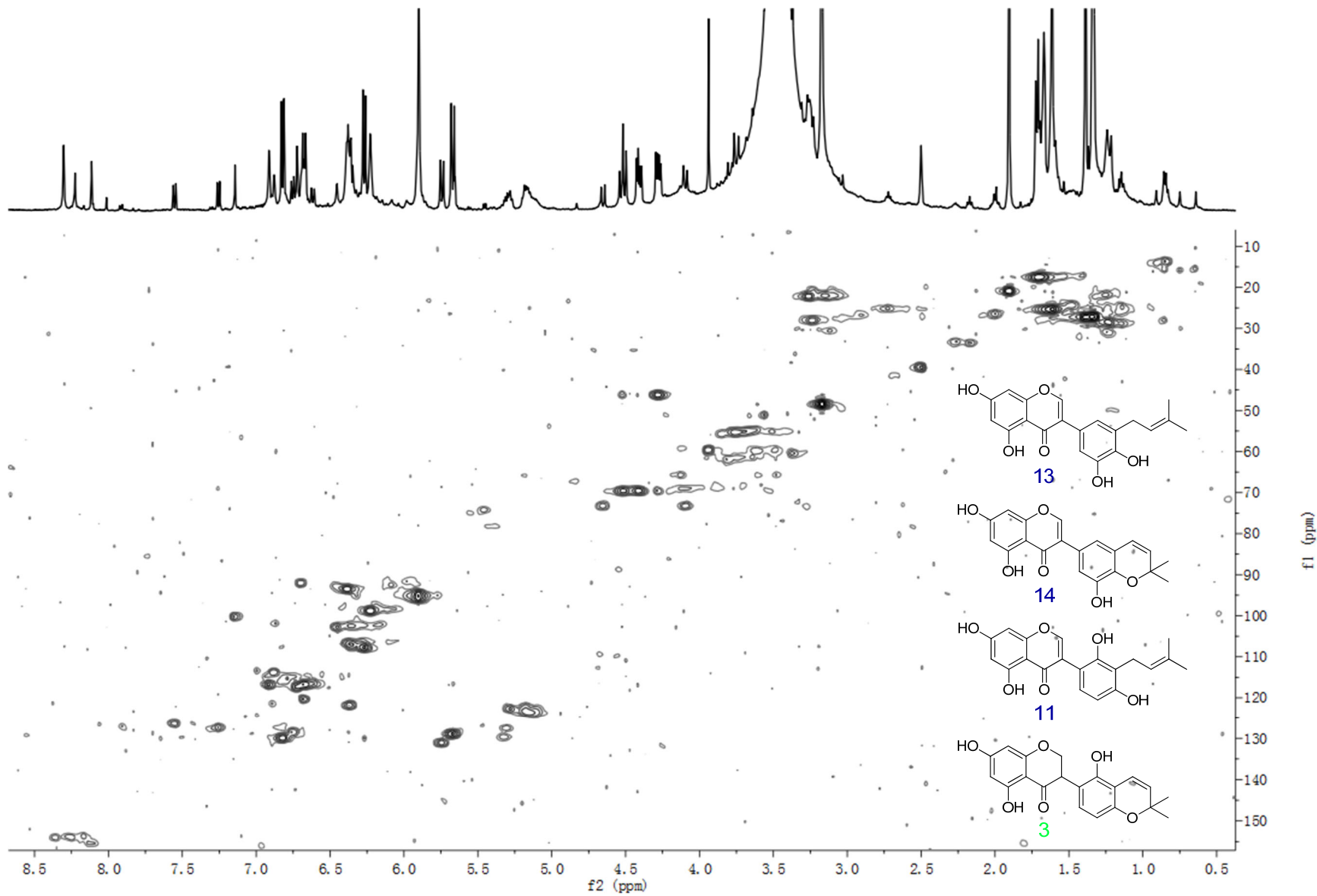


Figure S23. The HSQC spectrum of GU-MF-11 in $\text{DMSO}-d_6$.

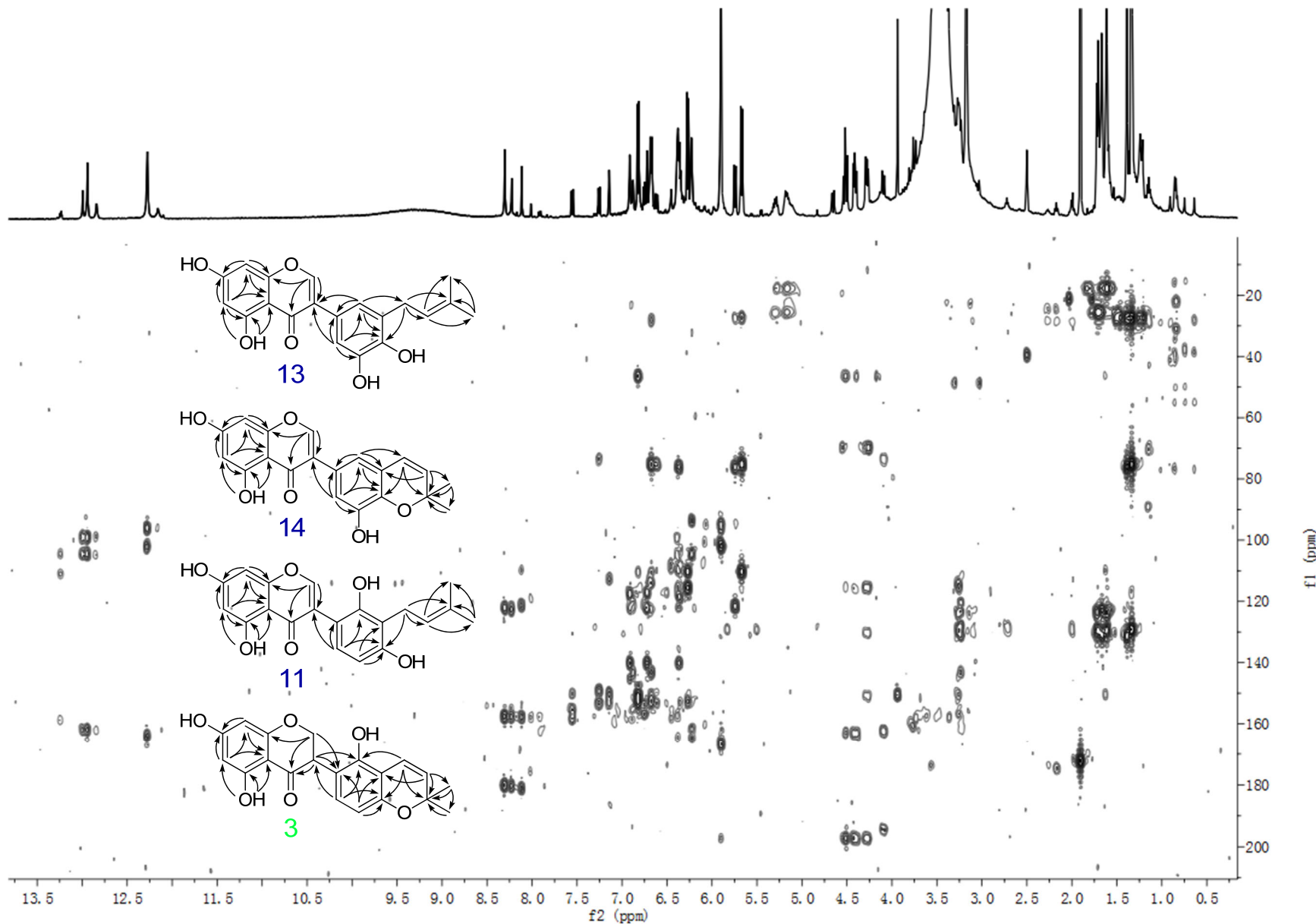


Figure S24. The HMBC spectrum of GU-MF-11 in DMSO-*d*₆.

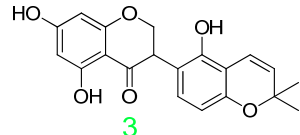
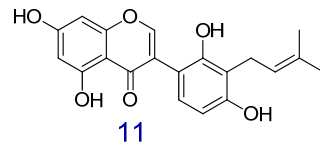
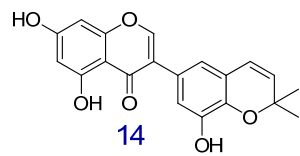
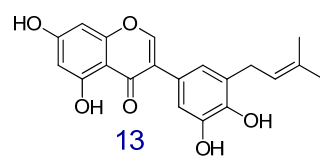
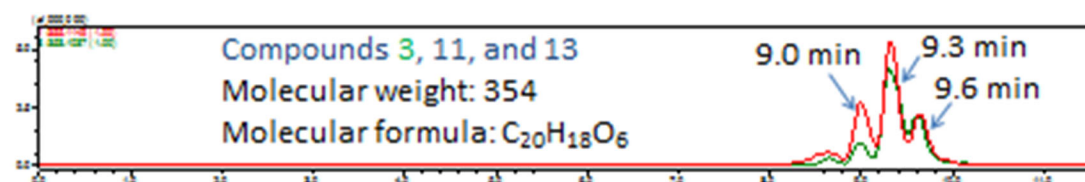
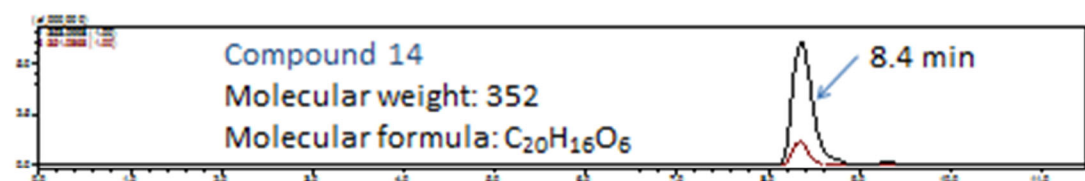
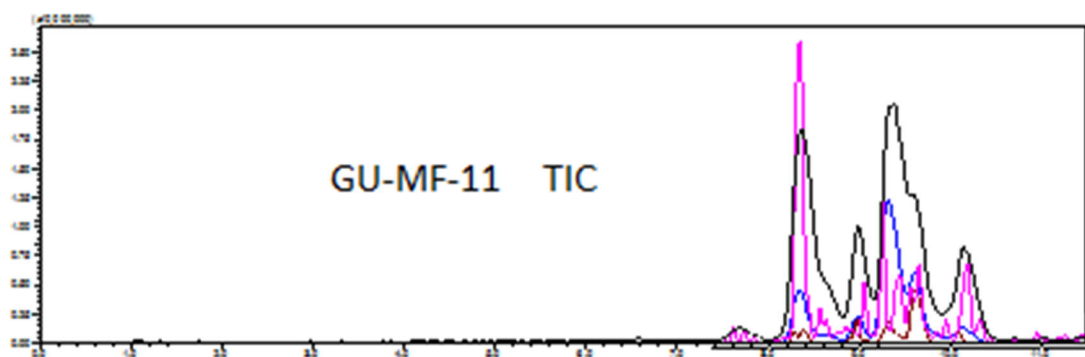


Figure S25. The IT-TOF TIC spectrum of GU-MF-11.

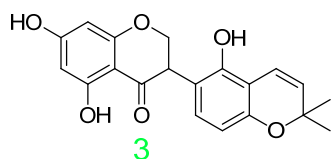
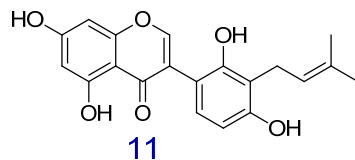
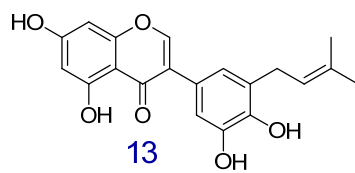
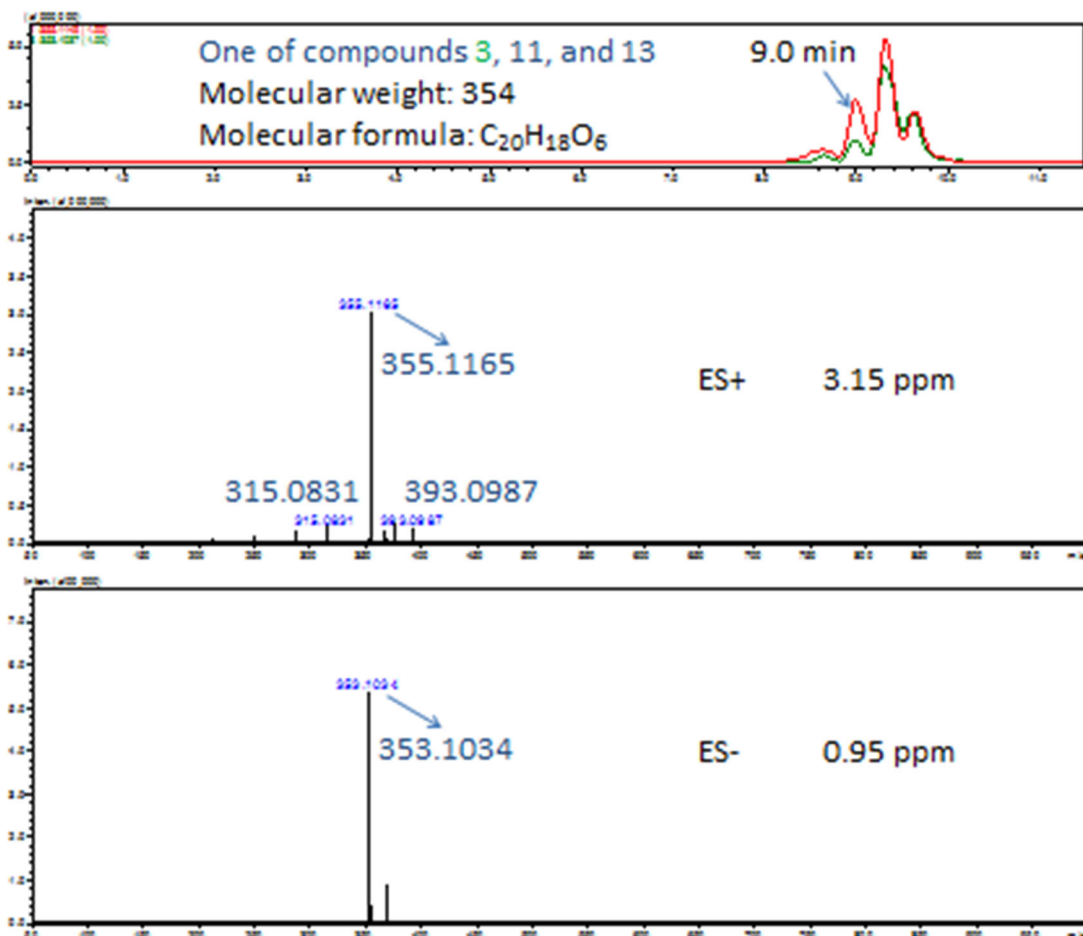


Figure S26. The (+)-HRESIMS and (−)-HRESIMS spectra of one of compounds **3**, **11**, and **13** in GU-MF-11 with extracted ions (positive and negative) for m/z 355 and 353, respectively.

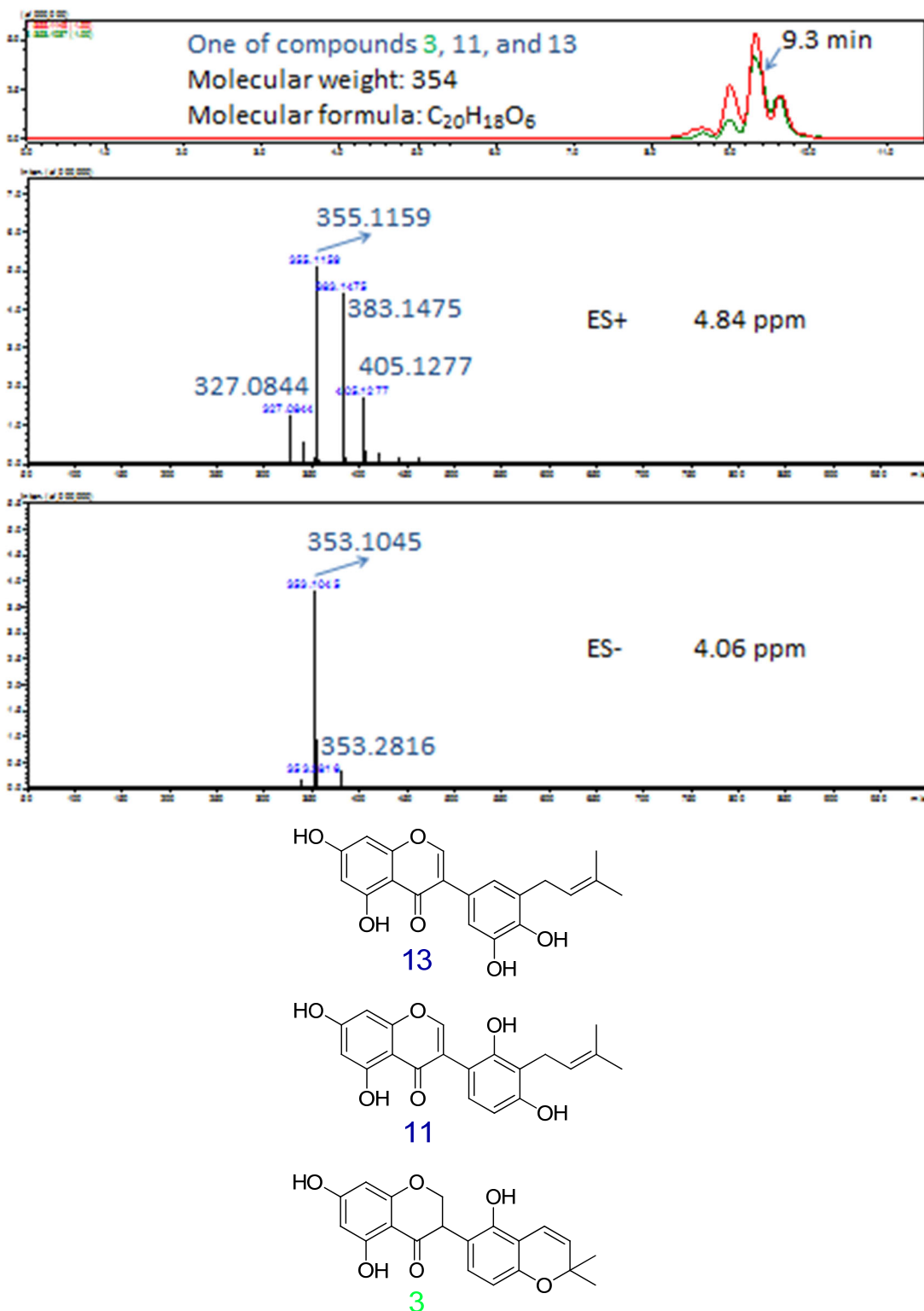


Figure S27. The (+)-HRESIMS and (-)-HRESIMS spectra of one of compounds **3**, **11**, and **13** in GU-MF-11 with extracted ions (positive and negative) for m/z 355 and 353, respectively.

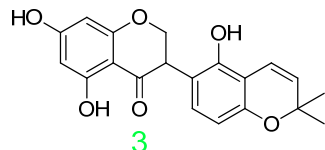
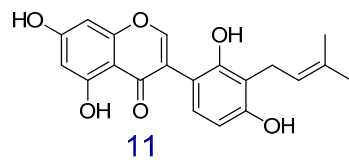
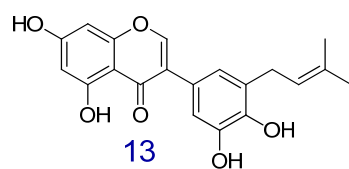
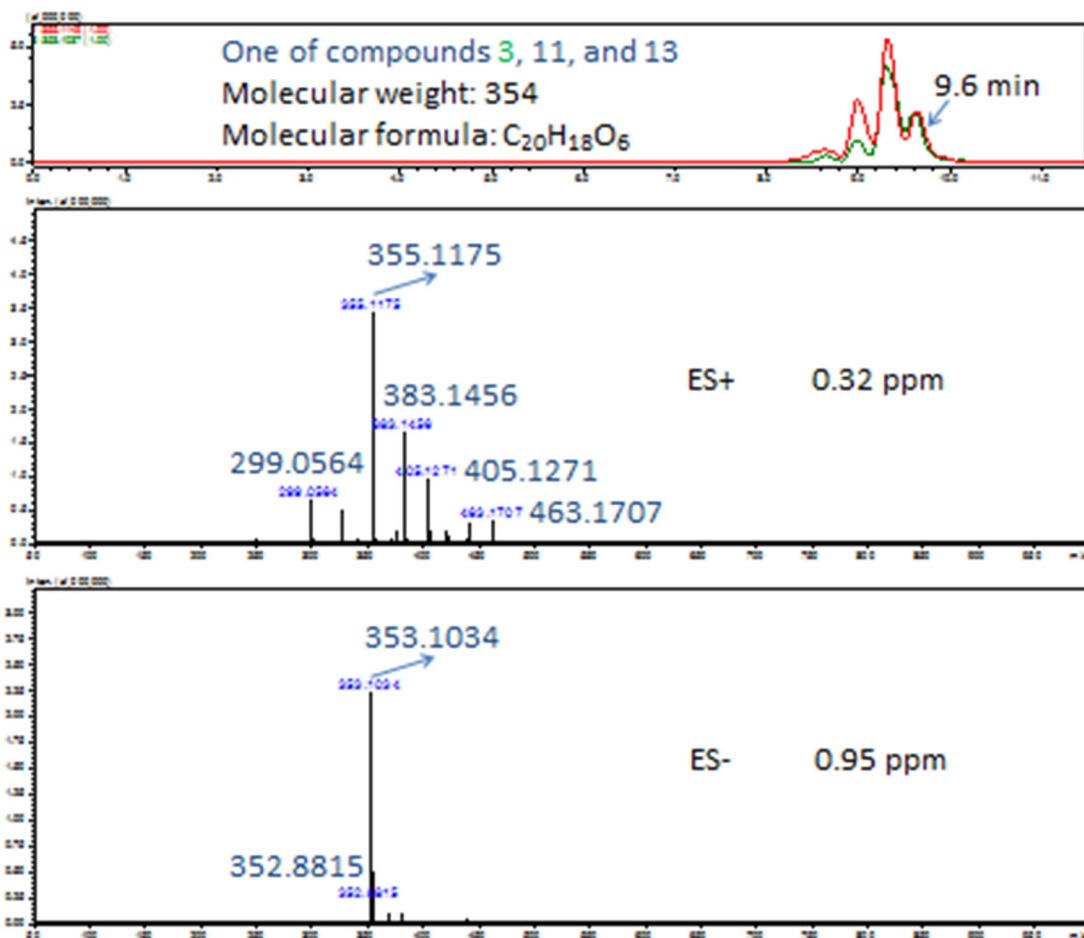


Figure S28. The (+)-HRESIMS and (-)-HRESIMS spectra of one of compounds **3**, **11**, and **13** in GU-MF-11 with extracted ions (positive and negative) for m/z 355 and 353, respectively.

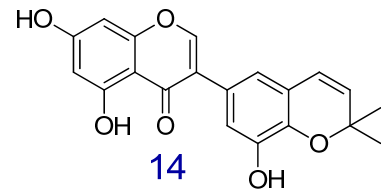
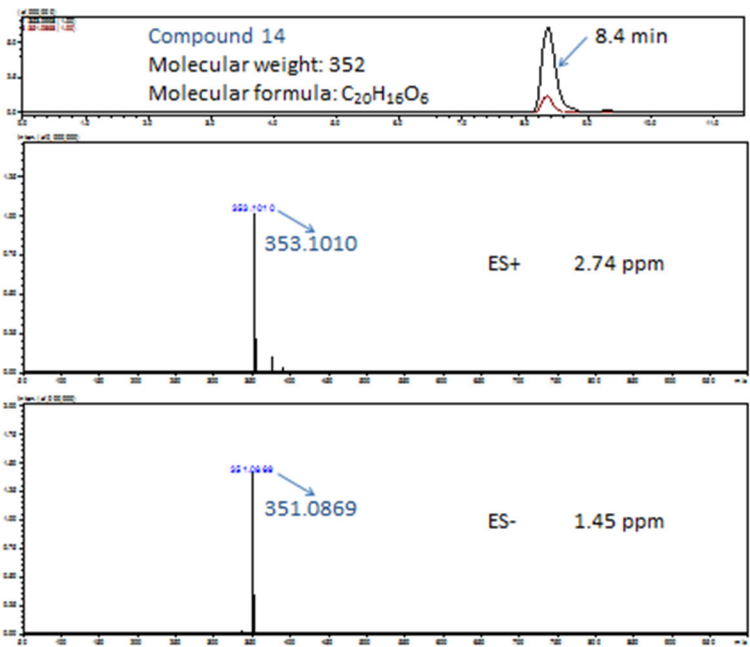


Figure S29. The (+)-HRESIMS and (-)-HRESIMS spectra of compound **14** in GU-MF-11 with extracted ions (positive and negative) for m/z 353 and 351, respectively.

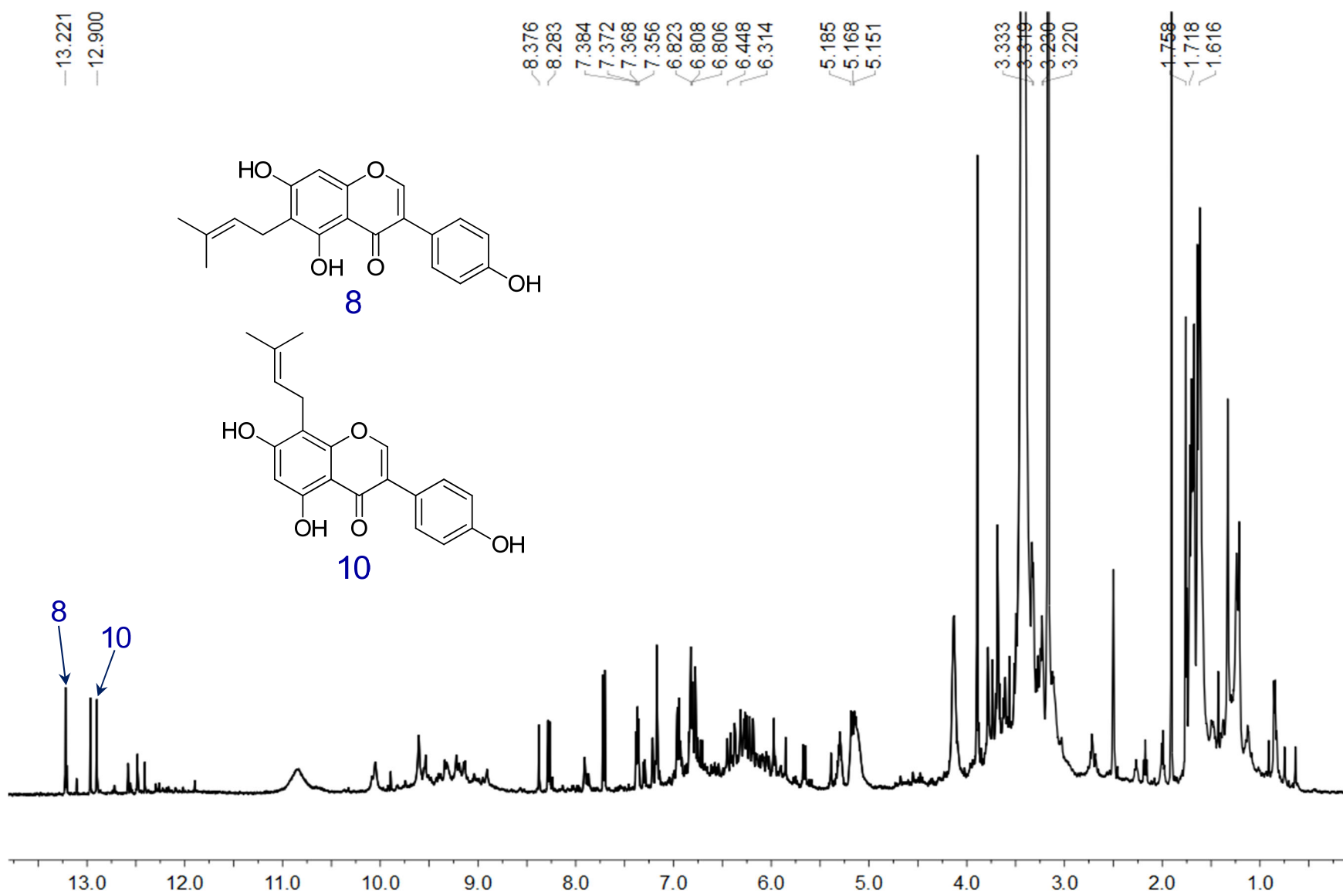


Figure S30. The ^1H NMR spectrum of GU-MF-12 in $\text{DMSO}-d_6$.

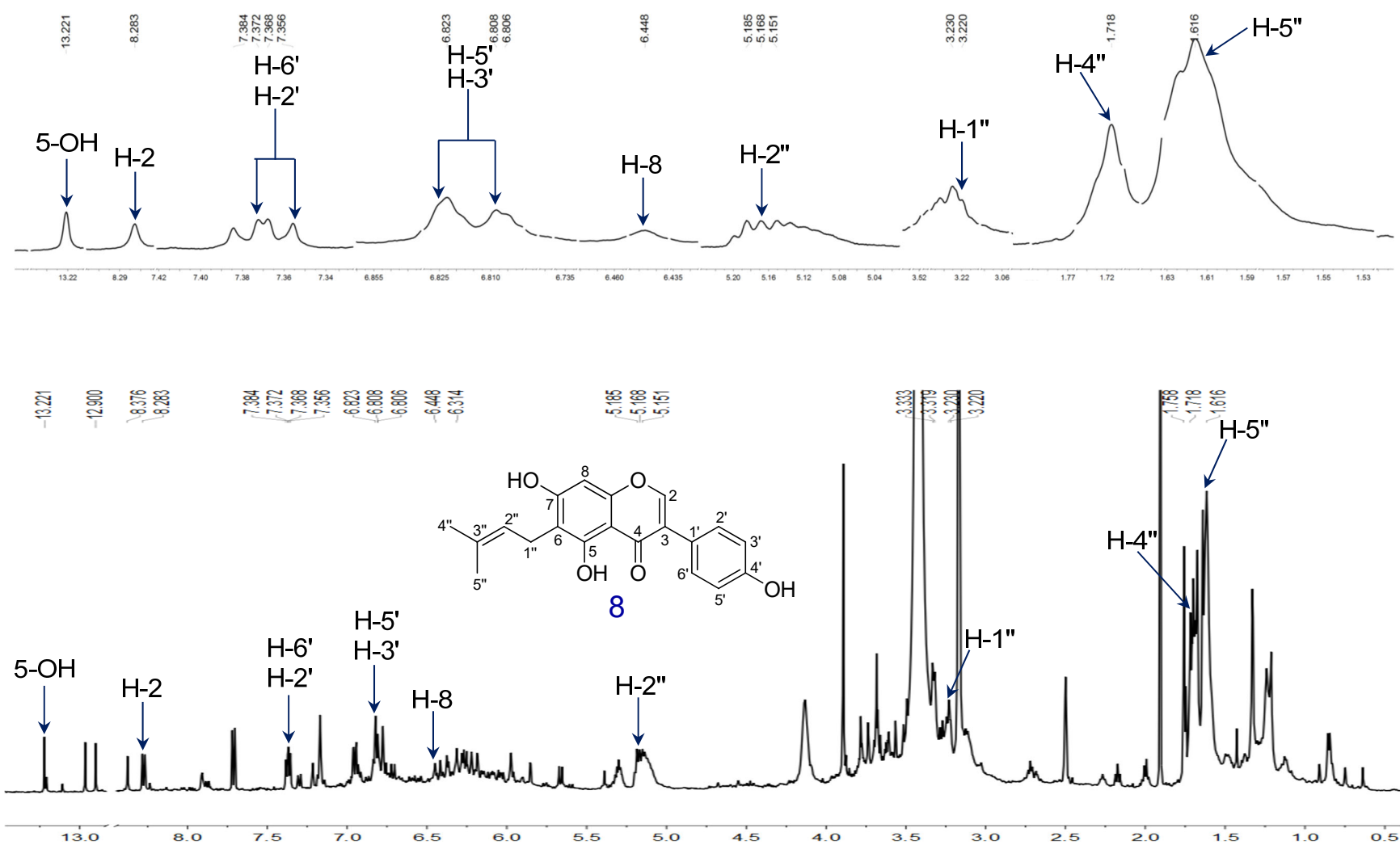


Figure S31. The ^1H NMR spectrum of compound **8** in GU-MF-12 in $\text{DMSO}-d_6$.

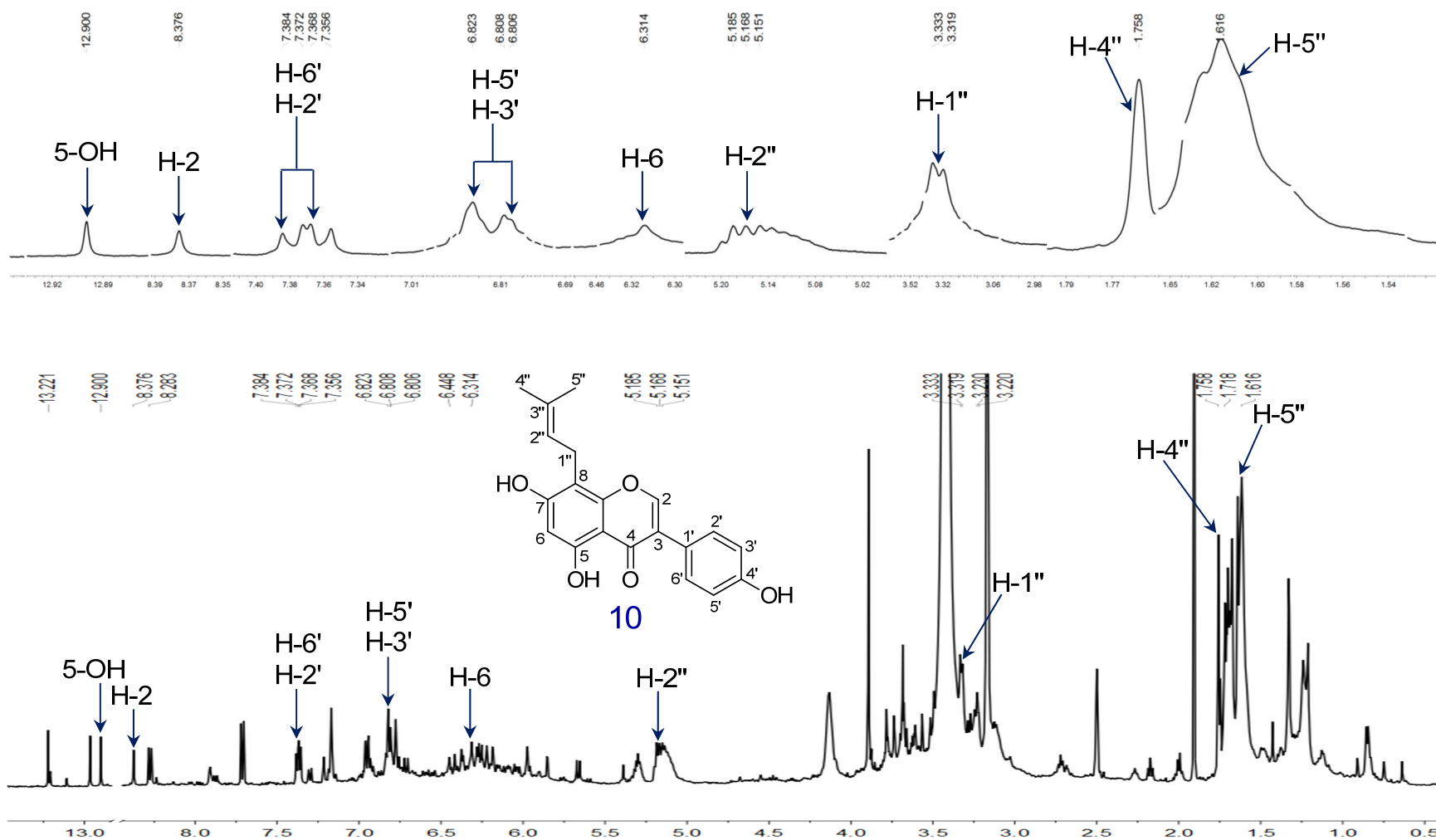


Figure S32. The ^1H NMR spectrum of compound **10** in GU-MF-12 in $\text{DMSO}-d_6$.

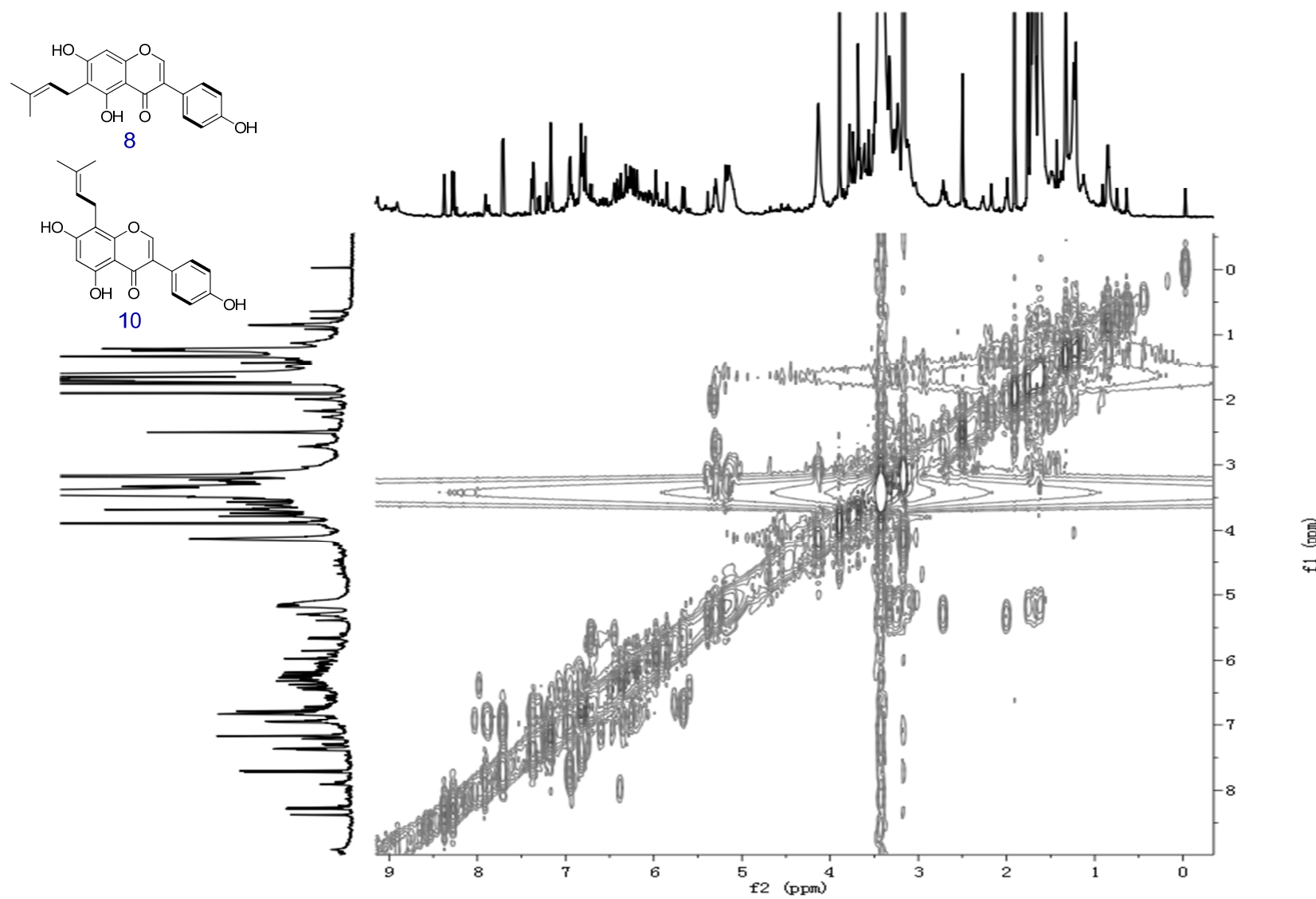


Figure S33. The ${}^1\text{H}$ - ${}^1\text{H}$ COSY spectrum of GU-MF-12 in $\text{DMSO}-d_6$.

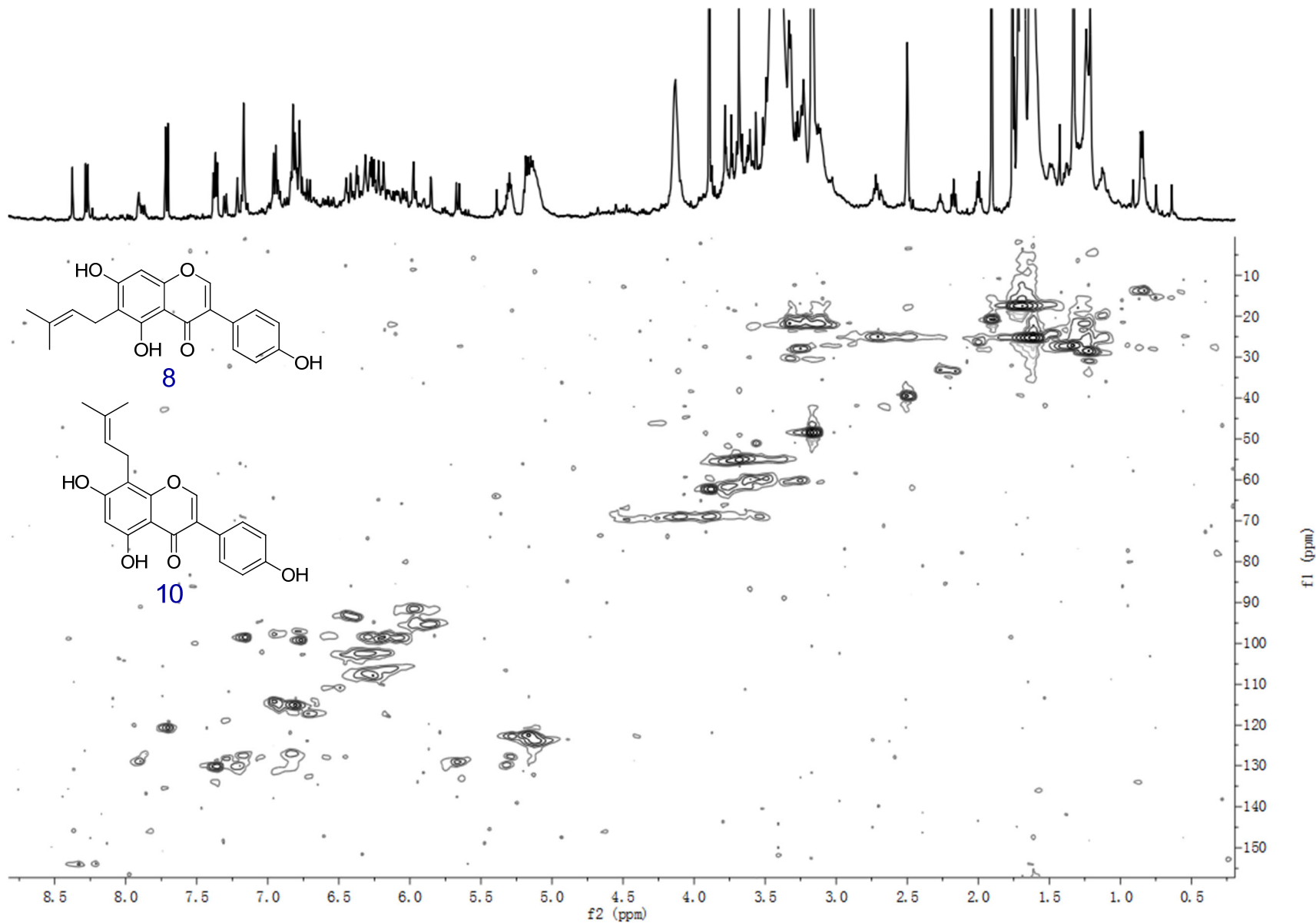


Figure S34. The HSQC spectrum of GU-MF-12 in $\text{DMSO}-d_6$.

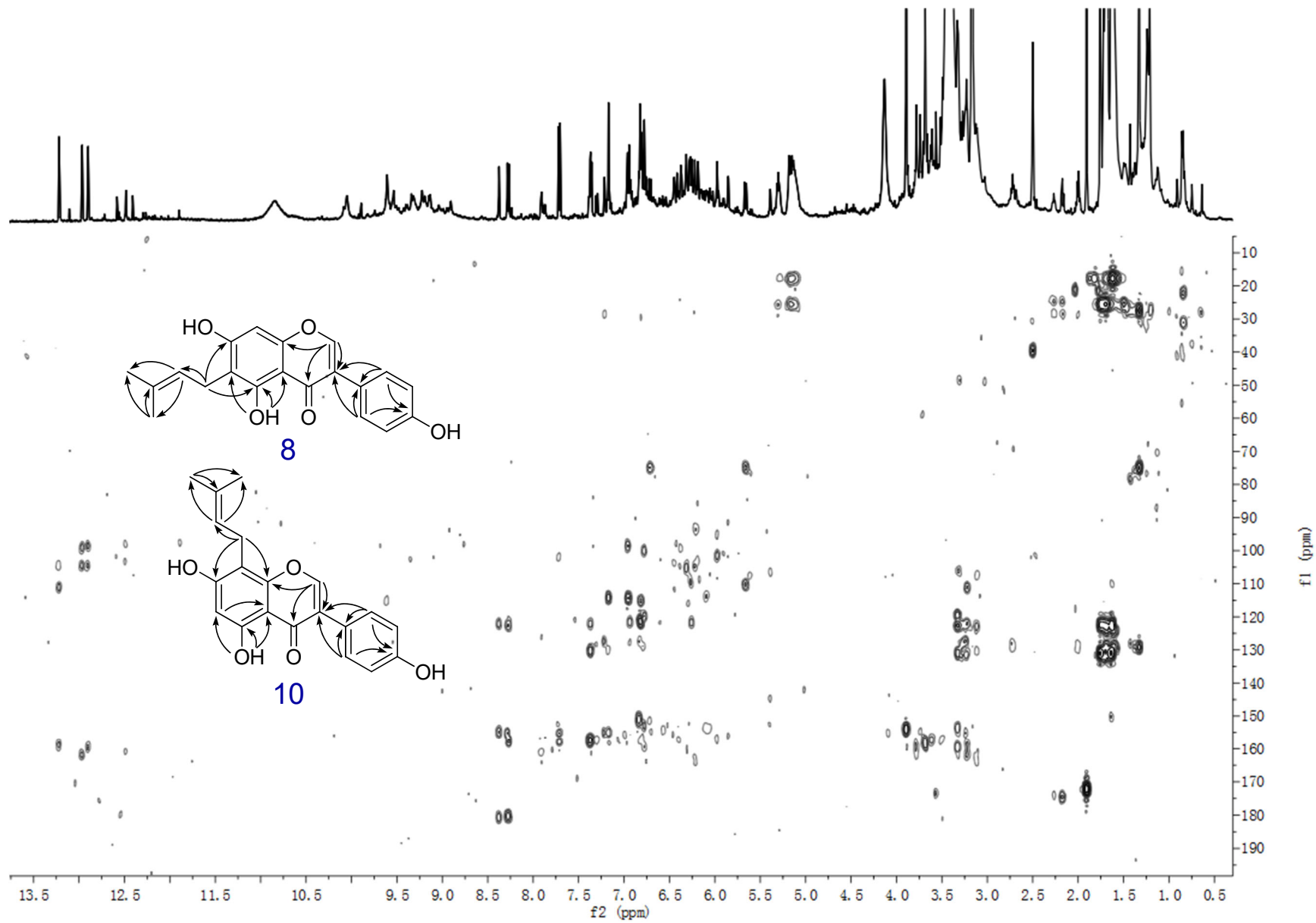


Figure S35. The HMBC spectrum of GU-MF-12 in $\text{DMSO}-d_6$.

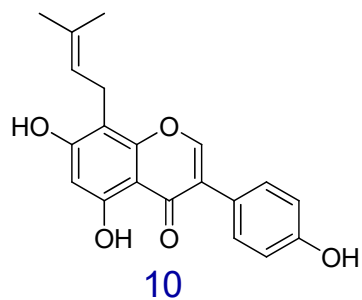
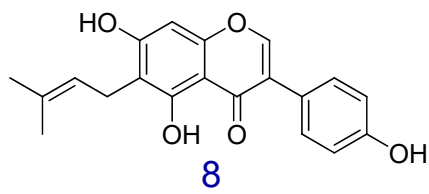
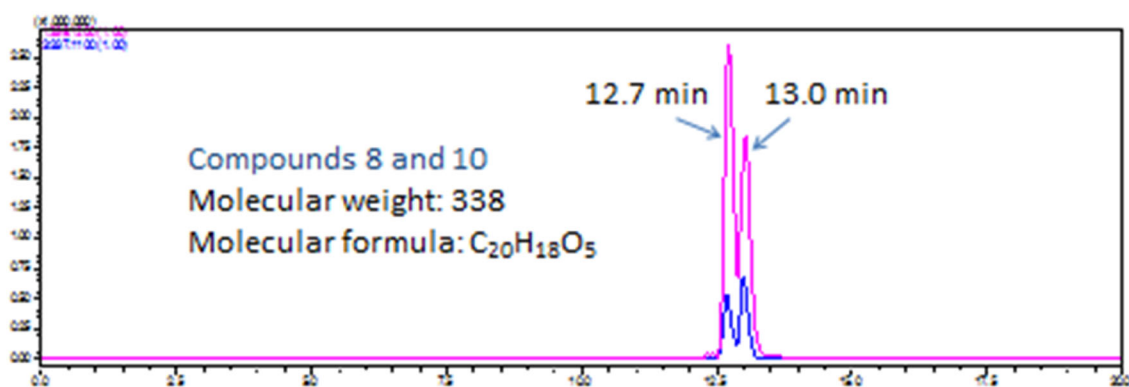
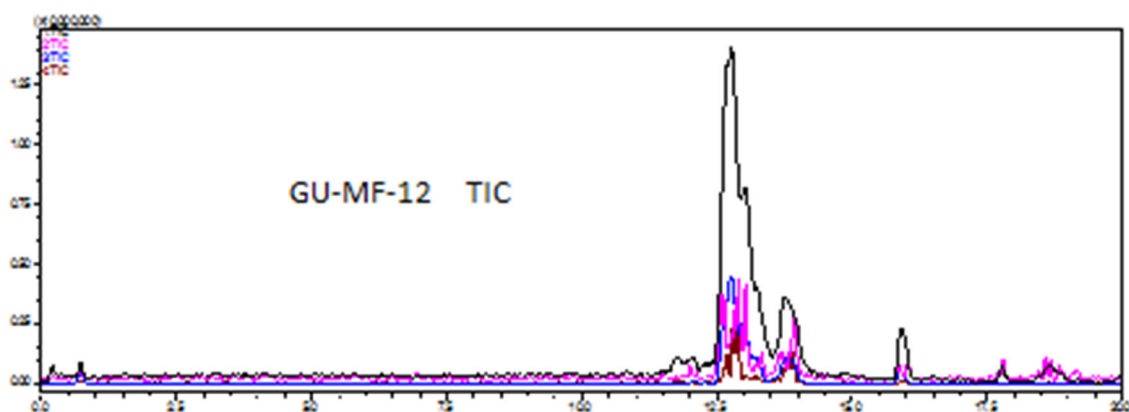


Figure S36. The IT-TOF TIC spectrum of GU-MF-12.

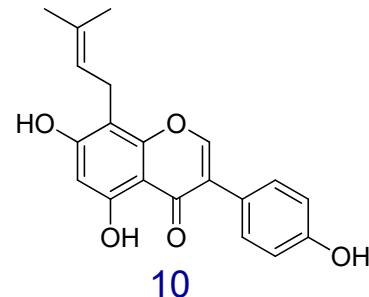
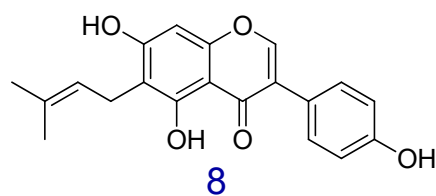
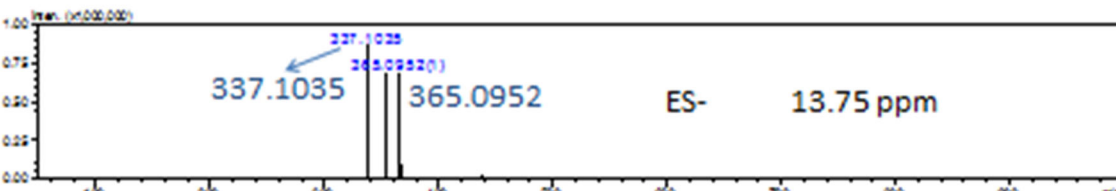
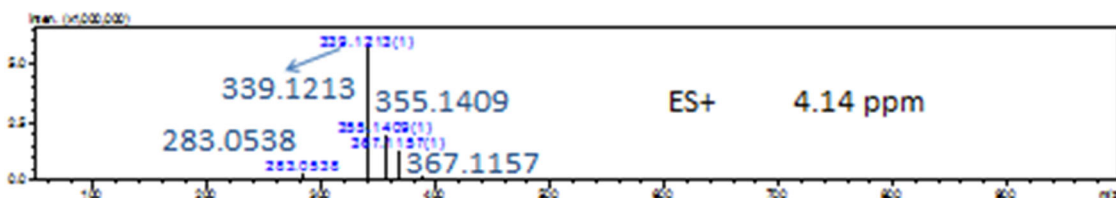
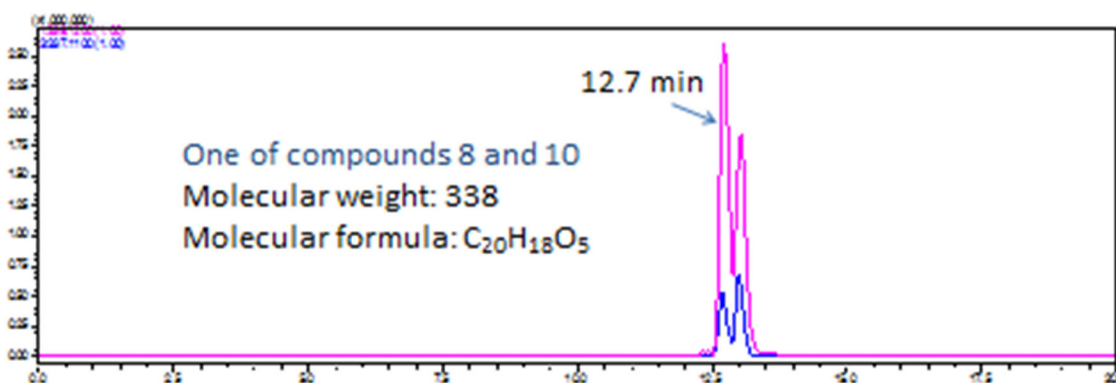


Figure S37. The (+)-HRESIMS and (-)-HRESIMS spectra of one of compounds **8** and **10** in GU-MF-12 with extracted ions (positive and negative) for *m/z* 339 and 337, respectively.

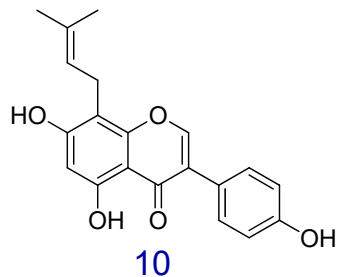
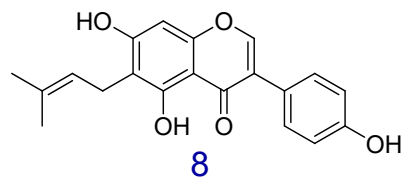
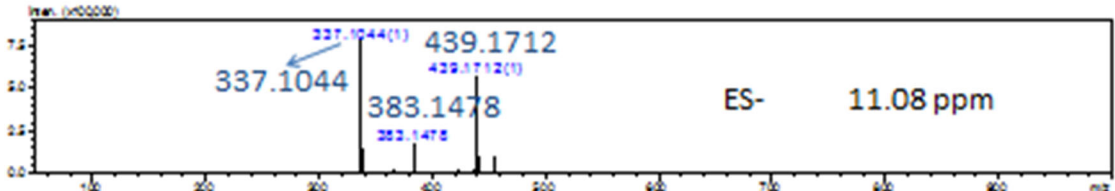
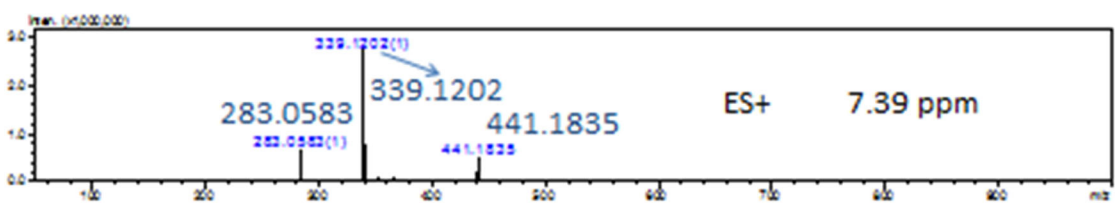
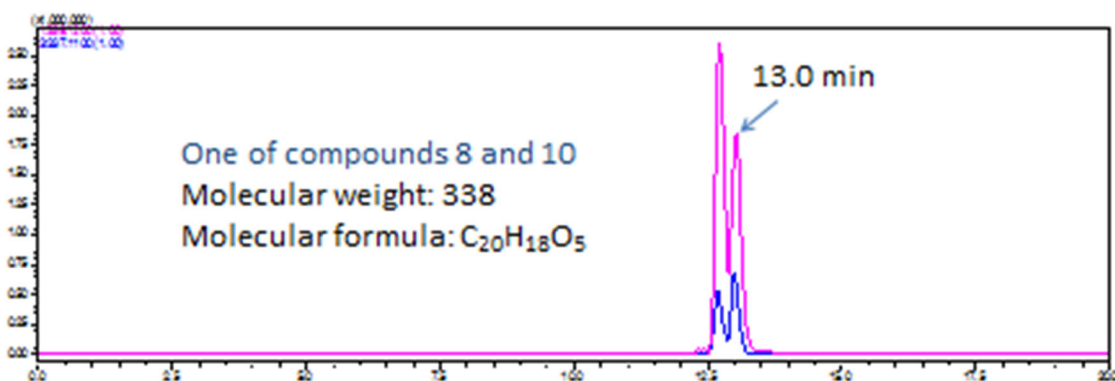


Figure S38. The (+)-HRESIMS and (-)-HRESIMS spectra of one of the compounds **8** and **10** in GU-MF-12 with extracted ions (positive and negative) for m/z 339 and 337, respectively.

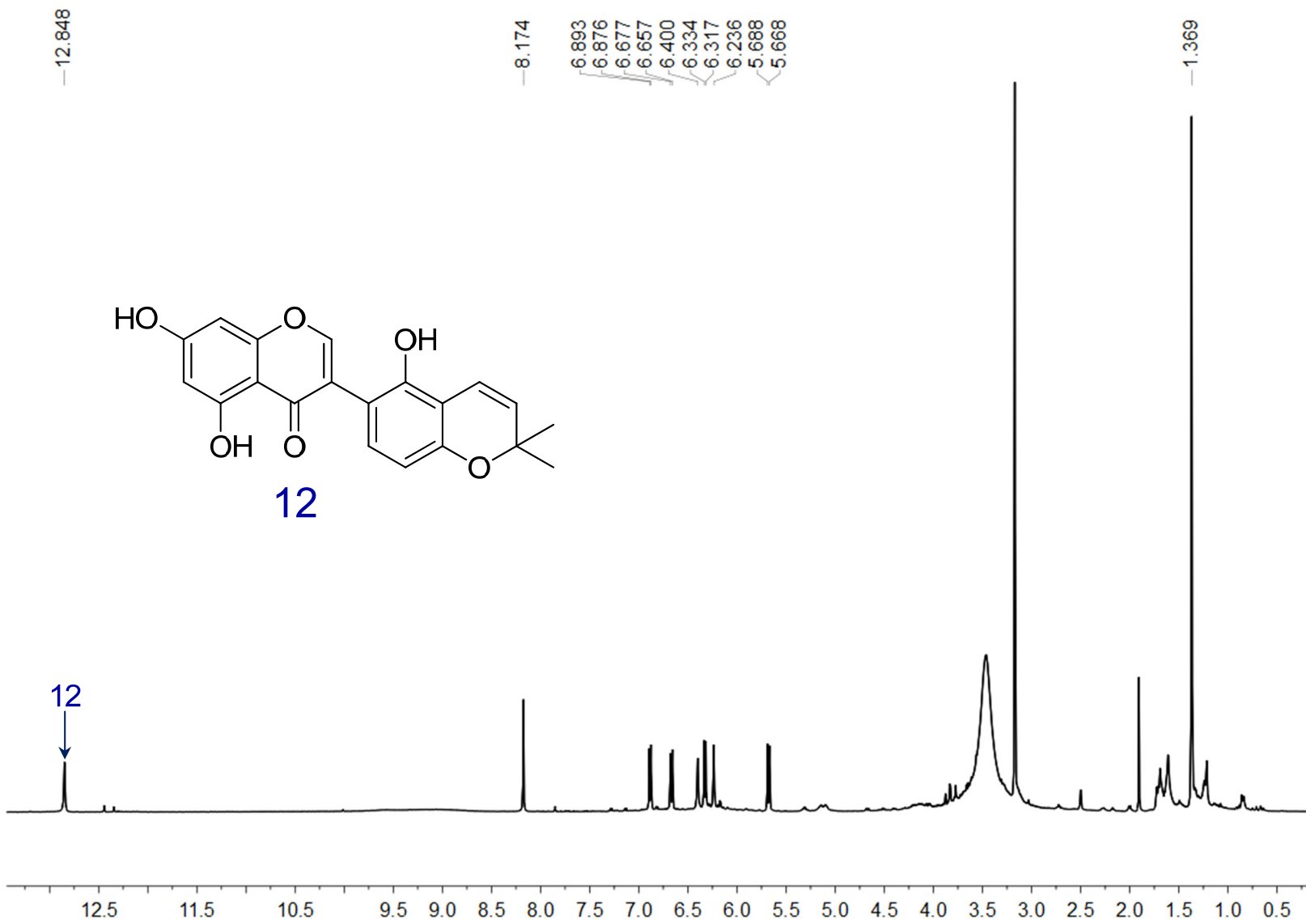


Figure S39. The ^1H NMR spectrum of GU-MF-14 in $\text{DMSO}-d_6$.

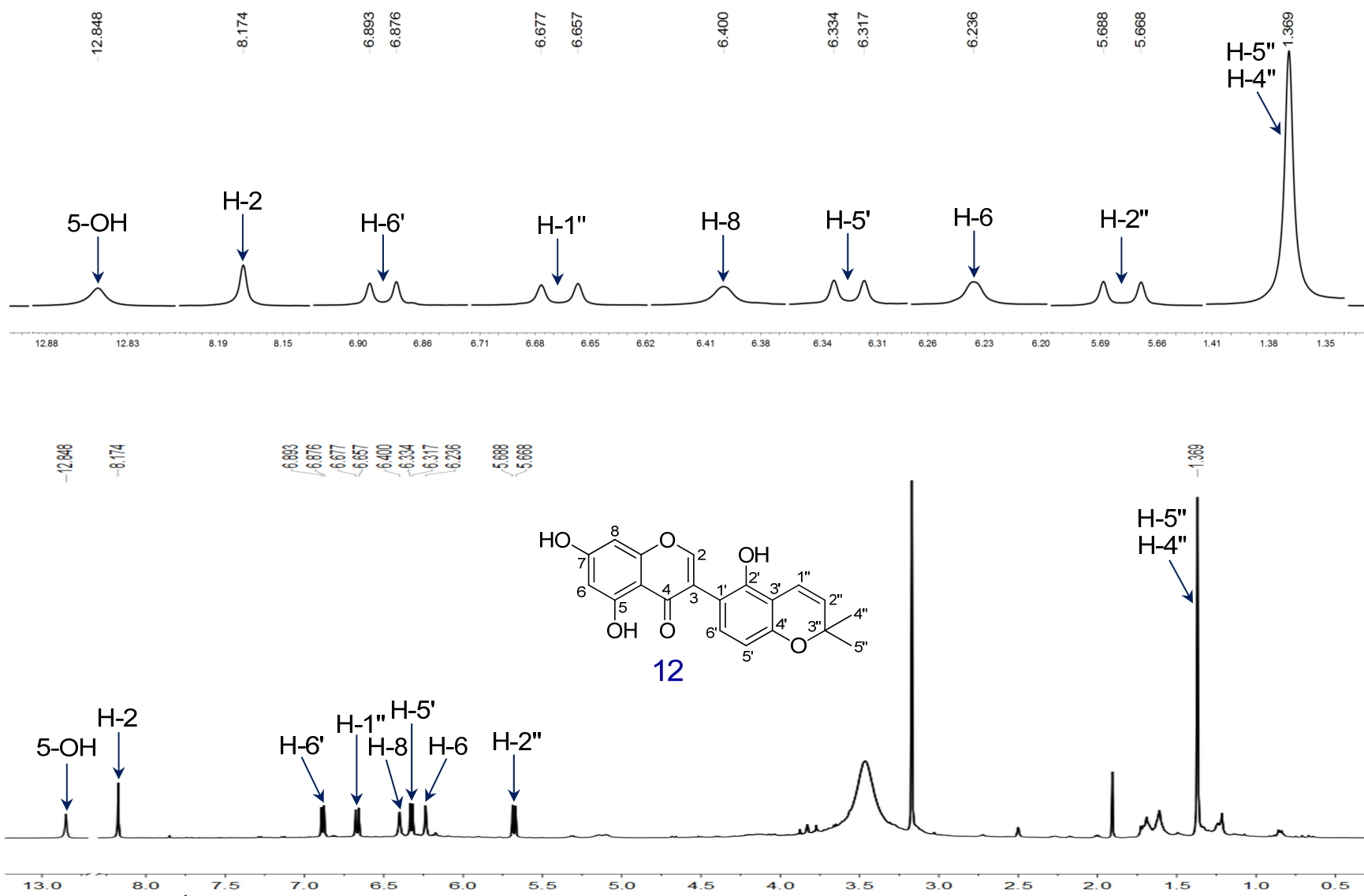


Figure S40. The ^1H NMR spectrum of compound **12** in GU-MF-14 in $\text{DMSO}-d_6$.

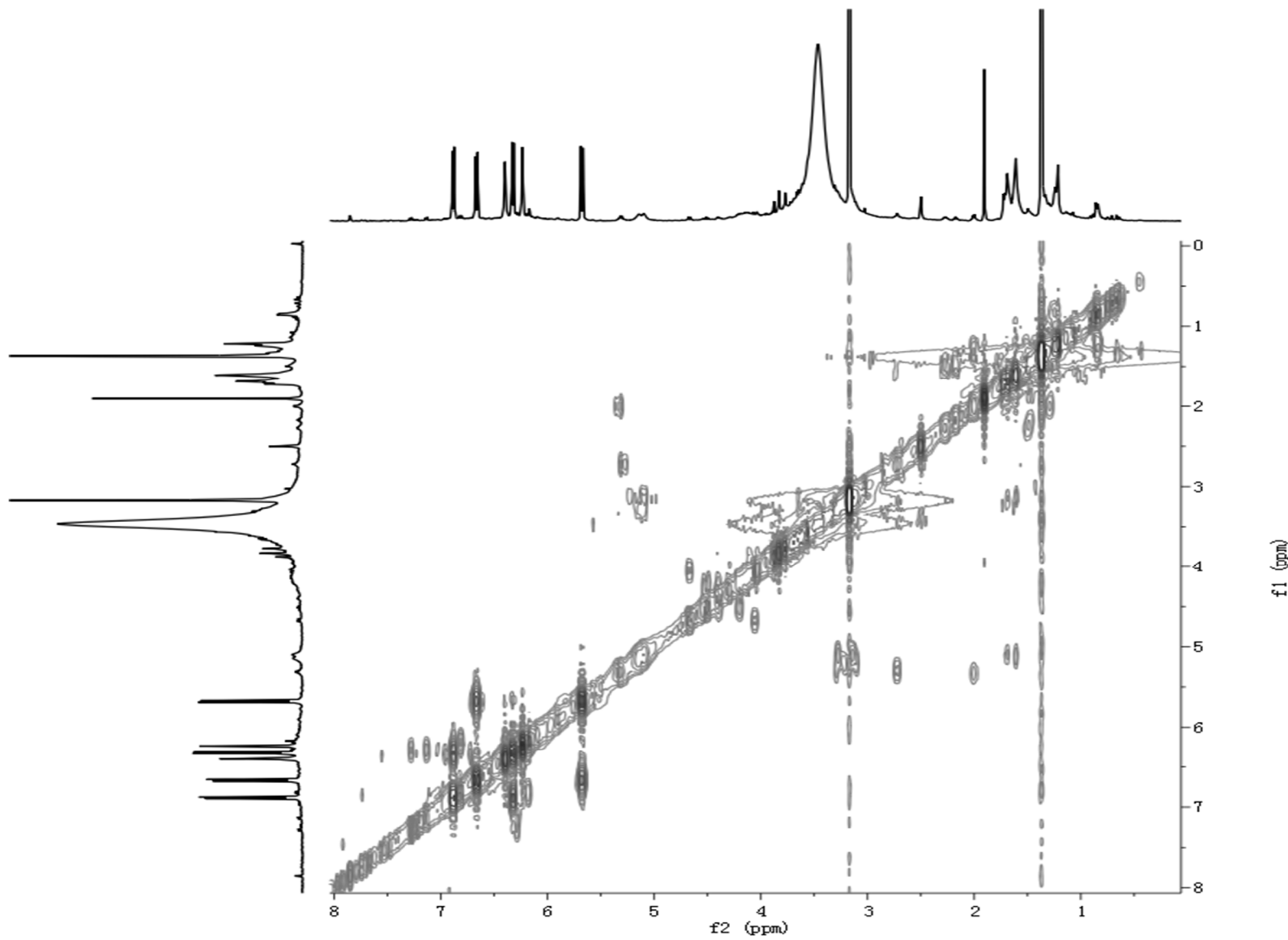


Figure S41. The ^1H - ^1H COSY spectrum of GU-MF-14 in $\text{DMSO}-d_6$.

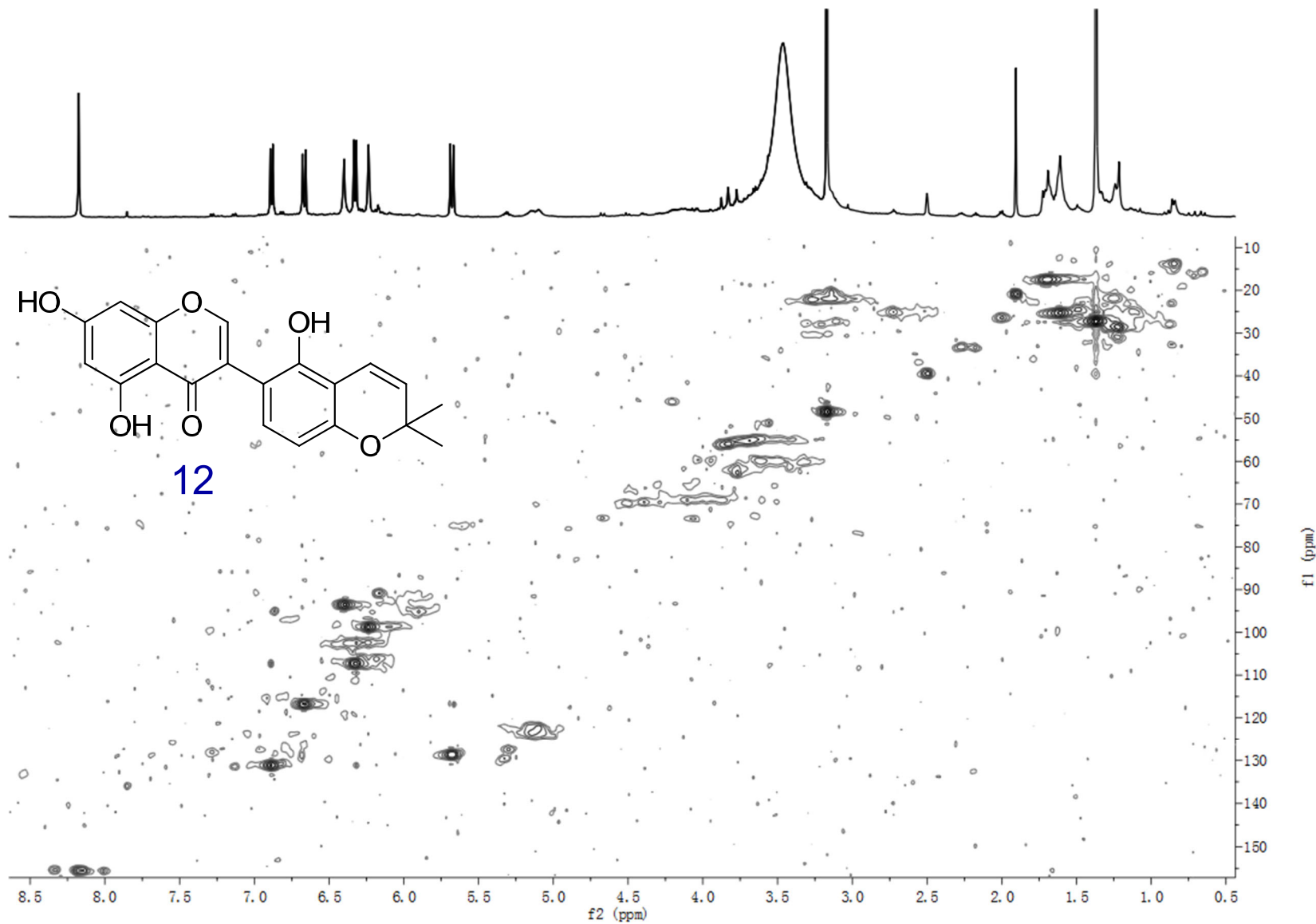


Figure S42. The HSQC spectrum of GU-MF-14 in DMSO-*d*6.

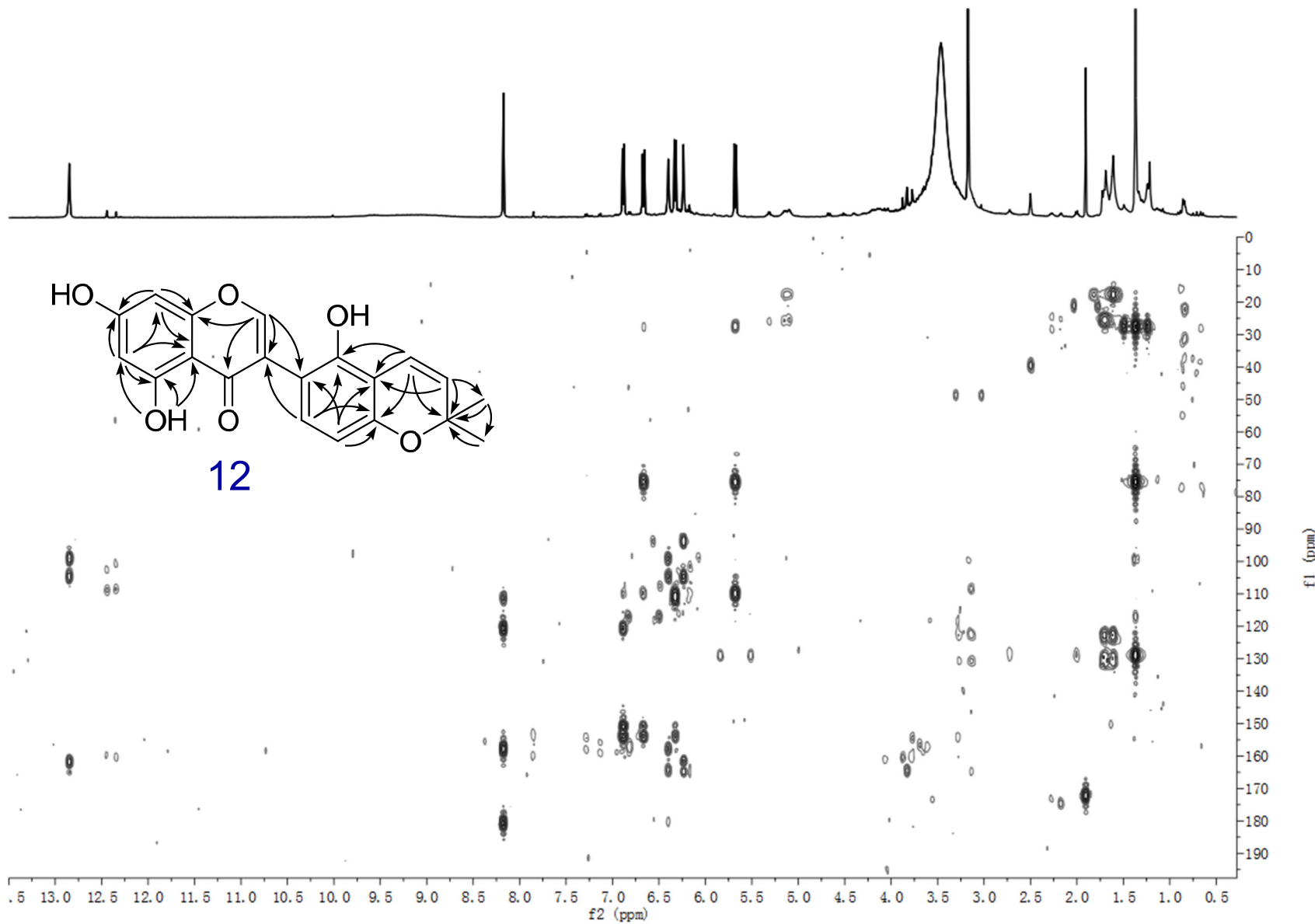


Figure S43. The HMBC spectrum of GU-MF-14 in DMSO-*d*₆.

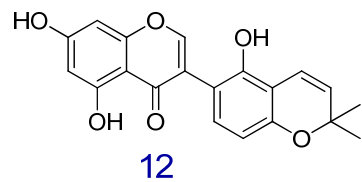
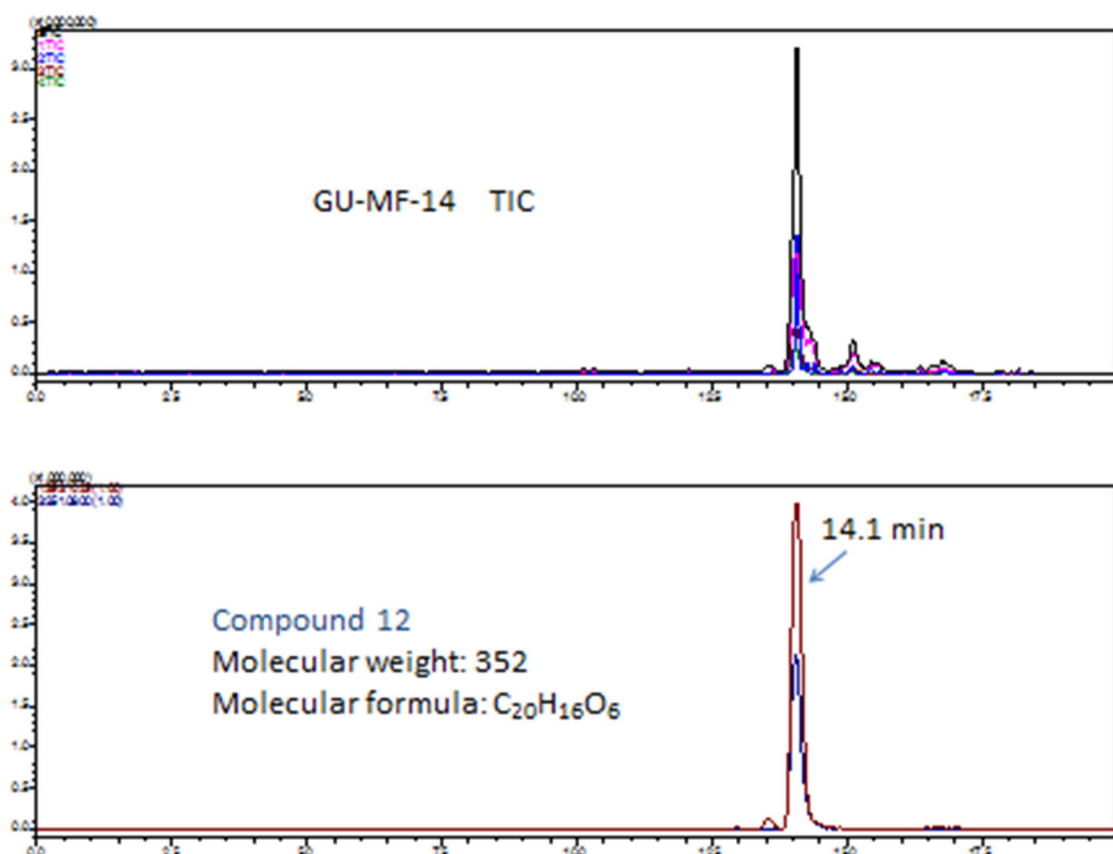


Figure S44. The IT-TOF TIC spectrum of GU-MF-14.

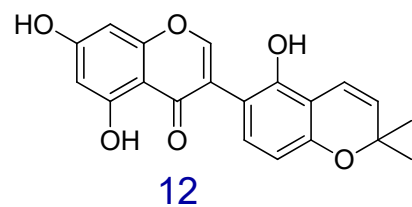
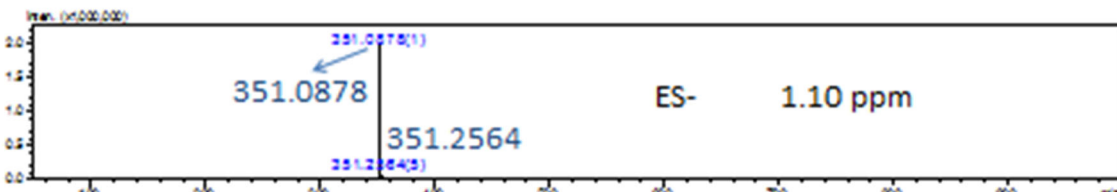
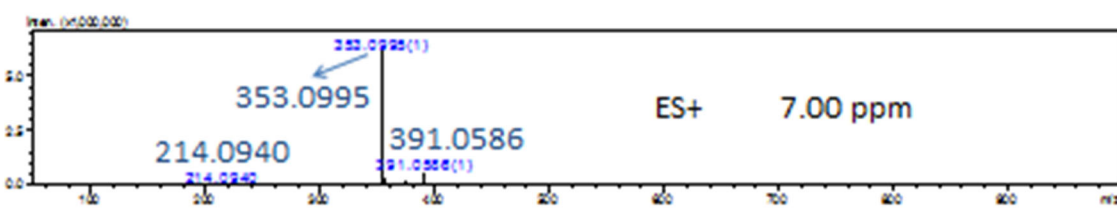
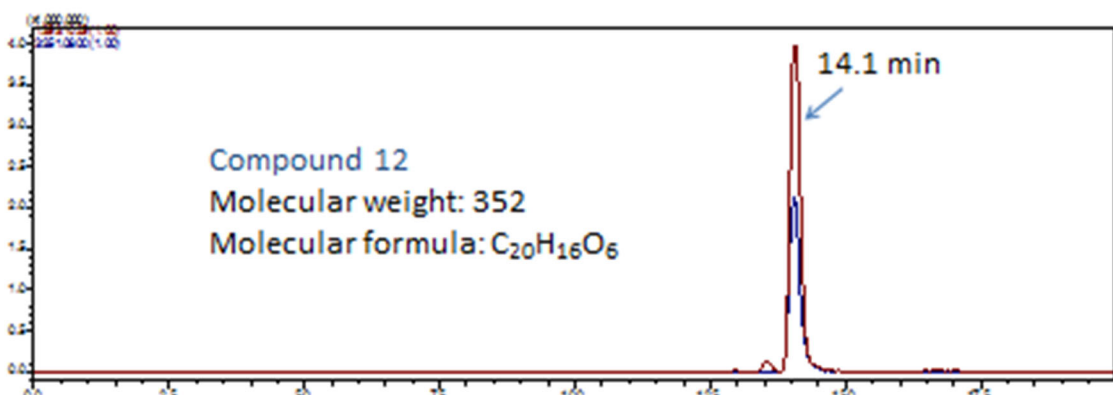


Figure S45. The (+)-HRESIMS and (-)-HRESIMS spectra of compound **12** in GU-MF-14 with extracted ions (positive and negative) for m/z 353 and 351, respectively.

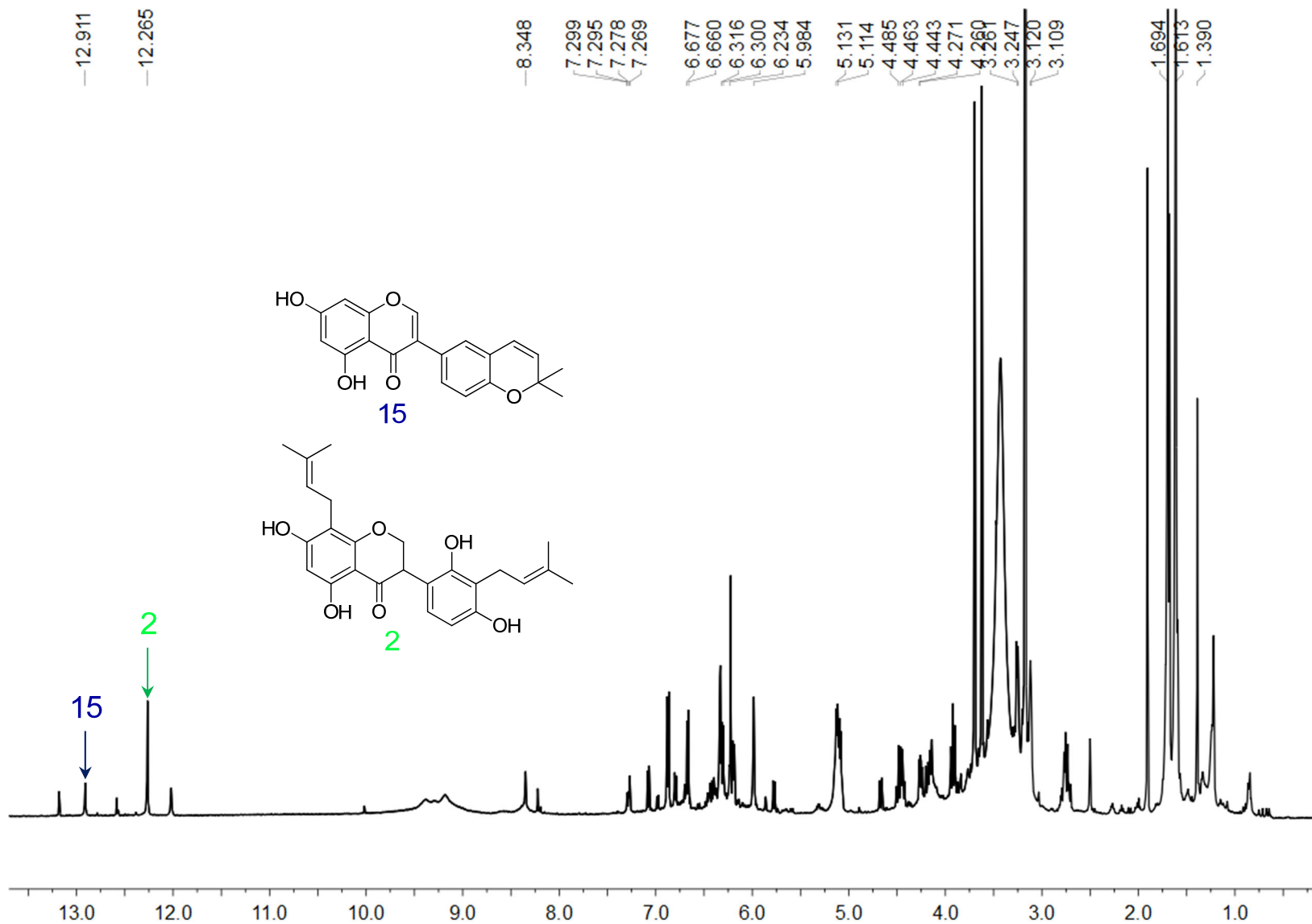


Figure S46. The ^1H NMR spectrum of GU-MF-15 in $\text{DMSO}-d_6$.

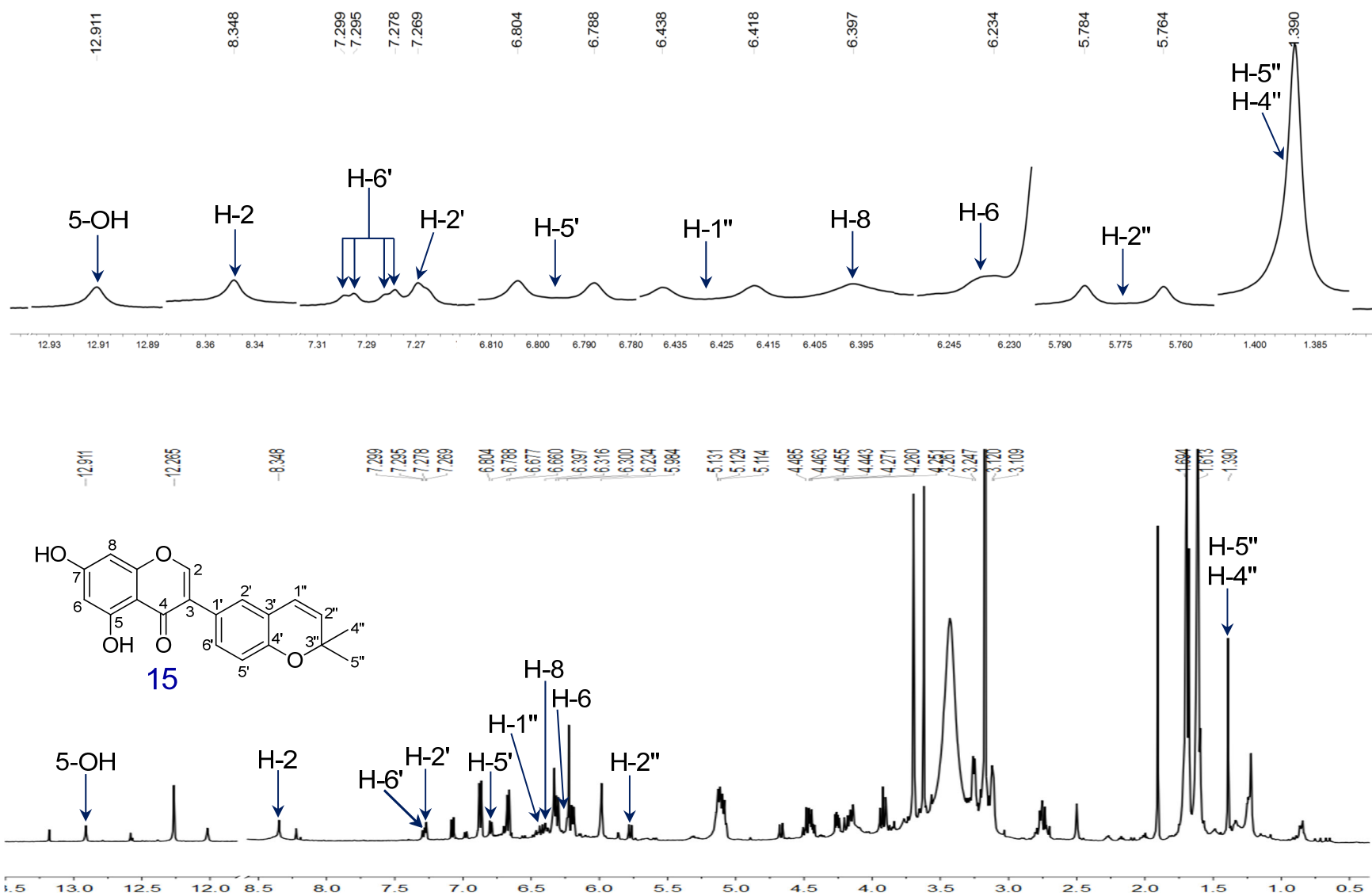


Figure S47. The ^1H NMR spectrum of compound **15** in GU-MF-15 in $\text{DMSO}-d_6$.

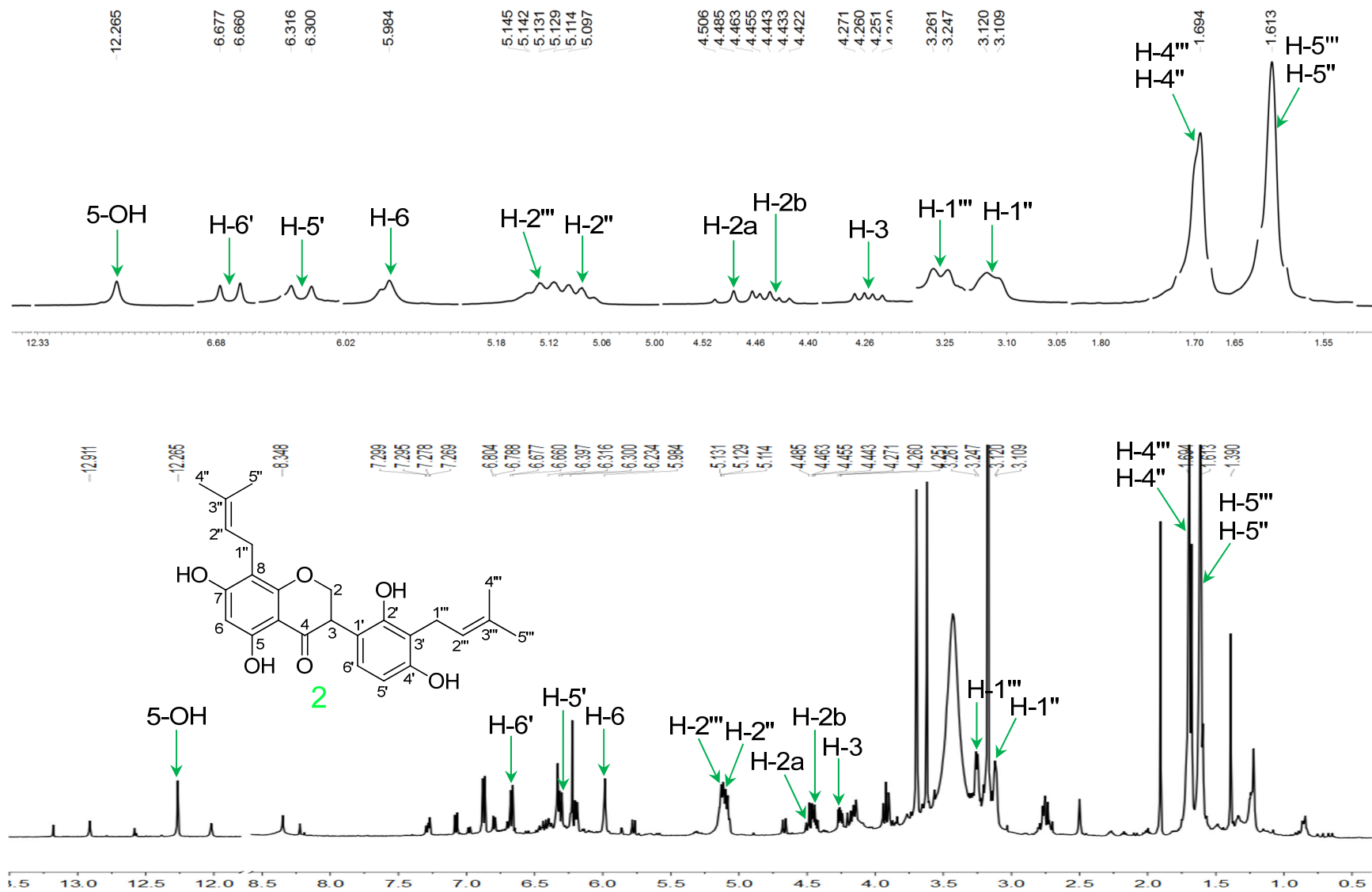


Figure S48. The ¹H NMR spectrum of compound **2** in GU-MF-15 in DMSO-*d*₆.

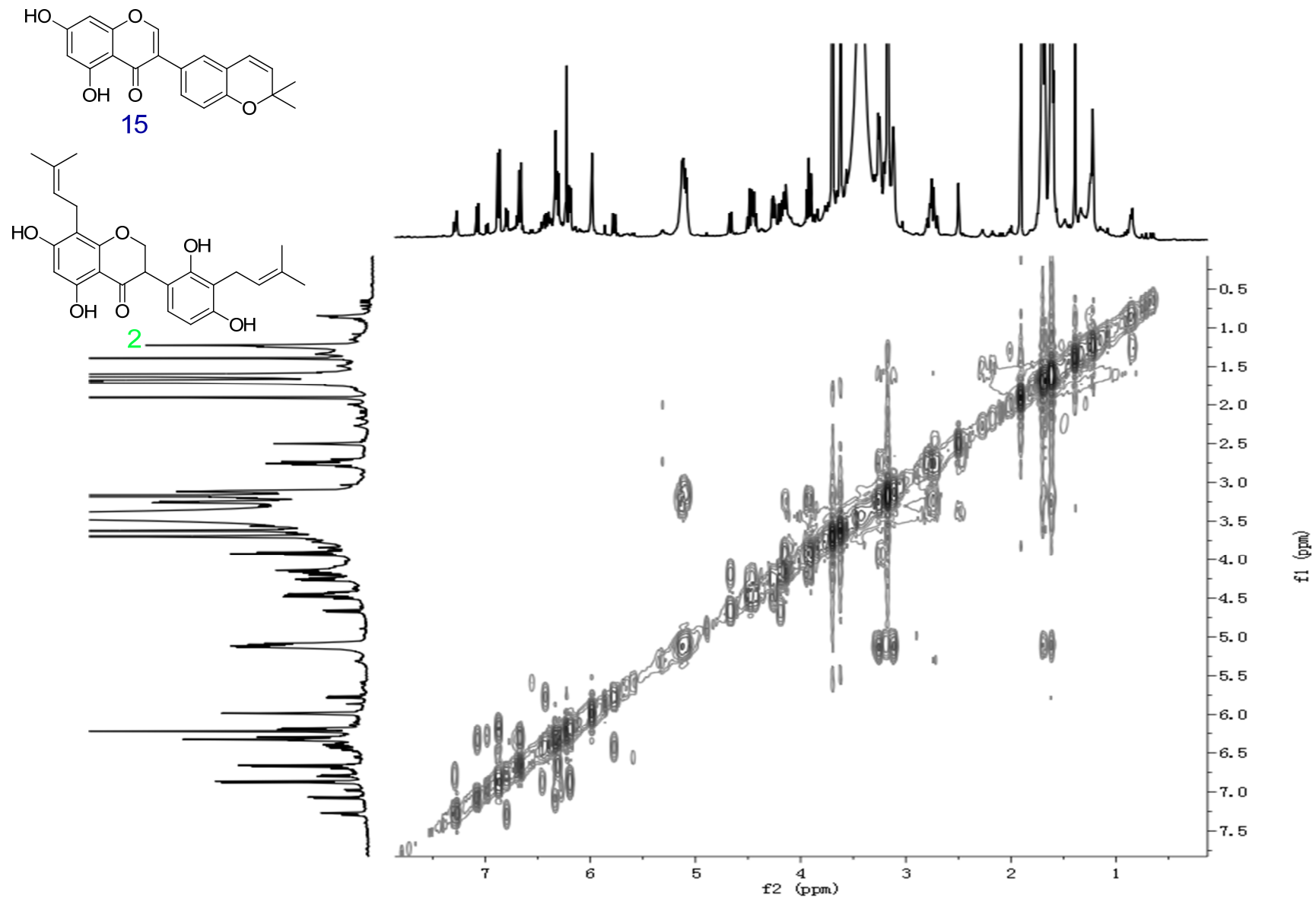


Figure S49. The ^1H - ^1H COSY spectrum of GU-MF-15 in $\text{DMSO}-d_6$.

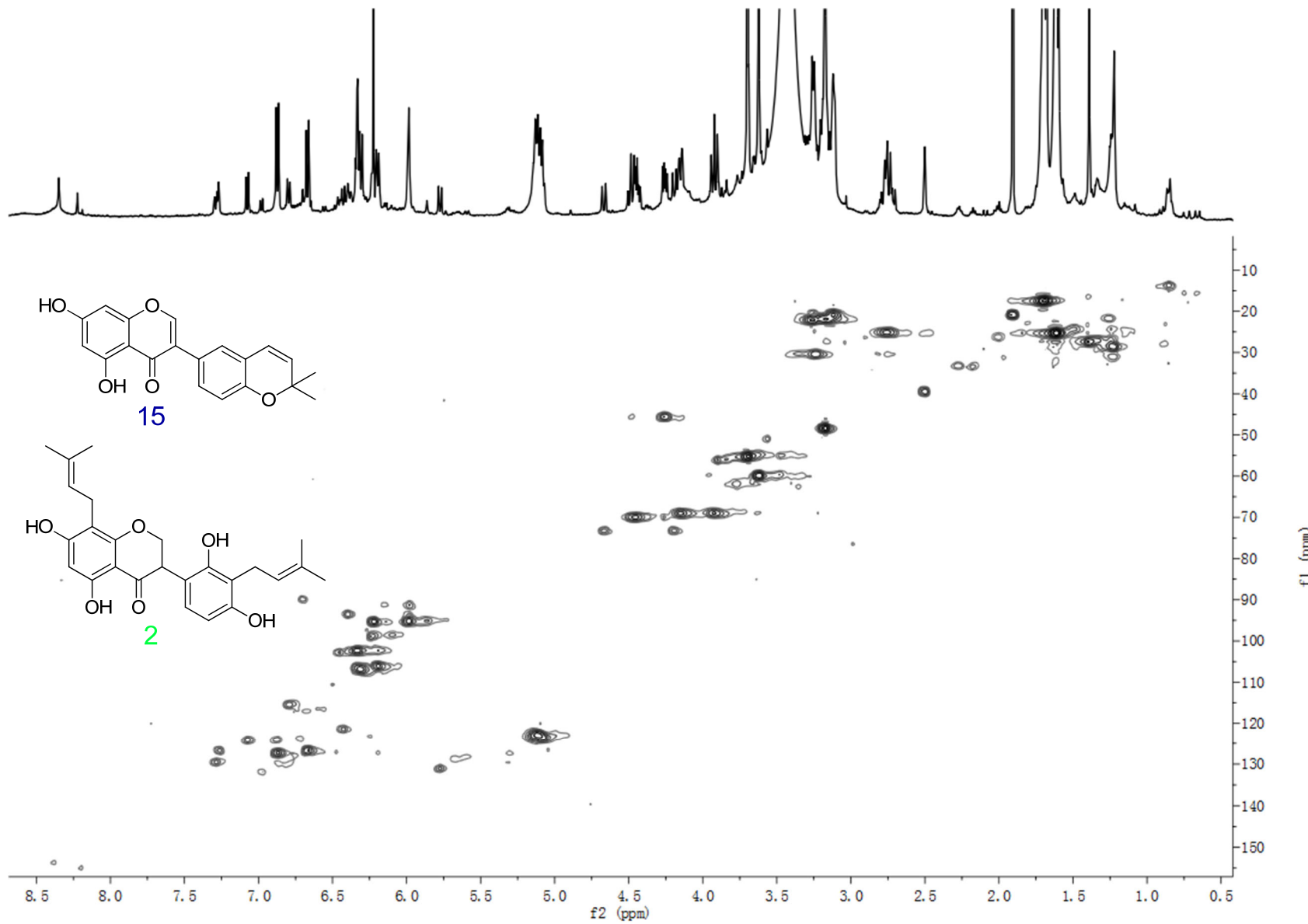


Figure S50. The HSQC spectrum of GU-MF-15 in $\text{DMSO}-d_6$.

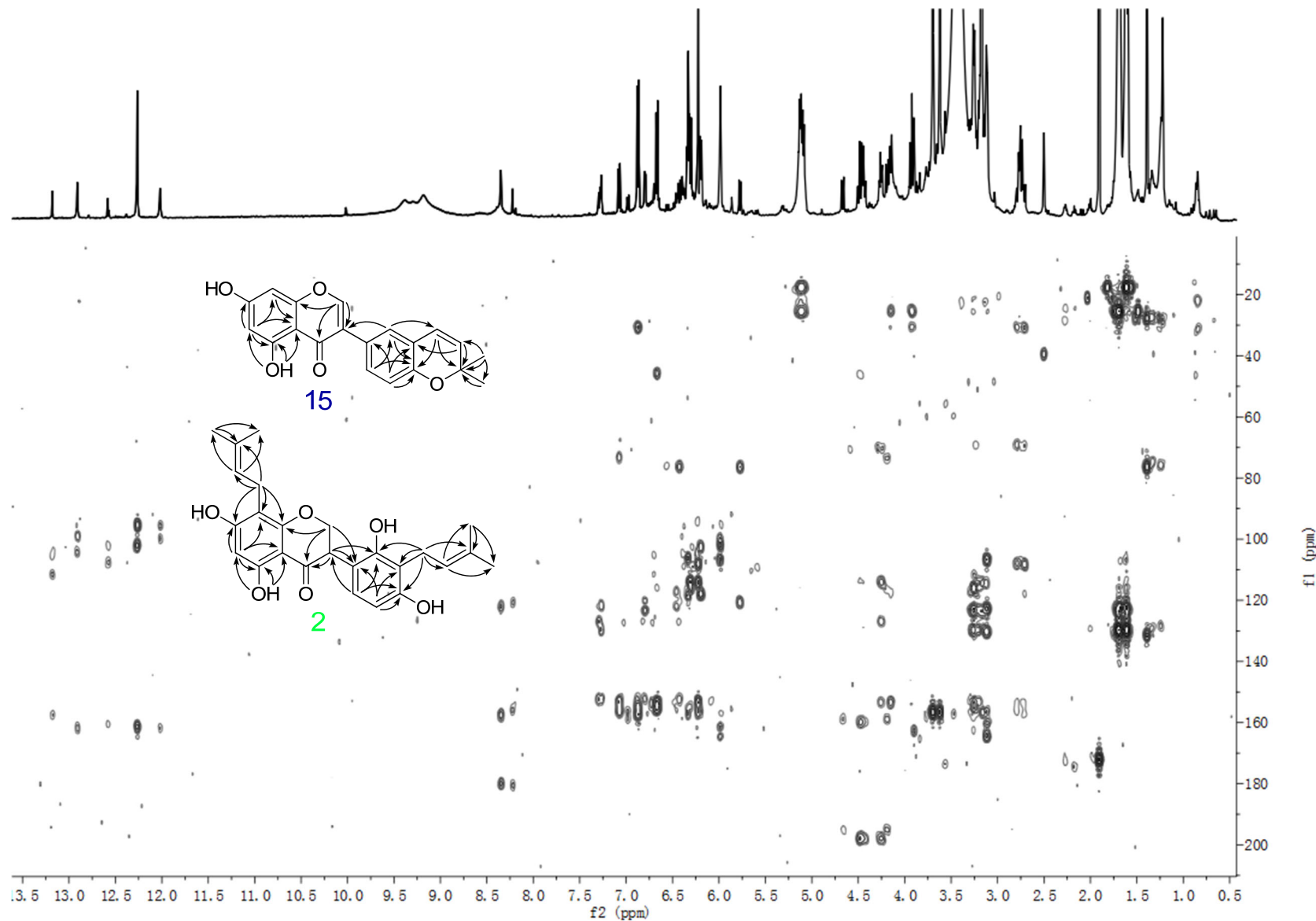


Figure S51. The HMBC spectrum of GU-MF-15 in $\text{DMSO}-d_6$.

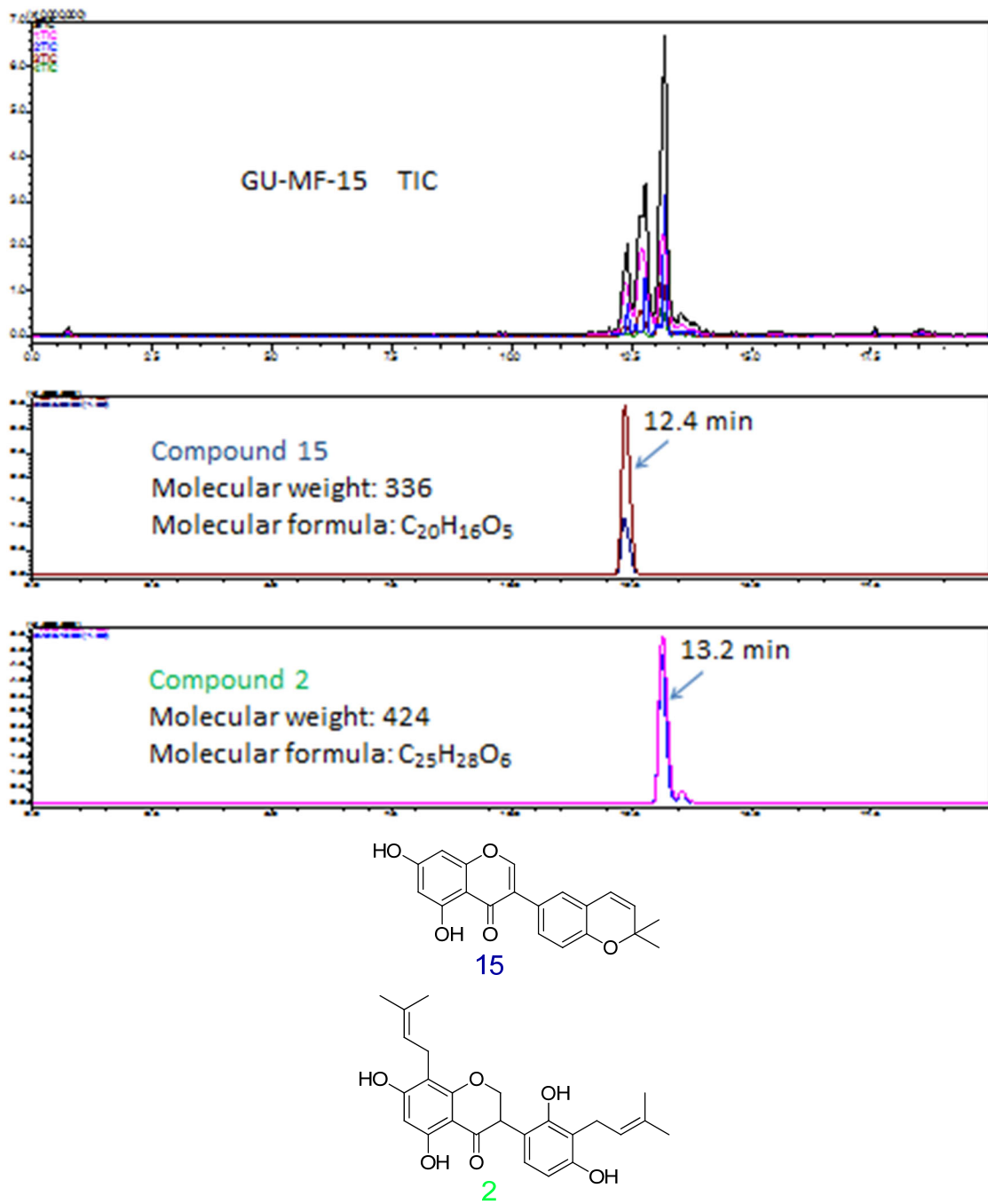


Figure S52. The IT-TOF TIC spectrum of GU-MF-15.

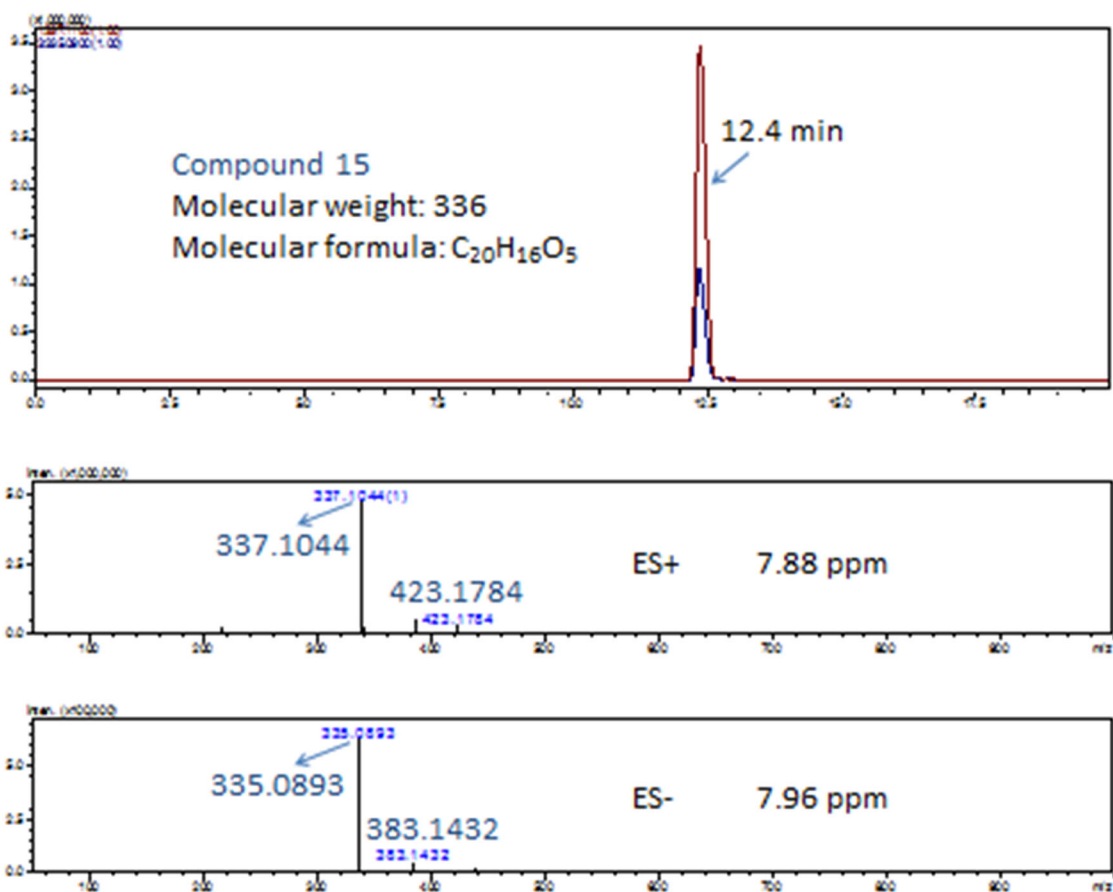


Figure S53. The (+)-HRESIMS and (-)-HRESIMS spectra of compound **15** in GU-MF-15 with extracted ions (positive and negative) for m/z 337 and 335, respectively.

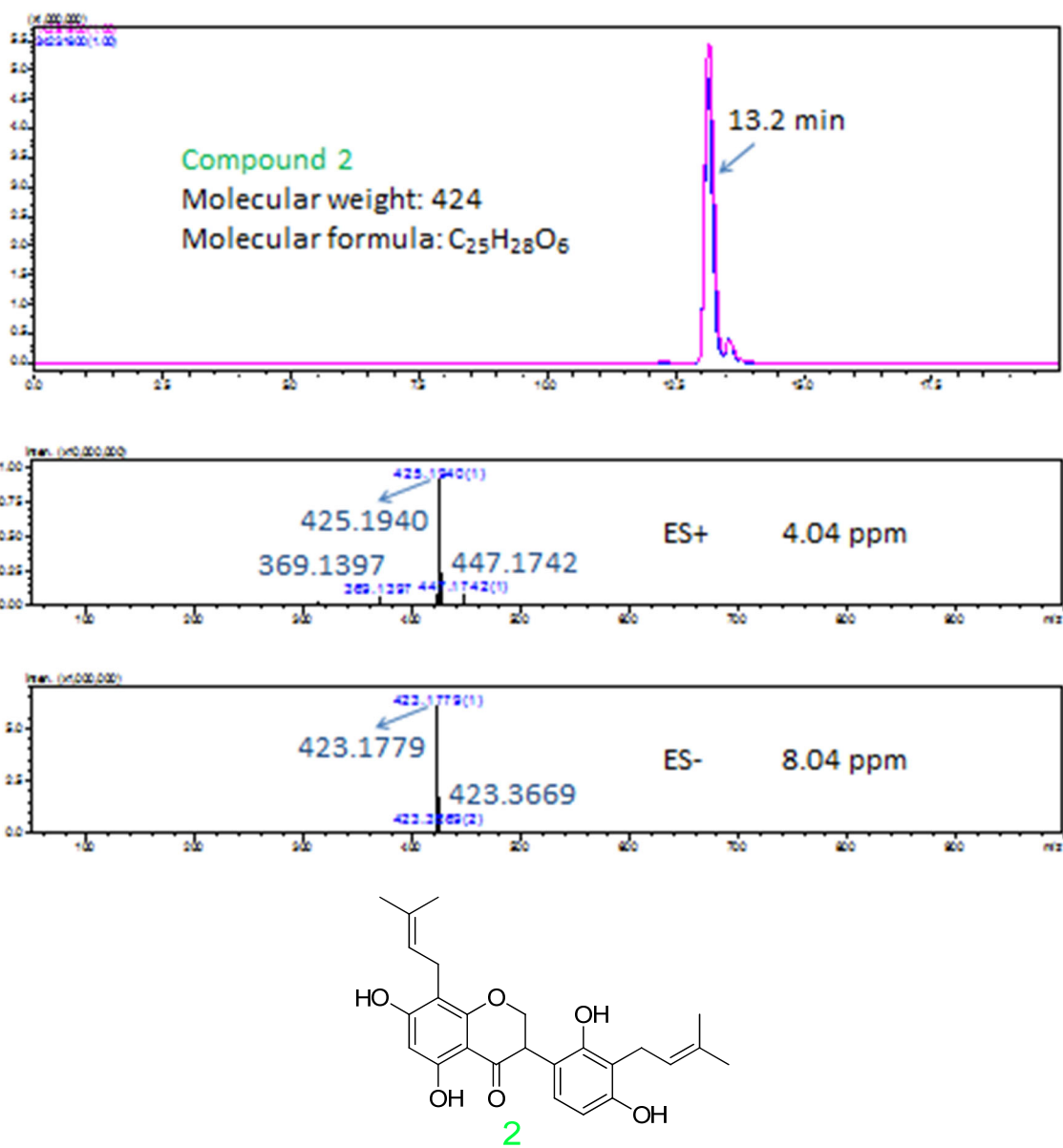


Figure S54. The (+)-HRESIMS and (-)-HRESIMS spectra of compound **2** in GU-MF-15 with extracted ions (positive and negative) for m/z 425 and 423, respectively.

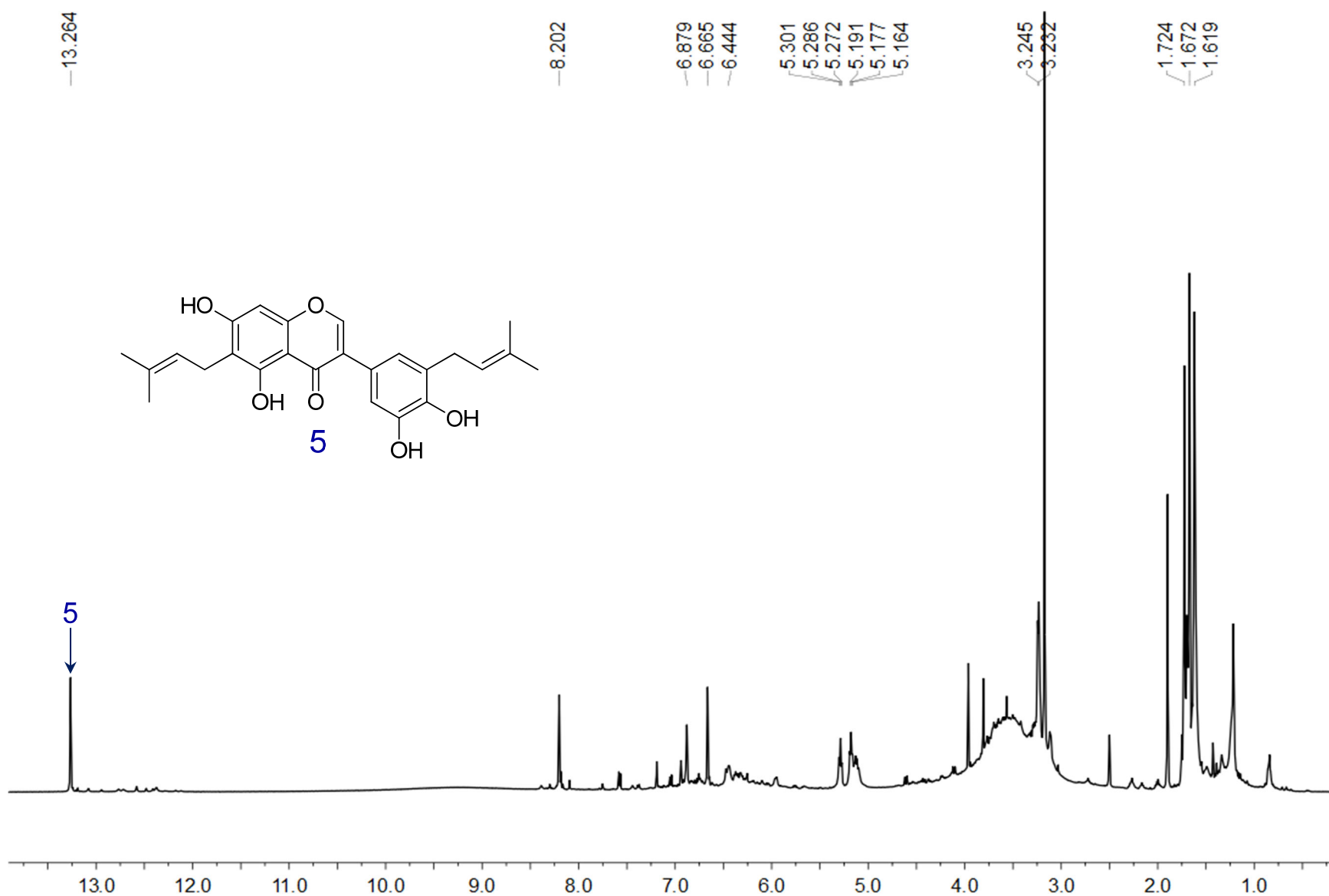


Figure S55. The ^1H NMR spectrum of GU-MF-16 in $\text{DMSO}-d_6$.

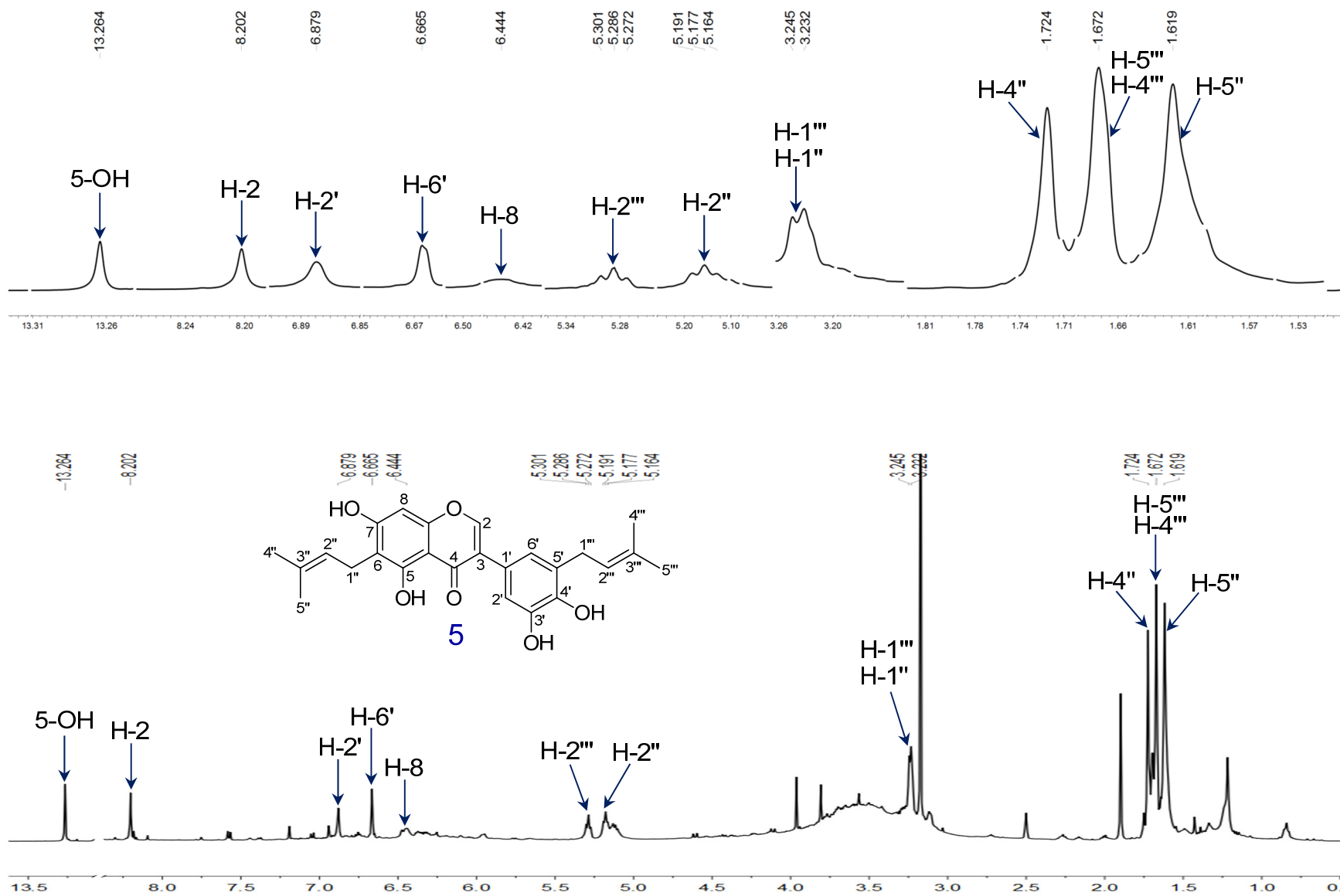


Figure S56. The ^1H NMR spectrum of compound **5** in GU-MF-16 in $\text{DMSO}-d_6$.

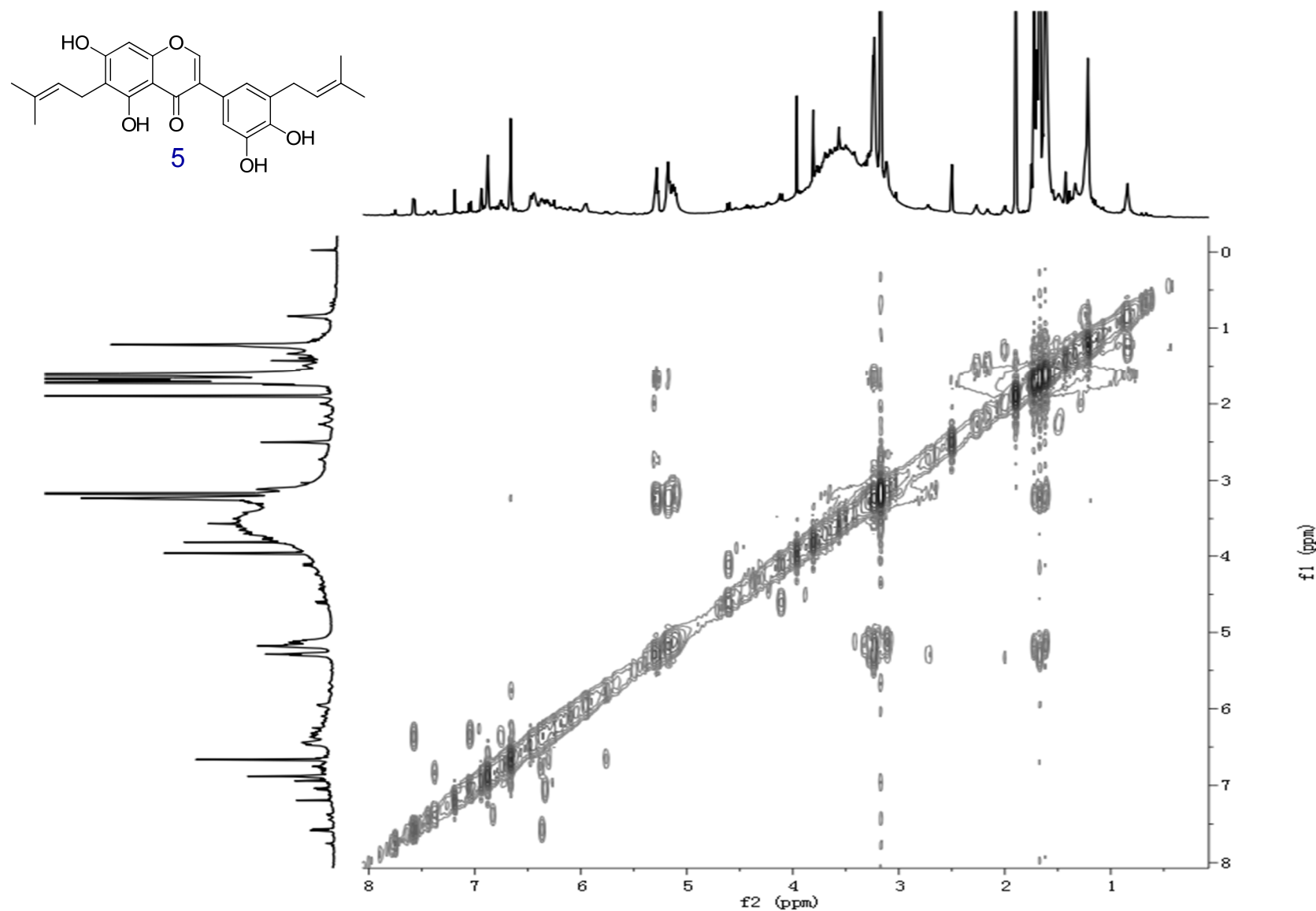


Figure S57. The ^1H - ^1H COSY spectrum of GU-MF-16 in $\text{DMSO}-d_6$.

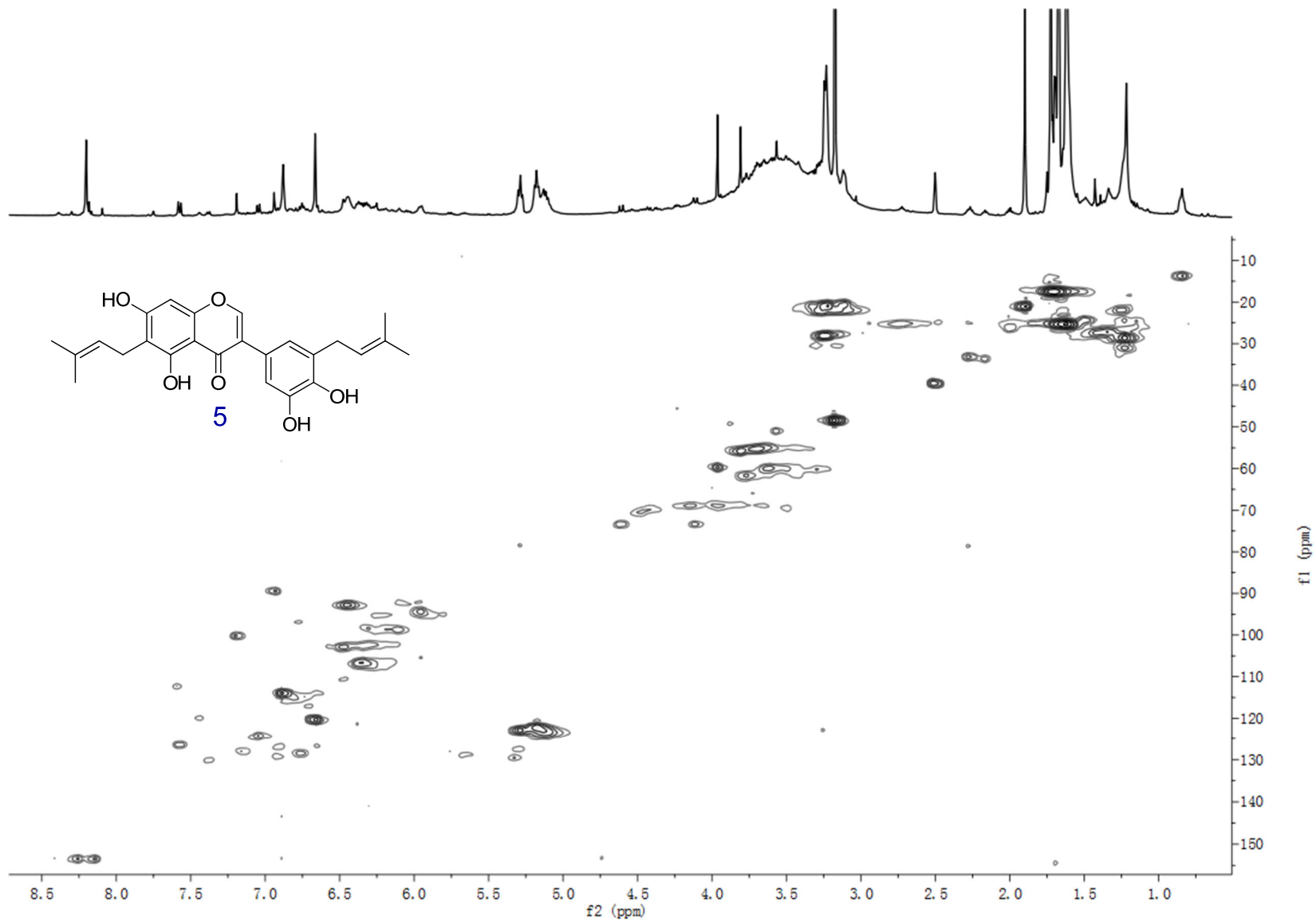


Figure S58. The HSQC spectrum of GU-MF-16 in $\text{DMSO}-d_6$.

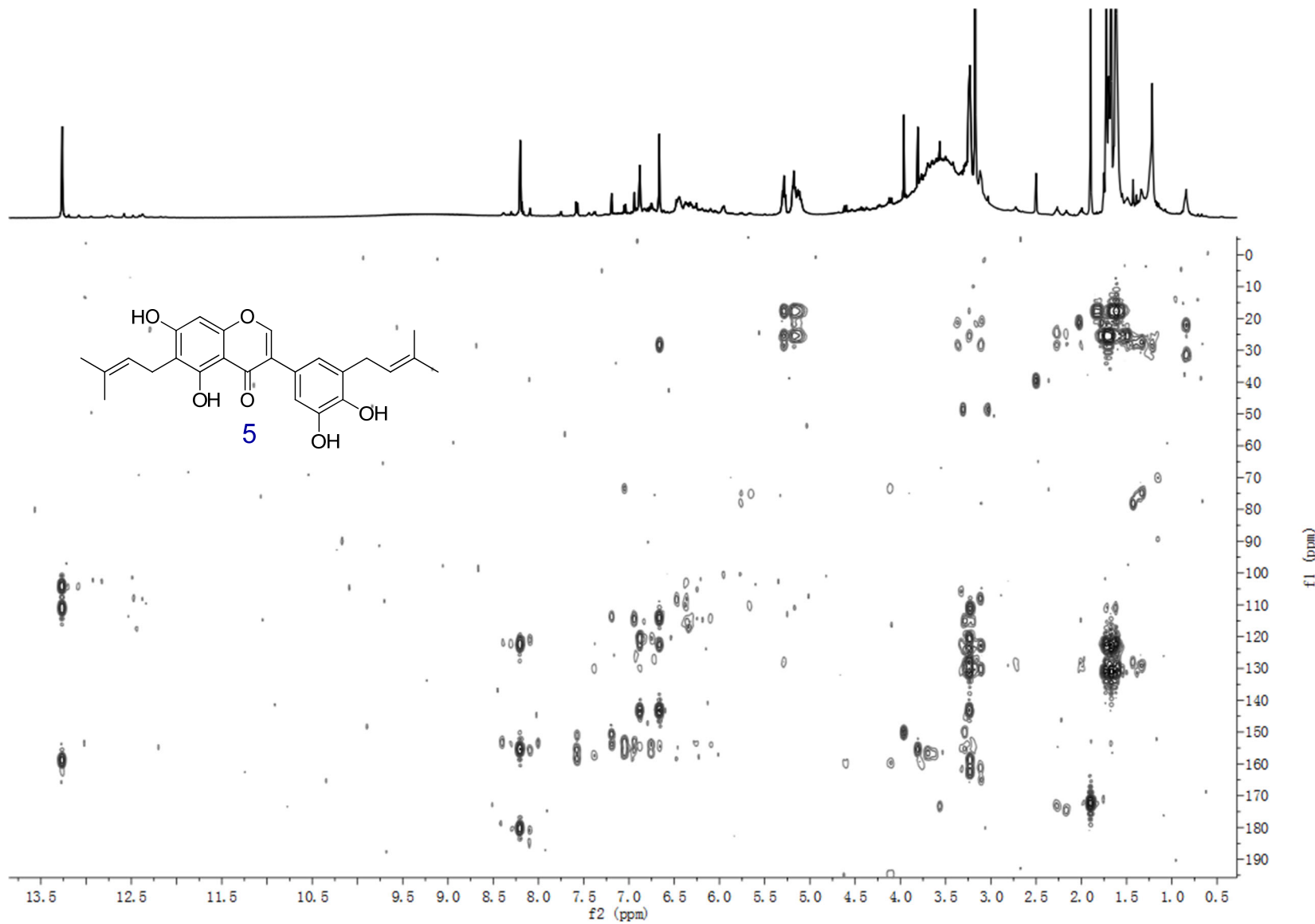


Figure S59. The HMBC spectrum of GU-MF-16 in ¹DMSO-*d*₆.

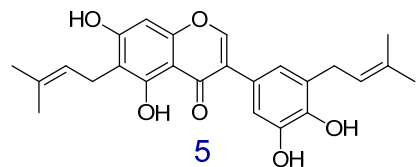
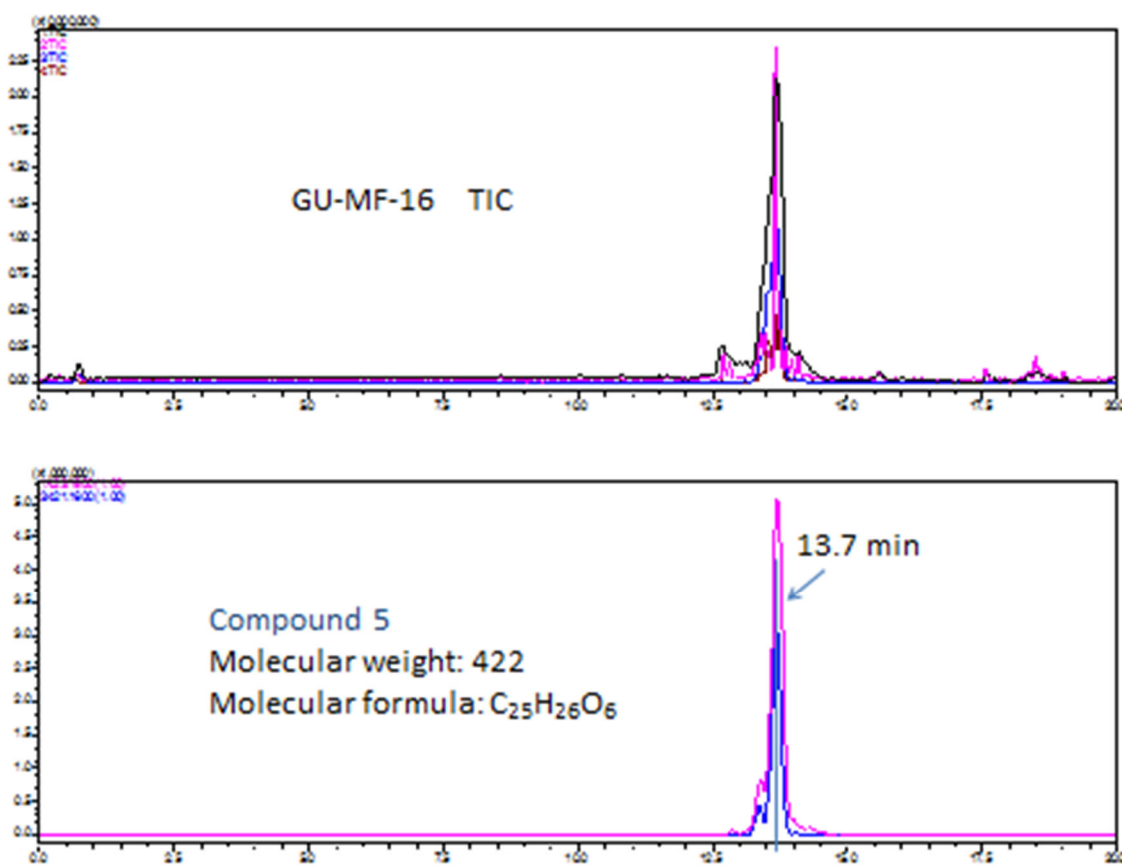


Figure S60. The IT-TOF TIC spectrum of GU-MF-16.

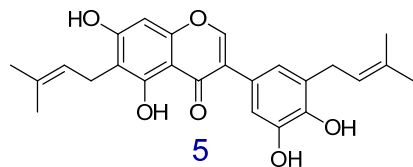
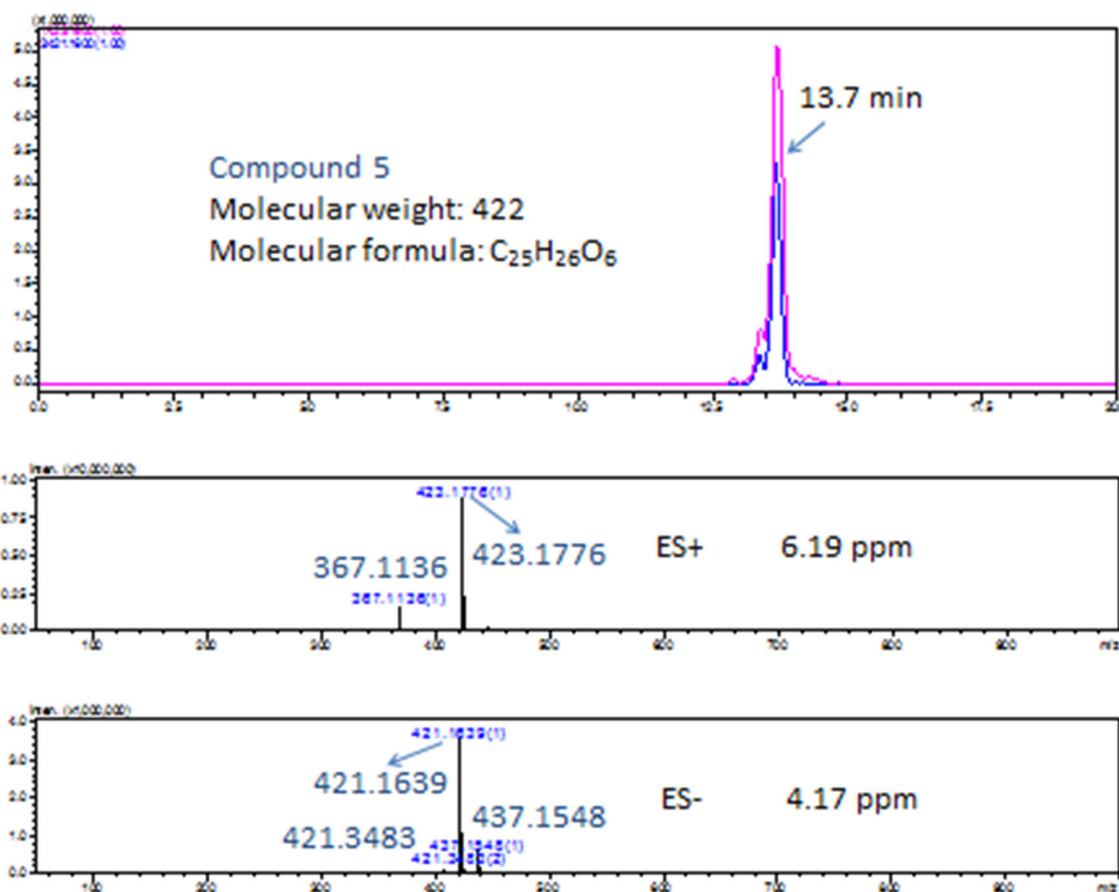


Figure S61. The (+)-HRESIMS and (-)-HRESIMS spectra of compound **5** in GU-MF-16 with extracted ions (positive and negative) for m/z 423 and 421, respectively.

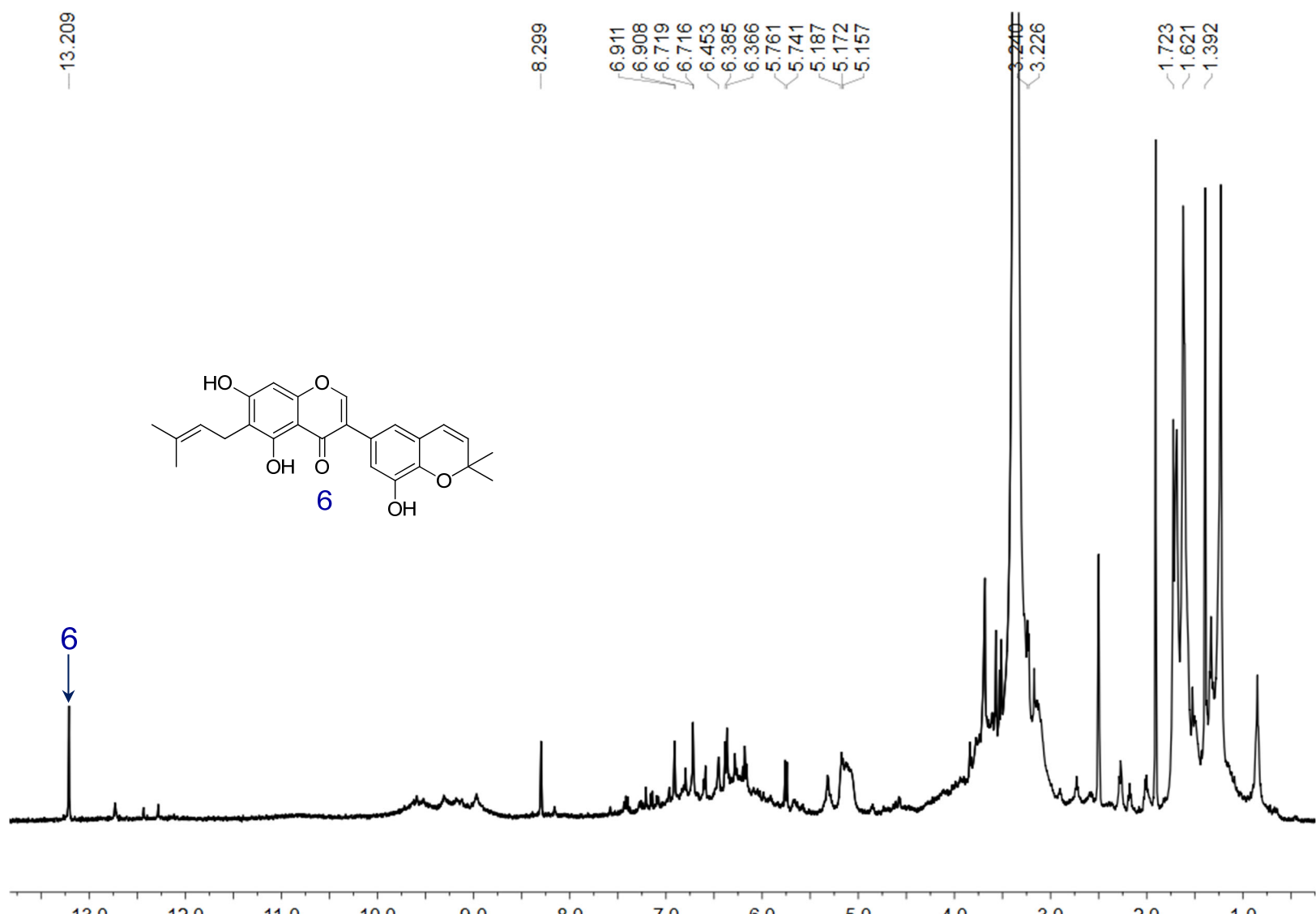


Figure S62. The ^1H NMR spectrum of GU-MF-17 in $\text{DMSO}-d_6$.

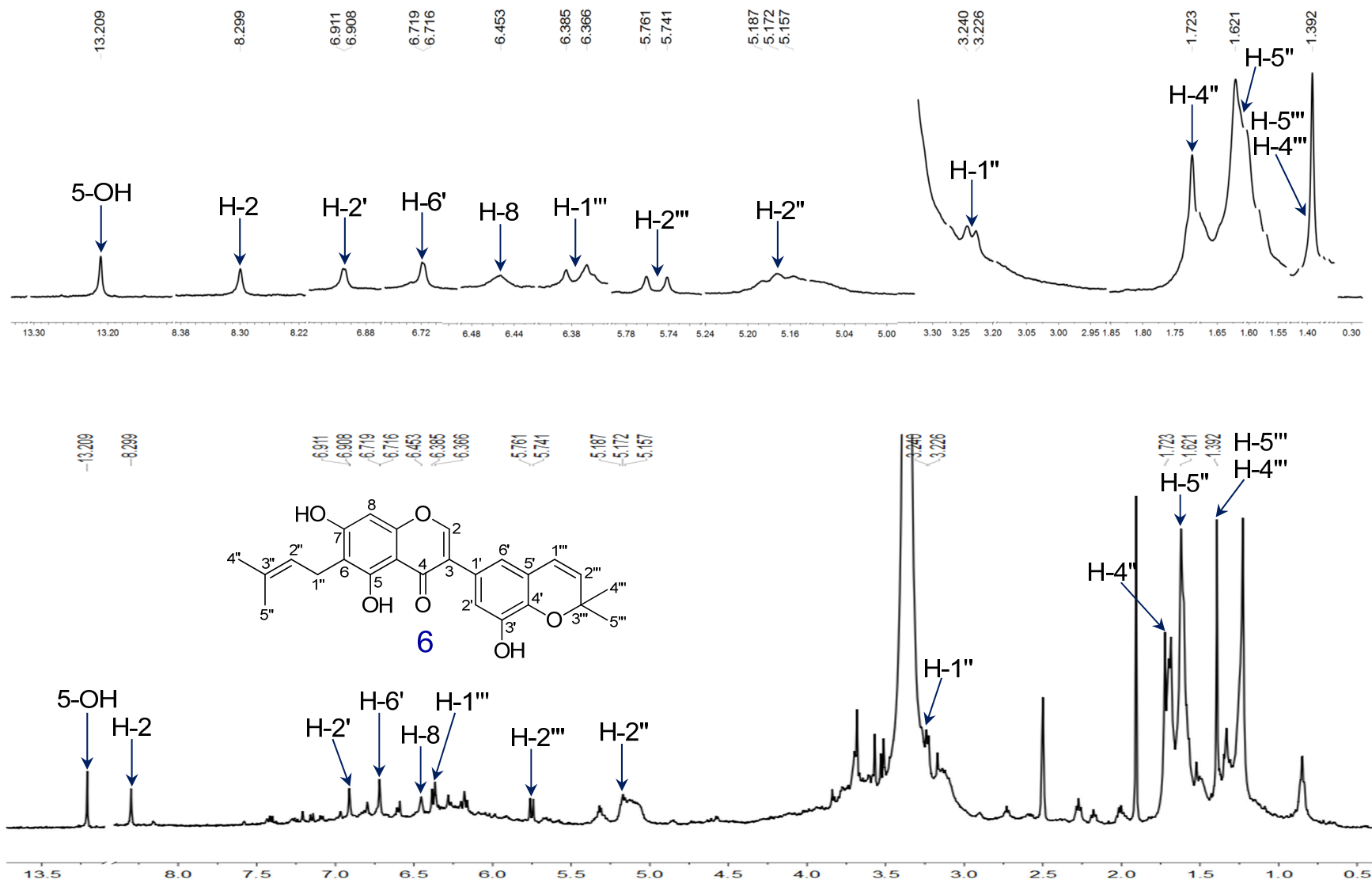


Figure S63. The ^1H NMR spectrum of compound **6** in GU-MF-17 in $\text{DMSO}-d_6$.

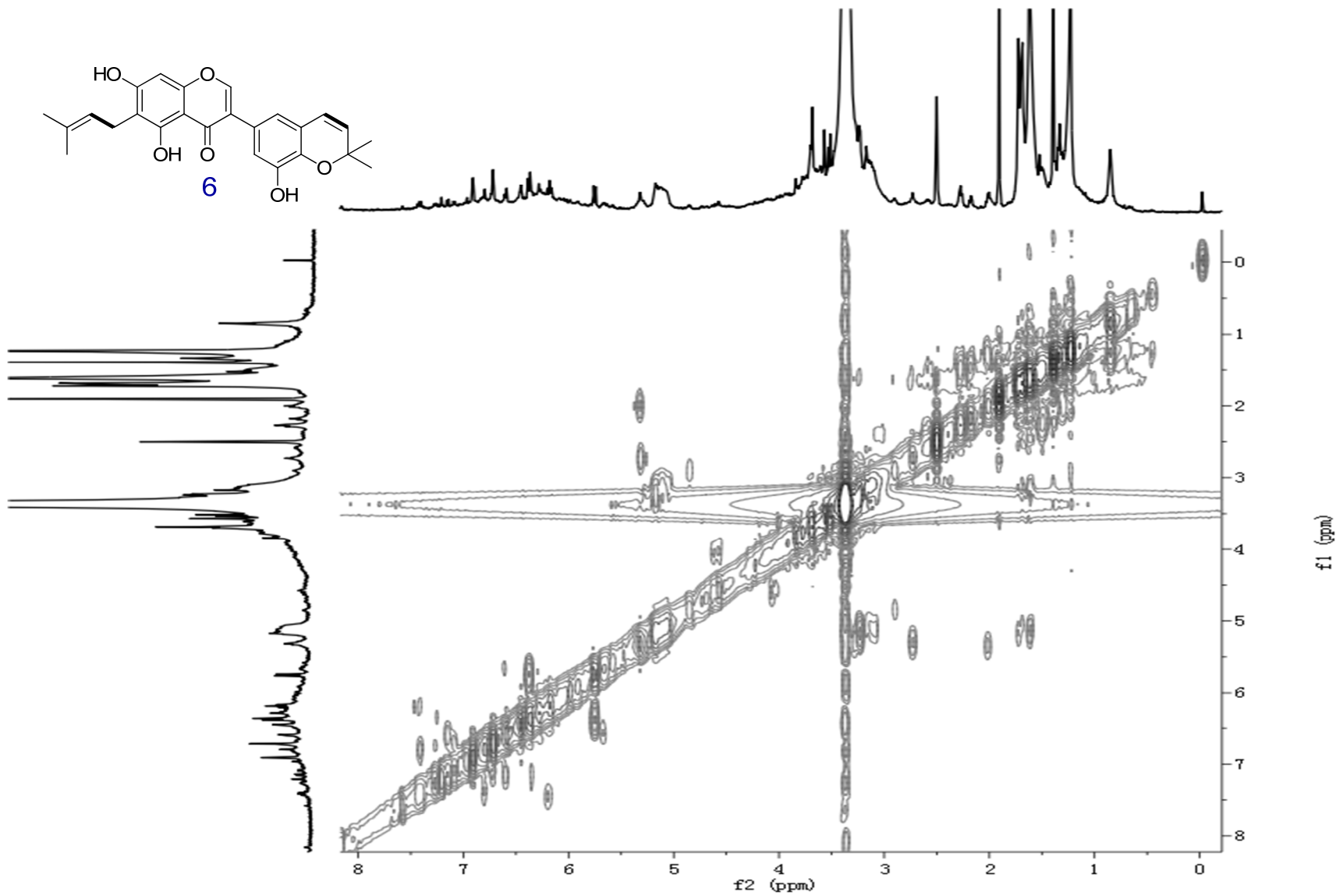


Figure S64. The ^1H - ^1H COSY spectrum of GU-MF-17 in $\text{DMSO}-d_6$.

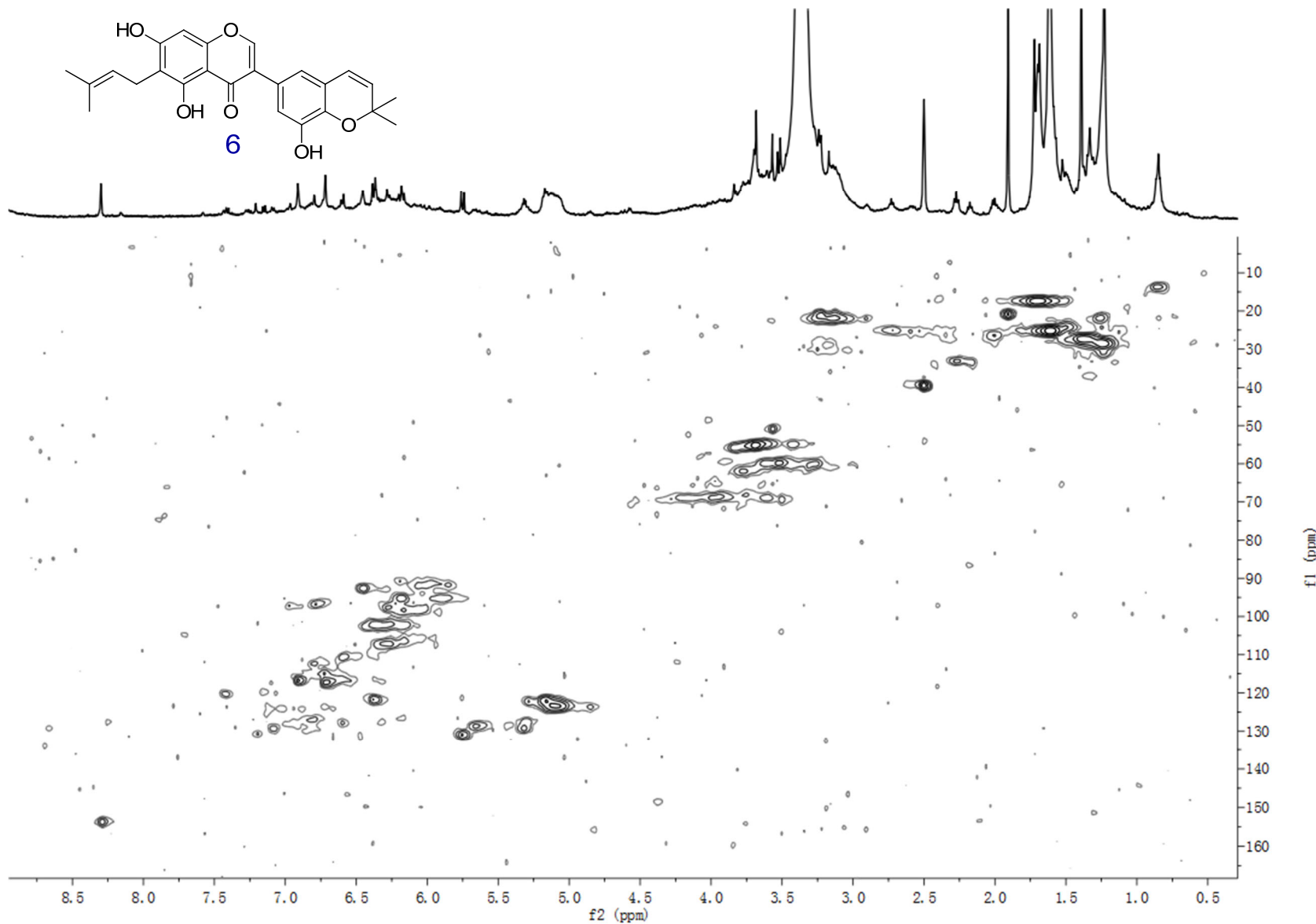


Figure S65. The HSQC spectrum of GU-MF-17 in $\text{DMSO}-d_6$.

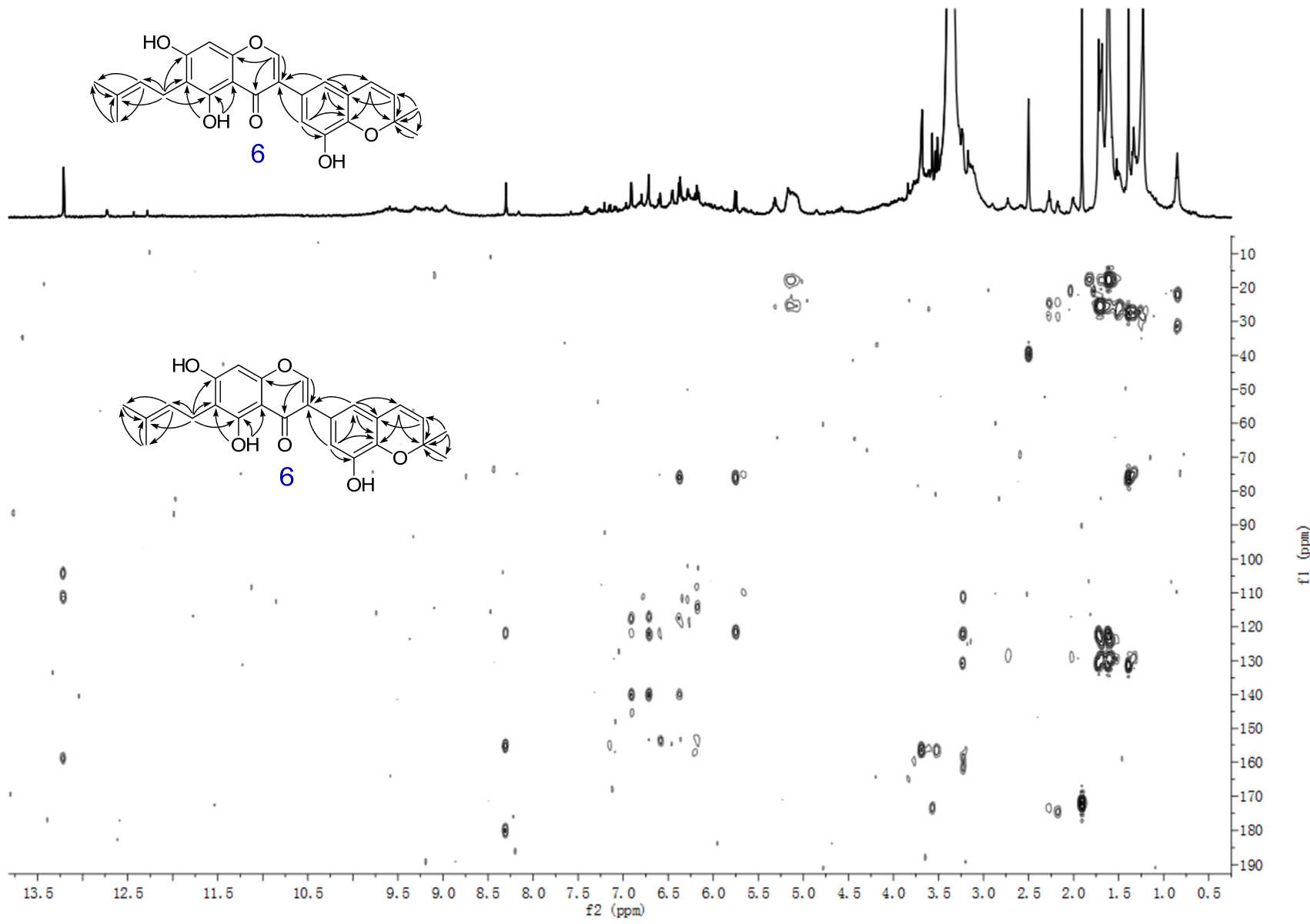


Figure S66. The HMBC spectrum of GU-MF-17 in $\text{DMSO}-d_6$.

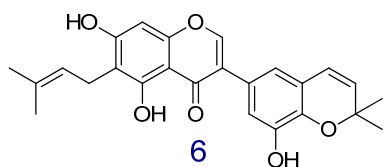
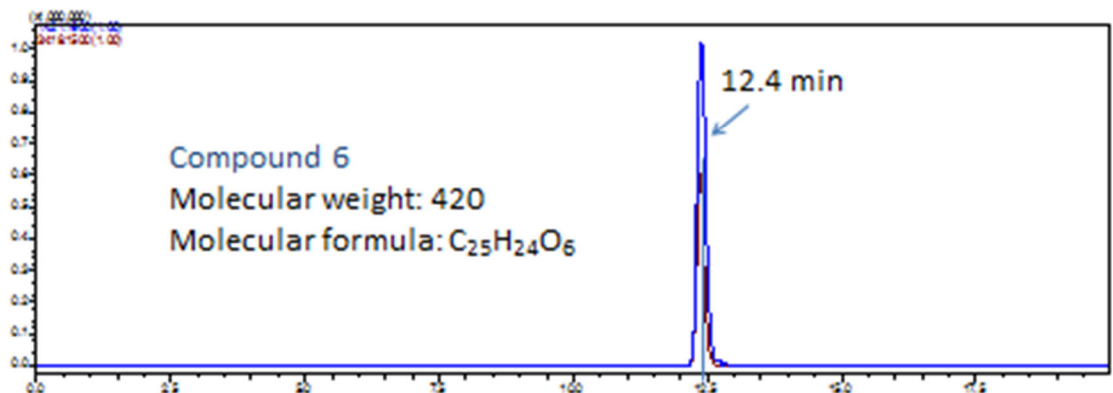
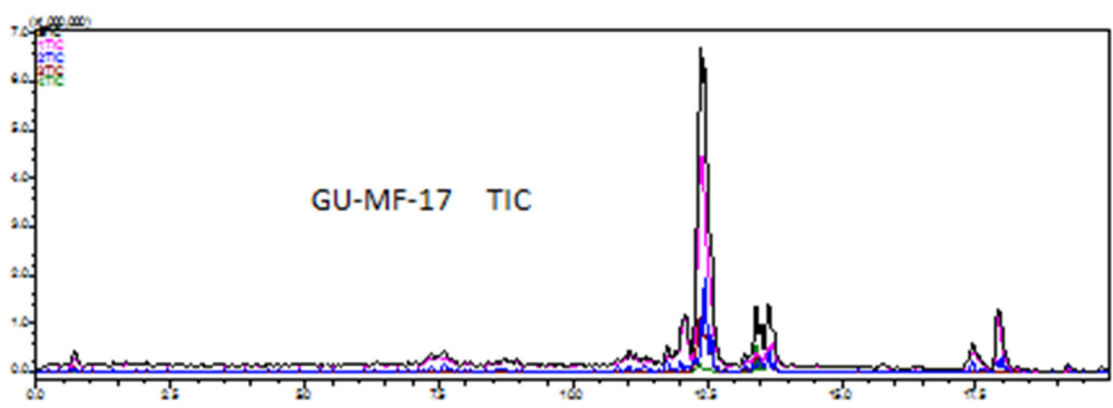


Figure S67. The IT-TOF TIC spectrum of GU-MF-17.

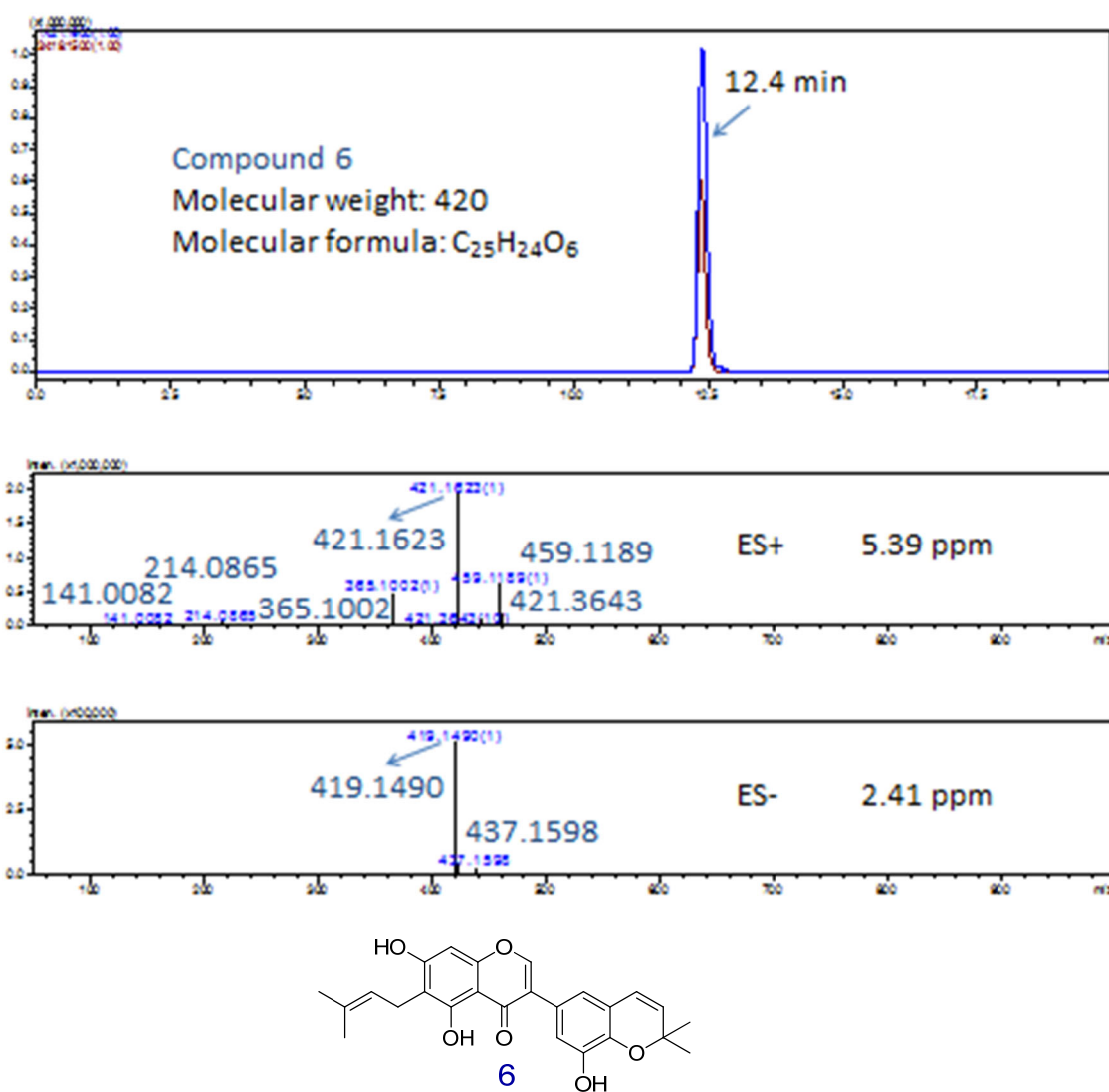


Figure S68. The (+)-HRESIMS and (-)-HRESIMS spectra of compound **6** in GU-MF-17 with extracted ions (positive and negative) for m/z 421 and 419, respectively.

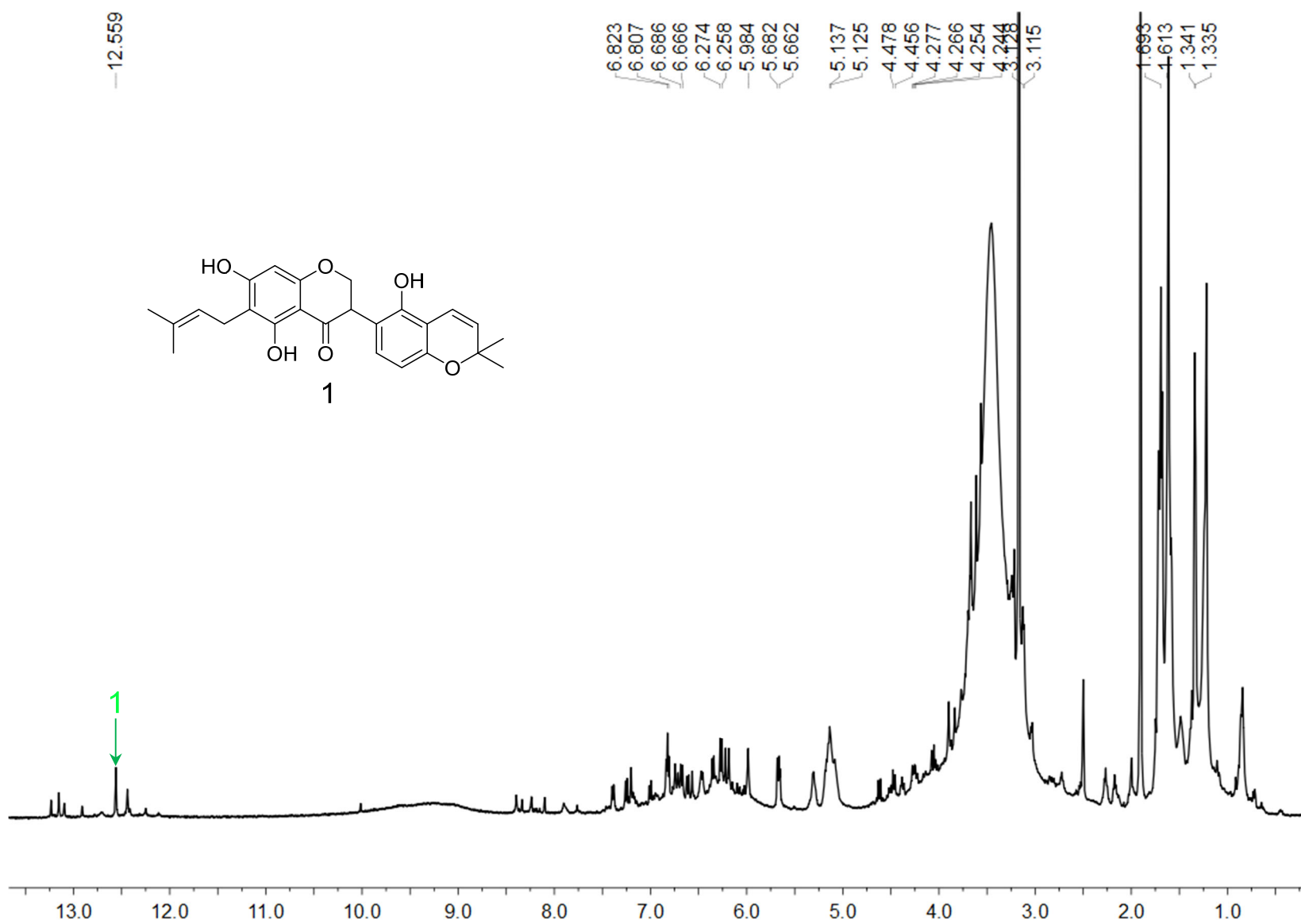


Figure S69. The ^1H NMR spectrum of GU-MF-18 in $\text{DMSO}-d_6$.

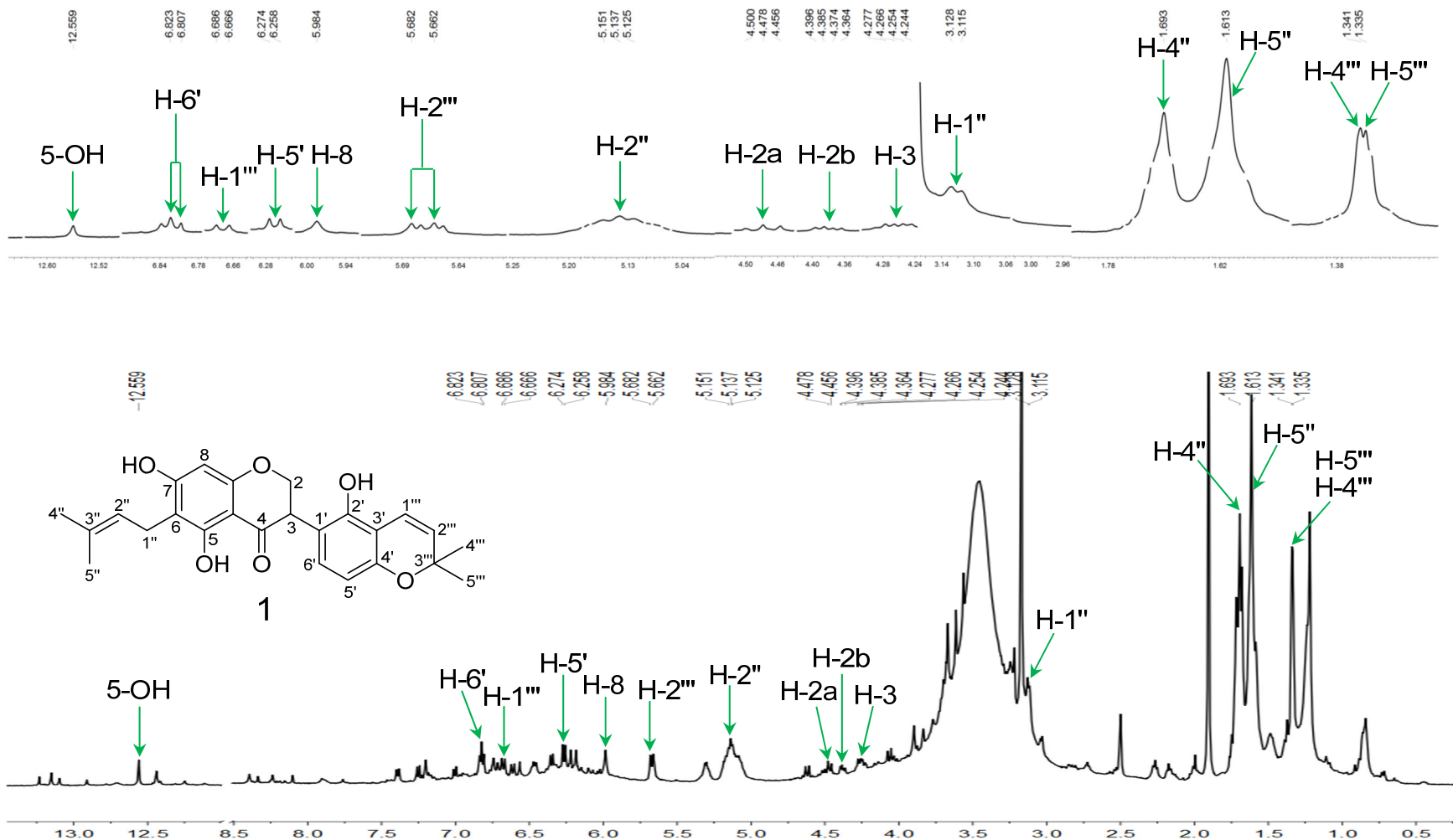


Figure S70. The ^1H NMR spectrum of compound **1** in GU-MF-18 in $\text{DMSO}-d_6$.

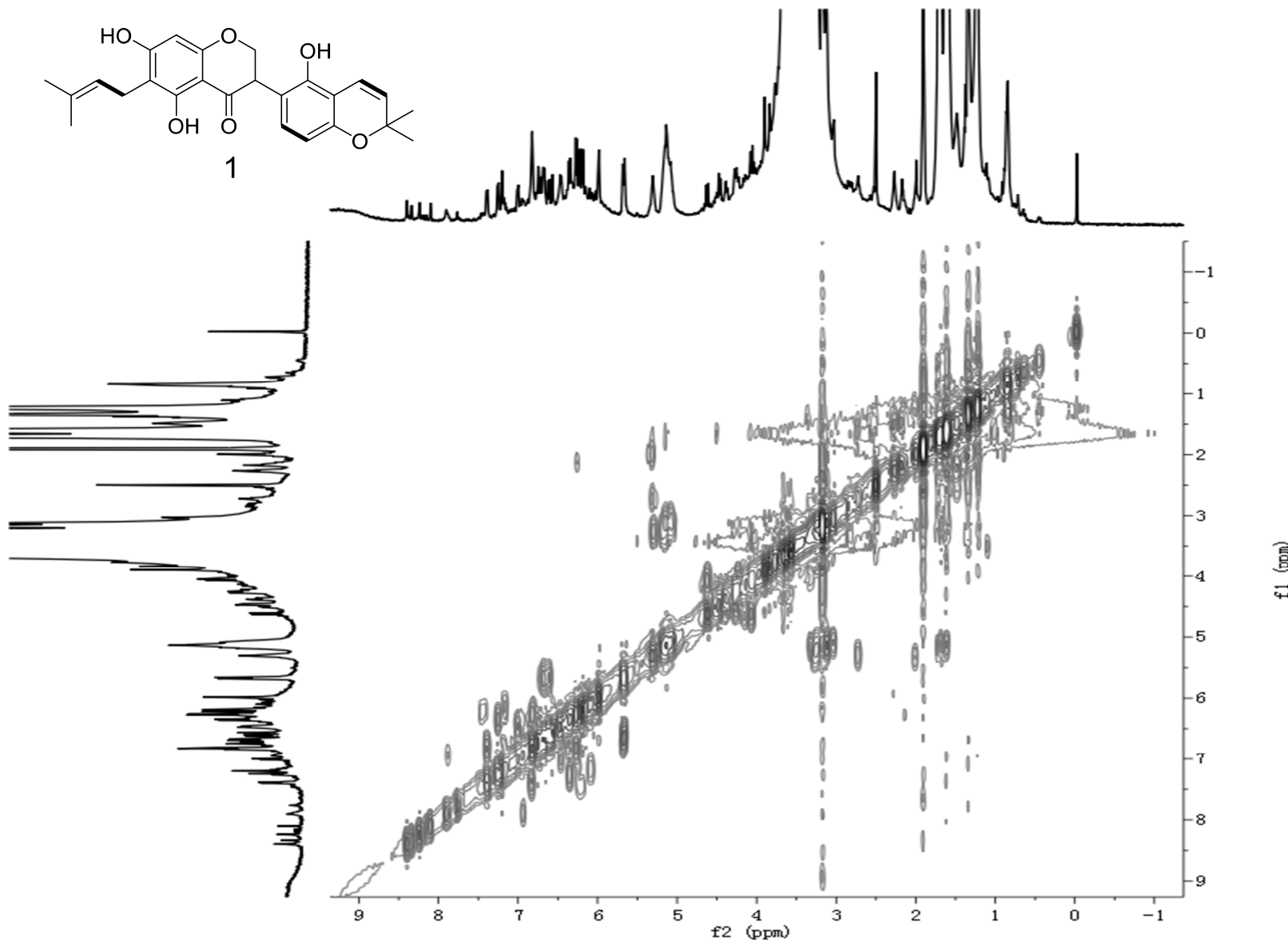


Figure S71. The ^1H - ^1H COSY spectrum of GU-MF-18 in $\text{DMSO}-d_6$.

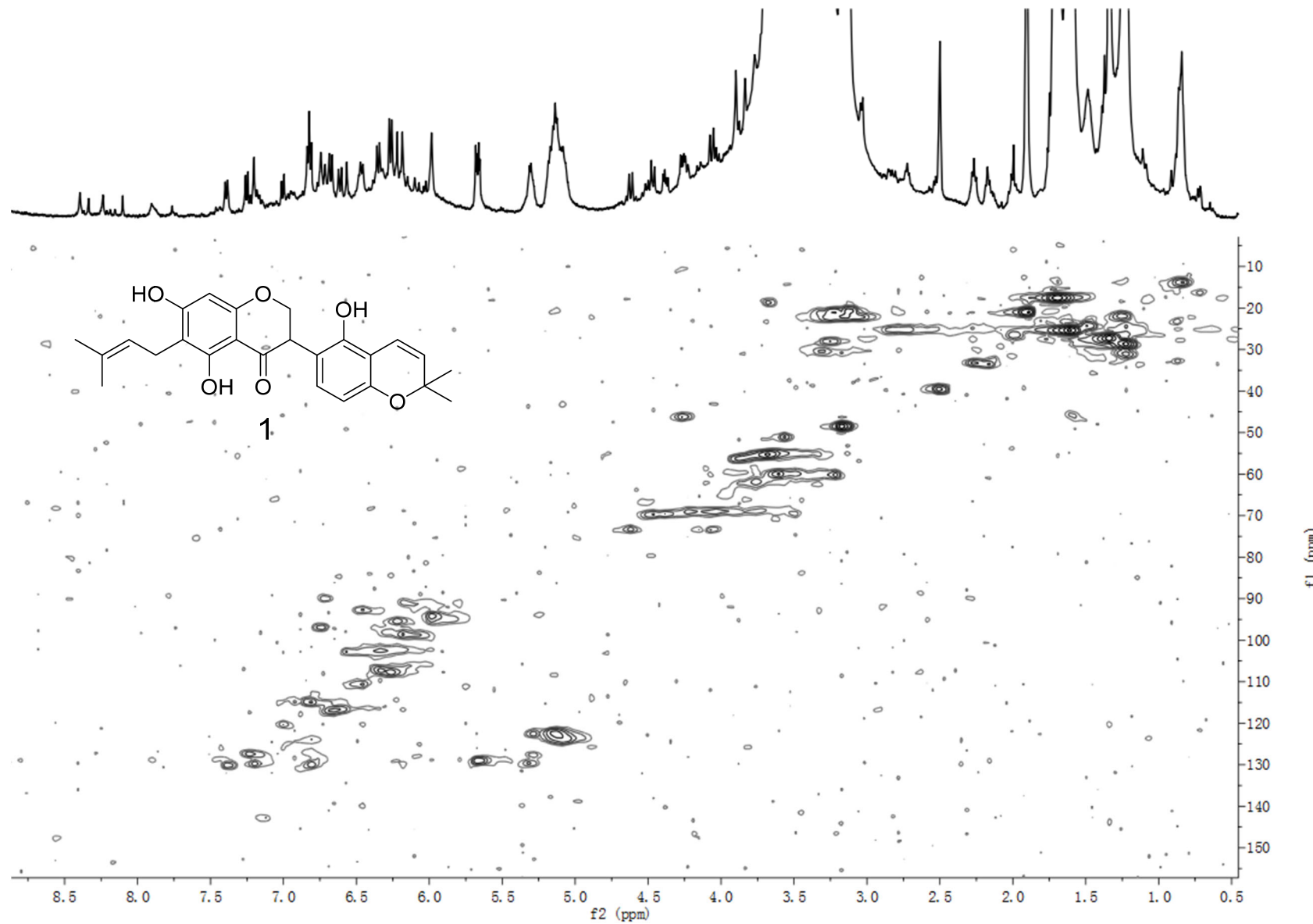


Figure S72. The HSQC spectrum of GU-MF-18 in DMSO-*d*6.

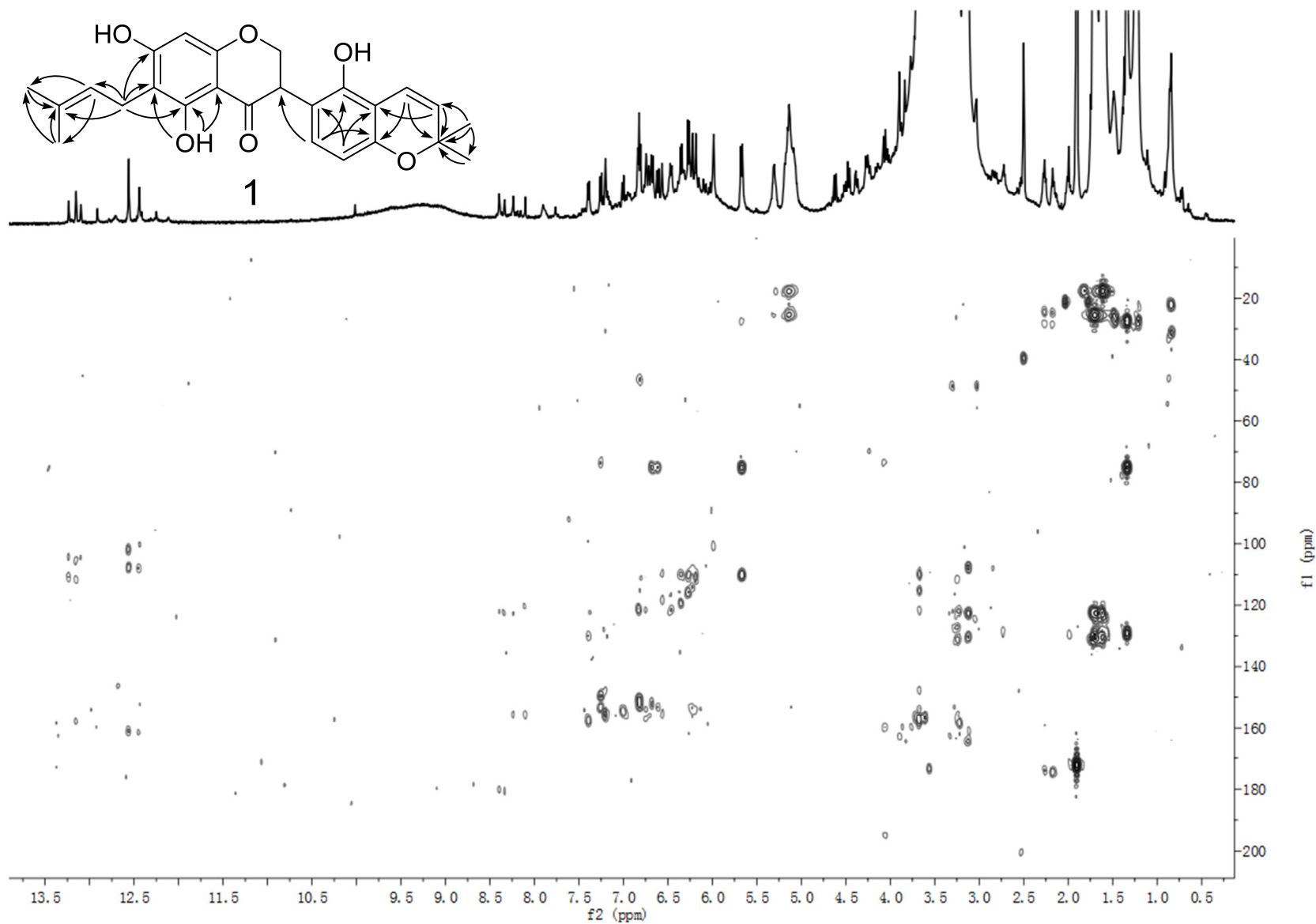


Figure S73. The HMBC spectrum of GU-MF-18 in $\text{DMSO}-d_6$.

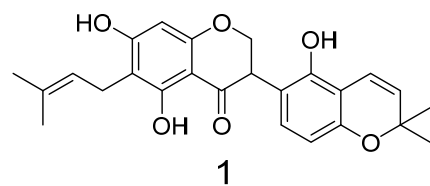
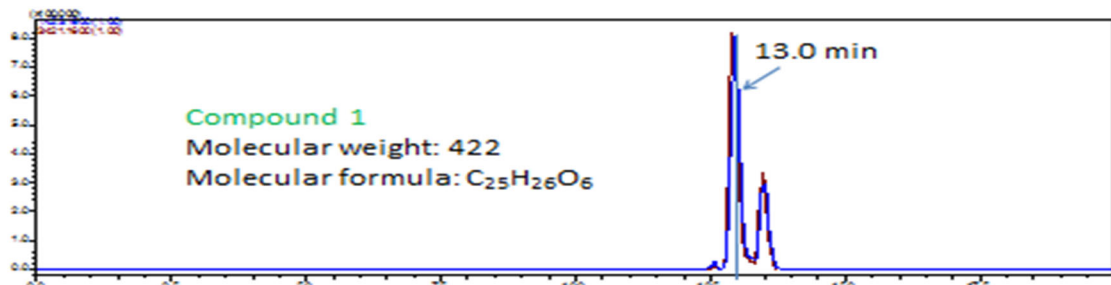
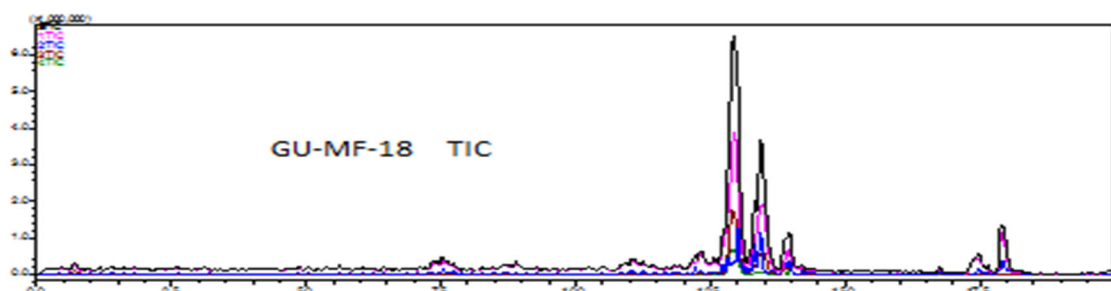


Figure S74. The IT-TOF TIC spectrum of GU-MF-18.

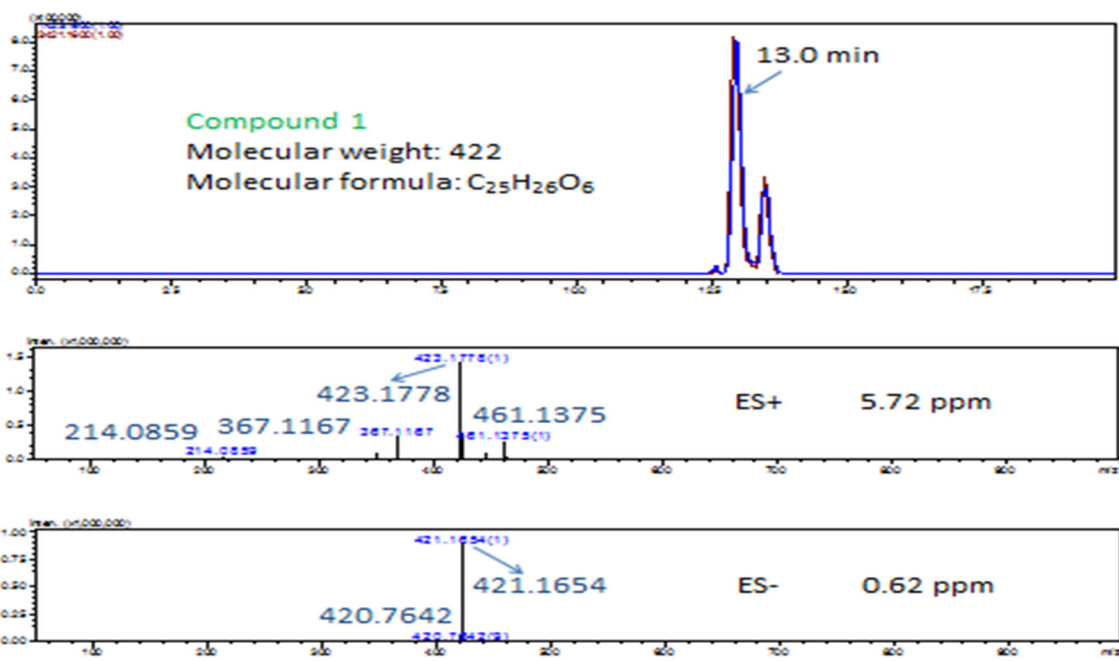


Figure S75. The (+)-HRESIMS and (-)-HRESIMS spectra of compound **1** in GU-MF-18 with extracted ions (positive and negative) for m/z 423 and 421, respectively

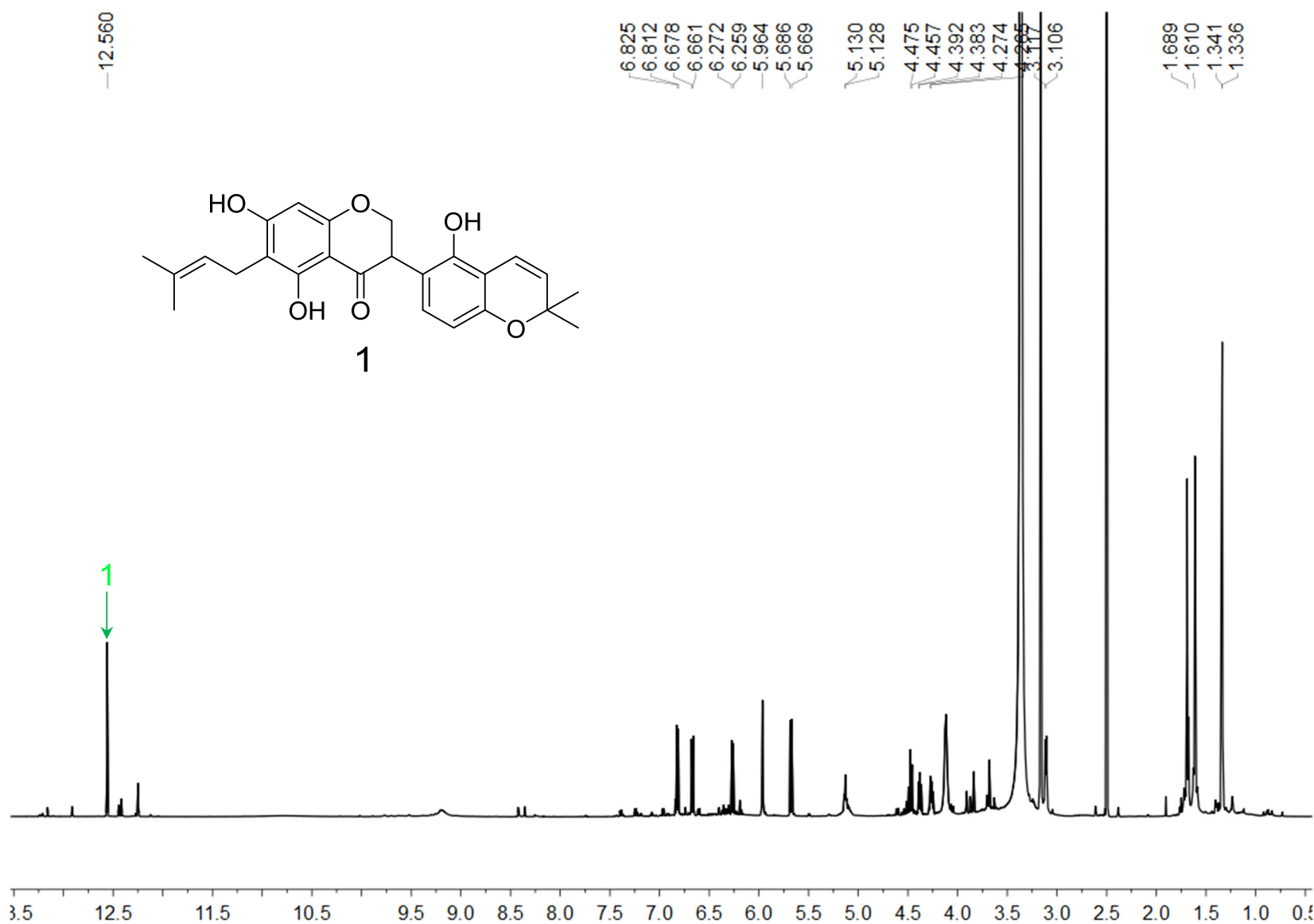


Figure S76. The ^1H NMR spectrum of GU-MF-18-1 in $\text{DMSO}-d_6$.

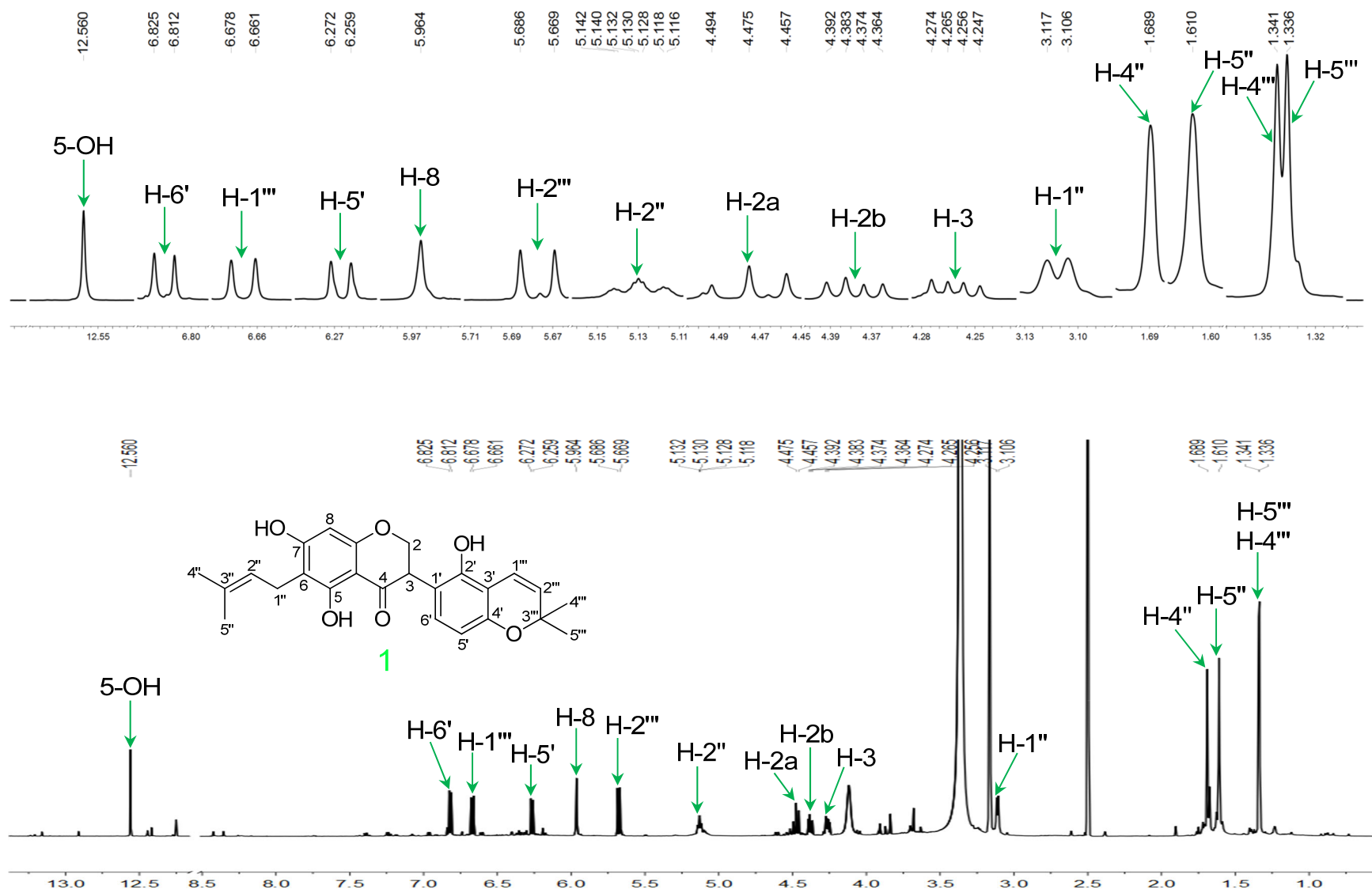


Figure S77. The ^1H NMR spectrum of compound **1** in GU-MF-18-1 in DMSO- d_6 .

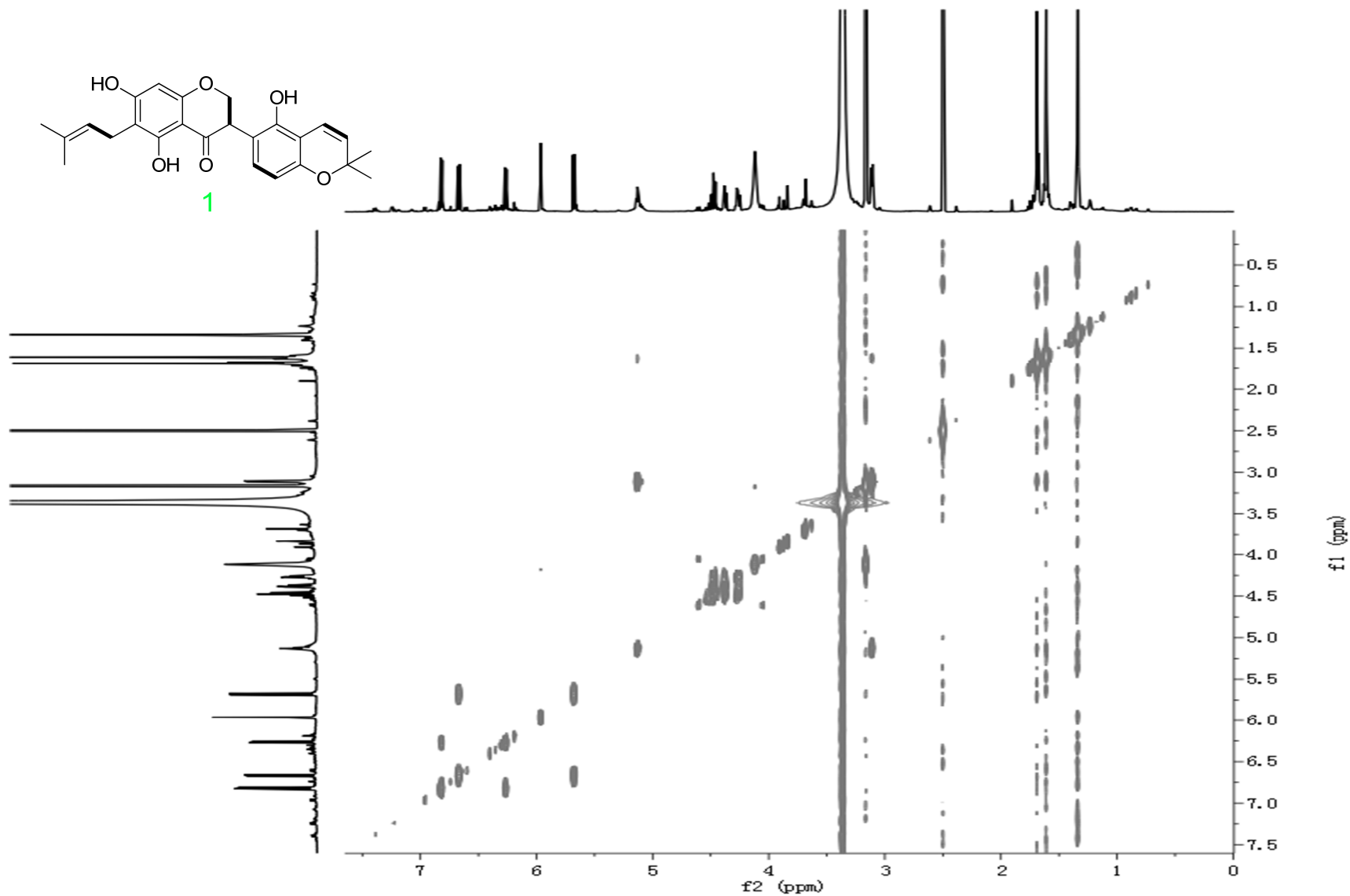


Figure S78. The ^1H - ^1H COSY spectrum of GU-MF-18-1 in $\text{DMSO}-d_6$.

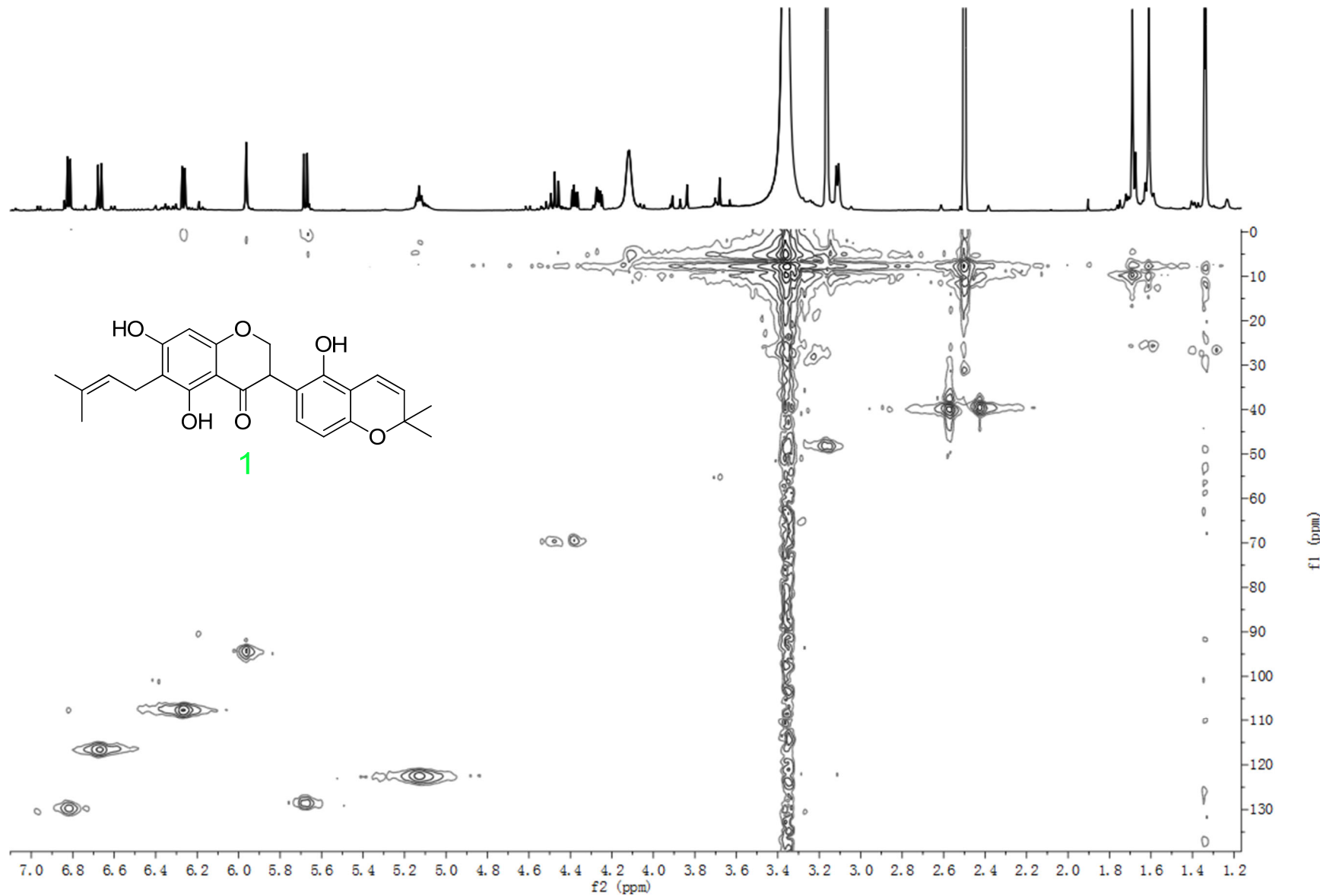


Figure S79. The HSQC spectrum of GU-MF-18-1 in DMSO-*d*6.

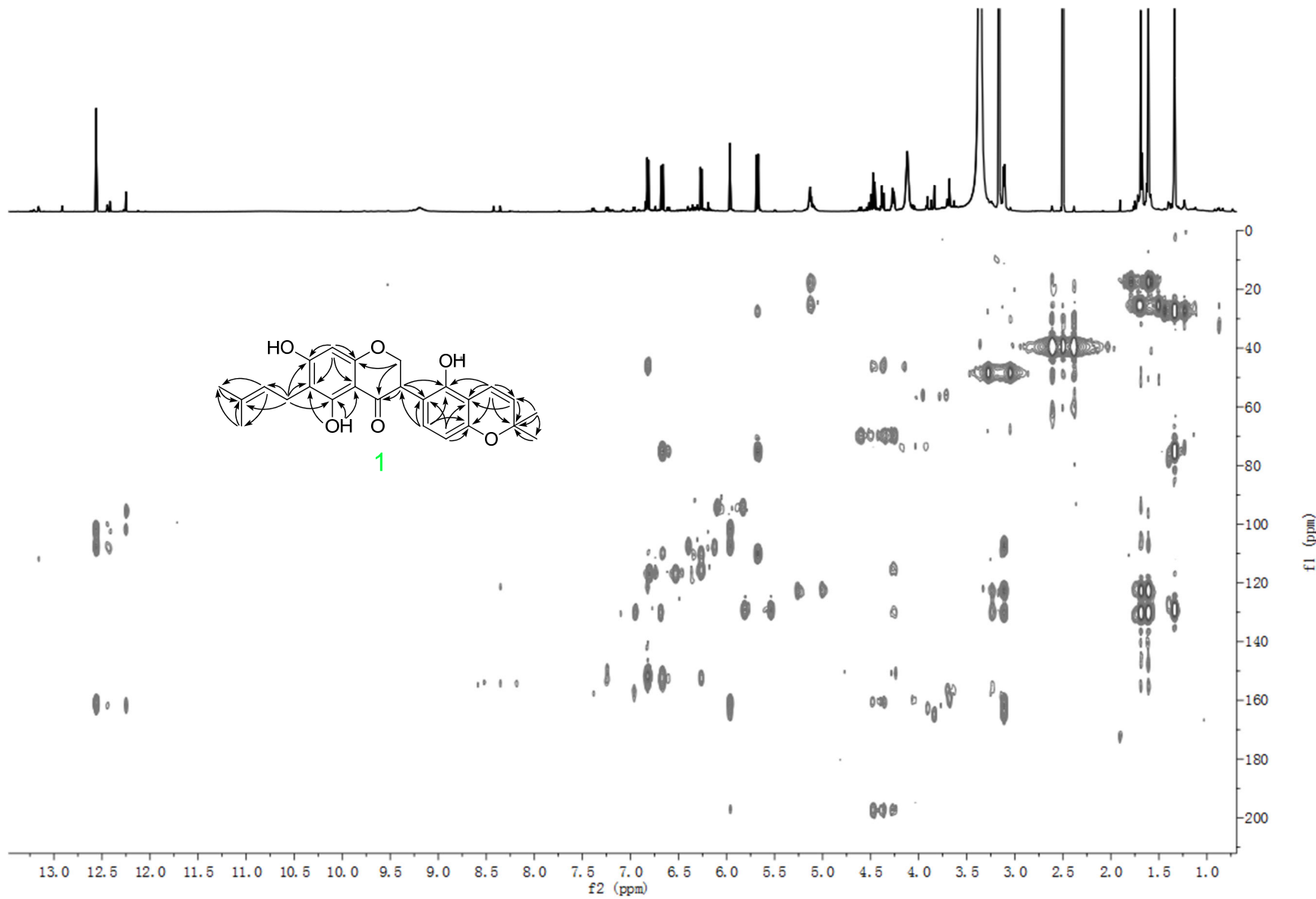


Figure S80. The HMBC spectrum of GU-MF-18-1 in $\text{DMSO}-d_6$.

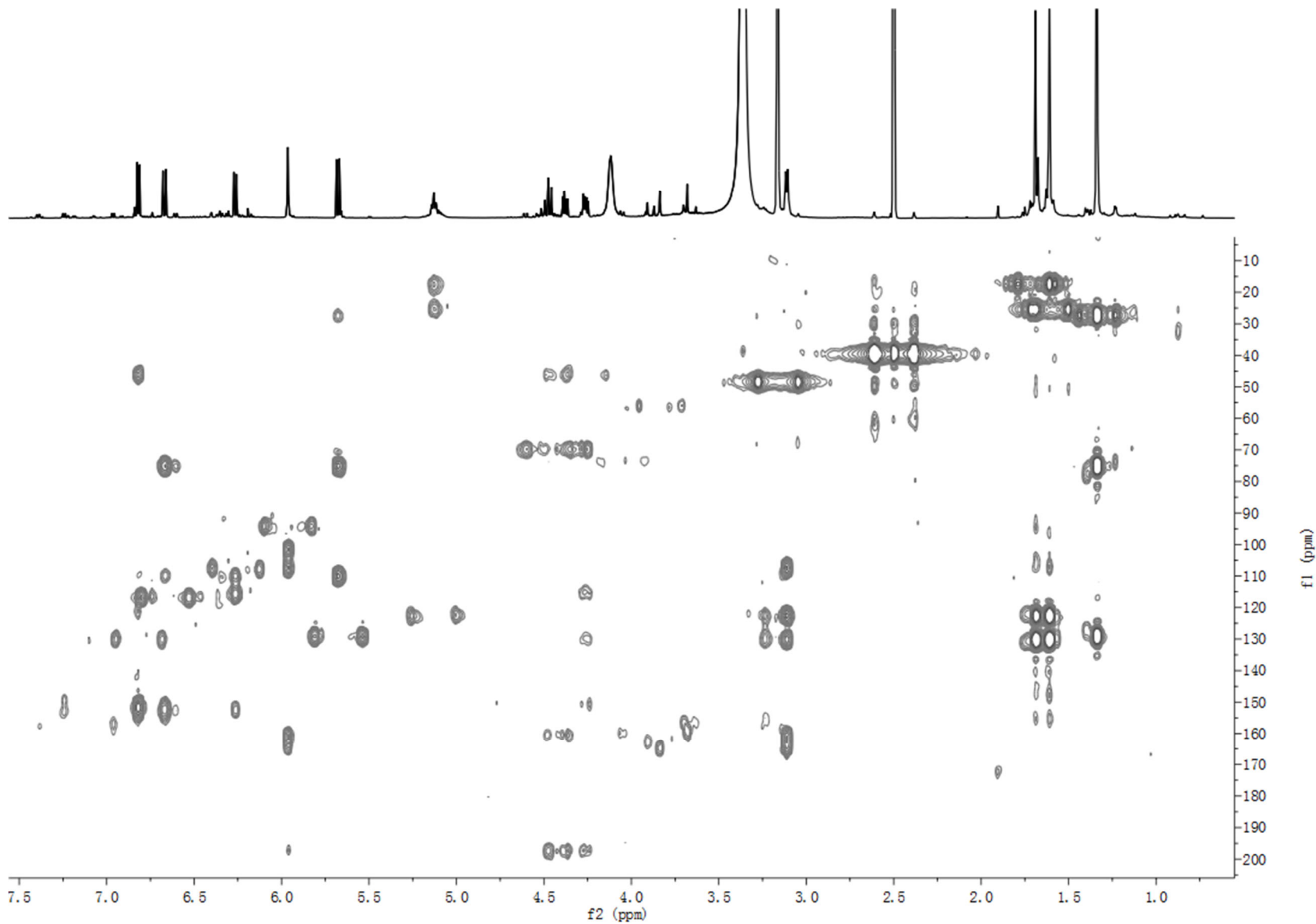


Figure S81. Expansion of the HMBC spectrum of GU-MF-18-1 for the range δ_{H} 0.55-7.56 and δ_{C} 2.5-206.0.

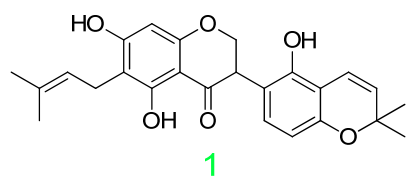
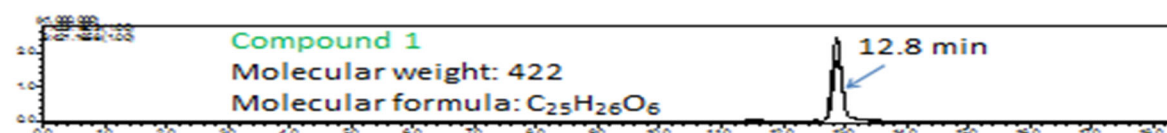
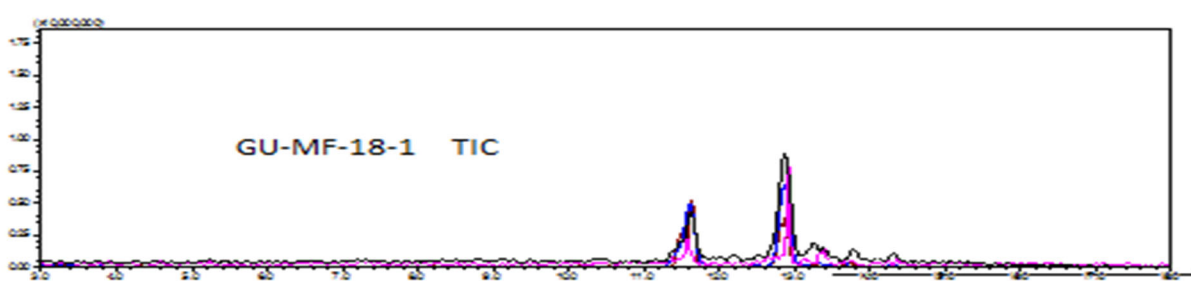


Figure S82. The IT-TOF TIC spectrum of GU-MF-18-1.

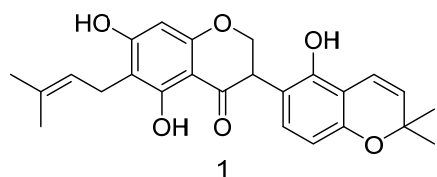
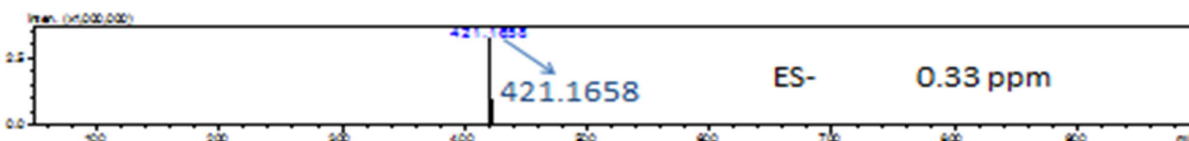
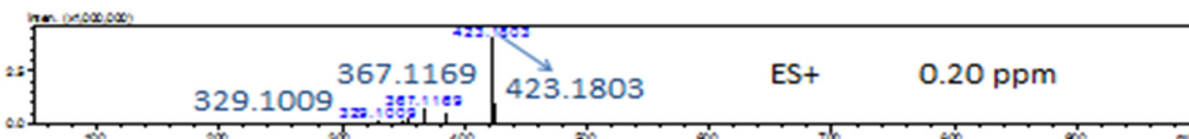
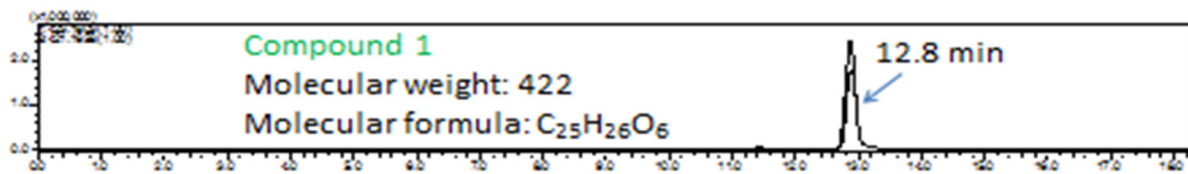


Figure S83. The (+)-HRESIMS and (-)-HRESIMS spectra of compound **1** in GU-MF-18-1 with extracted ions (positive and negative) for m/z 423 and 421, respectively.

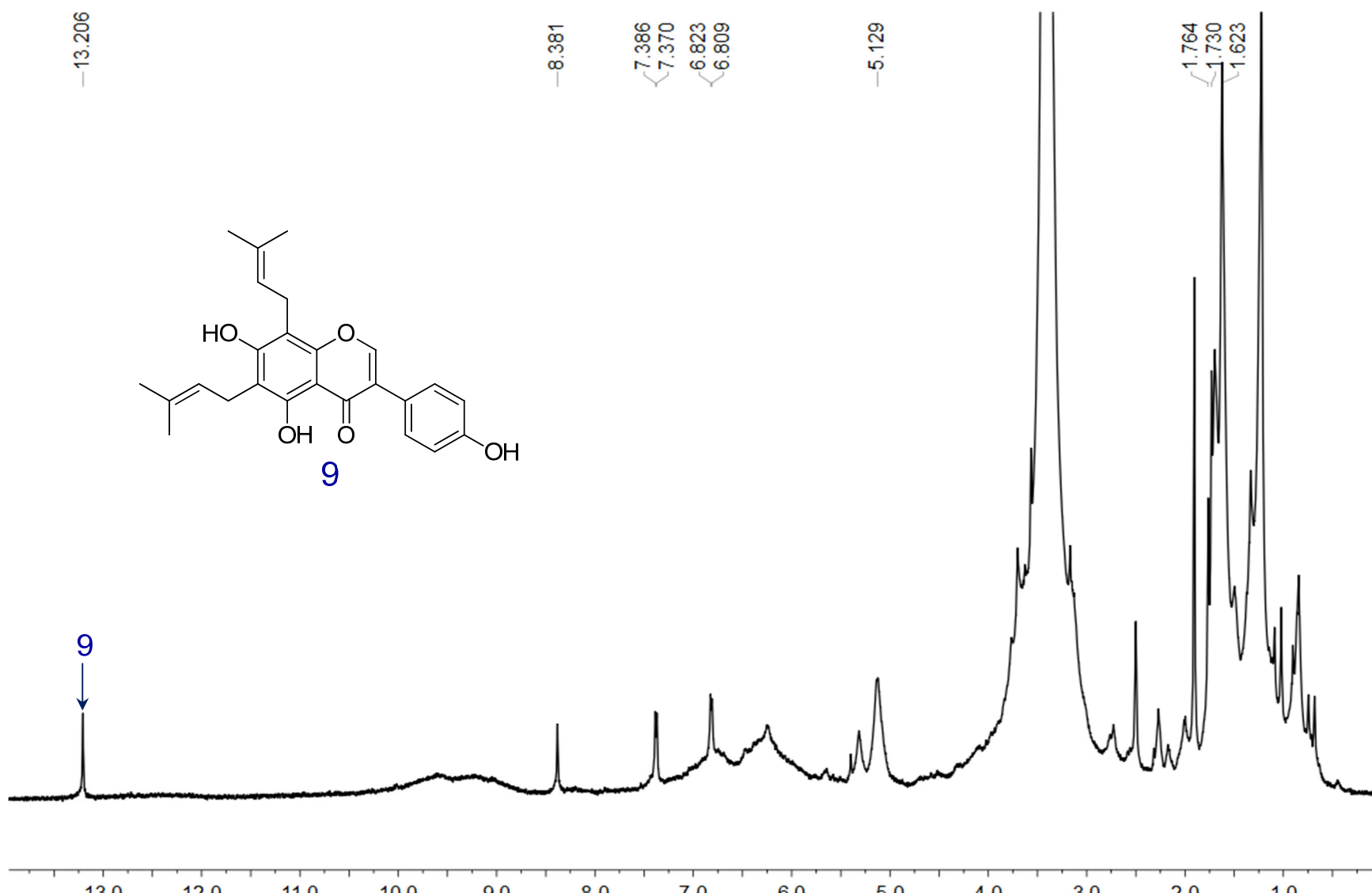


Figure S84. The ^1H NMR spectrum of GU-MF-19 in $\text{DMSO}-d_6$.

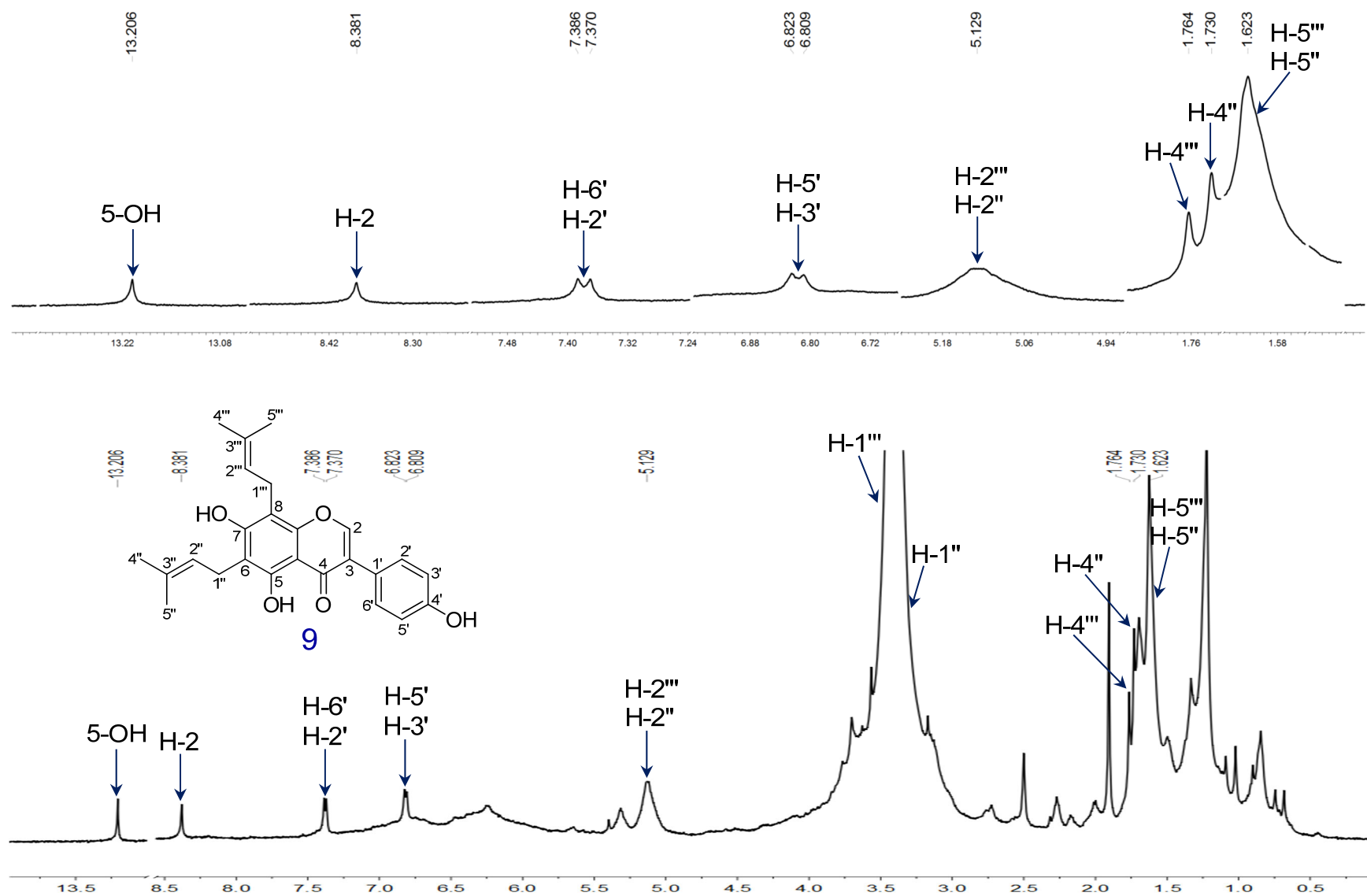


Figure S85. The ^1H NMR spectrum of compound **9** in GU-MF-19 in $\text{DMSO}-d_6$.

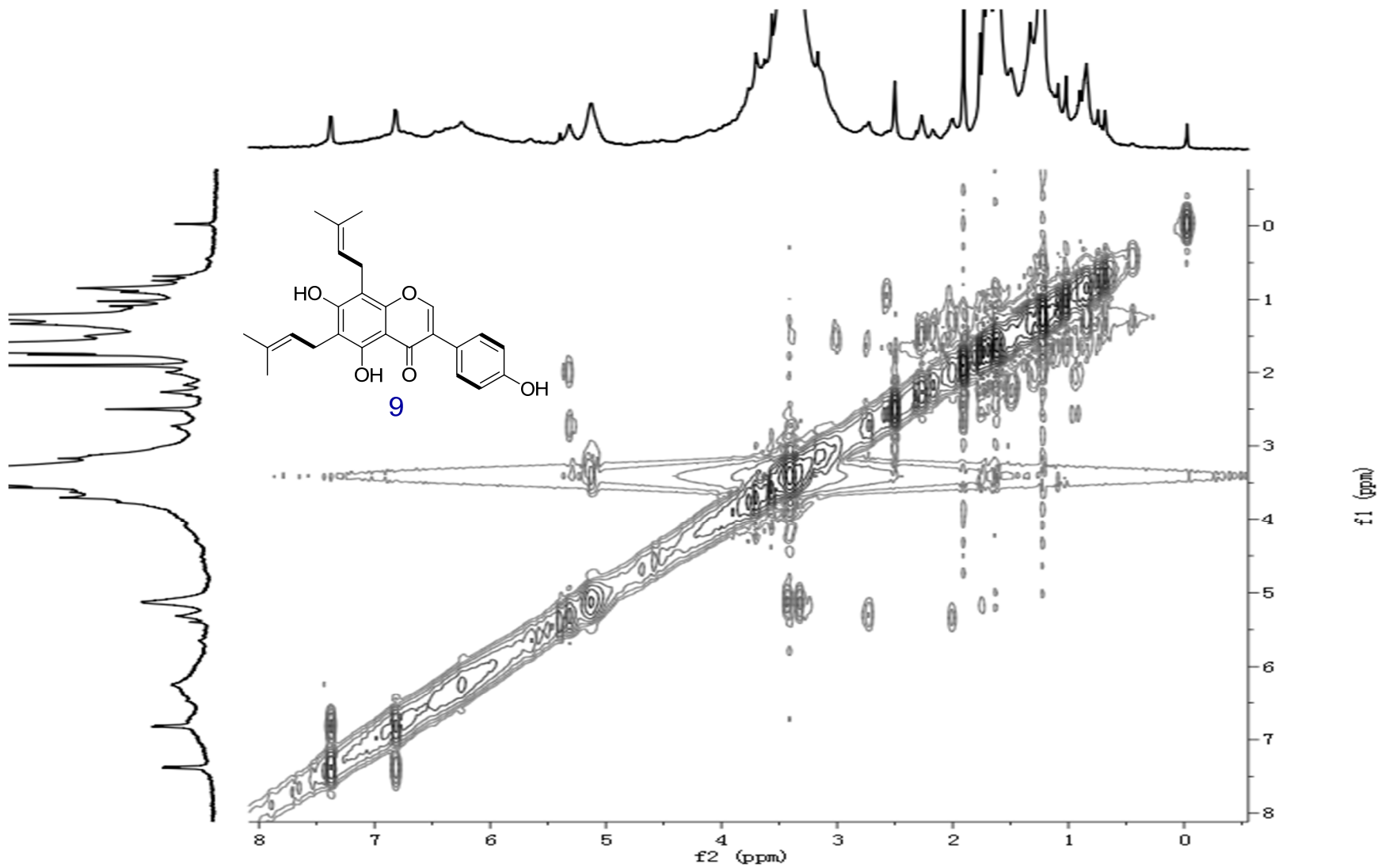


Figure S86. The ^1H - ^1H COSY spectrum of GU-MF-19 in $\text{DMSO}-d_6$.

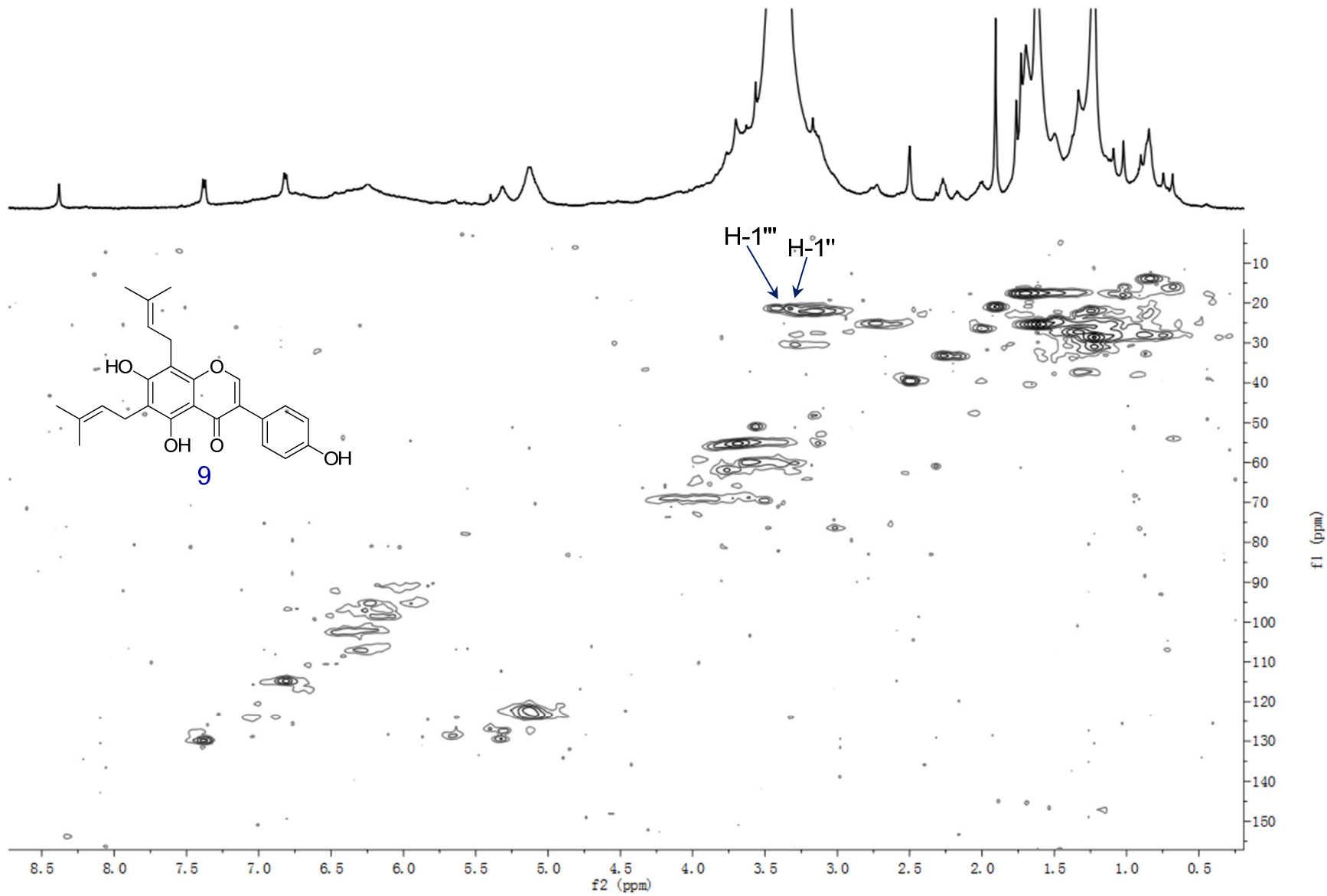


Figure S87. The HSQC spectrum of GU-MF-19 in *DMSO-d*₆.

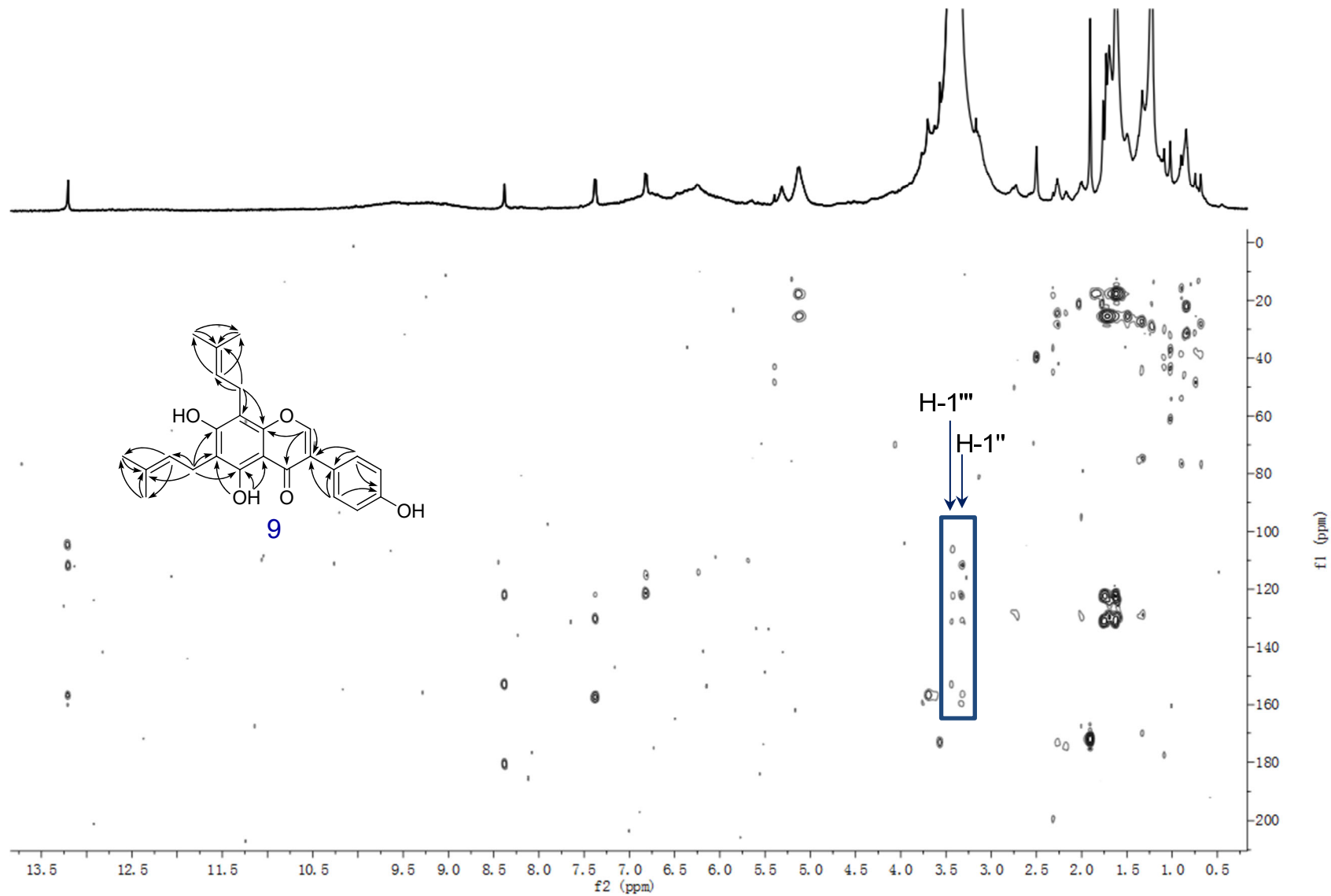


Figure S88. The HMBC spectrum of GU-MF-19 in $\text{DMSO}-d_6$.

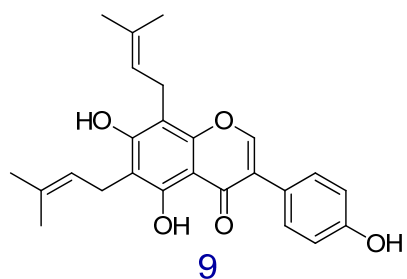
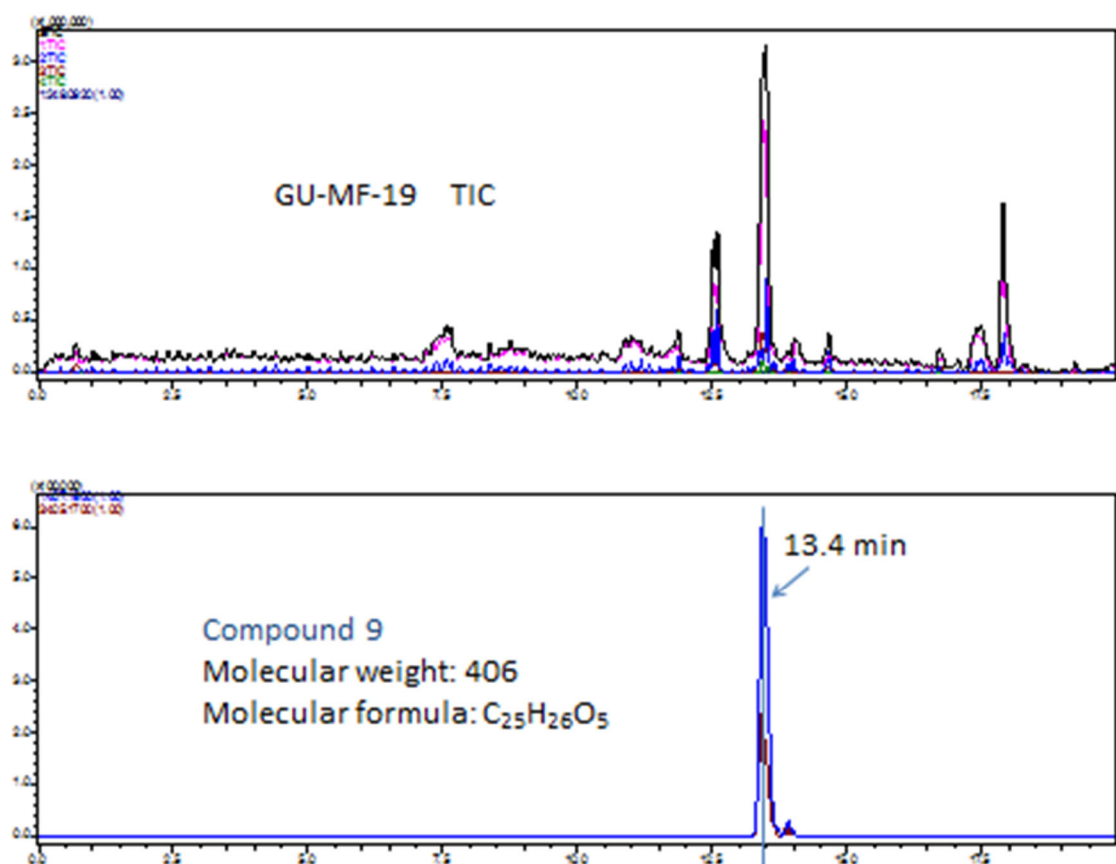


Figure S89. The IT-TOF TIC spectrum of GU-MF-19.

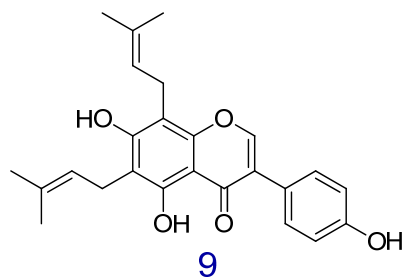
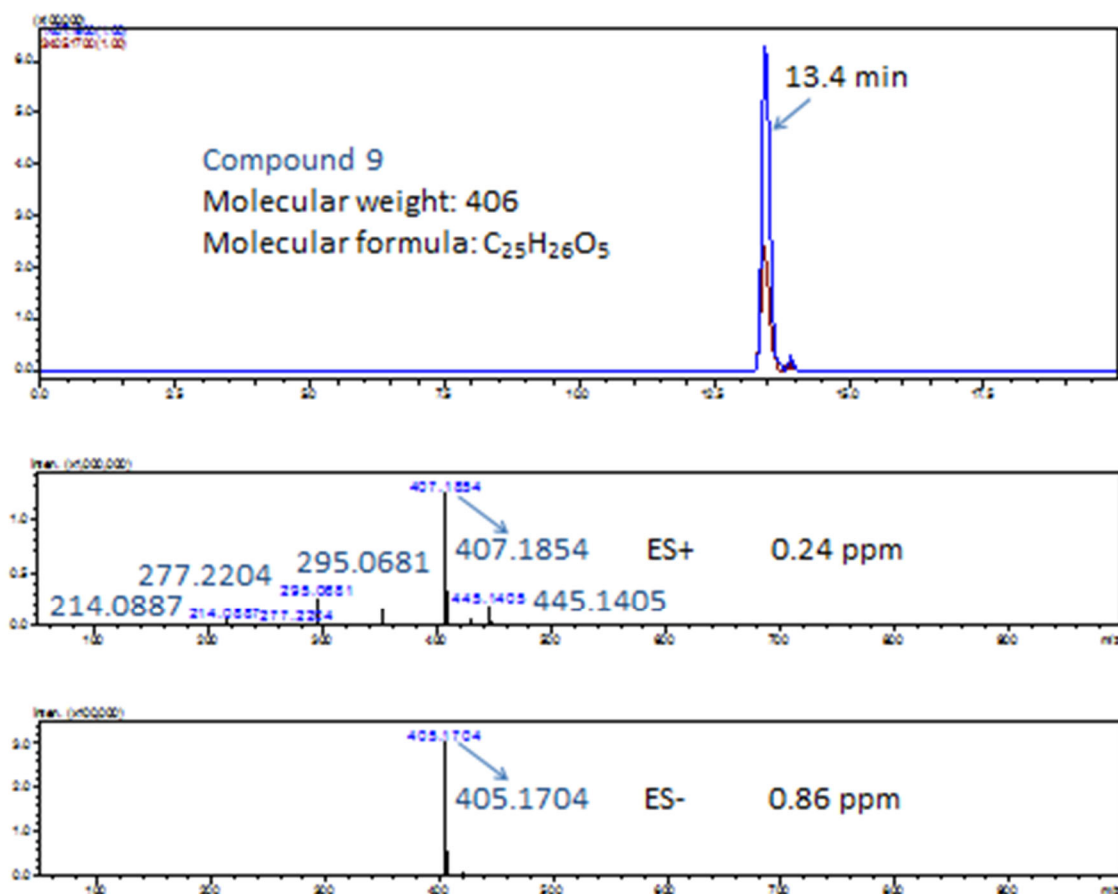


Figure S90. The (+)-HRESIMS and (-)-HRESIMS spectra of compound **9** in GU-MF-19, with extracted ions (positive and negative) for m/z 407 and 405, respectively.

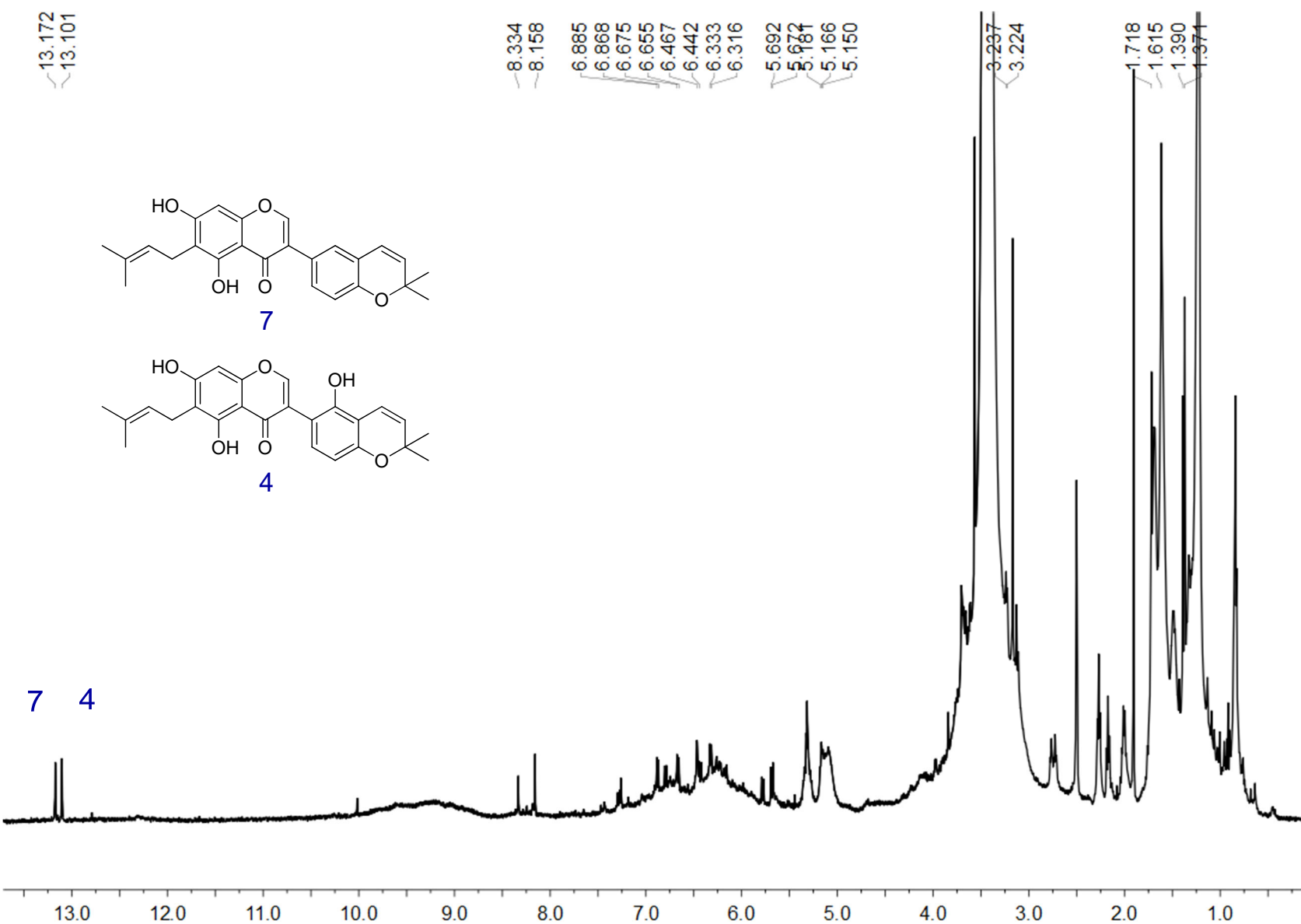


Figure S91. The ^1H NMR spectrum of GU-MF-20. in $\text{DMSO}-d_6$.

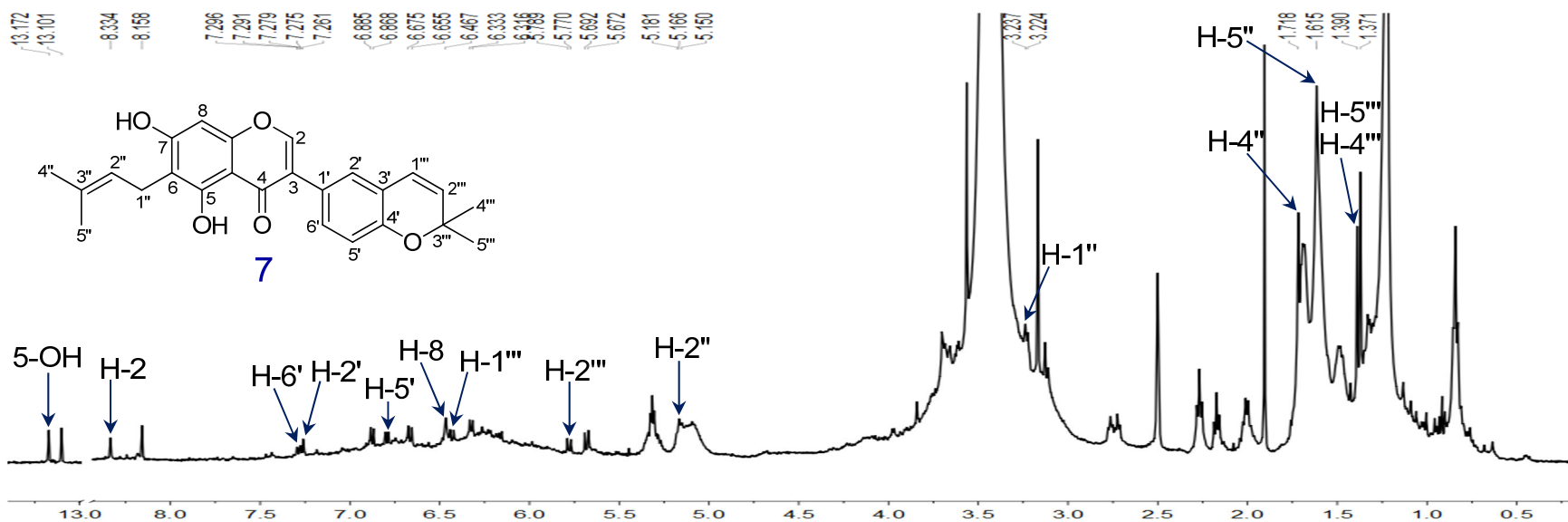
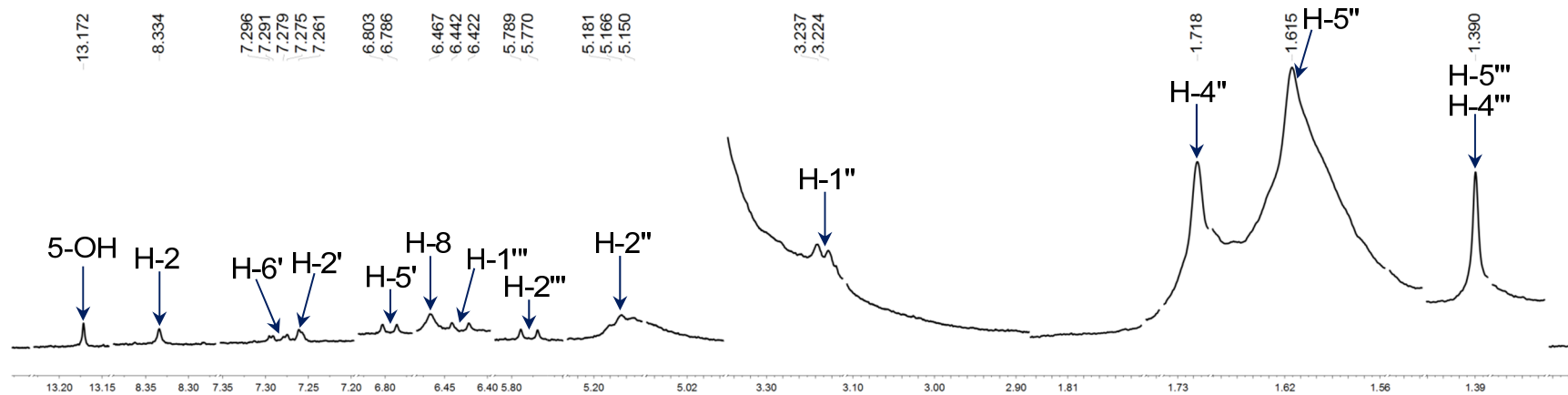


Figure S92. The ^1H NMR spectrum of compound **7** in GU-MF-20 in $\text{DMSO}-d_6$.

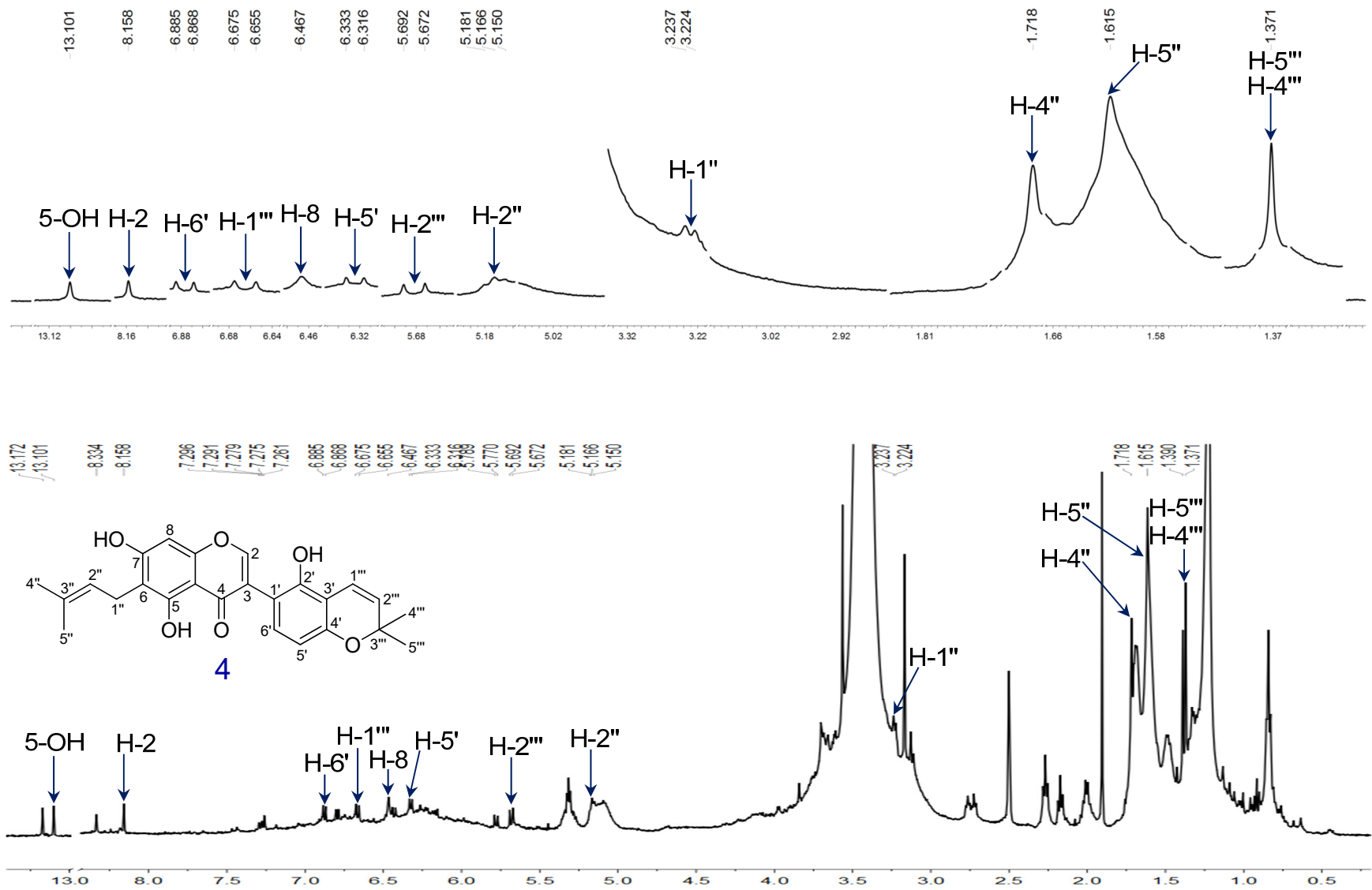


Figure S93. The ^1H NMR spectrum of compound 4 in GU-MF-20 in $\text{DMSO}-d_6$.

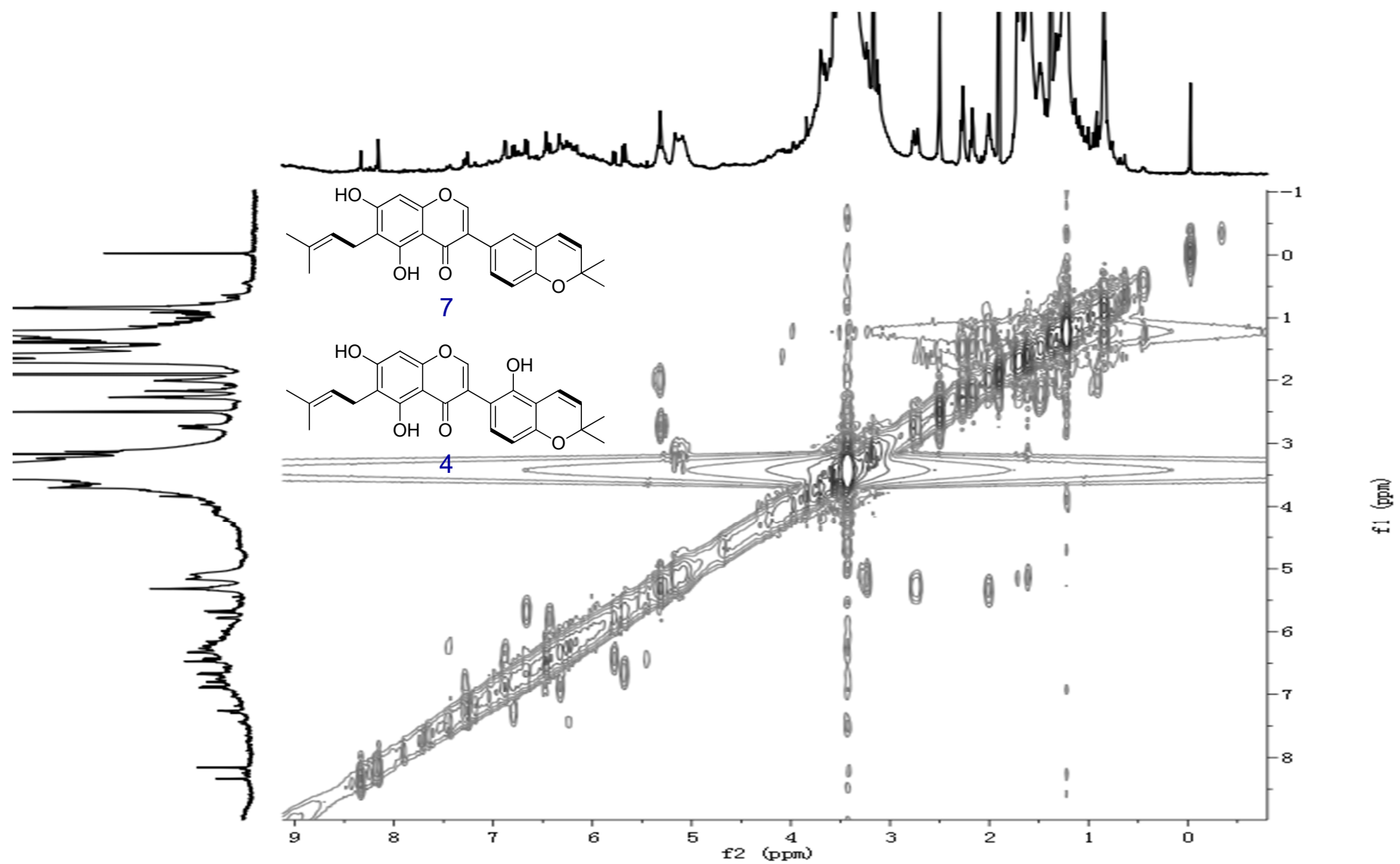


Figure S94. The ^1H - ^1H COSY spectrum of GU-MF-20 in $\text{DMSO}-d_6$.

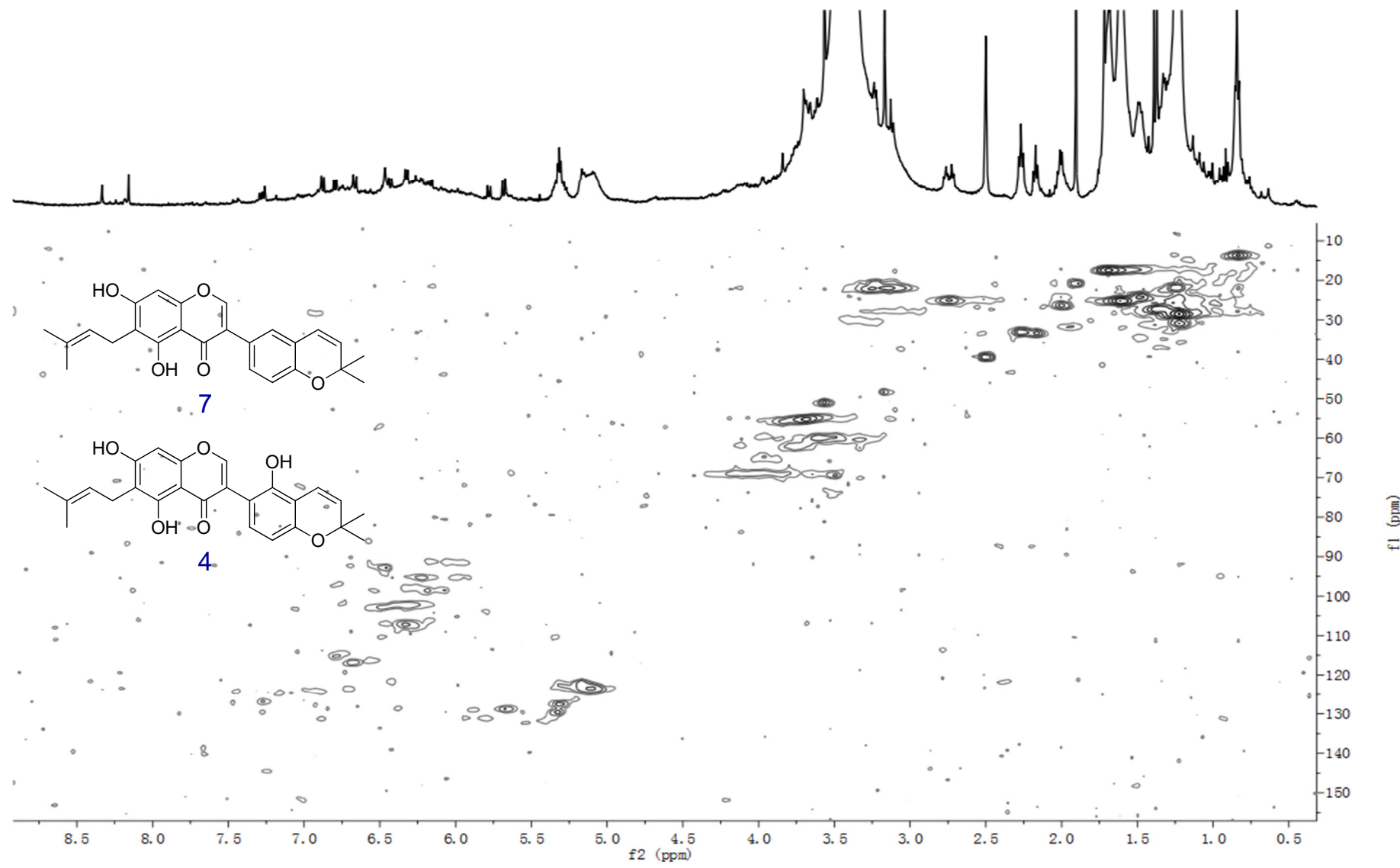


Figure S95. The HSQC spectrum of GU-MF-20 in ⁶DMSO.

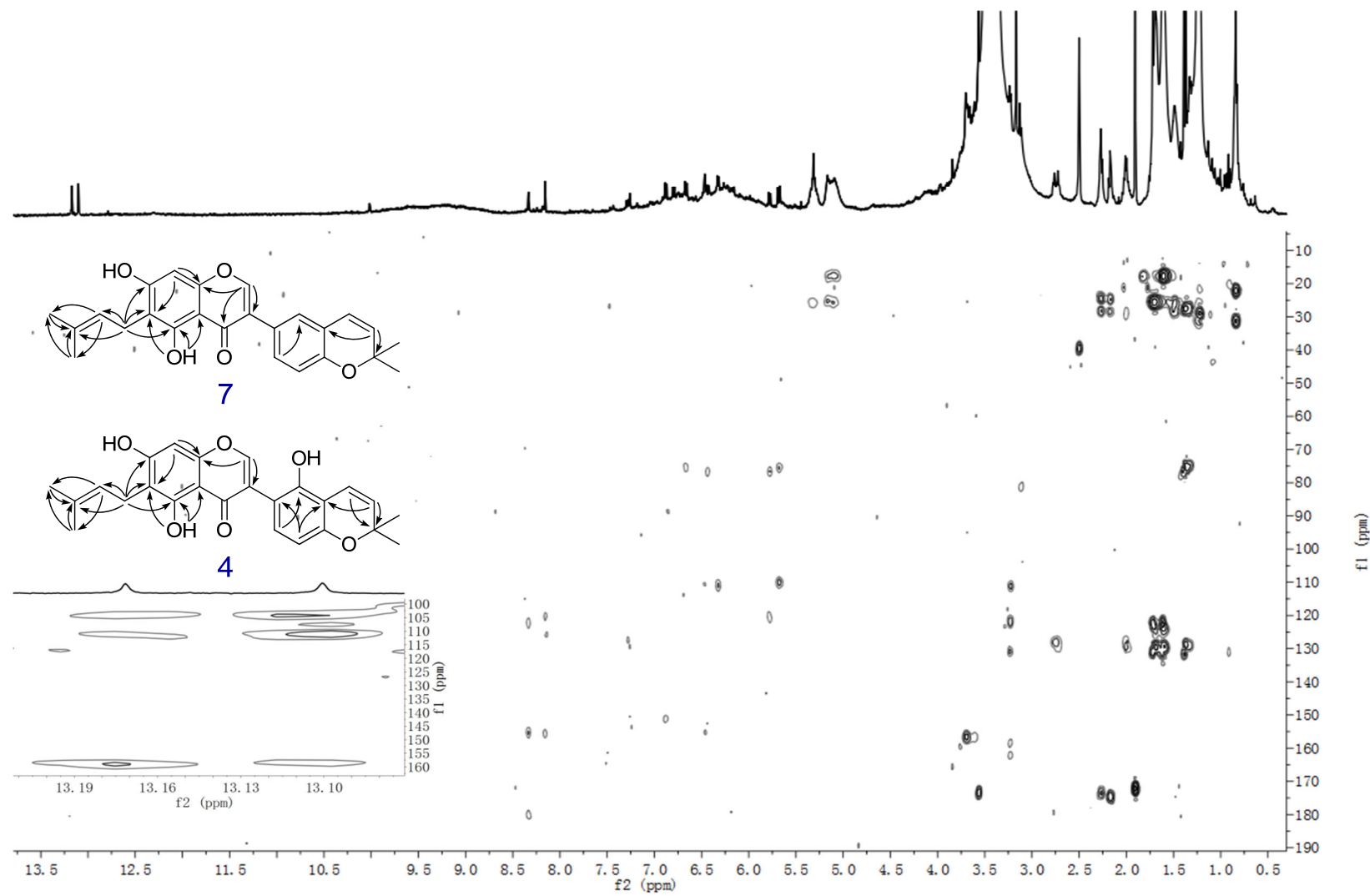


Figure S96. The HMBC spectrum of GU-MF-20 in $\text{DMSO}-d_6$.

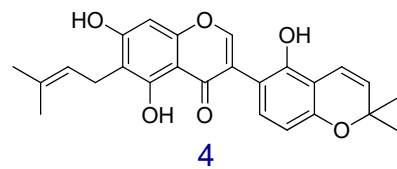
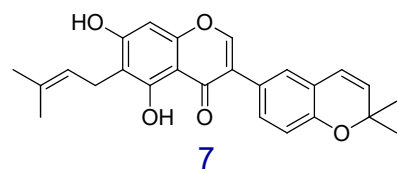
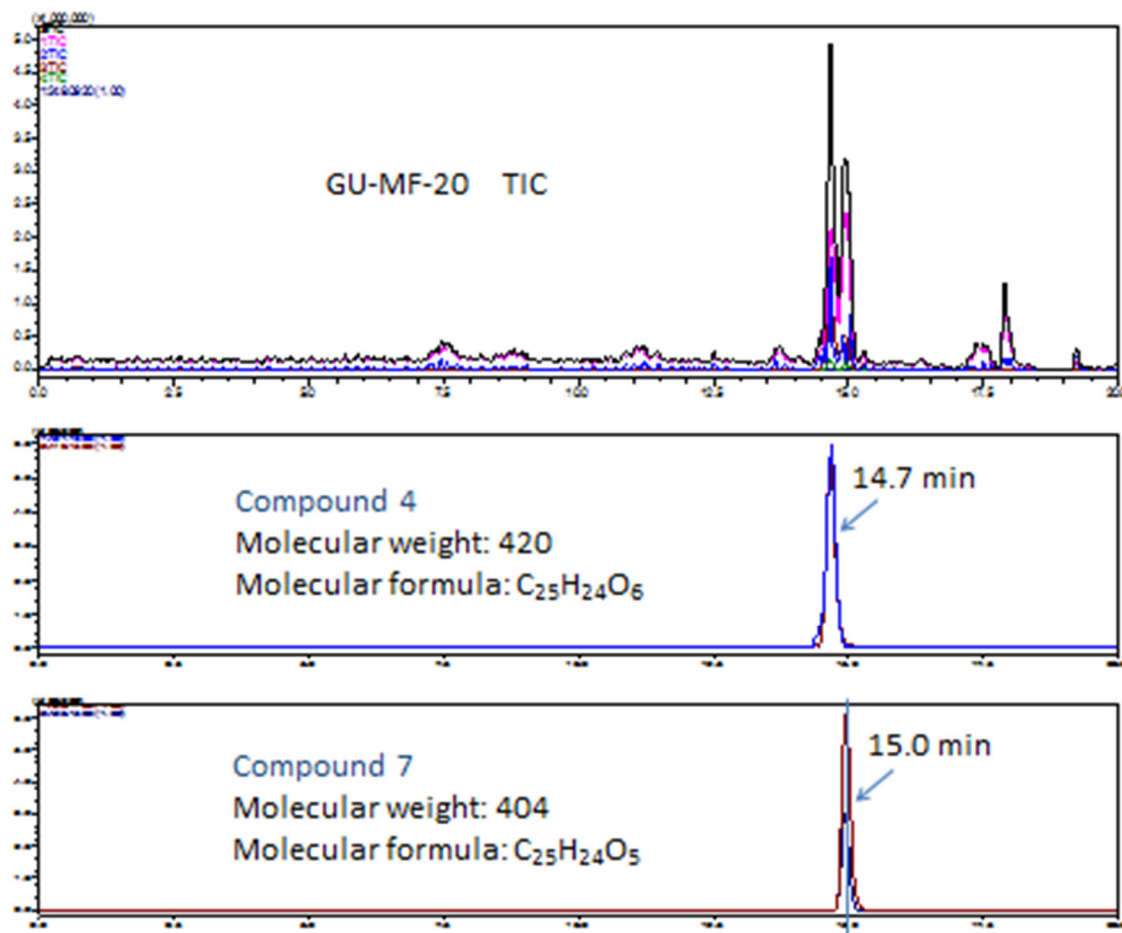


Figure S97. The IT-TOF TIC spectrum of GU-MF-20.

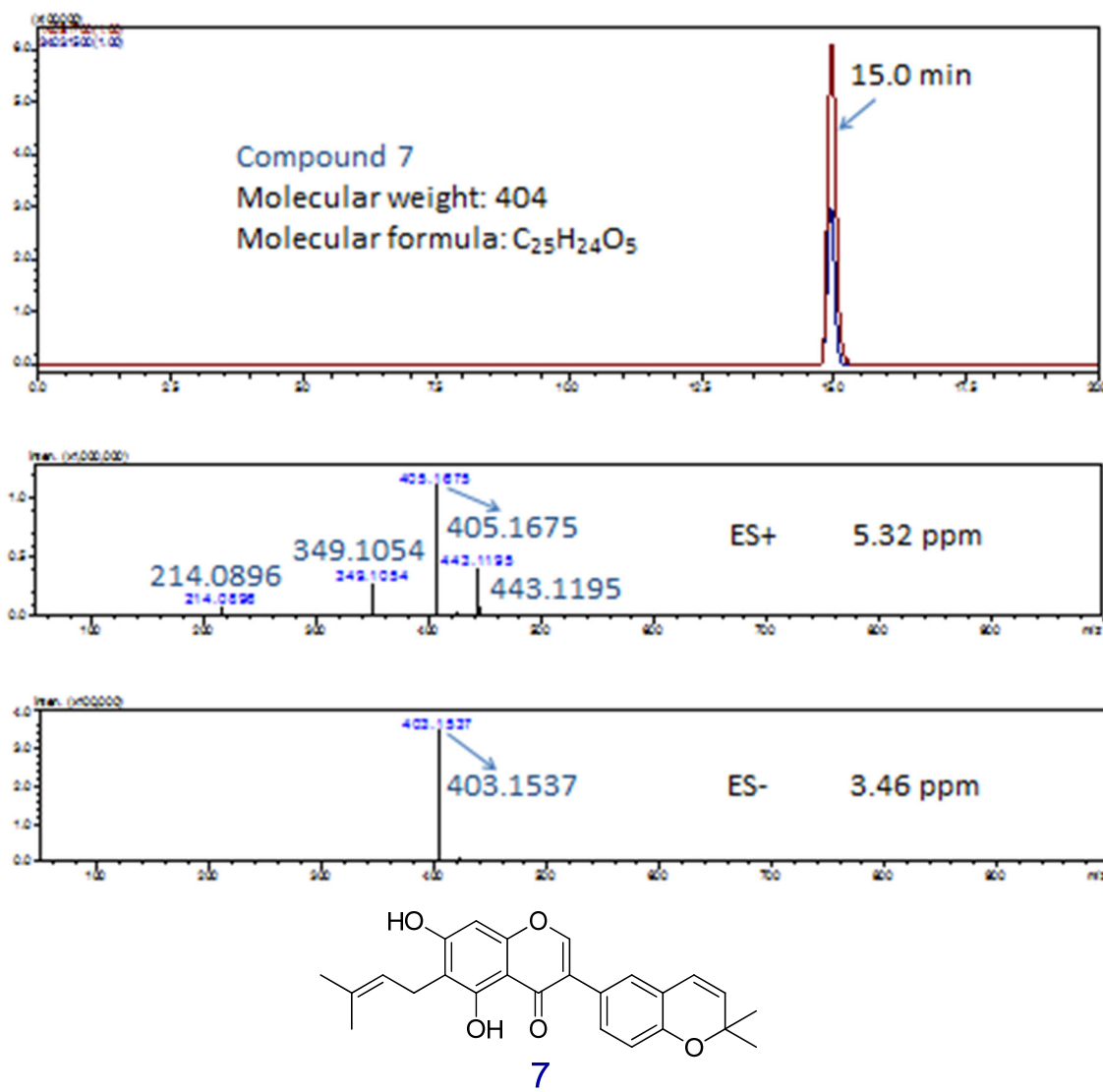


Figure S98. The (+)-HRESIMS and (-)-HRESIMS spectra of compound 7 in GU-MF-20 with extracted ions (positive and negative) for m/z 405 and 403, respectively.

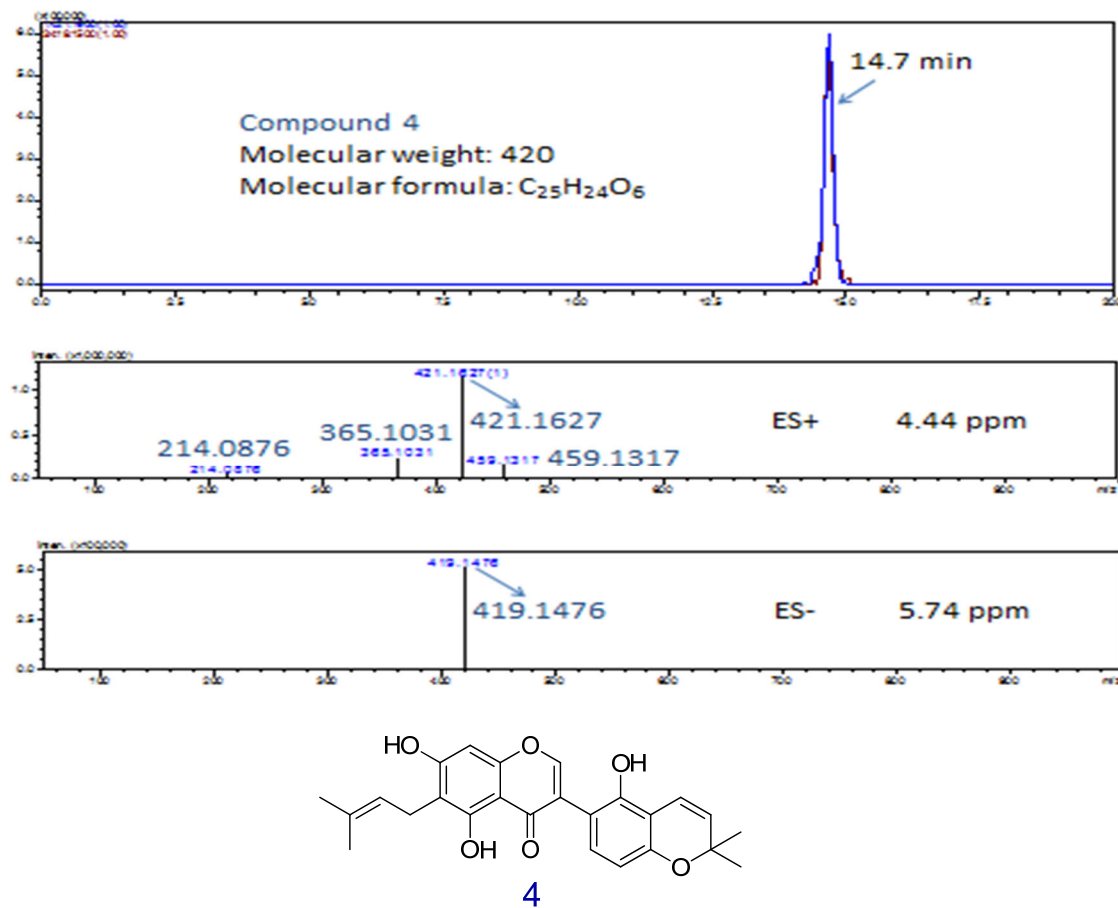


Figure S99. The (+)-HRESIMS and (-)-HRESIMS spectra of compound 4 in GU-MF-20 with extracted ions (positive and negative) for m/z 421 and 419, respectively.